D2-113016-7
April 10, 1967

STUDY OF NAVIGATION AND GUIDANCE OF LAUNCH VEHICLES HAVING CRUISE CAPABILITY FINAL REPORT, VOLUME 4 OF 4 DETAILED STUDIES OF TWO SELECTED NAVIGATION-GUIDANCE CONCEPTS

by

J. A. Retka, D. Harder, D. S. Hague,
C. R. Glatt, T. Seavoy, and D. Minden

Prepared for

NATIONAL AERONAUTICS AND SPACE ADMINISTRATION

Contract NAS 2-3691

Technical Management
NASA Mission Analysis Division
Moffett Field, California
Mr. Hubert Drake

Aerospace Group
THE BOEING COMPANY
Seattle, Washington

FOREWARD

This document reports on an investigation by The Boeing Company from June 10, 1966 to March 10, 1967 of the navigation and guidance of a two stage launch vehicle (hypersonic stage 1/rocket stage 2) under contract NAS 2-3691. The Technical Monitor for the study was Mr. Hubert Drake of the NASA Mission Analysis Division, Moffett Field, California with comonitor Mr. Frank Carroll of the NASA Electronics Research Center, Cambridge, Massachusetts.

The Final Report is prepared in four volumes:

Volume 1 - Summary Report, Boeing Document D2-113016-4

Volume 2 - Trajectory Parametric and Optimization Studies, D2-113016-5

Volume 3 - Alternate Navigation-Guidance Concepts (Phase I), D2-113016-6

Volume 4 - Detailed Study of Two Selected Navigation-Guidance Concepts (Phase II), D2-113016-7.

Boeing personnel who participated in the study reported in this volume (Volume 4) include J. A. Retka, program manager; D. Harder, empirical/explicit rendezvous guidance; D. S. Hague and C. R. Glatt, lambda matrix guidance; T. Seavoy, navigation-guidance mechanization, and D. Minden, cost estimates.

TABLE OF CONTENTS

FIGURES

FIGURES (Continued)

FIGURES (Continued)

FIGURES (Continued)

TABLES

1.0 INTRODUCTION

The study is directed to determining the feasibility, capabilities, and limitations of navigation and guidance systems for a two-stage launch vehicle having an aerodynamic, air breathing first stage and a rocket second stage. The basic mission is to fly a 3704 km (2000 nautical mile) offset distance to the orbital plane of a satellite, turn into the plane and separate the second stage which then accomplishes rendezvous of the payload with a target satellite; the first stage then returns to its base. The overall objective of the study is to determine if substantial improvements in navigation and guidance technology are required or if significant losses in mission performance occur in carrying out a rendezvous mission with this launch vehicle. Phase I, the first four months of the nine month study, was a comparative analysis of alternate navigation - guidance studies concluding with the recommendation of two concepts for detailed study during Phase II, the second half of the study.

The Final Report for the Study of Navigation and Guidance of Launch Vehicles Having Cruise Capability has four volumes:

Volume 1 - Summary Report, Boeing Document D2-113016-4.

Volume 2 - Trajectory Parametric and Optimization Studies, D2-113016-5.

Volume 3 - Analyses and Tradeoffs of Alternate Navigation - Guidance Concepts (Phase I), D2-113016-6.

Volume 4 - Detailed Studies of Two Selected Navigation - Guidance Concepts (Phase II), D2-113016-7.

This volume presents the results of the Phase II study of the two selected navigation - guidance concepts.

The Phase II study emphasized four tasks: (1) Further work on optimization of the nominal flight profile for the rendezvous mission, (2) Study of advanced rendezvous guidance techniques, specifically, the lambda matrix guidance technique, (3) Description of the explicit rendezvous guidance techniques developed by more conventional procedures, and (4) Description of the hardware mechanization, crew displays and controls, and operational studies. This emphasis resulted from the judgement at the conclusion of the Phase I study that the rendezvous navigation - guidance function is feasible within the state-of-the-art for the hypersonic Stage 1/Rocket Stage 2 launch vehicle. This is a distinct contrast with structure and propulsion problems for this launch vehicle. The above emphasis for the Phase II studies was given after NASA review of the Phase I study results.

As a starting point for developing rendezvous guidance, the following description of the problem by R. E. Roberson in "Technology of Lunar Exploration", Academix Press 1963, p. 217, is quoted. "The formal solution of the optimization problem is extremely difficult..... It goes without saying that machine solutions rather than literal ones will be obtained. Although there has been some investigation of closely related problems in astrodynamical

literature, an existing treatment of precisely the rendezvous trajectory sequence problem is not known. At the moment it will have to be categorized as unsolved. If this is the case, what is done in practice? As best one can tell from the discussions of such problems in the literature, the selection seems to be made on the basis of sub-optimization studies, i.e. of trajectory segments taken one at a time, liberally salted with intuition. The results can be quite senstive to details of the overall operational concept"

Empirical/Explicit Guidance

The "empirical/explicit" guidance approach suggested in Section 2 for the particular rendezvous problem of this study has the following steps: (1) Trajectory optimization computer programs are used to define optimum flight profiles for a small number of specific cases covering the range of mission variables, (2) From the results of (1) find empirical functions of the mission variables (e.g. offset distance) that define the flight profile variations, (3) Use the functions from (2) to define a nominal flight profile generator which has the capability of predicting terminal errors at the rendezvous point and iterating until the desired nominal is obtained, (4) Define guidance laws for the path segments obtaining boundary conditions for each segment from the nominal profile generator. The guidance laws use explicit forms where possible and empirical forms where necessary such as for the air-breathing stage.

The results of the Phase II trajectory optimization work were not available during the Section 2 work so that the details given should be considered only as an example of the approach. Considerable detail has been given so that technical feasibility of the approach is clear, and to define the methods of modifying the details when the results of further trajectory work are available.

The on-board nominal profile generator gives the capability for flexible mission control such as the selection of direct ascent, parking orbit ascent, or abort destinations. The design of the guidance equations is done to meet the requirement that fuel penalties due to approximations are small compared to expected off-nominal conditions and navigation error effects.

Lambda Matrix Guidance

The lambda matrix guidance investigation was accomplished by adding a simulation subroutine to a steepest-descent trajectory optimization computer program. (The optimization logic and iteration routines are not used in the guidance simulation.) A nominal flight profile is used as the reference for generating the guidance coefficients for the lambda guidance. When a steepest-descent optimization program is used to define the nominal, the required coefficients are obtained directly. Lambda guidance is a perturbation technique which minimizes the weighted control variable deviations from the nominal control history, where the control deviations are required to correct for off-nominal conditions.

Other perturbation guidance techniques that have had operational application are the Q-matrix and delta guidance techniques. Lambda guidance is analytically somewhat more complex than the other pertubation concepts, but has the advantage that development of the technique for an application is a relatively

well defined analytical process in the frame work of optimization and modern control theory. Advances in computer technology have occurred so that it is not imperative that the very simplest guidance concept be used. Q-matrix and delta guidance are possible candidates for segments of the mission but do not have the convenient adaptability to the complex rendezvous problem under consideration that the lambda guidance approach has.

The lambda guidance study results are reported in Section 3.

Either the lambda guidance or the "conventional" self-contained guidance is technically feasible for the two-stage launch vehicle rendezvous mission. It would be premature to choose between the techniques at this time. It is probable that the lambda guidance technique will be applied to less complex missions before the hypersonic Stage 1/Rocket Stage 2 launch vehicle is developed. An evaluation of the success of these applications will be possible before it is necessary to select the guidance law approach. The conventional guidance law approaches can be extended to this rendezvous mission application. Considerable simulation and design improvement of the details is necessary to implement the self-contained approach. The flexibility that can be obtained with the self-contained approach may be a requirement for the possible alternate missions of the hypersonic launch vehicle. The same degree of flexibility may be possible with the lambda guidance approach taking advantage of computer technology advances anticipated. Development effort on lambda guidance is needed to obtain this flexibility. Further development of the conventional approach would be part of the launch vehicle development program.

Navigation-Guidance Mechanization

The equipment characteristics described are for a current state-of-the-art approach using an inertial platform as the basic navigation sensor and for an advanced technology concept using strapdown inertial techniques with position updating from a navigation satellite system. Weight, volume, and electrical power estimates are made. Crew functions, preflight checkout and preflight alignment operational considerations are described. Accuracy analyses and reliability estimates are made for the two navigation concepts.

Alternate Missions

Payload performance estimates are made for the 9,250 Km (5000 N.M.) cruise mission by using segments of the trajectory obtained from the rendezvous trajectory optimization results reported in Volume 2. The accuracy performance of the navigation system is also described.

Cost Estimates

Estimates for the navigation-guidance system development and recurring costs are made on the assumption that existing technology equipment is adapted to the hypersonic vehicle without major new development.

2.0 RENDEZVOUS GUIDANCE SYSTEM BASED ON A PARAMETRIC DEFINITION OF THE OPTIMUM CONTROL PROFILES

2.1 INTRODUCTION

The objective of this chapter is to describe a system concept for development of a self-contained, vehicle-borne rendezvous guidance system for the launch and space vehicles under study. The concept is based on the hypothesis that the family of optimum control profiles, whatever their form, can be approximated by parametric functions of the mission variables. The implications of this are much more straightforward for Stage 2 than for Stage 1 guidance. Explicit control functions containing the boundary conditions as parameters have been developed which produce approximately optimum flight profiles outside of the atmosphere. In the implementation of this type of guidance for the first burn of Stage 2, the optimum staging and optimum transfer orbit injection conditions would be specified as the boundary conditions. Similar solutions for aerodynamic flight do not exist, complicating the characterization of the Stage 1 optimum control profiles. The concept is nevertheless feasible through the development of empirical functions which fit the optimum control profiles. A two-phase analysis and design process would be required to develop the empirical control functions. On the first phase, the methods of steepest ascent and parametric analysis would be combined to define the optimum integrated Stage 1 - Stage 2 profiles for a selected set of cases covering the range of mission variables. On the second phase, trajectory control models would be synthesized and tested in a search for forms that meet efficiency specifications. The work conducted in this study consisted of the synthesis of one representative model to test the feasibility of this guidance concept.

The principal system requirements which have been considered in the development of the guidance equations are:

- o Adaptability to off-nominal conditions in take-off time, atmosphere, and vehicle performance;
- o Efficiency in terms of fuel consumption;
- o Real time end condition prediction, including fuel reserves;
- o Secondary and abort mode guidance requirements;
- o Adaptability to operational variables such as enroute target updates and planned deviations in take-off weight.

An analysis of payload penalties for the representative guidance model was made for the rendezvous mission with target plane offset distance equal to 3704 Km (2000 N. M.). The payload penalty for the RSS of estimated three-sigma dispersions in knowledge of atmosphere and engine characteristics is 1.3%. This is a satisfactory result, indicating that the method is a competitive candidate for design.

The representative guidance model to be presented is influenced by the structure of the family of optimum nominal flight profiles. A model of this structure which is consistent with the optimization results for the 3704 KM (2000 nautical miles) offset mission is presented in Paragraph 2.2. This is followed by a functional description of the process of generating the nominal profiles for specific command situations in Section 2.3. The guidance concept and equations are presented in Section 2.4, followed by an analyses of payload penalties and computer requirements in Sections 2.5 and 2.6. Detailed equations for nominal profile generation and Stage 2 guidance are presented in Section 2.7.

2.2 A MODEL OF NOMINAL FLIGHT PROFILES

A member of the family of missions to be flown is defined by specification of eight input parameters -- six target orbit parameters and the geographic latitude and longitude of the base. These eight parameters are reduced to seven by a coordinate conversion to the system shown in Figure 2-1, in which the target orbit plane at the time of injection of Stage 2 into the rendezvous transfer orbit is the equator and the base location is on a meridian. The arc length of base latitude in this system is called the target plane offset distance, represented by the symbol R_o. The two parameters geographic latitude and longitude are replaced by the one parameter R_o. The basic parameter set is further reduced to six variables by restricting take-off time to one window per target orbit revolution so that time does not influence the shape of the nominal flight profile.

An important reduction in the complexity of the parametric representation of the family of profiles is realized by noting that the Stage 1 profiles are influenced by only two mission parameters - offset distance (R_o) and the inertial velocity-to-be-gained by Stage 2 on its boost phase, ΔV_g. The inertial velocity required at the end of Stage 2 boost is a function of the apogee altitude of the first coast ellipse on the orbital profile. The difference between the velocity at staging and at boost cut off is the total velocity-to-be-gained. All combinations of the basic parameters which produce a given value of the parameter pair R_o and ΔV_g will have essentially the same nominal Stage 1 profile shape. Another factor that greatly simplifies the problem of flight profile parametric representation is that the Stage 1 nominal is strongly influenced by R_o but is only weakly influenced by ΔV_g.

Consideration of the simplifying factors outlined above strongly influenced the formulation of the guidance model presented in paragraph 2.4. It was also strongly influenced by the concept that the flight profile can be described as a sequence of phases or segments. Segment boundaries are generally well-defined by the physics of the problem. For instance, the stage point defines the end of the Stage 1 outbound flight and the beginning of the Stage 2 initial boost phase; the end of the Stage 1 climb and acceleration phase and the beginning of the supersonic cruise phase on long range missions are sharply defined by the attainment of supersonic cruise conditions; the attainment of specified state vector relative to the orbit plane defines the start of the pullup phase.

TARGET PLANE ORIENTED COORDINATE SYSTEM

FIGURE 2-1

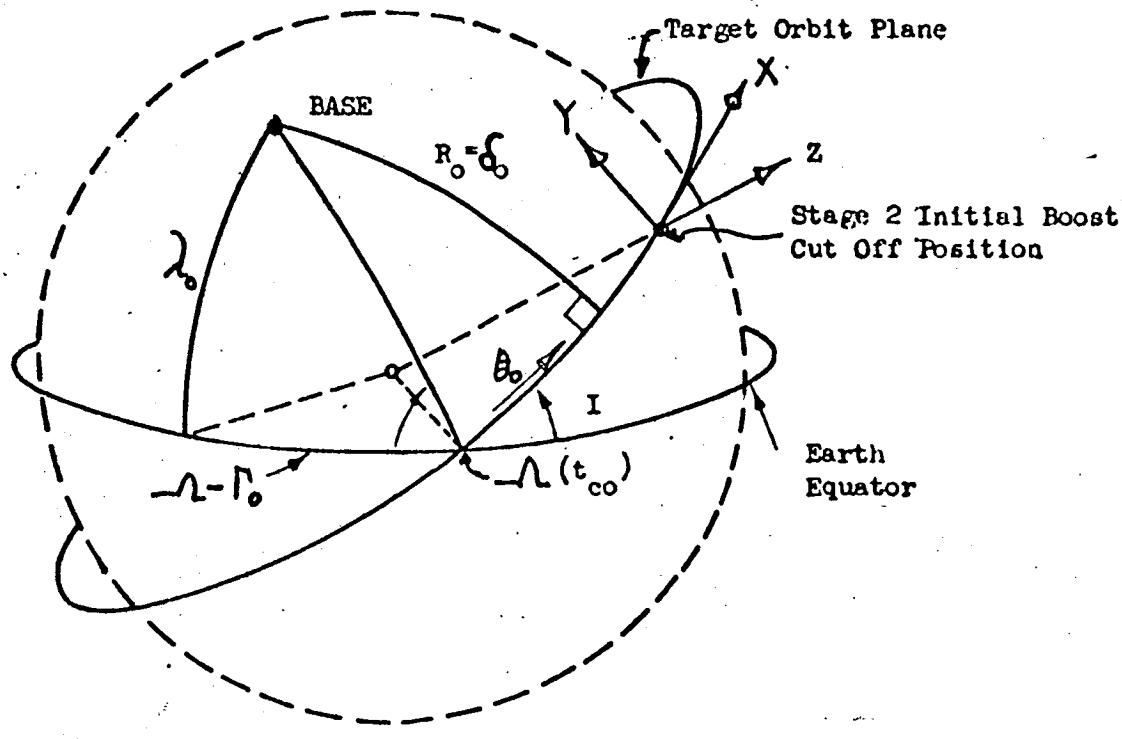

t_{co} - Time of Stage 2 injection into rendezvous transfer orbit (initial boost cut off position)

I - Target orbit inclination

$\Lambda(t_{co})$ - Target orbit node at t_{co}

λ_o, Γ_o - Base geographic latitude and longitude

δ_o, θ_o - Base latitude and longitude in target oriented reference system

(XYZ) - Inertial reference system, defined by local vertical system in target orbit plane at initial boost cut off position

A structure of flight segments was postulated which is based on optimization results for the 3704 Km (2000N. M.) offset mission and on preliminary observations about the short offset profiles. For offset distances of 1852 Km (1000 N. M.) or greater, the Stage 1 nominal outbound flight profiles are asymmetric with respect to the line passing through the base and normal to the target orbit plane. The outbound cruise heading varies with offset distance, from about 26 to 12 degrees as offset distance varies from 1852 to 3704 Km. A turn into the orbit plane follows cruise, and the stage point occurs prior to intercept of the orbit plane. The essential difference between this profile and that for short offset missions is that the acceleration and climb phase and turn phase merge on the short offset profiles. Consider the zero-offset case. Neglecting the effect of the Stage 1 return path and of Earth rotation, the minimum energy profile obviously is the one which heads straight into the desired orbital plane. This, however, produces the maximum length return path. If there are gains to be realized by giving up efficiency on the outbound leg to gain efficiency on the return leg, it will be necessary to move the staging point toward the base. Assuming that the climb and acceleration total path length cannot be shortened, the profile required to fly to a nearer staging point must include a spiral or an initial cruise leg away from the staging point. Curves 1, 2, and 3 of Figure 2-2 show climb and acceleration paths at maximum throttle with constant bank angles of 15, 30, and 45 degrees respectively. These profiles indicate that these pure spiral paths or combinations of them are expensive for moving the staging point toward the base: the fuel requirements for climb and acceleration increase markedly, and there is no effective maneuverability for end point control. Specifically, they result in cross plane final displacements of 178 Km (96 N. M.) or greater, which would be very expensive to null in the terminal phase of the maneuver. It was postulated, therefore, that the zero-offset Stage 1 profile would start with a subsonic cruise phase heading away from the staging point, followed by a turn toward the orbital plane combined with climb and acceleration. Curve 4 of Figure 2-2 shows a path with a subsonic cruise phase at 305 meters per second, (1000 ft. per second), following acceleration at full throttle to the cruise velocity. A turn through 180° is followed by acceleration and climb to the staging point in the plane 500 Km (260 N. M.) down range from the base. The excess fuel requirement for this maneuver was 3180 KG (7000 pounds). This is an expensive maneuver, but it does move the stage point 260 Km (140 N. M.) toward the base while meeting the required cross plane end condition. Considering both the zero-offset profile description and the 3704 Km offset profile, the sequence of segments for outbound Stage 1 flight are defined as follows:

- o Take-off and turn to initial heading (AZ_1).
- o Acceleration and climb to subsonic cruise conditions when $R_o \leq R_c$, acceleration and climb to supersonic cruise when $R_o > R_c$, (R_c is the magnitude of offset distance which defines the mission as short range or long range.)
- o Subsonic cruise when $R_o \leq R_c$; supersonic cruise when $R_o > R_c$.

SHORT OFFSET PROFILES

FIGURE 2-2

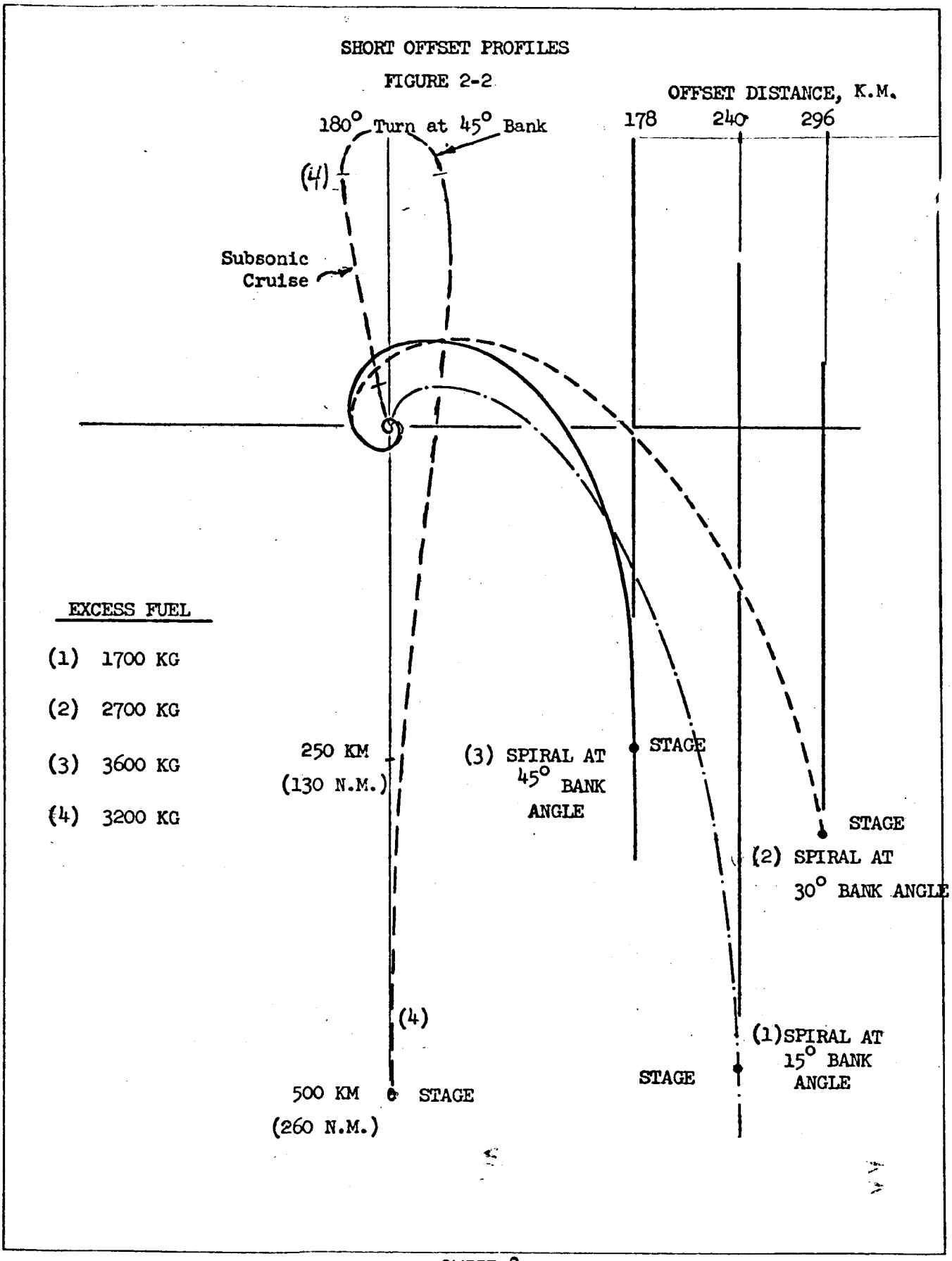

- Phase 1 of acceleration, climb, and turn after subsonic cruise ($R_o \leq R_c$) or Phase 1 of turn after supersonic cruise ($R_o > R_c$).
- Phase 2 of acceleration, climb, and turn after subsonic cruise ($R_o \leq R_c$) or Phase 2 of turn after supersonic cruise ($R_o > R_c$).
- Pull up and stage.

Figure 2-3 shows a possible pattern of latitude-longitude paths fitting this model. The attitude control profile on each segment is defined by the pitch angle and bank angle profiles. The pitch angle profile on each segment is defined by the optimum altitude-velocity for that segment. The bank angle profile on each segment is controlled to maintain the optimum latitude-longitude profile for that segment. Throttle setting is always at maximum except in the cruise phases.

The Stage 2 nominal orbital profiles are functions of target orbit semi-major axis, eccentricity, and argument of perigee, as well as of Stage 2 initial boost cut off conditions. They are defined explicitly by Keplerian orbital mechanics with approximations for perturbations due to gravitational anomalies. When the target orbit is nearly circular, there are two types of nominal orbital profiles - direct ascent and parking orbit, illustrated in parts (a) and (b) of Figure 2-4. When the target orbit is eccentric, the orbital profile consists of a two phase parking orbit as shown in part (c) of Figure 2-4. The vehicle coasts in the first parking orbit until it crosses the target orbit line of apsides in conjunction with the orbit apogee, injecting there into an eccentric orbit with apogee coincident with the target orbit perigee. The nominal point of transfer out of this orbit occurs on the line of apsides with injection into an ellipse such that rendezvous occurs at target orbit apogee. This flight profile sequence for the eccentric target orbit is designed to minimize the fuel required to accomplish rendezvous.

The sequence of segments on the Stage 2 profile to rendezvous are:

- Stage 2 initial boost segment, with cut-off conditions for a near Hohmann transfer to target altitude or parking orbit altitude.
- First orbital coast period with nominal coast angle of 180°+ on the near Hohmann transfer to target altitude or parking orbit altitude. If the rendezvous mode is direct ascent, this coast period is followed immediately by the terminal phase.
- First orbital ΔV (not used for direct ascent) placing the target in a circular orbit.
- Second orbital coast period in parking orbit.
- Second orbital ΔV, establishing a Hohmann transfer to target orbit perigee altitude. It is the final transfer if target orbit is circular; it is the second parking orbit if the target orbit is eccentric.

STAGE 1 OUTBOUND LATITUDE-LONGITUDE PROFILES (HYPOTHETICAL)

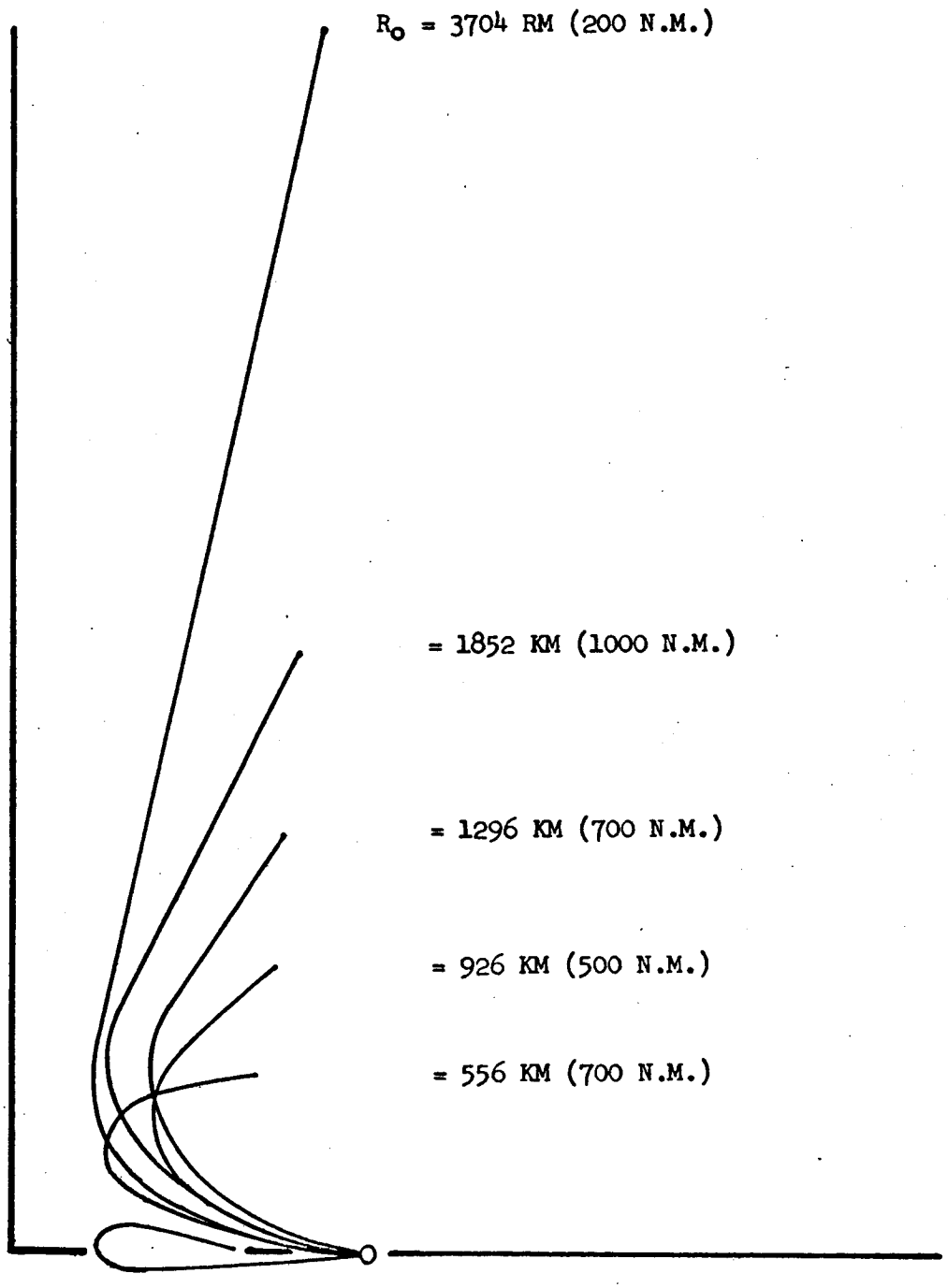

STAGE 2 NOMINAL ORBITAL PROFILES

FIGURE 2-4

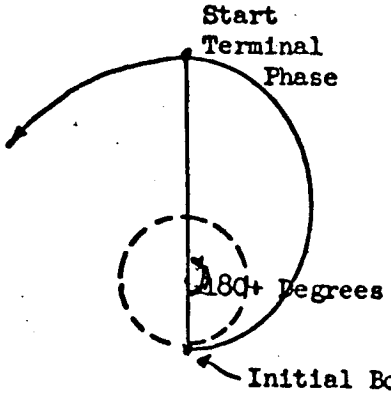

(a) DIRECT ASCENT

(Circular Target Orbit)

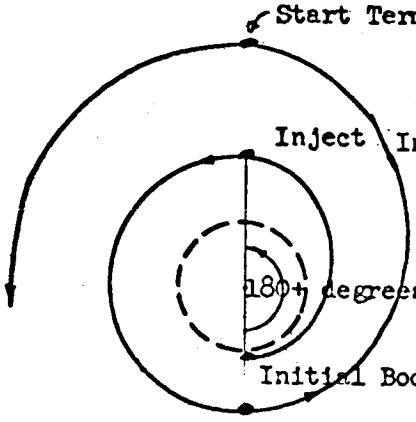

Inject Into Transfer Orbit

(b) SINGLE-PHASE PARKING ORBIT

(Circular Target Orbit)

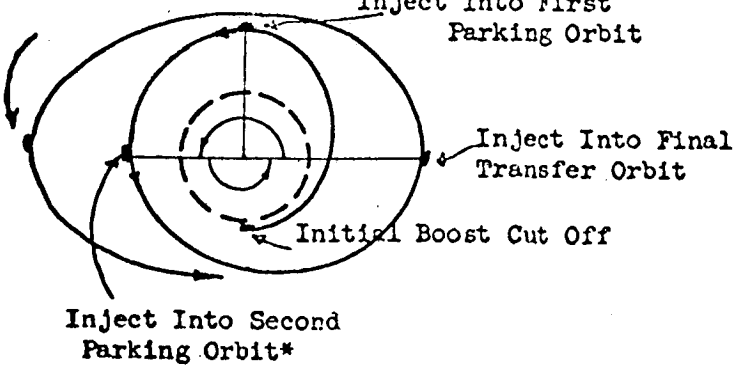

(c) TWO-PHASE PARKING ORBIT

(Eccentric Target Orbit)

*Parking orbit altitudes varied under off-nominal timing to provide phasing for rendezvous.

- Third orbital coast period with nominal coast angle of 180° on a Hohmann transfer to target perigee altitude (final altitude if target orbit is circular.)
- Third orbital ΔV, applying only to eccentric target orbits; magnitude is that required for a Hohmann transfer from perigee altitude to apogee altitude.
- Fourth coast period, applying to eccentric target orbits; nominal coast angle is 180° from coast orbit perigee to target apogee.
- Terminal rendezvous phase.

To illustrate the combined Stage 2 - Stage 1 profile, part (a) of Figure 2-5 shows the ground projection of the Stage 1 segments of a long range mission, and part (b) shows the Stage 2 direct ascent orbital segments for the profile. The target position Θ_T at the time of arrival of Stage 2 at the rendezvous position Θ_f is shown for an arbitrary take-off time. The error angle $\Theta_T - \Theta_f$ is reduced to zero by specifying the proper take-off time.

2.3 FUNCTIONAL DESCRIPTION OF THE NOMINAL FLIGHT PROFILE GENERATOR

The model of flight profiles described in Section 2.2 establishes a framework for defining nominal profiles which are close approximations of the optimum profiles. The segment boundary conditions are to be defined as parametric functions of R_o and ΔV_g. The functional forms are to be such that the boundary conditions defined by the parametric functions for a set of primary cases are coincident with corresponding points on the optimum profiles. The simplifying factors outlined in Section 2.2 suggest that an efficient family of profiles can be defined by fitting the parametric functions to the optimization data of a small number of primary cases, perhaps as few as ten. The purpose of this paragraph is to define the process by which the nominal profiles will be generated.

The parametric representation of the family of optimum flight profiles is implemented in a computer program called the Nominal Flight Profile Generator, (NPG). This program may be included in the vehicle computer system or in a ground-based computer. If it is included in the vehicle computer, the vehicle guidance system is self-contained in the sense that the only targeting inputs required are the target orbit parameters at some epoch. The characteristic of being self-contained is of interest. More important, however, is the fact that the parametric system eliminates the requirement for repeating the steepest-ascent trajectory optimization process for every flight.

A simplified outline of NPG is shown in Figure 2-6. Initial estimates of the mission parameters R_o and ΔV_g are obtained by a geometric solution which is accurate in R_o to within ± 37 Km (20 N.M.). Then the flight is simulated under the control of the guidance equations using constants determined as functions of the estimated values of R_o and ΔV_g. The terminal conditions of the simulated profile are then analyzed and corrections are made in R_o and

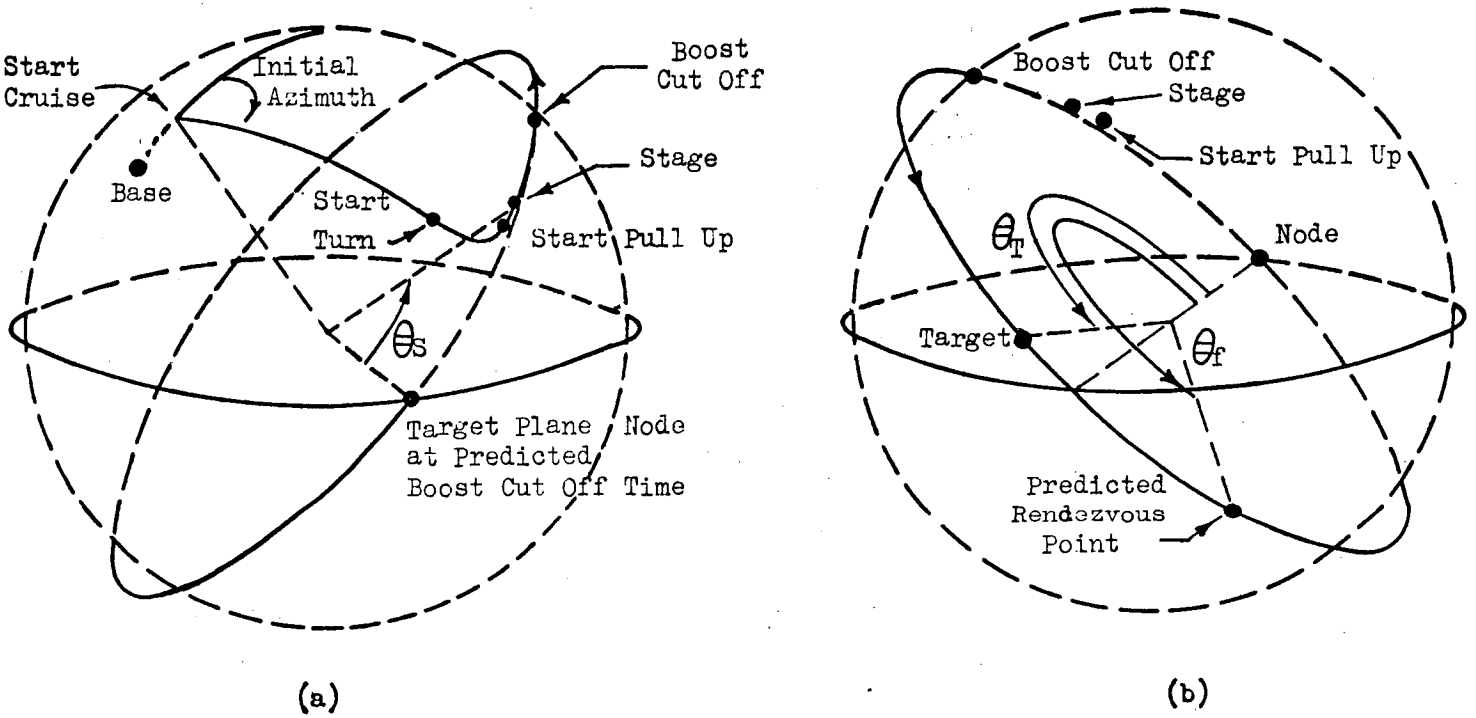

FLIGHT PATH SEGMENTS ON LONG RANGE PROFILE

FIGURE 2-5

FIGURE 2-6

SIMPLIFIED OUTLINE OF NOMINAL PROFILE GENERATOR

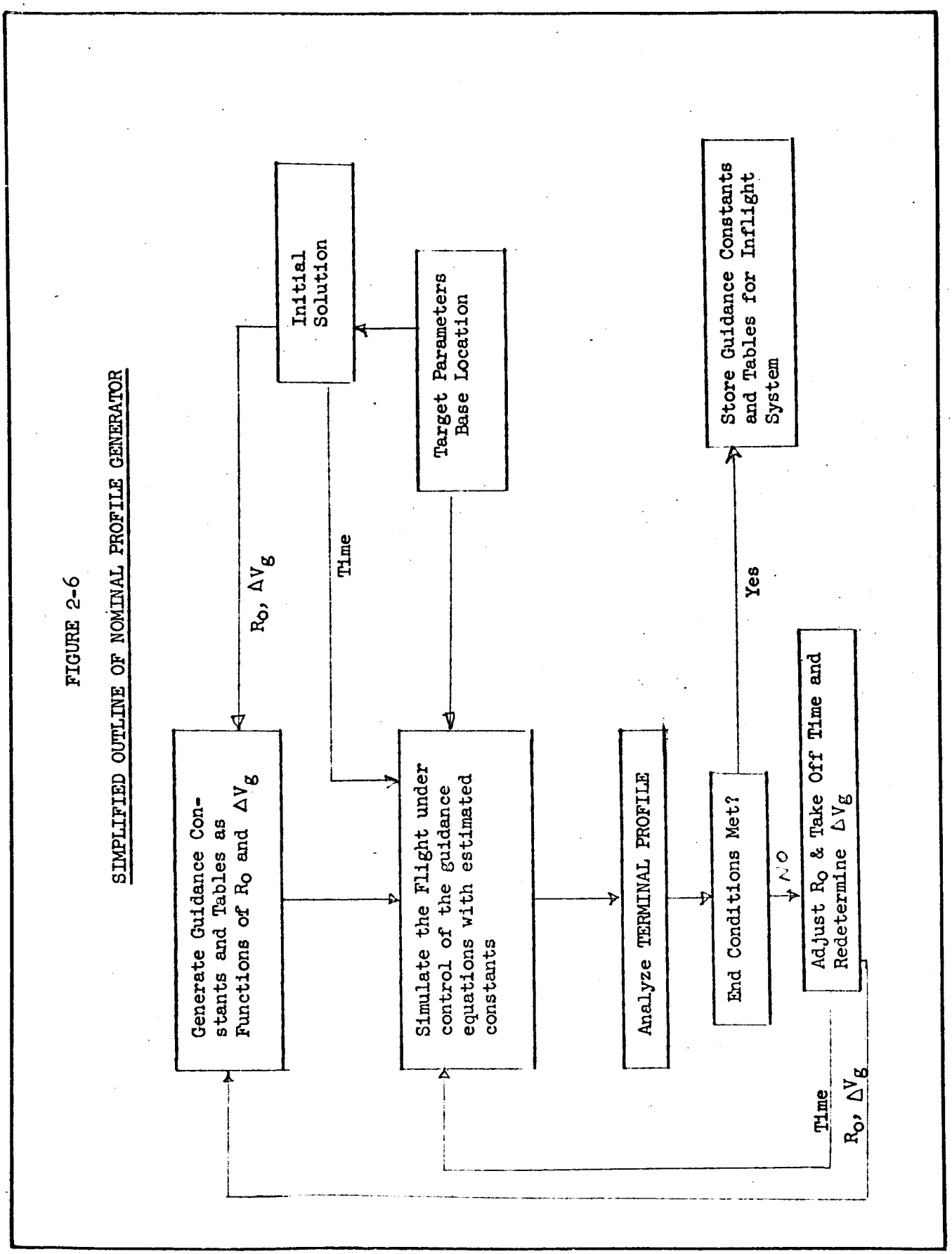

in take-off time to meet end conditions for rendezvous. The guidance equations are designed so that the profile flown on the second or third iteration meets the end conditions required for rendezvous, while maintaining specified altitude-velocity and latitude-longitude (or bank angle) profiles throughout Stage 1.

The following discussion is intended to clarify the method of representation of the boundary conditions and altitude-velocity profiles as functions of R_o and ΔV_g.

Assume that the curves shown in Figure 2-3 represent the latitude-longitude profiles (in target orbit plane parameters) of the family of optimum nominal profiles. The optimum stage point longitude (Θ_s) varies from 0.75° at R_o = 3700 Km to 3.° at R_o = 10 Km. The value of the optimum stage point for any value of R_o from O Km to 3700 Km is assumed to lie on the smooth curve which passes through the model points. These would be represented in NPG by a table or by a mathematical function which fits the data. Similarly, the variation in initial heading (AZ_1) from -10° when R_o = 0.0 Km to 80° when R_o = 3700 Km would be represented by a table of points on the curve through these points. If the optimum stage point longitude and the initial heading are not invariant with ΔV_g, the representation is more complex, but the principle remains the same. The representation of the variations in the optimum altitude-velocity profiles with R_o and ΔV_g is considerably more complex in detail than the representation of the heading and position boundary conditions; but, again, the principle is the same.

For illustration, consider the optimum altitude-velocity profile from take-off to the attainment of supersonic velocity. The solid line in Figure 2-7 represents this profile for the 3704 Km offset mission, with the acceleration and climb being executed at maximum throttle and essentially zero bank angle. The form of the variations from the reference profile when the vehicle is banked and throttled are not known at this time. One hypothesis to be tested is that there is no significant variation in the shape of the profile of altitude versus velocity when the vehicle is banked at full throttle. If this hypothesis is valid, the altitude-velocity profile for the acceleration and climb is represented by one profile for all missions that do not have a subsonic cruise phase. A subsonic cruise phase for short range missions is expected to introduce variations in the altitude-velocity profile. A purely hypothetical set of curves are sketched in Figure 2-7 to illustrate possible variations in the profile with respect to R_o in the region from the termination of cruise to attainment of supersonic velocity. The circled data points would be stored to define the three-dimensional array of altitude versus velocity versus R_o.

Illustrations of exactly the same form as those given above apply to all of the other constants and tables required by the guidance system to control the flight. There are many forms available for implementing the variations to fit the data of the optimum trajectories. Storage of the data in tables with suitable interpolation routines however is the most flexible method, and is expected to require about 800 constants and table values.

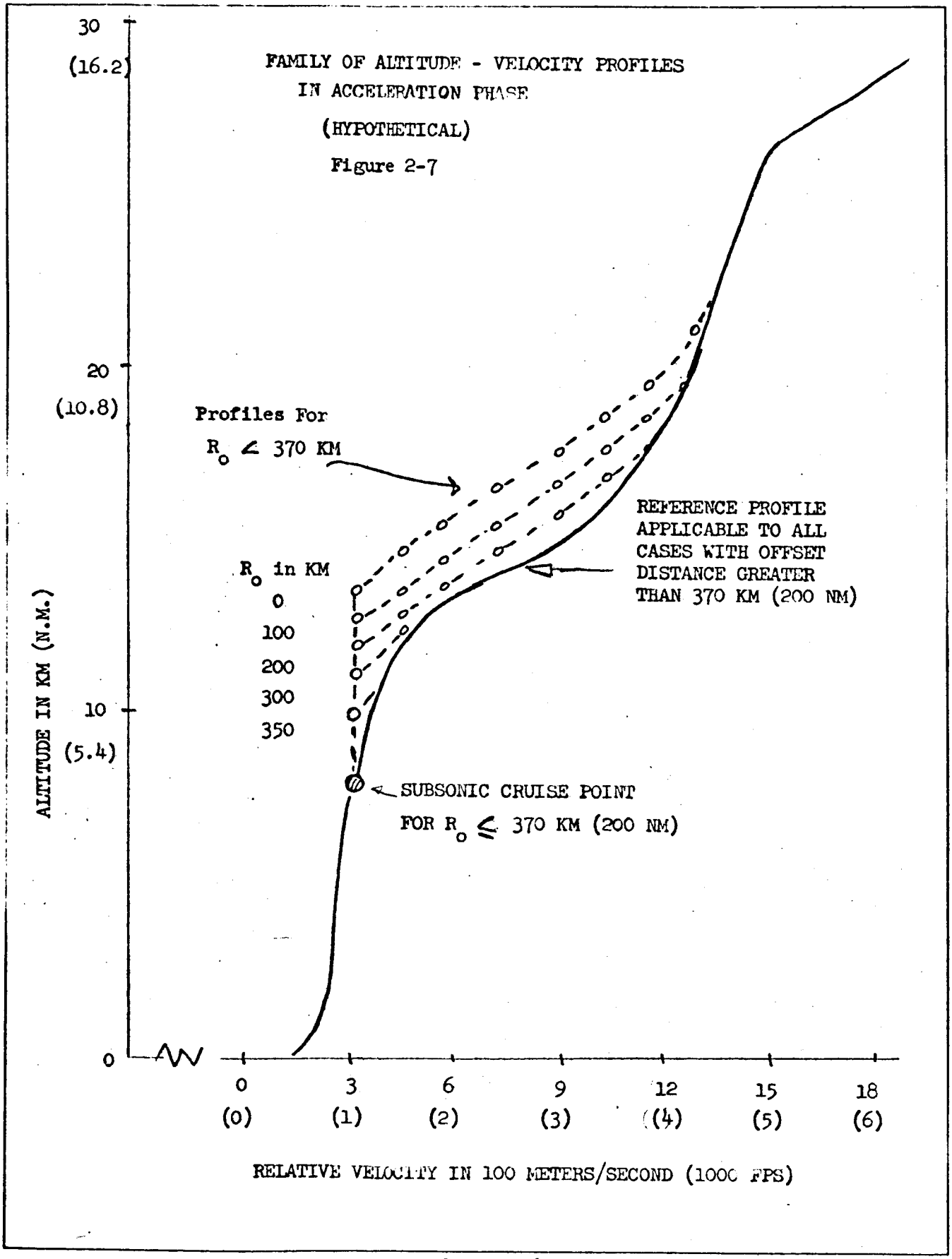

2.4 THE GUIDANCE EQUATIONS

The system of guidance equations defined in this section implements a combination of nominal path-following and explicit end condition control for Stage 1, and an essentially explicit form of end condition control for Stage 2.

2.4.1 STAGE 1 GUIDANCE

The definition of the Stage 1 guidance equations is divided into two parts. The first part defines the equations involved in following a nominal profile, neglecting off-nominal conditions on all segments except on the final phase of the turn and on the pullup maneuver. The second part defines the equations for detecting and treating off-nominal conditions to control stage position and time, to predict the fuel margin, and to switch rendezvous modes on the basis of the fuel margin prediction.

THE NOMINAL STAGE 1 GUIDANCE EQUATIONS

In the nominal mode, pitch is controlled at all times to maintain the nominal altitude-velocity profile, while bank angle is controlled in various modes depending on the phase of flight. Initially, it is controlled to turn toward and then hold an initial azimuth command. On the cruise phases, it is controlled to steer the great circle course to the commanded nominal start turn position. On the coordinated acceleration, climb, and turn of short range profiles, it is controlled by an empirically derived form in time which fits the optimum profile. In the last part of the turn and throughout pullup, it is controlled to achieve the optimum cross plane inertial position and velocity at the stage point. Throttle is maintained at its maximum setting in all except the cruise phases. The equations of the prestaging maneuver define a terminal controller which causes the profile to converge to the desired altitude, velocity, heading, and cross plane position at staging. The stage time, which is a free variable, is the principal independent variable in the control equations. It is predicted in a simplified integrable form of the equations of motion.

The nominal equations are defined in detail in Section 2.7.3. Only the details of the principal equations for the treatment of off-nominal conditions are given in this section.

STAGE TIME AND POSITION CONTROL FOR OFF-NOMINAL EFFECTS

The Supersonic Cruise Phase

For long range missions, when $R_o > R_c$, no corrections for off-nominal timing are made on the acceleration and climb phase. Course and throttle variations are started after reaching cruise conditions and are continued within specified limits throughout the cruise phase. Figure 2-8 illustrates the problem geometry. At time t, the vehicle is at position (δ , Θ), steering to the start turn position (δ_3, Θ_3) on a great circle which intersects the orbit plane with the azimuth angle A. The guidance equations for this phase are designed so that Stage 1 arrives at the staging point at some commanded time, not

SUPERSONIC CRUISE PHASE TIME CORRECTION DIAGRAM

FIGURE 2-8

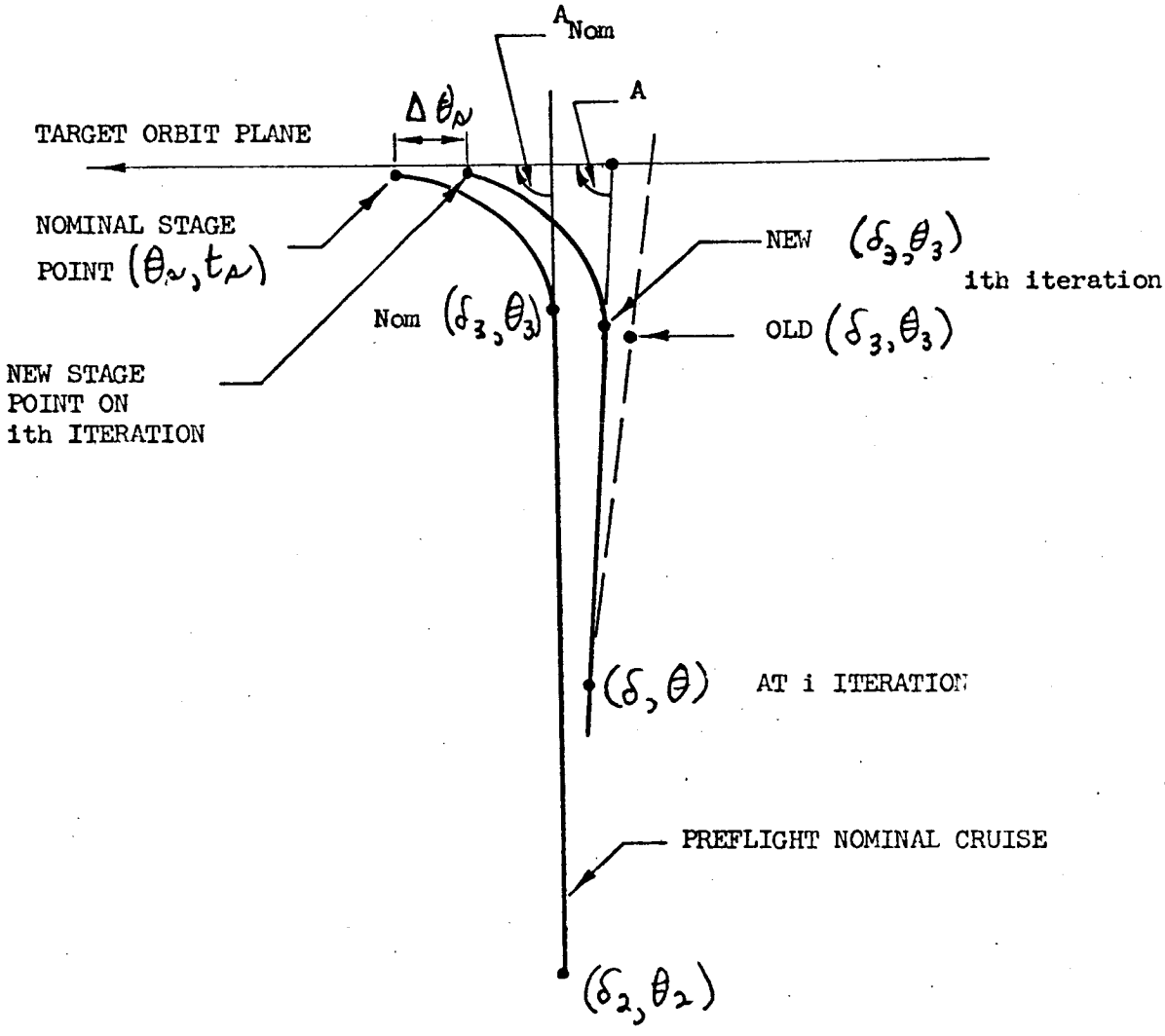

necessarily equal to the nominal staging time, but such that rendezvous conditions will be met. The first step in the control process is the prediction of stage position and time under the current command profile. Assuming constant turn characteristics and cross plane staging conditions, the variation of time in the turn is a linear function of the variation in angle A. The stage time predicted at time t is given by:

$$\hat{t}_s = t + R_{cr} / \eta_c S_{cr}) + C_1 + C_2 (A - A_{nom}) \qquad (2.4.1)$$

where η_c is the throttle command; S_{cr} is the nominal central angle rate in cruise; R_{cr} is the cruise range angle; C_1 is the time to turn through the nominal value of angle A; and C_2 is the inverse of the azimuth angular turn rate. The cruise range central angle is calculated from present position and start turn coordinates as follows:

$$R_{cr} = \cos\delta\cos\delta_3\cos(\Theta - \Theta_3) + \sin\delta\sin\delta_3 \qquad (2.4.2)$$

The predicted position of staging is now computed for the off-nominal conditions

$$\hat{\Theta}_s = \Theta' + C_3 + C_4 (A - A_{nom}) \qquad (2.4.3)$$

where Θ' is the longitude of the intercept of the cruise great circle with the target orbit plane and C_3 and C_4 are constants of the nominal turn profile. Next the correction required in stage time, δt_s, to meet rendezvous conditions when staging at Θ_s is given by:

$$\delta t_s = \hat{t}_s - \left(t_s - \frac{\hat{\Theta}_s - \Theta_s}{W_T} \right) \qquad (2.4.4)$$

where Θ_s and t_s are the nominal stage point longitude and time and W_T is the target orbit angular rate in the region of the rendezvous point, Θ_f. The stage time error δt_s is corrected by two control actions -- cruise heading angle change and throttle command change. Thresholds and limits are established; if the control commands exceed the limits or are below the thresholds, the residual time errors are corrected on the Stage 2 flight profile. Cruise course and throttle are commanded within limits to correct the stage time error δt_s. The logic for course correction is given by:

$$\text{New A} = \text{Old A} + C_5 (\delta t_s - \varepsilon_1), \text{ if } \delta t_s > \varepsilon_1 > 0$$
$$\text{or} \quad \text{New A} = \text{Old A} + C_5 (\delta t_s - \varepsilon_2), \text{ if } \delta t_s < \varepsilon_2 < 0 \qquad (2.4.5)$$

The constants ε_1 and ε_2 are threshold settings which may be asymmetrical about zero.

Angle A is limited to the region:

$$C_7 < (A - A_{nom}) < C_6$$

The new value of A determines the new value of the start turn position as follows:

$$\text{New } \Theta_3 = \text{Old } \Theta_3 + \frac{1}{C_8}\left(\tan\frac{A}{2} - \tan\frac{A_{nom}}{2}\right)\cos A_{nom} - \frac{(A - A_{nom})}{R_{cr}}\sin A_{nom} \qquad (2.4.6)$$

$$\text{New } \delta_3 = \text{Old } \delta_3 + \frac{1}{C_8}\left(\tan\frac{A}{2} - \tan\frac{A_{nom}}{2}\right)\sin A_{nom} + \left(\frac{A - A_{nom}}{R_{cr}}\right)\cos A_{nom}$$

Where C_8 is the turn radius and R_{cr} is the cruise range angle from present position to the current start turn position. After computing the new value of range angle to the new start turn position, the new heading command is given by:

$$AZ_c = \arcsin\left(\frac{\cos\delta_3 \sin R_{cr}}{\sin(\Theta - \Theta_3)}\right) \qquad (2.4.7)$$

The logic for correction of throttle is given by:

$$\eta_c = \dot{\eta}(\text{nom})\left(1 - \frac{C_9(\delta t_s - \varepsilon_1)}{R_{cr}}\right), \text{ if } \delta t_s > \varepsilon_1 > 0 \qquad (2.4.8)$$

or $$\eta_c = \dot{\eta}(\text{nom})\left(1 + \frac{C_9(\delta t_s - \varepsilon_2)}{R_{cr}}\right), \text{ if } \delta t_s < \varepsilon_2 < 0$$

within the limits:

$$C_{10} \leq \eta_c < 1$$

The constants ε_1 and ε_2 set the threshold of stage time correction by course and speed control. Factors considered in setting the threshold are accuracy of prediction and the mode of rendezvous. If the rendezvous mode is by parking orbit, the threshold is in the neighborhood of one minute; if the rendezvous mode is direct ascent, the threshold is in the neighborhood of twenty seconds. The constants C_6 and $C_{}$ set nominal limits on the range of course changes allowed; the constant C_{10} limits the range of throttle control; and the constants $C_{}$ and $C_{}$ determine the relative weight of course and speed corrections when the commanded variations are above the thresholds and within the nominal limits.

Stage Time Control When $R_o \leq R_c$.

For short offset missions when $R_o \leq R_c$, the Stage 1 profile does not include a supersonic cruise phase of sufficient duration to employ the explicit method of prediction and control of stage conditions defined above. A form of implicit control is proposed for this case. Bank angle is controlled to constrain the trajectory to follow the nominal latitude-longitude profile; throttle is controlled to maintain the nominal time schedule within specified limits; and pitch is controlled -- as before -- to follow the nominal altitude velocity profile.

DIAGRAM OF COURSE CORRECTION IN COORDINATED TURN CLIMB AND ACCELERATION

FIGURE 2-9

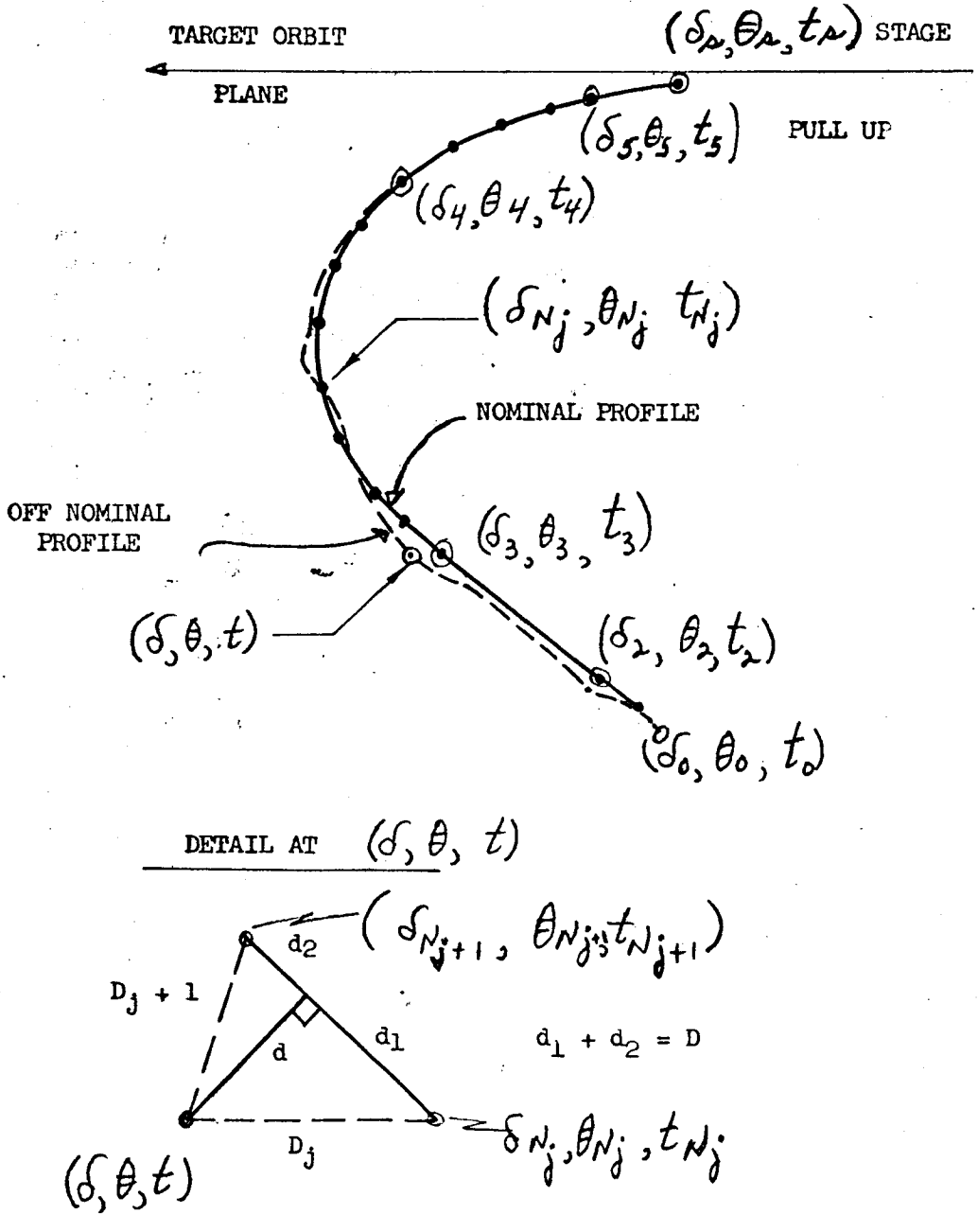

The problem geometry is illustrated in Figure 2-9. The nominal latitude-longitude-time profile is defined by a three argument table of points $(\delta_N, \Theta_N, t_N)$; recorded by the Nominal Profile Generator on the last iteration of NPG 2. The segment boundary conditions, which are part of this profile, are denoted by $(\delta_i, \Theta_i, t_i)$, $i = 1, 2, \ldots 6$. The present position of the vehicle in flight is denoted by (δ, Θ) without subscripts.

The equations on take-off and acceleration and climb to subsonic cruise conditions are identical with the nominal guidance equations. In cruise, the bank angle is controlled to steer the start turn point (δ_3, Θ_3) and throttle is varied from nominal within limits to arrive at (δ_3, Θ_3) at the nominal time t_3. Throttle control is given by:

$$\eta_c = \eta\,(\text{nom.})\,(1 + C_{11} \cdot \frac{(t = t_N))}{R_{cr}}) \qquad (2.4.9)$$

where $t_N - t = t_2 - \left[\frac{t - t_2}{t_3 - t_2}\right]\left[\frac{\delta - \delta_2}{\delta_3 - \delta_2}\right]$

to give a time correction that is a function of the cross-plane distance to go.

η_c is constrained within the limits:

$$C_{12} \leq \eta_c \leq C_{13}$$

The next phase of off-nominal control begins at (δ_3, Θ_3) and ends at (δ_4, Θ_4), which are the boundary conditions for the first phase of the coordinated climb, acceleration, and turn. The pitch control equations for this path segment are such that the nominal altitude-velocity profile is followed. The bank angle control equations are such that the nominal latitude-longitude profile is followed. Off-nominal conditions on the latitude-longitude profile are measured by the perpendicular and parallel distances of present position from the nominal profile. These off-nominal variations are corrected by bank angle and throttle commands. The steps to implement these commands follow.

Let the vehicle be at position (δ, Θ) at time t. The normalized distance on a unit sphere from (δ, Θ) to the ith point on the (δ_N, Θ_N) profile is given by:

$$D_i = \sqrt{(\delta - \delta_{N_i})^2 + ((\Theta - \Theta_{N_i}) \cos \delta_{N_i})^2} \qquad (2.4.10)$$

Neglecting the time variable, the cross track trajectory error is defined as the normal distance from (δ, Θ) to the nearest segment connecting two consecutive points of the nominal profile. The nearest segment is found by a simple search on D_i, selecting the two points with the smallest value of D_i. Let their subscripts be j and j + 1. The length of the segment defined by the two points is given by:

$$D = \sqrt{(\delta_{N_{j+1}} - \delta_{N_j})^2 + ((\Theta_{N_{j+1}} - \Theta_{N_j}) \cos \delta_{N_j})^2} \qquad (2.4.11)$$

The length of the normal distance from (δ , Θ) to the segment is given by:

$$d = D_j + \frac{(D_j^2 - D_{j+1}^2 - D^2)}{2D} \qquad (2.4.12)$$

The intercept of the normal and the segment divides the segment into two parts of length:

$$d_1 = \frac{D_j^2 - D_{j+1}^2 - D^2}{2D} \qquad (2.4.13)$$

and $d_2 = D - d_1$

The nominal time at the interior point of the segment is approximated by:

$$t_N = t_{Nj} + d_1 \frac{(t_{n_{j+1}} - t_{N_j})}{D} \qquad (2.4.14)$$

$$\delta t_s = t - t_n$$

The trajectory cross-track and time deviations from nominal at time t are equal respectively to d and (t - t_N). A weighted average of the d - deviations over a time period preceding time t yields an estimate of the rate of change in the deviations under the commanded control. The nominal bank angle control is perturbed in proportion to the cross-track error history as follows:

$$\phi_c = \phi_c \text{ (Nom)} + C_{13} \cdot d + C_{14} \dot{d} \qquad (2.4.15)$$

where $\dot{d}$ is the output of the d-averaging process.

Throttle control is given by:

$$\eta_c = \eta_c \text{ (nom)} \cdot \left(1 + \frac{C_{15}}{C_{16}(t_4 - t) + C_{17}}\right) \cdot (\delta t - \varepsilon_3), \text{ if} \qquad (2.4.16)$$

or $$\eta_c = \eta_c \text{ (nom)} \cdot \left(1 + \frac{C_{15}}{C_{16}(t_4 - t) + C_{17}}\right) (\delta t - \varepsilon_4), \text{ if}$$

η_c is constrained within the limits:

$$C_{18} \leq \eta_c \leq C_{19}$$

The constants ε_3 and ε_4 set the threshold for time corrections on the turn. The threshold magnitude is a function of the accuracy of prediction and control. Work to date indicates that it will be in the neighborhood of one minute. The constants C_{15}, C_{16} and C_{17} determine the response characteristics of the throttle control to the estimated error in time schedule. The equation given is of the simplest-first order- form, in which the constants will be selected to produce an over-damped system. The constants C_{18} and C_{19} set limits on the range of throttle control.

The control described above is terminated at the start of the second phase of the turn at (δ_4 , Θ_4 , t_4). From this point through staging the in-flight control equations are identical with the nominal equations defined for the Nominal Profile Generator. These equations are adaptive in seeking to follow a well-defined nominal cross-plane profile as well as the altitude-velocity profile.

FUEL MARGIN PREDICTION AND RENDEZVOUS MODE CONTROL

The nominal thresholds and limits imposed on Stage 1 course and throttle perturbations in Equations 2.4.5 and 2.4.16 leave a residual stage time deviation from nominal to be accounted for on the Stage 2 profile. This deviation and the predicted fuel margin at staging are the two independent variables in the logic for determining the rendezvous mode and for signalling abort conditions. The equations for predicting Stage 1 fuel margin are outlined first and then the logic for mode control is defined.

STAGE 1 FUEL MARGIN PREDICTION, SUPERSONIC CRUISE PHASE

The estimate of Stage 1 fuel margin at staging on the supersonic cruise phase is based on the current time prediction and on the profile of fuel weight flow as a function of throttle profile. The equations contain the following constants which are to be derived in preflight analysis:

C_{20} --nominal fuel weight flow on the supersonic cruise phase;

C_{21} --the deviation from nominal fuel weight flow with respect to throttle deviation from nominal for the supersonic cruise phase;

C_{22} --nominal fuel weight flow on the turn phase prior to the start of pullup;

C_{23} --nominal total fuel weight for the turn and pullup phase;

Let $E(t)$ and $E(\hat{t}_s)$ represent respectively the fuel weight remaining at present time t and at the predicted stage time t_s. $E(t)$ is given in flight by a fuel gauge reading and $E(\hat{t}_s)$ is the difference between the fuel gauge reading and the estimate of the fuel required on the remainder of the flight to the staging point. From Equation 2.4.1, the predicted time to the start turn position from time t is $R_{cr}/\eta_c S_{cr}$ and the deviation from nominal in the turn time is equal to $C_2(A-A_{nom})$. The fuel weight flow on the supersonic cruise phase under the throttle command η_c is equal to $C_{20} + C_{22}(\eta_c - \eta_{nom})$. Combining the product of fuel weight flow and time on the cruise, turn, and pullup phases, the estimate of fuel remaining at stage time is given by:

$$E(\hat{t}_s) = E(t) - \frac{R_{cr}}{\eta_c \cdot S_{cr}} \left[C_{20} + C_{21} (\eta_c - \eta_{nom}) \right] - C_{22} (A - A_{nom}) - C_{23}$$

STAGE 1 FUEL MARGIN PREDICTION ON THE COORDINATED TURN OF SHORT OFFSET MISSIONS

The fuel margin prediction on short offset missions is based on the fuel requirement on the nominal profile. The vehicle is constrained to follow the nominal latitude-longitude profile stored by the Nominal Profile Generator, as illustrated in Figure 2-9. With each point (δ_{Nj}, Θ_{Nj}, t_{Nj}) on the nominal profile, a fourth profile variable is recorded, namely ΔW_{Nj}, the nominal fuel weight expended from time t_{Nj} to the nominal stage time. Equation 2.4.14 gives the formula for the interpolated nominal time t_N corresponding to the present time t when the vehicle is at position (δ, Θ). The corresponding estimate of ΔW_N is found by interpolation in the table of fuel weights versus time, with t_N being the argument of the independent variable. The estimate of fuel margin at staging is then given by the difference between the present fuel gauge reading and ΔW_{Nj}:

$$E(t_s) = E(t) - \Delta W_{Nj}$$

The minimum allowable fuel margin at staging will be given by a tabular function of the distance from the stage point to the landing point. Let the value of this variable for the chosen landing site be represented by E_m. When $E(t_s) - E_m$ reaches a specified minimum, stage time control is suppressed for the remainder of the mission. On the short offset profile, this means that throttle is maintained at nominal. On the long range mission, throttle is maintained at nominal and the cruise heading is controlled to follow the current great circle course. These limits, imposed by the critical state of Stage 1 fuel margin, supercede the limits defined in Equations 2.4.8 and 2.4.16.

RENDEZVOUS MODE CONTROL

On long range missions, the nominal rendezvous mode is by direct ascent, with the nominal orbit to the start of the terminal phase being a near-Hohmann transfer. The guidance equations implemented for Stage 2 solve explicitly for the initial boost cut off conditions required to meet rendezvous conditions, and are therefore adaptive to off-nominal staging conditions. However, as stage time deviates from nominal, the Stage 2 fuel requirements increase. The constants ε_1 and ε_2 set the upper and lower bounds on stage time corresponding to the allowable Stage 2 fuel penalty for stage time. When the stage time deviation is greater than ε_1, that is, when stage time is too late for a direct ascent, the rendezvous mode is switched to the parking orbit mode. When the stage time deviation is less than ε_2, that is, when stage time is too early for a direct ascent, a secondary mode or an abort mode must be activated.

On short range missions, the nominal rendezvous mode is by parking orbit. The constants ε_3 and ε_4 set the lower and upper limits on stage time deviation for the nominal parking orbit attitude. The upper limit ε_4 is determined by the maximum allowable parking orbit time. When stage time deviation exceeds ε_4

a secondary or abort mode must be activated. The lower limit ε_3 is a function of the parking orbit altitude. When stage time deviation is less than ε_3, the rendezvous mode is switched to direct ascent or to a secondary mode.

Several forms of secondary modes may be specified within the framework of the guidance equations for the primary modes. The Stage 1 landing site may be changed to open the limits on Stage 1 course and speed control; the parking orbit altitude may be varied from the minimum altitude to altitudes above the target orbit altitude; or a secondary orbital mission not involving rendezvous may be executed.

2.4.2 STAGE 2 BOOST GUIDANCE EQUATIONS

Transfer to Parking Orbit

When the rendezvous profile includes a parking orbit, the Stage 2 boost profile is controlled to achieve boost cut off conditions for a near Hohmann transfer to the parking orbit altitude. The optimum boost cut off radius, r_{co}, and flight path angle, γ_{co}, are functions of ΔV_g to be derived in preflight analysis. The form for r_{co} is one of the variables defined by the Nominal Profile Generator, and γ_{co} is expected to be a linear function of ΔV_g as follows:

$$\gamma_{co} = C_{60} + C_{61} * \Delta V_g$$

The magnitude of the cut off velocity is an explicit function of r_{co}, γ_{co}, and the radius of the parking orbit r_a:

$$V_{co} = \sqrt{2\mu\left[\frac{r_a}{r_a + r_{co}}\right]}$$

An explicit solution for thrust axis control, based on a linear form of attitude versus time-to-cut-off, is proposed for Stage 2 guidance to the desired transfer orbit conditions. The equations are documented in Reference 1, and have been programmed in a simulation documented in Reference 2. This simulation was used to obtain the accuracy and payload penalty numbers reported in Section 2.5.

DIRECT ASCENT TRANSFER TO RENDEZVOUS

The equations for guiding Stage 2 to a specified cut off altitude and velocity vector must be modified to constrain time and position in the direct ascent rendezvous application. As they stand, time and down range angle are treated as free variables but they are calculated as part of the cut off condition prediction equations. A method of meeting the rendezvous time and position constraint is outlined in Figure 2-10. The system of equations defined in Reference 1 are utilized exactly as for injection into a parking orbit, with the exception that the injection flight path angle is perturbed instead of fixed. The perturbation is determined on each iteration as a function of the commanded boost cut off radius and velocity, the predicted boost cut off

FIGURE 2-10

BOOST GUIDANCE PROGRAM

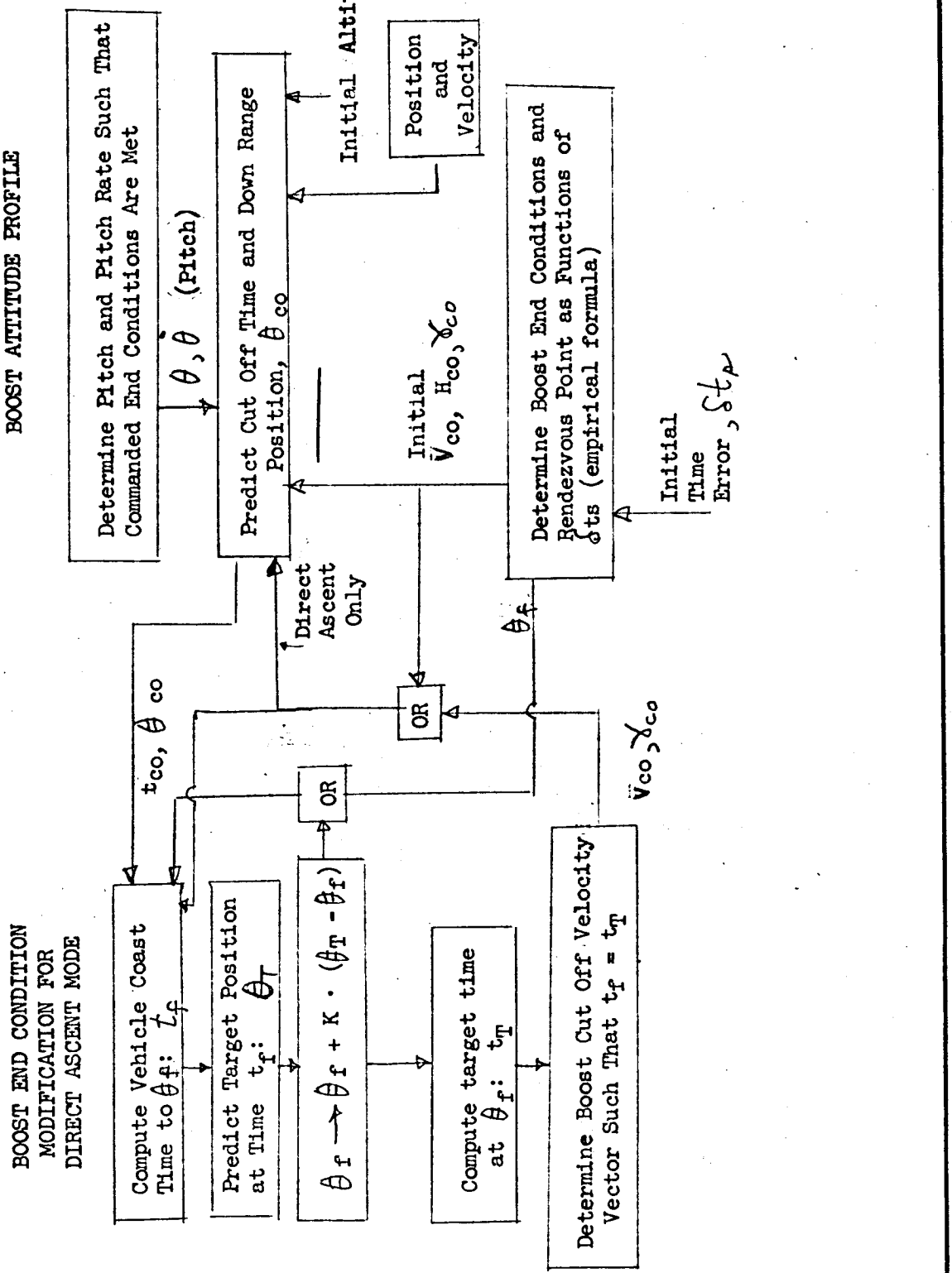

time and range angle, and of the commanded rendezvous position Θ_f. The rendezvous position is also varied within limits in seeking a solution for rendezvous conditions. The initial boost cut off conditions, including flight path angle, are determined as functions of ΔV_g using the same equations defined above for parking orbit injection. The computation steps on each iteration are:

(1) Predict boost cut off time and down range angle, using the current solution for the attitude profile. (Equations of reference 1).

(2) Solve for the attitude control parameters as a function of commanded boost cut off radius, velocity, flight path angle, and predicted boost cut off time. (Equations of reference 1)

(3) Compute vehicle coast time $\Delta t_{2,1}$ from boost cut off to Θ_f, using Lambert's equation. Predicted rendezvous time: $t_f = t + \Delta t_{2,1}$

(4) Predict target position at time t_f, Θ_T.

(5) Move the rendezvous point to reduce the angle between Θ_T and Θ_f: New Θ_f = Old $\Theta_f + K(\Theta_T - \Theta_f)$

(6) Compute target time at the new Θ_f.

(7) Correct boost cut off flight path angle differentially in proportion to the time difference $(t_T - t_f)$.

Repeat Steps (1) through (7) on the next computation cycle, using the updated values of flight path angle and attitude angle profile parameters.

The equations for coast time $\Delta t_{2,1}$ are an implementation of Lambert's equations, as follows:

$$l = V_{co}^2 \sin^2\gamma \cdot r_{co}^2$$ coast ellipse semilatus rectum

$$e = \frac{r - l}{r\cos(\theta_f - \theta_o)}$$ coast ellipse eccentricity

$$a = \frac{l}{1 - e^2}$$ coast ellipse semi-major axis

$$\Delta t_{2,1} = \sqrt{\frac{a^3}{\mu}} \left[\alpha - \sin\alpha - \beta + \sin\beta \right] \quad \text{if } \gamma > 0$$

$$\text{or } \Delta t_{2,1} = 2\pi \left(\sqrt{\frac{a^3}{\mu}} - 1 \right) \left[\alpha - \sin\alpha - \beta + \sin\beta \right] \quad \text{if } \gamma < 0$$

where

$$\alpha = 2 \arcsin \sqrt{\frac{r_{c0} + r_a + c}{4a}}$$

$$\beta = 2 \arcsin \sqrt{\frac{r_{c0} + r_a - c}{4a}}$$

$$c = \sqrt{r_{c0}^2 + r_a^2 - 2 r_{c0} r_a \cos(\theta_f - \theta_0)}$$

2.5 ESTIMATED PAYLOAD PENALTIES DUE TO GUIDANCE EFFECTS

Estimated payload penalties associated with off-nominal conditions are summarized in this section for the 3704 KM (2000 n.m.) offset mission. The Stage 1 and orbital guidance penalties were obtained analytically, while the Stage 2 boost penalties were obtained by combining simulation and analytical results.

The Stage 1 penalty estimates are based on the following assumptions:

- o the command altitude-velocity profile is accurately maintained without a significant fuel penalty in the presence of all off-nominal environmental and vehicle parameters;
- o continuous adjustment of vehicle course to maintain a fixed start-turn point after the supersonic cruise phase does not incur a significant fuel penalty in the presence of cross-track winds and thrust axis control errors.

Under the above assumptions, the penalty due to the off-nominal conditions on Stage 1 flight is completely identified with the penalty for overcoming time schedule errors. Thus the combination of all off-nominal conditions from take-off to the start of the cruise phase are represented by a time error. Open loop simulation runs were made to determine the sensitivity in time at the start of the supersonic cruise phase with respect to off-nominal environmental and vehicle parameters. These are summarized in Figure 2.5-1, Volume 3. The one-sigma time error due to each source error is the product of the sensitivity coefficient and the one sigma estimate of the dispersion in the source parameter. Assuming that the error sources are independent, the total time error at the start of cruise is equal to the root sum square of the one-sigma errors due to each source. Appendix A2 of Volume 3 gives the method of analysis by which the fuel penalty was computed for correction of time errors at the start of cruise by several methods of guidance, including that of cruise course adaption and speed control defined in Section 2.4 of this Volume. Table 2.5-1 of Volume 3 summarizes the results of that analysis. Information from that table is extracted in the summary which follows.

Finally, the explicit guidance system for Stage 2 boost was tested in a set of simulation runs to determine the sensitivity in payload penalty to initial condition errors and vehicle parameter uncertainties. The first run was with no errors in the initial conditions or vehicle parameters, but with an arbitrary constant thrust level equal to the maximum thrust level of the optimum profile described in Volume 2. The mass at boost cut off was the reference mass for the remaining mass penalty studies. The mass in orbit for the explicit guidance method was obtained by subtracting an analytically determined fuel weight for injection into orbit at rendezvous. The difference between this mass in orbit and that obtained on the optimum profile is negligible. The payload penalty, therefore, for non-ideal profile generation by the

explicit guidance technique is estimated to be negligible when the rendezvous mode is by direct ascent. When the rendezvous mode is by parking orbit, the penalty due to the use of the parking orbit mode is in the neighborhood of fifty pounds.

The payload penalties due to navigation system errors are also included in the summary which follows. The numbers are extracted from the analysis reported in Section 2.5 of Volume 3.

All of the material referred to above is summarized in Table 2-1 with the levels of environmental and vehicle parameter error sources set at their expected one-sigma level, and with the navigation system accuracy of both Stage 1 and Stage 2 at the medium high level. It is seen that the total estimated payload penalty for direct ascent is 90 KG (200 pounds) and for the parking orbit mode 93 KG (205 pounds).

Table 2-1 Payload Penalties Versus Rendezvous Mode For Three Sigma Dispersions

3704 KM (2000 N.M.) Offset Mission

Payload Penalty in kg (lbs.)

Off Nominal Condition	Direct Ascent		Parking Orbit	
	Each Source	RSS	Each Source	RSS
Stage 1				
One minute time error, start cruise	27 (60)	27 (60)	---	---
Stage 2 boost		34 (75)		32 (70)
Initial Conditions:				
±20 secs, stage time	11 (25)			
-190m (-620 ft), altitude	28 (62)		28 (62)	
-3m/sec (-10 FPS), velocity	11 (25)		9 (20)	
-3m/sec (-10 FPS), alt. rate	3 (11)		3 (11)	
Propulsion:				
±5% thrust	9 (20)		9 (20)	
±5% specific impulse	7 (16)		7 (16)	
Stage 2 Orbital				23 (50)
Non-ideal trajectory			23 (50)	
Terminal Rendezvous		32 (70)		36 (80)
±20 secs, stage time	23 (50)			
Navigation errors	23 (50)		36 (80)	
TOTAL RSS		93 (205)		91 (200)

2.6 COMPUTER REQUIREMENTS

The memory and computation speed requirements for implementing the guidance system outlined in section 2.4 are presented. The memory requirements are defined in terms of the number of instructions and the number of constants which must be stored. The speed requirements are defined by the peak load computation relative to allowable computation time interval. The estimates are based on detailed programming work performed on a number of projects, including Dynasoar vehicle computer work, the Saturn V Launch Vehicle Guidance and Navigation functional description, and computer studies for the AGM-69 program.

The computation functions involved in the Stage 1 guidance equations are listed in Table 2-2 with the estimated number of instructions and constants for each function. The navigation system computations are included. They constitute about 17% of the total number of 12500 instructions and constants. Given a six-bit operation code --- 64 basic instructions --, a three-bit address index and instruction modifier code, a 14-bit address code, and one parity bit, the instruction word size is 24 bits. Allowing 2000 24-bit data words for scratch pad memory and 1500 words for estimate error, the total memory consists of 16000 24-bit words.

The maximum computation speed requirement on Stage 1 occurs in the real-time in-flight integration of the acceleration data on the acceleration phases of flight. The acceleration components are integrated by summing increments of velocity over very small periods of time, so the computation speed requirement is a function of acceleration magnitude. Since the acceleration on Stage 1 flight is less than on typical booster flights, and the guidance functions are of no more complex form, it is concluded that state of the art computers designed for space boosters will meet the requirements for Stage 1 in-flight computations. The add and multiplication times are in the neighborhood of 12 μs and 50 μs, respectively, which may be classified as of medium speed in the state of the art. The preflight Stage 1 flight simulation equations are of a more complex form than the in-flight navigation equations, but the computation speed requirement is not higher. It is estimated that the simulation of the 2000 n.m. flight will take less than five minutes on a medium speed computer. Profile generation will require nominally two iterations, but never more than three, bringing the maximum time for final profile generation to fifteen minutes. The approximate profile, sufficient for the early part of the count-down, will be obtained in less than one minute. Since the minimum lead time for each launch opportunity is 1.5 hours -- the time between launch opportunities -- it is concluded that a medium speed computer will meet the Stage 1 requirements.

The computation functions for Stage 2 navigation and guidance are listed in Table 2-3, with estimates of the number of instructions. A medium speed computer -- 12 μs add and 50 μs multiplication times -- meets the Stage 2 computer requirements.

TABLE 2-2

STAGE 1 COMPUTER FUNCTIONS AND
ESTIMATED NUMBER OF INSTRUCTIONS

Function	Estimated Number of Instructions
Executive Program	500
Arithmetic Subroutines	400
Computer Loading	150
Telemetry Input-Output	300
System Checkout*	1300
Inertial Navigation System Equations	
Pre-process of Accelerometer & Gyro Data	200
Integrate Acceleration Equations to Obtain Position and Velocity	500
Update Inertial System With Optimal Filter Of Observations (Omega and/or Nav Sat)	1500
Navigation Updating System	
Omega or Navigation Satellite	1800
Nominal Profile Generator	
Executive Routine (Includes Iteration Control)	500
Approx. Stage 1 & Stage 2 Boundary Conditions (NPG1)	750
Nominal Stage 1 Guidance Equations	800
Simulate Total Acceleration Vector**	800
Integrate Equations of Motion	500
Coordinate Conversion	200
Data Recorder	100
Control Tables & Constants	800
In-Flight Guidance Equations* **	
Supersonic Cruise	200
Coordinated Turn-Climb	300
Fuel Margin Estimation & Rendezvous Mode Control	200

TABLE 2-2 (Continued)

STAGE 1 COMPUTER FUNCTIONS AND
ESTIMATED NUMBER OF INSTRUCTIONS

Function	ESTIMATED NUMBER OF INSTRUCTIONS
Prelaunch Second Stage Checkout & Range Safety	200
Recovery and Return to Base	200
Pilot Displays and Controls	500
TOTAL	12,500

* Portions of this are utilized for in-flight system checkout
** Includes thrust and air density tables
*** In addition to the nominal guidance equations

TABLE 2-3

STAGE 2 COMPUTATION FUNCTIONS

FUNCTIONS	ESTIMATED NO. OF INSTRUCTIONS
Executive Program	300
Arithmetic Subroutines	300
Computer Loading	100
System Checkout	600
Inflight Checks	200
Navigation System	
Inertial Navigation	800
Platform Alignment	300
Target Prediction	500
Explicit Boost Guidance to V,h,γ Conditions	1000
Explicit Orbital Prediction	
Time Prediction	500
Time Pred. Applied in Boost Guidance for Rendezvous	300
Time Prediction Applied in Orbital Guidance	300
Terminal Guidance	800
Constants	100
TOTAL	6100

2.7 Development of Detailed Equations for the Nominal Profile Generator

2.7.1 Introduction

A system of profile generating equations is defined for preflight construction of the flight profile to the rendezvous point with a specified target in orbit. The nominal profile generator (NPG) consists of a two-phase process. The first phase, designated NPG-1, produces an approximate solution with end condition errors in the order of ± 20 N.M. The second phase, designated NPG 2, reduces the end condition errors to ± 1 N.M.

Two coordinate systems are employed in the equations: the conventional Earth-relative system with geographic latitude and longitude (λ, Γ) respectively, and the inertial system (XYZ) shown in Figure 2-11. The Z axis is directed along the vertical vector at the predicted position of Stage 2 boost cut off. The X and Y axes are directed along the horizontal vectors in and normal to the target orbit plane at the position of boost cut off. The geographic coordinates relative to the target plane are represented by (δ, θ) with the longitude (θ) measured in the target orbit plane from the ascending node (Λ), and with latitude (δ) measured from the orbital plane.

The transformation from (λ, Γ) geographic coordinates to (δ, θ) orbital plane coordinates is given by:

$$\delta = \arcsin \left[\sin (I + \beta) - \sin \alpha \right] \qquad 2.7.1$$

$$\theta = \arccos \left[\frac{\cos \alpha}{\cos \delta} \right]$$

where,

$$\alpha = \arccos \left[\cos \lambda \cos (\Lambda - \Gamma) \right]$$

$$\beta = \arcsin \left[\frac{\sin \lambda}{\sin \alpha} \right]$$

2.7.2 The Nominal Flight Profile Generator Initial Mode (NPG-1)

The system of equations for generating the approximate nominal flight profile for rendezvous with a specified target is defined. The nomenclature involved is summarized in Table 2-4.

The principal features of NPG-1 are:

- The Stage 1 profile is divided into segments which are represented by arcs on a non-rotating Earth. The segment boundary conditions and arc lengths are approximated by empirical functions of the great circle distance from the base to the

FIGURE 2-11

TARGET PLANE ORIENTED COORDINATE SYSTEM

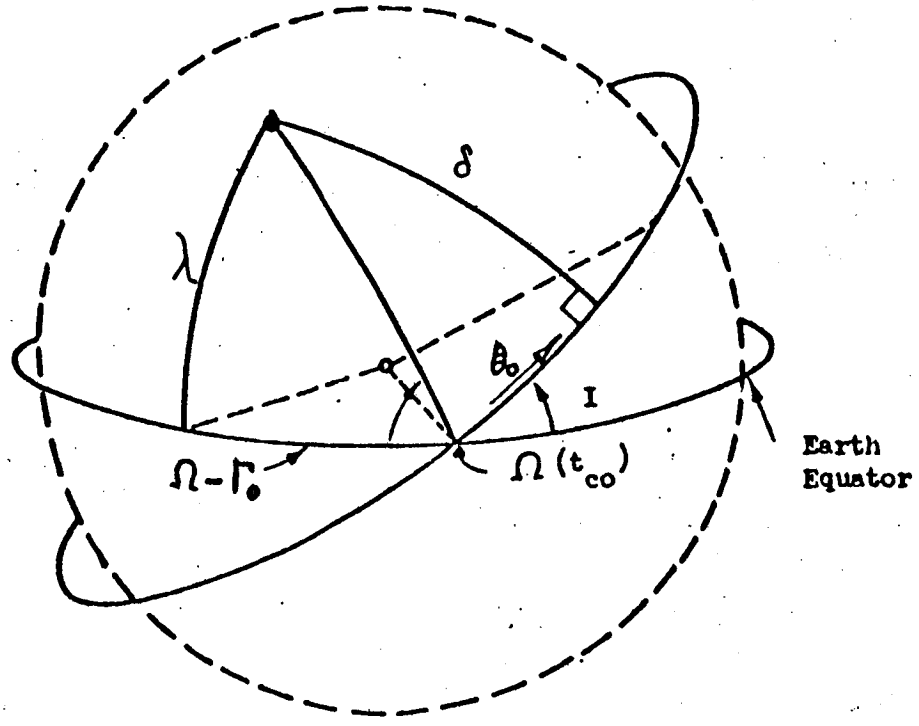

λ	CONVENTIONAL GEOGRAPHIC LATITUDE
Γ	CONVENTIONAL GEOGRAPHIC LONGITUDE
$\Omega\ (t_{co})$	TARGET ORBIT PLANE ASCENDING NODE
I	TARGET ORBIT PLANE INCLINATION
δ	LATITUDE RELATIVE TO TARGET ORBIT PLANE
θ	LONGITUDE IN TARGET ORBIT PLANE

TABLE 2-4 NOMENCLATURE FOR NPG 1 GEOMETRIC REPRESENTATION OF PROFILE

δ_i, Θ_i, t_i	position and time of ith Stage 1 segment end point in spherical coordinates relative to the target plane
$\Delta\Theta_{2,i}$	Stage 2 orbital segment arcs
$\Delta t_{2,i}$	time on orbital arcs
$\Delta\Theta_B$	Stage 2 boost arc
$\Theta_s = \Theta_6$	longitude of stage position in orbit plane (measured from node)
$\delta_s = \delta_6$	latitude of stage position from orbitplane
Θ_f, t_f	predicted rendezvous point
t_T	target time at Θ_f
w_e, V_e	Earth rotation rate and easterly horizontal velocity at equator
μ	Earth gravitational constant
r_p	radius vector of circular parking orbit
a	semi-major axis
e	eccentricity
w	argument of perigee
I	inclination
Ω	ascending node
t_p	time at perigee
r_p, ra	radius vector at perigee and apogee

Target Parameters

target orbit plane, R_o. These functions are obtained by the process of fitting curves to profile data generated in preflight simulation, as illustrated in paragraph 2.3.

- The Stage 2 boost segment boundary conditions are approximated by empirical functions of the variation in inertial velocity-to-be-gained ΔV_g on the boost phase. These boundary conditions also are obtained by the process of fitting curves to profile data generated in preflight simulation.

- The orbital profile segments are obtained explicitly by the formulae of Keplerian orbit mechanics.

The overall process of NPG-1 is iterative, starting with an estimate of Stage 2 boost cut off time, t_{co}. The computations on each iteration consist of the following set of consecutive operations:

(1) Determine the position of the orbital plane at estimated time t_{co}.

(2) Determine the polar coordinates of the base location in the δ, θ system. The offset distance, R_o, is equal to base latitude in the system.

(3) Select the rendezvous mode, with selection depending upon the magnitude of R_o and eccentricity of the target orbit. Determine the central angle and time increments of Stage 2 orbital segments for the mode selected.

(4) Determine the variation, ΔV_g, of inertial velocity at Stage 2 boost cut off from a reference cut off velocity. Determine the Stage 2 boost segment cut off altitude, central angle, and time increments as functions of the velocity-to-be gained variations, ΔV_g.

(5) Determine the stage position coordinates, δ_s and Θ_s as functions of the parameters R_o and ΔV_g.

(6) Combine the segment arc and time increments obtained in 3,4, and 5 with the current estimate of boost cut off time, t_{co}, to obtain the estimate of rendezvous position Θ_f and time t_f and stage time t_s.

(7) Determine the time t_T at which the target arrives at the predicted rendezvous position, Θ_f. The new estimates of Stage 2 boost cut off and stage time are:

$$t_{co} = \text{OLD } t_{co} + K_T (t_T - t_f)$$

$$t_s = \text{OLD } t_s + K_T (t_T - t_f)$$

(8) Determine the segment arc and time increments on Stage 1 from take off to the start of subsonic or supersonic cruise.

(9) Determine the segment arc and time increments on Stage 1 from the stage point backward to the end of the cruise phase.

(10) Determine the time interval on the cruise arc defined by the end points obtained on 8 and 9.

(11) Add the Stage 1 segment time intervals obtained in 8, 9, and 10 and subtract from stage time to obtain take off time, t_o.

The process defined by operations 1 through 11 is iterated until convergence criteria are met on $(t_T - t_f)$. The equations for each of the operations follow.

NPG-1 Equations

(1) Target Orbit Plane Position at Time t_{co}.

The location of the target orbit plane is the first step in defining a specific mission profile. To predict the location of the plane, the effect of orbit perturbations must be considered. The ascending node of the target orbit plane at the last orbit parameter update time t_o', is computed from the orbit parameter input data. The node precesses at a rate which is a function of the semi-major axis (a), eccentricity (e), and inclination (I) of the orbit. Letting it be represented by f_1, the position of the node at time t_{co} is:

$$\Lambda(t_{co}) = \Lambda(t_o')-W_e(t_{co}-t_o') + f_1(t_{co}-t_o', a, e, I)$$

where W_e is Earth rotation rate.

(2) The Parameter R_o.

The target plane offset distance from the base, R_o, is equal to latitude of the base in the target-oriented coordinate system. The longitude of the base in this system is also required in later equations. These coordinates are obtained by substituting the base geographic coordinates, λ_o and Γ_o in the Equation 2.7.1.

(3) Rendezvous Mode Selection and Orbital Segments

The profile generator automatically selects one of three possible rendezvous modes depending on the value of R_o and the target orbit eccentricity e. The criteria for switching between modes are formulated during the preflight mission planning. The objective of alternate modes is to minimize fuel penalties for the specific flight conditions of the mission. The three modes or cases are:

Case 1: circular target orbit and $R_o > R_c$: the nominal rendezvous mode is by direct ascent.

Case 2: circular target orbit and $R_o \leq R_c$: the nominal rendezvous mode is by parking orbit.

Case 3: eccentric target orbit: the nominal rendezvous mode is via a two-phase parking orbit.

The offset distance R_c at which mode is switched from parking orbit to direct ascent is to be determined by study of payload penalties versus off-nominal conditions accumulated during the take off and accelerations phases of the mission. It is expected that for long range missions, adjustment in course and speed on the cruise phase will compensate effectively for off-nominal conditions accumulated during the take-off and accelerations phase of the mission. For short range missions on which the cruise range is limited, the parking orbit is used to compensate for off-nominal conditions.

The segments of the stage 2 orbital elements are now constructed from the rendezvous point in steps back to the staging point. When the staging point is defined later, the position of rendezvous and the time of arrival of the launch vehicle at that point are calculated by joining the orbital profile to the stage 1 profile at the stage point. The stage 2 orbital phase profile segments may have up to four arcs characterized by central angle increments $\Delta\theta_{2,i}$ and time increments $\Delta t_{2,i}$ ($i = 1,..,4$). These orbital arcs are defined for the three rendezvous mode cases as follows:

Case 1, Direct Ascent

$$\left.\begin{aligned} \Delta\theta_{2,i} &= 180^\circ. + g_1(r_a) \\ \Delta t_{2,i} &= \frac{\pi}{\sqrt{\mu}}\left(\frac{r_a + r_{co}}{2}\right)^{3/2} + g_2(r_a) \end{aligned}\right\} \quad 2.7.2$$

$$\left.\begin{aligned} \Delta\theta_{2,i} &= 0 \\ \Delta t_{2,i} &= 0 \end{aligned}\right\} \; i = 2,3,4$$

μ is the Earth's gravitational constant, r_a is the target orbit radius from the center of the Earth, and r_{co} is the radius of position at Stage 2 boost cut off. In general, the value r_{co} is a function of specific mission conditions and is one of the variables

determined by iteration. A later equation of the NPG-1 process produces the new value on each iteration. The initial value is that for a nominal mission. Case 1 implements a near Hohmann transfer directly to the target orbit from boost cut off. $g_1(r_a)$ and $g_2(r_a)$ define the slight variation from a Hohmann transfer due to drag.

Case 2: Single-Phase Parking Orbit

$$\Delta\Theta_{2,1} = 180^\circ + g_1(r_a)$$

$$\Delta t_{2,1} = \frac{\pi}{\sqrt{\mu}}\left(\frac{r_p + r_{co}}{2}\right)^{3/2} + g_2(r_a) \qquad 2.7.3$$

r_p is the radius of the circular parking orbit. Case 2 implements a Hohmann transfer to parking orbit altitude from boost cut off.

$\Delta\Theta_{2,2} = \Delta\Theta_{P\ nom}$ --coast angle in the parking orbit.

$\Delta\Theta_{P_1 nom}$ is selected by study of the expected value of off-nominal stage times.

$$\Delta t_{2,2} = \frac{\Delta\Theta_{P\ nom}}{180^\circ} \cdot \frac{\pi}{\sqrt{\mu}}\left(r_p\right)^{3/2} \qquad 2.7.4$$

$$\Delta\Theta_{2,3} = 180^\circ$$

$$\Delta t_{2,3} = \frac{\pi}{\sqrt{\mu}}\left(\frac{r_T + r_p}{2}\right)^{3/2}$$

$\Delta\Theta_{2,3}$ is the arc of the Hohmann transfer from the parking orbit to the target altitude.

$$\Delta\Theta_{2,4} = 0 \quad ; \quad \Delta t_{2,4} = 0 \qquad 2.7.5$$

Case 3: Eccentric target orbits, rendezvous by a two-phase parking orbit.

$$\Delta\Theta_{2,1} = 180^\circ + g_1(r_a)$$

$$\Delta t_{2,1} = \frac{\pi}{\sqrt{\mu}}\left(\frac{r_p + r_{co}}{2}\right)^{3/2} + g_2(r_a) \qquad 2.7.6$$

$\Delta\Theta_{2,1}$ is the arc of a Hohmann transfer to the initial parking orbit.

$$\Delta\Theta_{2,2} = W + 180^\circ - (\Theta_s + \Delta\Theta_B + \Delta\Theta_{2,1})$$

$$\Delta t_{2,2} = \frac{\pi}{\sqrt{\mu}} (r_p)^{3/2}$$

$\Delta\Theta_{2,2}$ is the coast arc in the parking orbit. It is terminated at the crossing of the line through target apogee. W is the angle of perigee of the target orbit relative to the line of nodes. Θ_s and $\Delta\Theta_B$ are segment parameters determined by later equations of NPG-1. The initial value of Θ_s is Θ_0, the longitude of the base in the XYZ system. The initial value of $\Delta\Theta_B$ is the boost angle for a nominal mission.

$$\Delta\Theta_{2,3} = 180^\circ$$

$$\Delta t_{2,3} = \frac{\pi}{\sqrt{\mu}} \left(\frac{r_p + r_p}{2} \right)^{3/2} \qquad 2.7.7$$

$\Delta\Theta_{2,3}$ is the arc of the Hohmann transfer from the parking orbit altitude to target orbit perigee altitude.

$$\Delta\Theta_{2,4} = 180^\circ$$

$$\Delta t_{2,4} = \frac{\pi}{\sqrt{\mu}} (r_p + r_a)^{3/2} \qquad 2.7.8$$

$\Delta\Theta_{2,4}$ is the arc of the Hohmann transfer from target perigee altitude to apogee altitude.

(4) The Stage 2 Boost Phase Parameters

The approximate Stage 2 flight profile is completed by determining the central angle increment $\Delta\Theta_B$ from staging to injection into the transfer orbit, and the associated time increment Δt_B, and the radius at transfer injection cut-off, r_{co}.

These parameters--$\Delta\Theta_B$, Δt_B, r_{co} -- are functions of the inertial velocity-to-be-gained during the Stage 2 boost phase. The velocity-to-be-gained depends on the target orbit inclination and the latitude at staging (the component of Earth's rotation) and also on r', the radius of apogee of the transfer ellipse.

$r' = r_T$, the target orbit radius, for case 1;

$r' = r_P$, the parking orbit radius, for cases 2 and 3.

The variation ΔV_g in the velocity-to-be-gained from a reference cutoff velocity $V_{co}(ref)$ and from the reference component of Earth's rotation rate $V_s(ref)$ is:

$$\Delta V_g = \left[V_{co} - V_{co}(ref)\right] - \left[V_s - V_s(ref)\right]$$

$$= \sqrt{\frac{2}{r_{co}} - \frac{2}{r_{co}+r1}} - V_{co}(ref) \qquad 2.7.9$$

$$- \left[V_e (\cos \lambda_a \cos I) - V_e (\cos \lambda_R \cos I_R)\right]$$

λ_a is the latitude of the staging point, I the inclination of the target orbit, V_e the easterly horizontal velocity at the equator due to the Earth's rotation, and (λ_R, I_R) are latitude and inclination at a reference staging point.

The parameters describing the second stage boost are now given as functions of the variation in the velocity-to-be-gained. The cut-off radius, r_{co}, is assumed to be quadratic function of ΔV_g:

$$r_{co} = r_{co}(ref) + c_1 + c_2 \Delta V_g + c_3 (\Delta V_g)^2 \qquad 2.7.10$$

The time variation during this segment is assumed to be a linear form plus an exponential in ΔV_g. The exponential term accounts for the substantial part of the excess velocity that will be achieved during the final seconds before boost cut-off.

$$\Delta t_B = \Delta t_B(ref) + c_4 \cdot \Delta V_g + c_5 e^{-c_6 \Delta V_g} + c_7 \qquad 2.7.11$$

The variation in central angle is derived explicity from the variation in Δt_B,

$$\Delta \Theta_B = \Delta \Theta_B(ref) + \frac{1}{c_8} (c_9 + c_8 \cdot \Delta t_B) \ln(c_9 + c_8 \Delta t_B) + c_{10} \qquad 2.7.12$$

The c_i in the above equations are constants that are to be determined to produce the best fit of these functional forms to the end conditions obtained by trajectory optimization.

Step (4) completes the construction of the stage 2 flight segments. The stage point parameters are now defined by step (5). The orbital segments are then added to the stage point parameters, to obtain the estimated rendezvous position and time.

(5) The Stage Point Parameters

The position of staging relative to the target orbit plane is primarily a function of offset distance R_o. An empirical function of R_o will be developed which best fits the data produced by optimization. For fixed values of geographic latitude at staging, target orbit inclination, and transfer orbit apogee, the stage point coordinates will be given by as yet undefined empirical functions of R_o:

$$\Theta_s = \Theta_o + G_2(R_o)$$
$$\delta_s = G_3(R_o) \qquad 2.7.13$$

The optimum stage point will also be effected in some degree by the variation in magnitude of velocity-to-be-gained, ΔV_g. Assuming that the variations with respect to R_o and ΔV_g are not correlated, the stage point coordinates are given by functions of the following form:

$$\Theta_s = \Theta_o + G_2(R_o) + G_4(\Delta V_g)$$
$$\delta_s = G_3(R_o) + G_5(\Delta V_g) \qquad 2.7.14$$

If the variations are significantly correlated, the best empirical form has to be found by experimentation.

(6) The Predicted Rendezvous Location and Time

The arc increments, $\Delta\Theta$, obtained in (3) and (4) are now added to the stage point coordinate Θ_s to obtain the predicted location of rendezvous:

$$\Theta_f = \Theta_s + \Delta\Theta_B + \sum_{i=1}^{4}\Delta\Theta_{2,i} \qquad 2.7.15$$

The orbital arc time increments defined in Equations 2 through 12 are added to the current estimate of t_{co} to obtain the predicted rendezvous time. The Stage 2 boost time increment obtained in (4) is subtracted from t_{co} to obtain stage time:

$$t_f = t_{co} + \sum_{i=1}^{4}\Delta t_{2,i}$$
$$t_s = t_{co} - \Delta t_B \qquad 2.7.16$$

(7) Target Position and Time Prediction and Time Error Signal

The target orbit parameters given with the most recent update include, t_o', at some perigee crossing before time t_f. The time at the perigee crossing, t_p, just prior to time t_f is obtained by adding a multiple of the orbit period to time t_o', with a correction for the precession of line of apsides in the interval $(t_p - t_o')$. The rate of precession is a function of target orbit semimajor axis, eccentricity, and inclination. Let the approximation be represented by the function f_2. Then:

$$t_p = t_o' + \frac{m \cdot 2\pi a^{3/2}}{\sqrt{\mu}} + f_2 (t_p - t_o', I, a, e) \qquad 2.7.17$$

The integer m is chosen so that $t_p \leq t_f$.

If the target orbit is circular, the function $f_2 = o$, and the perigee axis is set arbitrarily at the node so that target is at the node at time t_p. Since the reference for longitude is also at the node, the remainder of the target prediction is through the angle Θ_f:

$$t_T = t_p + \frac{\pi}{\sqrt{\mu}} \cdot \frac{\Theta_f}{180^\circ} a^{3/2} \qquad 2.7.18$$

If the target orbit is eccentric, the target reference time, t_p, is now at the argument of perigee W, measured from the node. The true anomaly of the rendezvous position is therefore $\Theta_f - W$. The target time at Θ_f is given by Kepler's equation:

$$t_T = t_p + \frac{a^{3/2}}{\sqrt{\mu}} (E - e \sin E), \text{ if } \sin (\Theta_f - W) \geq 0 \qquad 2.7.19$$

$$\text{or } t_T = t_p + (2\pi - 1) \frac{a^{3/2}}{\sqrt{\mu}} (E - e \sin E), \text{ if } \sin (\Theta_f - W) \leq 0$$

where E is the eccentric anomaly given by:

$$E = \arccos \left[\frac{1 - e \cos (\Theta_f - W)}{1 + e \cos (\Theta_f - W)} \right] \qquad 2.7.20$$

The time error signal for correction of boost cut off and stage time on the next ieration is $(t_T - t_f)$.

(8) Stage 1 Segment Intervals from Take Off to Start of Cruise

The profile from time (t_o) to the start of cruise consists of two segments: take off and the climb and acceleration to the start of the cruise phase. The take off segment includes the turn from the specified heading (AZ_o) to the desired initial cruise heading AZ_1. Cruise heading is an empirical function $G_1(R_o)$, to be defined by the optimization work. Estimates of several points on the curve, G_1, were obtained on the Phase I study. In the model of flight profiles defined in Reference 1, AZ_1 varies from -103° to -13° from the heading normal to the orbit plane.

The take off segment end conditions depend on AZ_1 and the specified take off heading AZ_o. Assuming that a take-off climb of fixed duration at heading AZ_o is followed be a turn through the heading angle $(AZ_o - AZ_1)$, the following formulae yield an approximation of the segment parameters.

$$\Delta\Theta_1 = d_1 \cos(AZ_o) + d_2 \cos(AZ_o - AZ_1)$$

$$\Delta\delta_1 = d_1 \sin(AZ_o) + d_2 \sin(AZ_o - AZ_1) \qquad 2.7.21$$

$$\Delta t_1 = d_3 + d_4 (AZ_o - AZ_1)$$

where $\Delta\Theta_1, \Delta\delta_1$ are the change in latitude and longitude from the take off point. The coordinate system is the [illegible] system with longitude measured in the reference orbital plane and latitude measured from the orbital plane. The constants d_i are selected to produce a good fit of the functions to the simulated vehicle paths on the takeoff phase over the range of the parameter $(AZ_o - AZ_1)$.

The take off phase is followed by an acceleration and climb to subsonic or supersonic cruise conditions. This segment consists of an arc (D) along the great circle defined by the heading (AZ_1) at (Θ_1, δ_1). The arc D is a specified constant for each type of cruise (subsonic or supersonic) selected by study of preflight simulation work. The arc and time intervals are obtained by application of spherical geometry formulas.

$$\Delta\Theta_2 = \arcsin\left[\frac{\sin D \sin AZ_1}{(\cos\delta_1 \cos D - \sin\delta_1 \sin D \cos AZ_1)}\right]$$

$$\delta_2 = \arccos\left[\frac{\sin D \sin AZ_1}{\sin(\Theta_2 - \Theta_1)}\right] \qquad 2.7.22$$

With the take off and climb acceleration phases defined the next step is to work backwards from the staging point for the turn into the orbital plane and stage 1 pull-up maneuvers. Then the end point of the climb-acceleration and the start point of the turn-pull up define the length of the outbound stage 1 cruise segment.

(9) Stage I Segment Intervals from Stage Point Backward to Cruise End Point

There are three control segments from the end of cruise to staging. In NPG-1, however, they are treated as one segment, with the parameters given by empirical functions of R_o. These functions, again, are obtained by finding the best form which fits data produced in preflight simulation. Let the great circle arc and time intervals be represented by the following:

$$\Delta\Theta_{sc} = G_6(R_o)$$

$$\Delta\delta_{sc} = G_7(R_o) + G_8(\Delta V_g) \qquad 2.7.23$$

$$\Delta t_{sc} = G_9(R_o) + G_{10}(\Delta V_g)$$

The cruise end point coordinates are then:

$$\Theta_3 = \Theta_s - \Delta\Theta_{sc}$$

$$\delta_3 = \delta_s - \Delta\delta_{sc}$$

(10) Time Interval on the Cruise Phase

The length of the great circle arc connecting the cruise end points obtained in 9 and 10 is derived from spherical geometry:

$$\hat{R}_{cr} = \arccos\left[\cos\delta_1 \cos\delta_2 \cos(\Theta_1 - \Theta_2) + \sin\delta_1 \sin\delta_2\right] \qquad 2.7.24$$

The cruise time is given by

$$\Delta t_3 = \hat{R}_{cr}/S$$

Where S is average ground speed on the cruise phase.

(11) Take Off Time

Finally, take-off time is obtained by subtracting the Stage I segment time intervals from stage time obtained in 7:

$$t_o = t_s - (\Delta t_1 + \Delta t_2 + \Delta t_3 + \Delta t_{sc}) \qquad 2.7.25$$

Iteration

Steps (1) through (9) are repeated until the time t_f that the payload arrives at the rendezvous point is equal to the time t_T that the target arrives there. The outputs of these steps define the boundary conditions at the start and end of each path segment. These boundary conditions are the inputs to the path simulation mode of the nominal profile generator.

2.7.3 The Nominal Flight Profile Generator, Phase 2: NPG 2

The next phase of the nominal profile generator, called NPG 2, carries out the detailed construction of the flight profile for each segment including the construction of the guidance constants and tables necessary to fly the path.

2.7.3.1 Outline of NPG 2

NPG 1 produces an estimate of flight segment boundary conditions without defining in detail the profile to be flown. This task is accomplished by NPG 2 in an iterative process. On the first iteration, the constants required by the guidance system to fly the desired profiles are computed as functions of the NPG 1 estimate of R_O and ΔV_g, and the flight is simulated from take-off through staging. Then the simulated Stage 1 turn and pull-up profile is analyzed to determine the cross plane profile deviation from a desired nominal. R_O is the independent parameter which determines the shape of the cross plane profile; it is corrected in proportion to the observed cross plane deviation from the desired nominal. Rendezvous position and time are predicted from the simulated stage point, and take off time is corrected to null the error in position relative to the target. Then the process is repeated, starting with calculation of the guidance constants as functions of the new R_O and ΔV_g. Iteration continues until convergence criteria on R_O and take-off time are met. An outline of NPG 2 is shown in Figure 2-12. The sequence of operations in further detail follows:

(1) Construct the Stage 1 guidance control tables as functions of R_O and ΔV_g. These include the nominal h-V, bank angle, and throttle profiles for each segment; the guidance mode switching conditions for each segment; and the cross-plane position profile on the final phase of the turn prior to pull-up.

(2) Simulate Stage 1 flight from take off through staging under control of the nominal guidance equations. The principal computational blocks of the simulation program are:

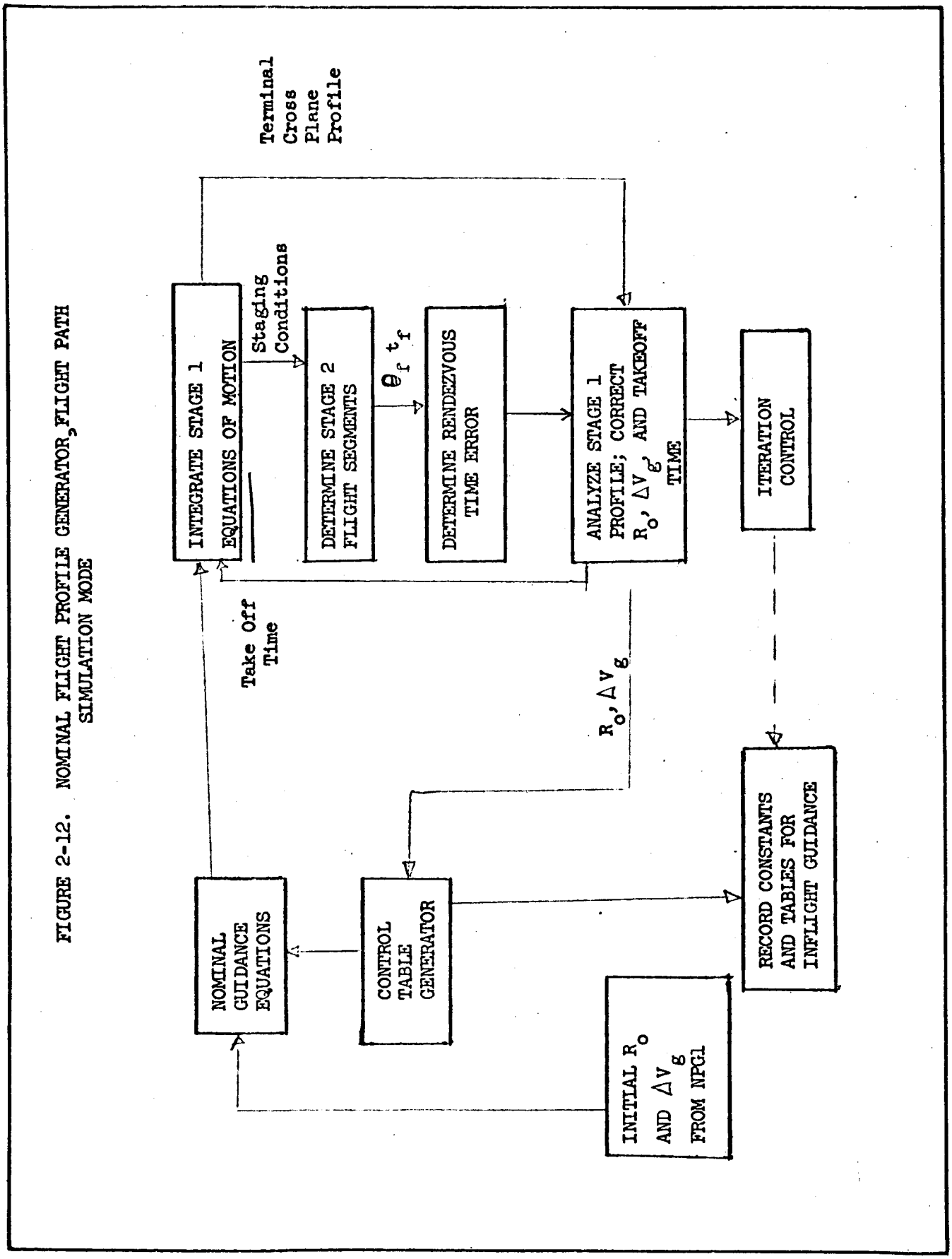

FIGURE 2-12. NOMINAL FLIGHT PROFILE GENERATOR, FLIGHT PATH SIMULATION MODE

- The Nominal Guidance Equations which produce angle of attack, bank angle, and throttle commands using the control functions generated in (1).
- The Flight Path Simulator which integrates the acceleration vector to produce position and velocity versus time.
- The Coordinate Converter which produces state vector components relative to the target orbit parameters as required in the guidance equations.
- The Data Recorder which saves simulated data for control of the next pass and for analysis of the profile after completion of each pass.

(3) Determine Stage 2 boost end conditions and orbital profile, obtaining rendezvous position and time (Θ_f, t_f) and the value of ΔV_g.

(4) Determine the time t_T at which the target arrives at Θ_f. Correct boost cut off, stage, and take off times, adding the term $K_T(t_T - t_f)$.

(5) Determine target plane position at new boost cut off time. Determine new value of R_O. Let ΔR_O = new R_O - Old R_O.

(6) Find the integral of the difference between the simulated cross plane position and the desired nominal as contructed in (1). Let $\Delta R_O'$ be an R_O correction term proportional to the integral:

$$\Delta R_O' = K_R' \left(\int_{t4}^{t5} (Y - Y_N) dt \right)$$

(7) Combine the results of (5) and (6) to correct R_O for the next iteration:

$$R_O = \text{OLD } R_O + \Delta R_O' - \Delta R_O$$

(8) Repeat operations (1) - (7) using the new values of R_O, ΔV_g and take off time. Iteration continues until convergence criteria on R_O and $(t_T - t_f)$ are met.

The equations for each NPG 2 operation are summarized in the following paragraphs.

2.7.3.2 The Control Table Generator Equations

The inflight guidance equations have a number of constants whose values are determined to specify the flight path for a particular mission. The control table generator is the portion of the nominal profile generator, NPG 2, that determines the constants as functions of the mission variables R_o and ΔV_g. Parameters for a number of reference flight profiles are stored in the computer memory for optimized flight paths that bracket the range of mission variables. For intermediate values of mission variables interpolation methods are used to determine the values of the constants.

The formal framework for describing a two parameter family (parameters are R_o and ΔV_g) of stage 1 control functions is developed. A general dependent variable is described by the symbol F_i as a function of a general independent variable u; n_1 dependent variables are used to define the flight profile ($i=1,\ldots, n_1$). The symbol $\overline{F}i(u)$ with a bar represents a set of stored table values for the i'th parameter. Each table $\overline{F}_i$ defines one desired nominal profile characteristic on a specified segment of flight, such as altitude versus velocity or bank angle versus time. The symbol $\overline{F}_{i,o}(u)$ represents the set of table values of $F_i(u)$ when the mission parameters R_o and ΔV_g have specified reference values for the reference trajectory cases. Interpolation formuluas are represented by the symbols $\overline{DF1_i}$ and $\overline{DF2_i}$ for increments from reference table values when the mission parameters R_o and ΔV_g are not equal to the reference values. The general form of the equations for generating a dependent variable as a function an independent variable is:

$$F_i(u) = \overline{F}_{i,o}(u) + \overline{DF1_i}(u,R_o) + \overline{DF2i}(u,\Delta V_g),\ i = 1,\ldots,n_1$$

The symbol K_j represents a constant for a particular mission which varies with the mission parameters R_o and ΔV_g from mission to mission. $G_k(R_o)$ and $G_1(\Delta V_g)$ are one dimensional tables or functions that define the constants K_j when the mission parameters are specified.

$$K_j = G_k(R_o) + G_1(\Delta V_g),\quad j \leq k + 1,\quad k = 1,\ldots,n_2$$
$$1 = n_2 + 1,\ldots,n_3$$

The constants K_j include:

(1) segment boundary conditions such as initial relative heading and stage position components; and

(2) constants in control variable equations that are fixed on a specific mission but vary with mission parameters.

The equations for the segment boundary conditions are for the most part the same as those appearing in NPG 1.

There are several candidates for the form of the incremental functions DF1 and DF2. They may be defined by two-dimensional tables, by combinations of one and two-dimensional tables, by combinations of tables and functions, or entirely by functions. Similarly, G_1 and G_K may be defined by one dimensional tables or by functions.

Not all profile characteristics are defined by tables of the form $\overline{F}_i$; some are defined by functional forms containing constants of the form K_i. In the guidance equations the symbol $F_i(u)$ is used to denote the value of the dependent profile variable depending on the independent variable u. No distinction is made as to form--that is whether F_i is obtained by table interpolation or by evaluating a function in u such as a polynomial or expotential form. When referring to the set of table values, a bar is placed above the function symbol. Similarly, $\overline{DF1}_i$, $\overline{DF2}_i$ and G_i represent functions of R_o or ΔV_g while $\overline{DF1}_i$, $\overline{DF2}_i$ and $\overline{G}_i$ represent sets of table values.

The foregoing merely sets up the formal framework for describing the two-parameter family of Stage 1 control functions for rendezvous missions. A control model is specified by defining the functions F_i, $DF1_i$, $DF2_i$, and G_i. One possible model will be described which is based on an interpretation of trajectory results obtained to date. The analysis and design process for synthesizing and testing guidance system models is outlined in Figure 2-13.

2.7.3.3 Nominal Guidance Equations for Preliminary Guidance System Model

Preliminary equations for the control variable commands required to simulate the vehicle nominal flight path are given. The control variables are scalar pitch (θ_c), bank angle (ϕ_c), and throttle (η_c), the subscript c denoting command. Scalar pitch is equal to angle of attack plus flight path angle, which are not in the same plane when the vehicle is banked. In actual flight, these commands are converted by the guidance system to Euler angle commands in the coordinate system of the inertial attitude reference system. These conversions are not included in the simulation since they have no effect on the simulated profile.

FIGURE 2-13

Development Steps - Nominal Profile Generator

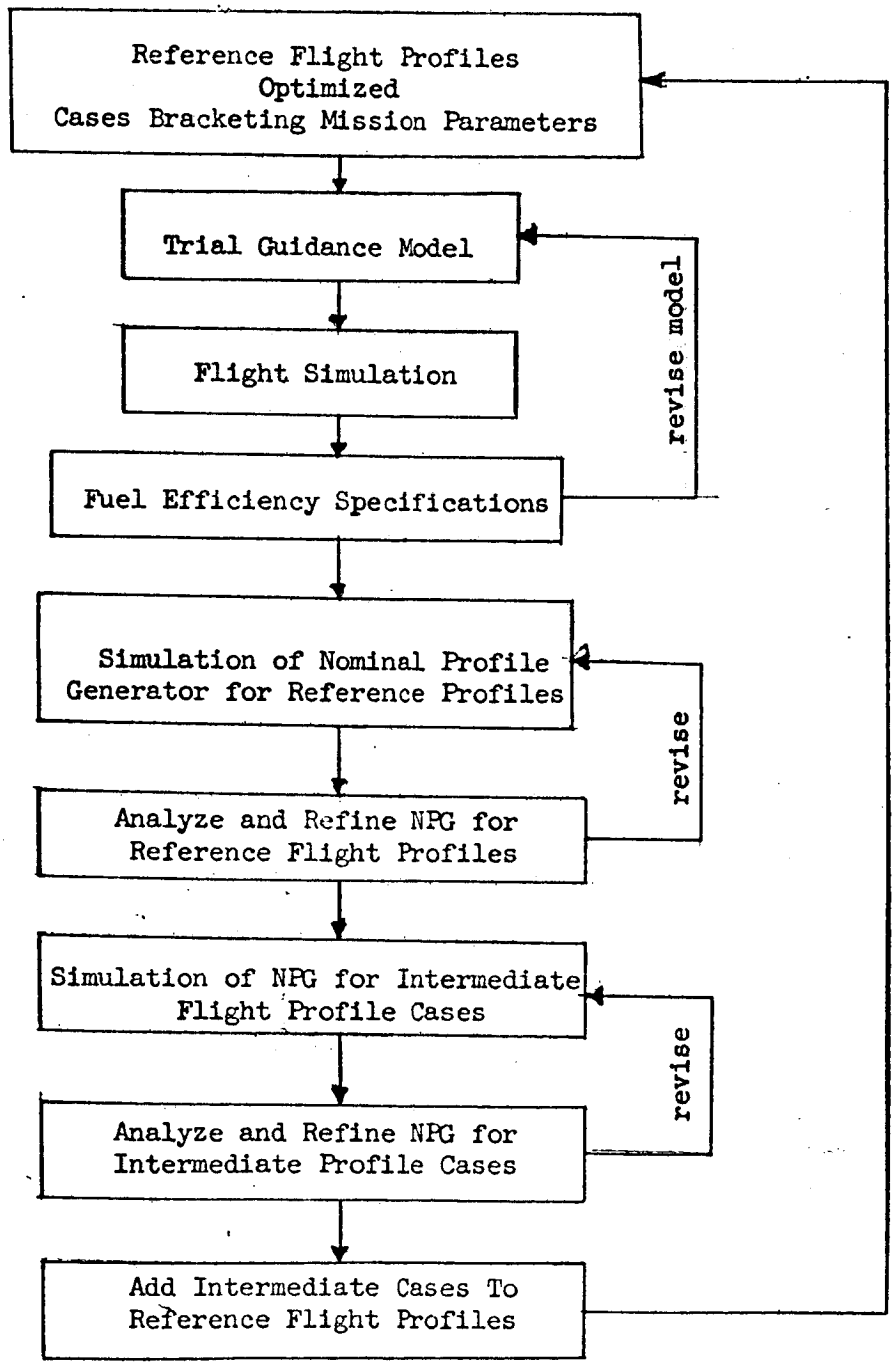

Inputs to the guidance equations include (1) simulated vehicle position and velocity in both the flight path coordinate system and the target oriented coordinate system defined in Figure 2-11; (2) the table values $\bar{F}_j$ and constants K_j produced by the Control Table Generator; and (3) a set of constants represented by c_j which are independent of the mission parameters R_o and ΔV_g. The guidance modes are in one-to-one correspondence with the flight segments defined in Section 2.2.

Mode 1. Take Off and Turn to Initial Heading

Taking off at heading AZ_o the vehicle flies a specified attitude profile at full throttle to a specified velocity, then banks until heading equals the desired initial value determined by the Control Table Generator (hereafter Control Table Generator is abbreviated CTG) as a function of R_o. The pitch and throttle equations are:

$$\Theta_c = c_o + c_1 (t-t_o)$$

$$\eta_c = 1. \qquad \text{throughout Mode 1}$$

The bank angle equation is:

Start with $\Delta \phi_c = c_2 (AZ-AZ_o)$

Switch to $\phi_c = c_3$ when V_R crosses the value c_4.

Switch to $\Delta \phi_c = c_5(AZ-K_1)$ when $(AZ-K_1) < c_6$.

K_1 is obtained by CTG through linear interpolation in a table of numbers, $\overline{G1(R_o)}$, which defines initial cruise heading as a function of R_o. Switch to Mode 2 when $|AZ - K_1| < c_7$.

Mode 2. Acceleration and Climb to Cruise Conditions

BRANCH I: When $R_o > R_c$, the vehicle is guided by Mode 2 to supersonic cruise conditions. The pitch angle and throttle profiles are invariant with R_o. Pitch angle is controlled to produce the altitude-velocity profile defined by the optimization work for long range missions shown in Figure 2-7. Throttle is held constant at its maximum value. The desired altitude is equal to $F1\ (V_R)$, obtained by a table interpolation in the table $\overline{F1(V_R)}$. $\overline{F1(V_R)}$ is equal to a reference table in CTG, denoted there by $\overline{F1_{,o}(V_R)}$ which is constructed to fit the optimum h-V profile for long range missions. The functions DF1, and DF2, are identically zero. The bank angle profile is determined by an equation formulated to cause the vehicle to fly the great circle containing present position and the desired start turn position $(\delta_3, \Theta_3) = (K_2, K_3)$. The desired start turn position components are

determined as functions of R_o by CTG, using the equations and tables defined in NPG 1. The control equations are:

$$\eta_c = 1.$$

$$\Delta\theta_c(t) = c_8(h - F_1(V_R)) + c_9[\Delta\theta(t) - \Delta\theta(t - \Delta t)]$$

$$\Delta\phi_c = c_5(AZ - AZ_c)$$

where

$$AZ_c = \arcsin \frac{\cos\delta_3 \sin R}{\sin(\theta - \theta_3)}$$

$$R = \arccos\left[\sin\delta \sin\delta_3 + \cos\delta \cos\delta_3 \cos\theta_3\right]$$

Switch to Mode 3 when V_R crosses C_{10}.

Branch Two of Mode 2: When $R_o \leq R_c$, the vehicle is guided by Mode 2 to subsonic cruise conditions. The pitch and the throttle profiles are the same as for Branch One, table $\overline{F_1(V_R)}$ being the altitude-velocity table, and throttle being at maximum. The bank angle is controlled to maintain heading at $AZ_1 = K_1$. Nominal guidance switches to Mode 3 when the specified subsonic cruise velocity, K_4, is attained. K_4 is determined by CTG as a function of R_o.

Mode 3. Subsonic or Supersonic Cruise

Subsonic

Pitch is controlled to maintain a specified altitude rate; throttle is controlled to maintain $\overline{V}_R$ equal to zero; and bank angle is controlled to maintain heading, K_1.

$$\Delta\theta_c = c_{11}(\dot{h} - K_5)$$

$$\Delta\eta = c_{12} \cdot \dot{V}_R$$

Initially, $\Delta\phi_c = c_5(AZ - K_1)$

Switch to $\phi_c = K_6$ when δ crosses $\delta_3 = K_3$

Switch to $\phi_c = c_5(AZ - K_7)$ when AZ crosses $(K_7 - .1°)$.

Nominal guidance switches to Mode 4 under control of the following logic:

Switch when latitude (δ) crosses K_8 if $R_o > 300$ NM
or switch when longitude Θ crosses K_9 if $R_o \leq 300$ NM.

The constants K_4 through K_8 are determined by CTG as a function of R_o.

Supersonic Cruise

Pitch is controlled to maintain a constant altitude; throttle is controlled to maintain constant ground speed; and bank angle is controlled so the vehicle flies on the great circle containing present position and the desired start turn position (δ_3, Θ_3) defined previously. Guidance switch to Mode 4 when δ crosses δ_3.

Mode 4. Phase 1 of Turn

BRANCH I: $R_o > R_c$

A maximum rate turn is executed with throttle at maximum setting. The pitch and bank angles are commanded to maximize the horizontal component of the normal acceleration vector within the constraint of $\dot{V}_R = o$ and $\dot{h} = o$.

$$\Delta\theta_c = c_{14}(\cos\phi\cos\alpha) + c_{15}(\cos\phi\cos\alpha)\cdot\dot{\gamma}$$

$$\phi_c = c_{16} + c_{17}\dot{V}_R + c_{18}(V_R - c_{18})$$

Guidance switches to Mode 5 when latitude (δ) crosses a specified value K_{10} which is a function of R_o.

Branch Two: $R_o \leq R_c$

When $R_o \leq R_c$, the climb, acceleration, and turn to the stage point are coordinated, the parameters of the profile being strong functions of R_o and weak functions of ΔV_g. The guidance equations for Mode 4 are based on the assumption that the profile on the first phase of the turn is independent of ΔV_g. The initial conditions at the start of the turn vary with the initial heading ($AZ_1 = G_1(R_o)$) and with the duration of the subsonic cruise leg, which also is dependent on R_o. The desired h-V profile is given by the table $\overline{F_2(V_R)}$ of M_1 pairs of points. $\overline{F_2(V_R)}$ is constructed by CTG as follows:

$$\overline{F_2(V_R)} = \overline{F_{1,o}(V_R)_J} + \overline{DF1_2}(R_o)$$

$\overline{DF1}_2$ is the table of differences in h with respect to R_o at the points in the middle region of the reference h-V profile shown in Figure 2-7. A schematic illustration of the family of profiles in this region is sketched in. The bank angle profiles on Mode 4 are defined by the following form:

$$\phi_c = K_{11} + K_{12}(t-t_3) + K_{13}(t-t_3)^2$$

where K_{11}, K_{12} and K_{13} are functions of R_o.

Guidance is switched to Mode 5 when latitude crosses $\delta = K_{14}$ where K_{14} is a function of ΔV_g.

Mode 5. Phase 2 of the Turn and Pull Up.

The form of the nominal guidance equations for the final turn prior to pull up is based on the hypothesis that the h-V profile in this phase is invariant with R_o, but varies with ΔV_g. The desired h-V profile table $\overline{F_3(V_R)}$ of M_2 pairs of points is given by:

$$\overline{F_3(V_R)} = \overline{F_{1,o}(V_R)} + \overline{DF2}_3(\Delta V_g)$$

$\overline{DF2}_3$ is the table of differences in h with respect to ΔV_g at the M_2 points on the reference h-V profiles. The bank angle profiles on Mode 5 are defined by the following form:

$$\phi_c = c_{20}(Y-Y_s) + c_{21}(\dot{Y}-\dot{Y}_s)(t-t_s) + c_{22}\ddot{Y}(t-t_s)^2$$

where Y_s, $\dot{Y}_s$ are the desired cross plane components of inertial position and velocity at staging and t_s is the current estimate of stage time. The desired stage point position was defined previously in terms of latitude and longitude (δ_s, Θ_s). The cross plane inertial velocity Y_s is given as a function of R_o and ΔV_g:

$$\dot{Y}_s = c_{23} + G_{22}(\Delta V_g) + G_{23}(R_o)$$

where the second and third terms are evaluated by CTG by interpolation in Tables $\overline{G22}$ and $\overline{G23}$.

Sometime during Mode 5, a prediction calculation for the time to start pull-up is initiated using a simplified form of the equations of motion with constant gravity and an idealized form of the accelerations due to lift and drag. These are still to be derived. An integrable form is sought such that the prediction involves the evaluation of a functional form for $(V_R)_5$ and h_5 at t_5.

Stage time is corrected then to:

$$\delta t = \text{New } t_5 - \text{Old } t_5 = c_{24}((\dot{V}_R)_5 - K_{15}) + c_{25}(h_5 - K_{16})$$
$$\text{New } t_s = \text{Old } t_s + \delta t$$

where K_{15} and K_{16} are the desired relative velocity at the start of pullup as functions of R_o and ΔV_g:

$$K_{15} = G_{24}(R_o) + G_{25}(\Delta V_g)$$
$$K_{16} = G_{26}(R_o) + G_{27}(\Delta V_g)$$

Guidance is switched to Mode 6 when $t = \text{New } t_5$.

Mode 6. Pullup and Stage

The equations for pitch control are the same on Mode 6 as Mode 5, the h-V profile, $F_3(V_R)$ extending from the start of Mode 5 through staging. The bank angle is controlled by an open loop time profile as follows:

$$\Delta\phi_c = c_{26}(F_4(t_s - t) - \phi)$$

where stage time is held constant at the value predicted at the start of pullup.

Staging occurs when $t = t_s$.

2.7.3.4 Stage 1 Flight Path Simulation

The Stage 1 equations of motion may be integrated in the Earth equatorial inertial system $(x, y, z, \dot{x}, \dot{y}, \dot{z})$ or in the flight path coordinate system $(V_R, \gamma, AZ, h, \Gamma, \lambda)$. Both sets of coordinates appear as variables in the control equations, requiring coordinate conversion in either case. The flight path coordinates are required to determine the applied force vector, and the inertial coordinates are required to determine position and velocity relative to the target. The choice of coordinates in integration depends on detailed considerations which are beyond the scope of the present study. For purposes of this discussion the equations of motion are arbitrarily presented in the flight path coordinate system.

The acceleration vector is defined by $\dot{V}_R$, $\dot{\gamma}_R$, and $\dot{AZ}$, as follows:

$$\dot{V}_R = \frac{T\cos\alpha - D}{m} - g\sin\gamma_R + W^2 r_e \cos\lambda(\cos\lambda\sin\gamma_R - \sin\lambda\cos\gamma_R\sin AZ)$$

$$\dot{\gamma}_R = \frac{T\sin\alpha + L}{mV_R} - \left(\frac{g}{V_R} - \frac{V_R}{r}\right)\cos\gamma_R + 2W\cos\lambda\cos AZ + \frac{Wr^2}{V_R}\cos\lambda(\cos\lambda\cos\gamma_R + \sin\lambda\sin\gamma_R\sin AZ)$$

$$\dot{AZ} = -\frac{(T\sin\ + L)\sin\phi}{mV_R\cos\gamma_R} - \frac{V_R}{r_e}\tan\lambda\cos\gamma_R\cos AZ - 2W(\sin\lambda - \tan\gamma_R\sin AZ\cos\lambda) - \frac{W^2 r\sin\lambda\cos\lambda\cos AZ}{V_R\cos\gamma_R}$$

The velocity vector in spherical coordinates is given by:

$\dot{h} = V_R\sin\gamma_R$ altitude rate

$\dot{\lambda} = \frac{V_R\cos\gamma_R\sin AZ}{r_e}$ latitude rate

$\dot{\Gamma} = V_R\cos\gamma_R\cos AZ/r_e\cos\lambda$, longitude rate

Mass rate, thrust, lift, and drag are approximated by a set of functions, f_i, involving state and control variables:

$\dot{m} = f_1(\eta, h, V_R)$ mass rate

$T = f_2(\eta, h, V_R, \gamma_s)$ thrust force

$D = f_3(h, V_R, \alpha)$ drag force

$L = f_4(h, V_R, \alpha)$ lift force

The gravitational acceleration is given by:

$$g = \mu / r_e^2$$

A development problem exists in the formulation of the functions, f_i, defining the mass rate and applied forces. Altitude and velocity appear as independent variables in all four of the functions; angle of attack appears in all except the mass rate function; and throttle appears in the mass rate and thrust functions. In existing simulations of aerodynamic flight these functions are given by a combination of formulae and table look up. This may be the best way of describing vehicle characteristics, but the potential of an analytical formulation should be investigated.

2.7.3.5 Analysis of Stage 1 End Conditions and Correction for Rendezvous.

Stage 2 Boost Segment and Orbital Segment Profiles

Having defined the Stage 1 profile by simulation, NPG 2 adds the Stage 2 boost and orbital segment arcs and time to the stage position and time to obtain the new estimate of rendezvous position and time.

The Stage 2 boost and first coast arc parameters are computed with the same formulae defined in NPG 1. Formulae of this type are accurate within a few seconds and one kilometer, so that simulation of the equations of motion may not be required.

Target Position Prediction

The target time t_f at position Θ_f is computed and the correction in takeoff time is determined as in NPG 1.

Cross Plane Error Correction.

The purpose of the Stage 1 simulation is to measure and correct the errors due to approximations in the representation of the Stage 1 profile by parametric functions of R_o and ΔV_g. The parametric representation shapes the profiles; end conditions are met by adjusting the profile cross plane profile and take off time after each simulation of the Stage 1 equations of motion. The proposed measure of cross plane profile error is the integral of the difference between simulated cross plane position and a desired nominal on the second phase of the turn. The profile on this segment is a strong function of R_o and a weak function of ΔV_g. It is constructed by CTG as follows:

$$Y_N(t) = F_5(t) + \overline{DF1_5}(R_o, t) + \overline{DF2_5}(\Delta V_g, R_o, t)$$

$$\overline{DF2_5} = G(R_o) \cdot \Delta V_g, \text{ for all } t$$

and $\overline{DF1_5}(R_o, t)$ is a matrix of table values.

The measure of cross plane profile error is:

$$\sum_{j=1}^{m_3} \left[Y(t_j) - Y_N(t_j)\right] \Delta t$$

Since R_o is the principle cross plane profile parameter, the profile is adjusted by correcting R_o by a term $\Delta R_o'$ proportional to the observed cross plane error.

The position of the target plane at the updated boost cut-off time and the resultant change in R_o, ΔR_o, are determined. The composite correction in R_o is then $\Delta R_o' - \Delta R_o$. The steps defined in 2.7.3.1 - 2.7.3.5 are repeated with the new values of R_o and ΔV_g. Iteration continues until convergence criteria on $(t_T - t_f)$ are met.

REFERENCES, SECTION 2.0

1. "An Explicit Multi-Stage Boost Guidance For Minimum Fuel Consumption", by A. A. Morgan and G. W. Braudaway, Boeing Document D2-90200, November, 1962.

2. "Dyna Soar Trajectory Simulation", Boeing Document D2-80674, May, 1963.

3. "Launch Vehicle Digital Computer Equation Defining Document For The AS502 Flight Program", Contract No. NAS 8-14000, May, 1966.

4. "Earth Orbit Rendezvous Guidance Studies", by C. D. Eskridge and M. S. O'Mahoney, Boeing Document D5-13344, February, 1967.

3.0 LAMBDA GUIDANCE

3.1 Introduction

Lambda guidance and the variational form of the steepest-descent optimization process share a common origin, small perturbation analysis of the motion of a nonlinear dynamic system. In both cases an optimal result, correct to first order, is sought. In steepest-descent problems the object is to maximize or minimize a function of the terminal state and time while simultaneously providing specified changes to an array of constraint functions. In Lambda guidance problems the object is to find the minimum control perturbation which retains terminal control about an arbitrary nominal path in the presence of small disturbances.

In flight control problems the disturbance may have several sources. The state at a particular time may be in error as a result of a combination of navigational, guidance or control errors. Localized environmental disturbances in the planetary atmospheric characteristics may be encountered during a particular mission. Finally, the predicted vehicle characteristics themselves may be in error; aerodynamic and propulsive forces in particular are subject to some uncertainty on most vehicles. In any non-linear system the propagated effect of uncorrected small errors in the state vector or its time derivative can become large, hence a guidance system which determines corrective control action once the errors have been detected is a necessity. If the errors are small, linearized perturbation analysis can be employed to determine control corrections which maintain some chosen subset of the original terminal state-vector components. In particular, if an acceptable measure of control perturbation cost can be devised, the optimal control correction, i.e., that which provides minimum "cost" in some generalized sense, can be analytically obtained. Lambda guidance is an optimal guidance scheme in this sense, the cost function employed being the control perturbation measure of Eqn. (2.1.5), Part II, Vol. 2.

The Lambda guidance approach retains the complete system dynamics to first order and hence is capable of providing control about an arbitrary vehicle flight path, providing the errors remain small in a mathematical sense. It should be emphasized that this definition of smallness may not always coincide with preconceived conceptions of smallness. Only actual simulations of the controlled dynamic systems can provide the correlation between mathematical and preconceived ideas of smallness. Since Lambda guidance can be applied to an arbitrary flight path it has the ability to provide guidance about the complex flight paths which often result from optimization calculations. This appears to be a significant point, since piecewise approximation of dynamic optimal paths by conventionally defined and controlled sub-arcs may result in significant performance losses.

The remainder of this part of the report is devoted to a derivation of the Lambda guidance equations, a brief description of a simulator developed for the study of Lambda guidance problems, and the results of applying the simulator to some typical recoverable launch system flight paths.

3.2 ANALYTIC DEVELOPMENT

3.2.1 Error Sources

The optimization analysis of Sections 2 and 3 in Part II, Volume 2 of the present report contains the nucleus of first order control theory as a by-product. For example, the trajectory sensitivities to various types of error are obtained, Eqns. (3.2.41) to (3.2.46) of Part II, Volume 2. These sensitivities permit the direct computation of the effect of various error sources at any point on the trajectory, on the quantities of interest at the trajectory termination, provided the magnitude of these errors is small.

In guidance problems several types of errors may exist at a point on the trajectory, including

(a) State variable errors on the terminal values of the payoff or constraint functions.
(b) Control variable errors on the terminal values of the payoff or constraint functions.
(c) Vehicle characteristic errors.
(d) Environmental errors in the planetary characteristics.

The remainder of this section is devoted to the study of type (a).

It will be assumed that a basic trajectory, along which the vehicle is to fly, is available. In this case, the state variables, which describe the trajectory history, and the control variable histories which generate this basic trajectory in the absence of errors, will be known functions of time, say

$$\left\{x(t)\right\} = \left\{X(t)\right\} \qquad 3.1$$

$$\left\{\alpha(t)\right\} = \left\{A(t)\right\} \qquad 3.2$$

The guidance problem considered here is that of determining control history corrections, $\left\{\Delta\alpha(t)\right\}$, which maintain the terminal conditions of Eqns. (2.1.2) to (2.1.4) of Part II, Vol. 2, or some selected subset of these conditions, in the presence of small state errors along the path. It should be emphasized at this point that for a variety of reasons the basic trajectory may be non-optimal. In these instances first order analysis can be used to predict the effect of small state and control perturbations on the terminal value of the payoff function.

3.2.2 Effect of State Variable Errors

Suppose that the flight of a vehicle on a basic trajectory is being monitored, and at some time, t', let it be noted that the actual vehicle flight path has deviated, in a state sense, from the basic trajectory. That is, an error in the state variable of position, velocity and mass exists, so that

$$\left\{x(t')\right\} = \left\{X(t')\right\} + \left\{\Delta x(t')\right\} \qquad 3.3$$

where $\left\{\Delta x(t')\right\}$ is the detected state error. Now apply Eqns. (2.2.20) of Part II, Vol. 2 to the remaining portion of the trajectory, assuming no control variable correction and no vehicle characteristic or environmental errors. This can be achieved by substituting t' for t_o to obtain

$$\Delta\phi = \left[\lambda_{\phi\Omega}(t')\right]\left\{\Delta x(t')\right\} \qquad 3.4$$

and

$$\left\{\Delta\psi\right\} = \left[\lambda_{\psi\Omega}(t')\right]'\left\{\Delta x(t')\right\} \qquad 3.5$$

The quantities $\Delta\phi$ and $\{\Delta\psi\}$ are the first order estimates of perturbations in the payoff and constraint functions, if the errors, $\{\Delta x(t')\}$, are left uncorrected, and allowed to propagate throughout the remainder of the trajectory.

In some instances, it may be desirable to obtain the history of the entire remaining portion of the perturbed trajectory, in addition to the final perturbations. This can be accomplished using a combination of the analysis of Section 2, Part II, Vol. 2, and the superposition principles contained in Reference 2. First, returning to Eqn. (2.2.13) of Part II, Vol. 2, it follows by integration between t' and $\bar{t}$, where

$$t' < \bar{t} < T \qquad 3.6$$

that

$$\left\{\lambda'\delta x\right\}_{\bar{t}} - \left\{\lambda'\delta x\right\}_{t'} = \int_{t'}^{\bar{t}} \left[\lambda\right]'\left[G\right]\left\{\delta\alpha\right\}\, dt \qquad 3.7$$

Now suppose the boundary conditions

$$\left[\lambda(\bar{t})\right] = \left[I\right] \qquad 3.8$$

are imposed.

It follows directly from Eqns. (3.7) and (3.8) of Part II, Vol. 2, that

$$\left\{\delta x(\bar{t})\right\} = \int_{t'}^{\bar{t}} \left[\lambda\right]'\left[G\right]\left\{\delta\alpha\right\} dt + \left[\lambda(t')\right]'\left\{\Delta x(t')\right\} \qquad 3.9$$

If the control variables are not perturbed, the first term on the R.H.S. disappears and

$$\left\{\delta x(\bar{t})\right\} = \left[\lambda(t')\right]' \left\{\Delta x(t')\right\} \qquad 3.10$$

Now applying the superposition principles at time $\bar{t}$

$$\left[\lambda(\bar{t})\right] = \left[L(\bar{t})\right]\left[\lambda(T)\right] = \left[I\right] \qquad 3.11$$

Premultiplying both sides by $\left[L(\bar{t})\right]^{-1}$, we obtain

$$\left[\lambda(T)\right] = \left[L(\bar{t})\right]^{-1} \qquad 3.12$$

and hence by the superposition principle applied at time t'

$$\left[\lambda(t')\right] = \left[L(t')\right]\left[L(\bar{t})\right]^{-1} \qquad 3.13$$

Combining Eqns. 3.1, 3.10 and 3.13, the time history of the perturbed trajectory in the region $t' \leq \bar{t} \leq T$ becomes

$$\left\{x(\bar{t}) + \delta x(\bar{t})\right\} = \left\{X(\bar{t})\right\} + \left[\left[L(\bar{t})\right]^{-1}\right]' \left[L(t')\right]' \left\{\Delta x(t')\right\} \qquad 3.14$$

If the control history is also perturbed, the state at any future time, t, can be found by substitution of Eqn. 3.13 into Eqn. 3.9. In this case

$$\left\{x(\bar{t}) + \delta x(\bar{t})\right\} = \left\{X(\bar{t})\right\} + \left[\left[L(\bar{t})\right]^{-1}\right]' \left\{\int_{t'}^{T} \left[L(t)\right]' \left[G\right]\left\{\Delta\alpha\right\} dt + \left[L(t')\right]' \left\{\Delta x(t')\right\}\right\} \qquad 3.15$$

3.2.3 Correction of State Variable Errors

Once a state variable error has been detected, the question of how it should be compensated arises. The compensation can only be made by a correcting perturbation to the basic control variable histories. Depending on the control system sophistication, this may be accomplished by means varying from a pulse correction in the control variables, to a continuously distributed perturbation in the remaining portion of the control variable histories.

3.2.3.1 Pulse Control Variable Corrections

In the simplest case, we must attempt to eliminate the effect of the state variable errors by a pulse in the controlling variables. That is, we will superimpose a control variable perturbation, $\{\delta\alpha(t)\}$, on to the basic control variable history, $\{A(t)\}$, of the form

$$\left\{\Delta\alpha(t)\right\} = \left\{\Delta\alpha(t') \cdot \delta(t - t')\right\} \qquad 3.16$$

Substituting the measure state variable errors, $\{\Delta x(t')\}$; the control variable perturbation, $\{\Delta\alpha(t')\}$; and t' for t_o; in Eqns. 2.2.20 of Part II, Vol. 2, we obtain

$$d\phi = \left[\lambda_{\phi\Omega}(t')\right]\left[G(t')\right]\left\{\Delta\alpha(t')\right\} + \left[\lambda_{\phi\Omega}(t')\right]\left\{\Delta x(t')\right\} \qquad 3.17$$

$$\left\{d\psi\right\} = \left[\lambda_{\psi\Omega}(t')\right]'\left[G(t')\right]\left\{\Delta\alpha(t')\right\} + \left[\lambda_{\psi\Omega}(t')\right]'\left\{\Delta x(t')\right\} \qquad 3.18$$

If the number of constraints plus payoff function, P+1, is equal to the number of control variables, M; Eqns. 3.17 and 3.18 can be solved. Further, by making the L.H.S. of each of these equations zero, the significant terminal conditions of the trajectory will be unaltered. Making this substitution and solving for the control variable pulse magnitudes, we obtain

$$\left\{\Delta\alpha(t')\right\} = -\left[\left[\frac{\left[\lambda_{\phi\Omega}(t')\right]}{\left[\lambda_{\psi\Omega}(t')\right]'}\right]\left[G(t')\right]\right]^{-1}\left[\frac{\left[\lambda_{\phi\Omega}(t')\right]}{\left[\lambda_{\psi\Omega}(t')\right]'}\right]\left\{\Delta x(t')\right\} \qquad 3.19$$

In Eqn. 3.19, it has been assumed that the matrix which is to be inverted is non-singular. If one of the controls were ineffective at t', so that corresponding column in the G matrix was null, the inversion would be impossible. In this case, that particular control variable could be ignored, and there would be (M-1) effective control variables.

When there are fewer control variables than terminal quantities of interest, $M < P+1$, then it is only possible to select M of the P+1 quantities and eliminate the error in them. The selection of which of the P+1 terminal quantities should be so chosen depends both on the importance

of each constraint, and the effect of the pulse correction on the remaining terminal quantities. This latter effect can be obtained by substituting the pulse corrections in the complete set of equations given by Eqns. 3.17 and 3.18.

When there are more control variables than terminal quantities of interest, M > P+1, any P+1 of the M control variables can be used to eliminate the terminal errors.

3.2.3.2 Distributed Control Variable Corrections

In a more sophisticated system than that considered in Section 3.2.3.1 the control variable correction may be distributed over the remaining portion of the trajectory. In this case, the requirement of $M \geq P+1$, to completely correct a state variable error disappears.

Substituting the state variable errors together with a control variable perturbation into Eqns. 2.2.20 of Part II, Vol. 2, and applying these equations at the point $t_o = t'$, we now obtain

$$d\phi = \int_{t'}^{T} \left[\lambda_{\phi\Omega}\right]\left[G\right]\left\{\Delta\alpha\right\} dt + \left[\lambda_{\phi\Omega}(t')\right]\left\{\Delta x(t')\right\} \qquad 3.20$$

and

$$\left\{d\psi\right\} = \int_{t'}^{T} \left[\lambda_{\psi\Omega}\right]'\left[G\right]\left\{\Delta\alpha\right\} dt + \left[\lambda_{\psi\Omega}(t')\right]'\left\{\Delta x(t')\right\} \qquad 3.21$$

Now suppose we take a control variable perturbation of total magnitude

$$\Delta P^2 = \int_{t'}^{T} \left[\Delta\alpha(t)\right]\left[W(t)\right]\left\{\Delta\alpha(t)\right\} dt \qquad 3.22$$

From the analysis of Part II, Vol. 2, Eqn. 2.2.38, the optimal way to distribute this perturbation while eliminating the terminal constraint errors is

$$\left\{\Delta\alpha\right\} = \mp\left[W\right]^{-1}\left[G\right]'\left\{\left\{\lambda_{\phi\Omega}\right\} - \left[\lambda_{\psi\Omega}\right]\left[I_{\psi\psi}(t')\right]^{-1}\left\{I_{\psi\phi}(t')\right\}\right\} \times \sqrt{\frac{\Delta P^2 - \left[\Delta\beta\right]\left[I_{\psi\psi}(t')\right]^{-1}\left\{\Delta\beta\right\}}{I_{\phi\phi}(t') - \left[I_{\psi\phi}(t')\right]\left[I_{\psi\psi}(t')\right]^{-1}\left\{I_{\psi\phi}(t')\right\}}} + \left[W\right]^{-1}\left[G\right]'\left[\lambda_{\psi\Omega}\right]\left[I_{\psi\psi}(t')\right]^{-1}\left\{\Delta\beta\right\} \qquad 3.23$$

where

$$\left\{\Delta\beta\right\} = -\left[\lambda_{\psi\Omega}(t')\right]' \left\{\Delta x(t')\right\} \qquad 3.24$$

The functions $\left[I_{\psi\psi}(t')\right]$, $\left\{I_{\psi\phi}(t')\right\}$, and $I_{\phi\phi}(t')$ are defined by Eqns. 2.2.31a to 2.2.31c of Part II, Vol. 2, respectively, with t_o replaced by t'. The change in ϕ is similarly derived from Eqn. 2.2.39 of Part II, Vol. 2, and is given by

$$\Delta\phi = \mp \sqrt{\left(I_{\phi\phi}(t') - \left[I_{\psi\phi}(t')\right]\left[I_{\psi\psi}(t')\right]^{-1}\left\{I_{\psi\phi}(t')\right\}\right)\left(\Delta P^2 - \left[\Delta\beta\right]\left[I_{\psi\psi}(t')\right]^{-1}\left\{\Delta\beta\right\}\right)}$$
$$+ \left[I_{\psi\phi}(t')\right]\left[I_{\psi\psi}(t')\right]^{-1}\left\{\Delta\beta\right\} + \left[\lambda_{\phi\Omega}(t')\right]\left\{\Delta x(t')\right\} \qquad 3.25$$

There are several ways in which the solution of Eqns. 3.23 and 3.25 can be used. All hinge on the choice of ΔP^2, the control variable perturbation magnitude. These are:

(a) Use the minimum ΔP^2 which will eliminate the end point changes. In this case,

$$\Delta P^2 = \left[\Delta\beta\right]\left[I_{\psi\psi}(t')\right]^{-1}\left\{\Delta\beta\right\} \qquad 3.26$$

(b) Use the minimum ΔP^2 which will eliminate both the end point changes and restore the performance. This solution is obtained from Eqns. 3.23 and 3.25, and is limited to non-optimal paths.

(c) Use a value of ΔP^2 which is known to be in a reasonably linear range, up to a maximum value obtained from (b).

In a highly complex system, we might utilize any of these three approaches and predict the anticipated conditions at predetermined sampling points. The value of ΔP^2 could then be adjusted according to how well the conditions at each successive sampling point were being predicted. If such a method was applied from the commencement of the trajectory, the probability of staying within the bounds of linearity would greatly increase. It should be remembered that throughout this section, we have linearized the true perturbation by making the assumption that $\left\{\Delta x\right\}$ and $\left\{\Delta\alpha\right\}$ are small. Some of the problems introduced by this technique become clear from Appendix I of Ref. 2. It would seem,

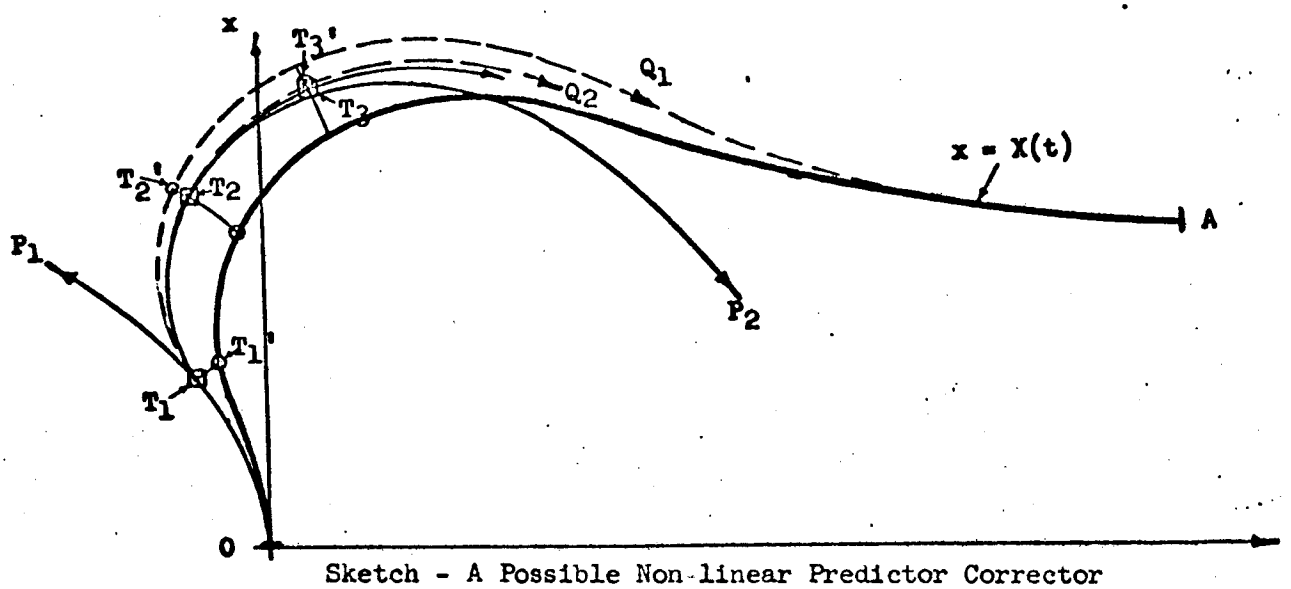

Sketch - A Possible Non-linear Predictor Corrector Guidance Scheme

from the experience gained to date, that a fairly complex set of logical decisions would need to be incorporated into a control system which attempts to correct errors by new optimal distributed corrections. For example, consider the sketch above where a trajectory X(t) is known. At the first predetermined sampling point, T_1, we expected to be at position T_1'. If no corrections are made to the control variable history, suppose the path OT_1P_1 will be followed. Now suppose that we attempt to completely eliminate the end point errors by perturbing the basic control variable histories by an amount $\Delta A_1(t)$, and let the trajectory OT_1Q_1A be the trajectory predicted by the linear analysis, Eqn. 3.15. It is possible, due to the essentially non-linear nature of the problem, that this perturbation will over-correct the end point error and that a trajectory similar to OT_1P_2 will result. At the second predetermined sampling point, however, the tendency to over-correct becomes apparent for instead of being at T_2' we are at T_2. At this point then the amount of end point error being corrected could be reduced and a new control variable perturbation $\Delta A_2(t)$ generated which leads to a predicted trajectory $OT_1T_2T_3'$ and an actual trajectory $OT_1T_2T_3$; at this point, the process is repeated and once the perturbed trajectory becomes reasonably linear, the amount of end point error correction could be gradually increased. This discussion is included to indicate the type of problem which might be encountered in an actual application of first order control theory to a complex dynamic trajectory.

Another point worthy of mention is that in Guidance and Control Problems, we will, in some cases, be interested in control variable perturbations which require the least expenditure of control fuel. The complete solution of this type of problem would normally require a complete six-degree-of-freedom analysis. In some cases, it may be possible to arrive at approximate solutions with a point mass analysis by a judicious choice of weighting function in Eqn. 3.22 and by utilizing

the control variable accelerations as the α instead of the actual control variables themselves.

3.2.4 Lambda Guidance

When the control perturbation is chosen according to Eqn. 3.26 the lambda guidance control perturbation algorithm is obtained. In this case it follows from Eqns. 3.23 and 3.24 that

$$\left\{\Delta\alpha(t)\right\} = \left[C_1(t)\right]\left[C_2(t')\right]\left\{\Delta x(t')\right\} \qquad 3.27$$

$$= \left[C(t,t')\right]\left\{\Delta x(t')\right\} \qquad 3.28$$

where

$$C_1(t) = -\left[W\right]^{-1}\left[G\right]'\left[\lambda_{\psi\Omega}\right] \qquad 3.29$$

$$C_2(t') = \left[I_{\psi\psi}(t')\right]^{-1}\left[\lambda_{\psi\Omega}(t')\right] \qquad 3.30$$

The algorithm of Eqn. 3.27 is used exclusively in the lambda guidance simulator described in the following section. It should be noted that since $\left[I_{\psi\psi}(t')\right]$ is singular when $t' = T$ lambda guidance becomes quite sensitive if updates near the trajectory termination are employed. Discussion of why guidance works for rendezvous where time control is needed.

3.3 Lambda Guidance Simulator (LAGS)

A generalized lambda guidance simulator has been developed during the present study. The simulator can be used for the study of arbitrary point mass flight paths in the following environment:

(1) A spherical planet

(2) A radially symmetric inverse square gravitational field

(3) ARDC 1959 or 1962 Standard Atmosphere

(4) Rotating or non-rotating planet

Vehicle characteristics are entered in tabular form and include,

(1) Propulsive characteristics - thrust force and fuel flow

(2) Aerodynamic characteristics - lift, drag and side forces

(3) Multi-stage capability - stages occur at fixed time

Point mass vehicle flight paths are generated with continuous control employing the following variables:

1. Scalar pitch - the algebraic sum of the flight path angle and the total angle-of-attack
2. Bank angle - A rotation about the velocity vector at constant scalar pitch
3. Throttle setting
4. Sweep angle of the primary lifting surface.

Nominal flight paths can be generated in several ways including:

1. Mach-altitude path following
2. Constant velocity cruise
3. Constant rate of climb
4. Open loop control

The last option, open loop control for the generation of reference nominal flight paths, is used exclusively in the present study. In this mode the simulator is able to accept previously generated control histories from the flight path optimization computer programs of Refs. 2 and 7.

Error sources are contained within the simulator and include

1. Multiplicative and additive aerodynamic lift and drag error constants, i.e., the aerodynamic force appears in the form

$$C_L = A_1 C_L + B_1$$

$$C_D = A_2 C_D + B_2$$

where the A_i and B_i are arbitrary error constants.

2. Multiplicative and additive thrust and fuel flow error constants, i.e.,

$$T = A_3 T + B_3$$

$$\dot{M} = A_4 \dot{M} + B_4$$

Again the error constants are arbitrary.

3. Arbitary state errors can be introduced at any point along the flight path.

4. Timing errors can similarly be introduced.

5. Atmospheric variations can be introduced. At the present time wind profiles are not included.

Terminal constraints may be imposed on any set of functions of the final state and time chosen from a preprogrammed array of 40 variables to a maximum of 14 on any one calculation. The 40 variables include several inflight inequality constraints which are automatically rephrased as terminal constraints using the penalty function technique described in Reference 2.

Program operation is straightforward. Forward integration of the nominal flight path, using either open loop control or one of the programmed flight path generators, is carried out together with a simultaneous computation of the state Jacobian, $\left[\frac{\partial \chi}{\partial \chi}\right]$, and the control partial derivatives, $\left[\frac{\partial \chi}{\partial \alpha}\right]$. The adjoint equations are then integrated backwards in time with the boundary conditions imposed. The control matrix elements, $\left[C(t,t')\right]$, are stored during this calculation. Following the reverse integration of the adjoint equations guidance trajectories are computed in the forward direction with any desired combination of the errors discussed above introduced. The guidance trajectory is integrated with error generation until a chosen start guidance time, t_{go}. At this point the control vector perturbation history which will maintain the specified end points for the then existing state error is computed and added to the nominal control vector history in the time region, $t_{go} \leq t \leq T$. Integration of the guidance trajectory then continues with the modified control history. The control history is updated in this manner at specified time points in the time region, $t_{go} \leq t_g \leq T_g$, where the discrete points t_g are of the form

$$t_g = t_{go} + N. \Delta t_g; \; N = 1,2\text{-------} \qquad 3.31$$

and T_g is a selected guidance update cut-off time chosen to avoid the control singularities discussed in Section 3.2.4. The trajectory continues to be integrated beyond this point until the nominal cut-off condition is satisfied. Throughout the guidance trajectory, limits, $\bar{\alpha}^L$ and $\bar{\alpha}^M$, can be directly imposed on the control perturbations, so that

$$\bar{\alpha}^L \leq \bar{\alpha}(t) \leq \bar{\alpha}^M$$

where $\bar{\alpha}(t)$ is the control perturbation computed from the lambda guidance algorithm. An over-ride of this type is sometimes necessary due to the non-linear nature of highly dynamic atmospheric trajectories, or if updates occur close to the trajectory termination.

A schematic diagram of the lambda guidance simulator is presented in Figure 3-1. The simulator is applied to the study of several trajectories during the remainder of this section. Since relatively few examples of the application of lambda guidance to complex atmospheric trajectories are extant, the simulator is initially applied to a short duration mission and its behavior studied on several typical situations. Problems of increasing complexity are then treated culminating with a complete launch mission from take-off to orbital rendezvous conditions.

3.4 Lambda Guidance Applications - Short Duration Trajectory

The analysis of Section 3.2 indicates that lambda guidance generates an infinite number of control laws. For each differing choice of the time varying weighting matrix $\underline{W}$, a new control correction is generated. The rational choice of these weighting matrices is discussed further in Section 3.6. The applications of the present section use a straightforward approach to this problem on a heuristic basis.

Strictly speaking, the Lambda guidance analysis of Section 3.2 applies to the correction of effects of detected state errors. Nevertheless it is clear that the method has a latent ability to correct small environmental and vehicle characteristic errors also. This can be seen from somewhat idealized argument, for these errors introduce small changes in the control matrices, $[C_1]$ and $[C_2]$. It follows that the control correction for a given state error in the presence of vehicle errors takes the form

$$\{\Delta\alpha\} = [C_1 + \Delta C_1][C_2 + \Delta C_2]\{\Delta x\}$$

$$\simeq [C_1][C_2]\{\Delta x\} \qquad 3.32$$

This assumes that the flight paths of the nominal vehicle and the vehicle subject to characteristic errors are identical. If the paths are not identical but are close to each other this merely introduces a further small error in the control matrices and Eqn. 3.32 remains approximately true.

In reality however small vehicle characteristic errors can rapidly propagate into large flight path errors on complex trajectories. Hence if the effect of vehicle characteristic errors is ignored in the analysis, lambda guidance may fail to provide reasonable terminal control. The errors however only propagate unchecked between the guidance update times, for at each update time the state error is re-established and a revised control correction computed. This point is discussed further in the following section where the behavior of lambda guidance in the presence of vehicle error is demonstrated. Similar remarks can be made with respect to environmental errors.

LAMBDA GUIDANCE SIMULATOR SCHEMATIC

Figure 3-1

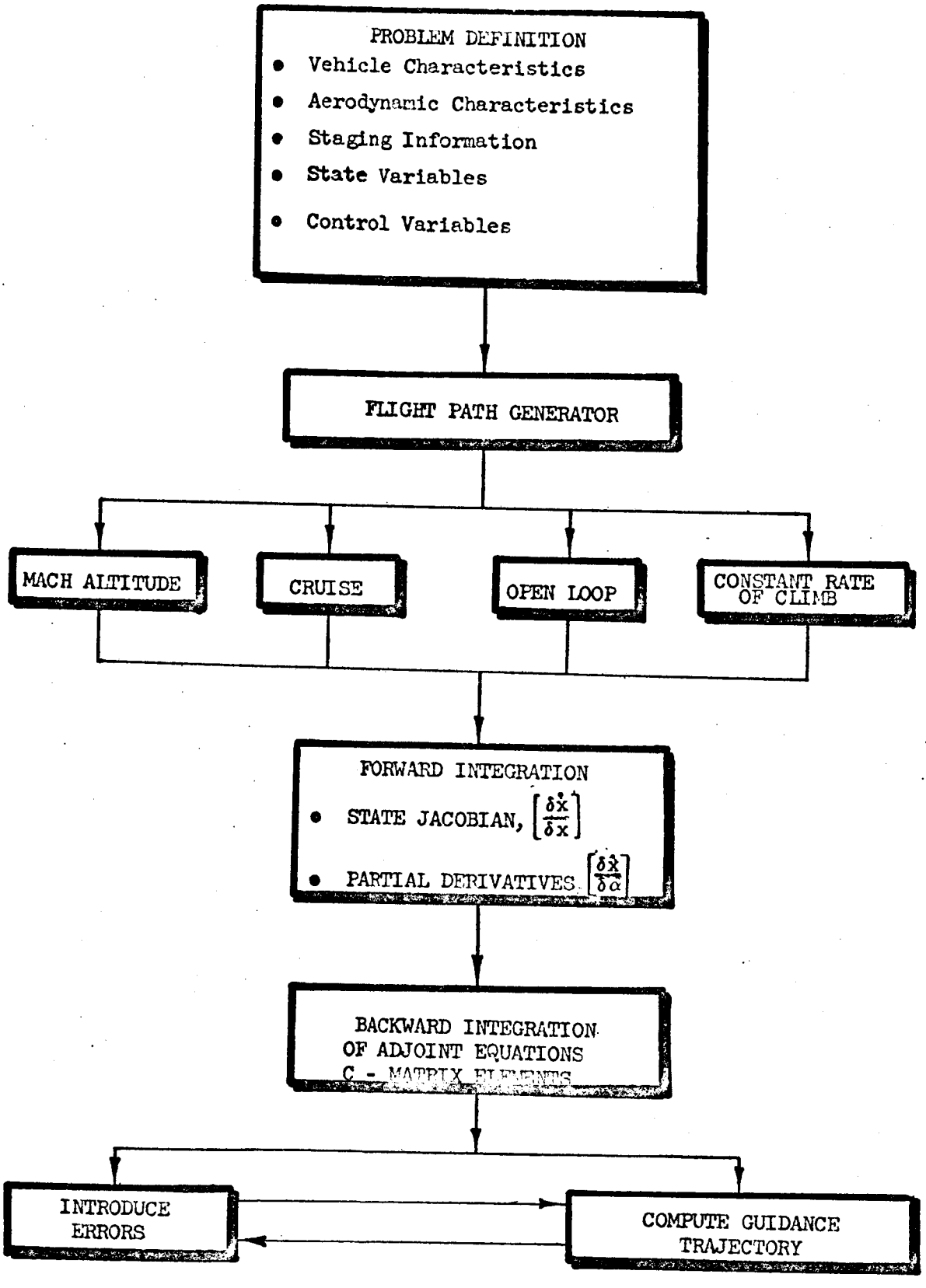

3.4.1 Short Duration Trajectory - Path Following

The initial demonstration of the generalized lambda guidance simulator is for a sequential series of short duration flight paths. The complete mission in these calculations is the first 300 seconds of the trajectory obtained after 32 iterations through the program of Reference 7. It consists of an almost level subsonic acceleration followed by a near constant velocity climb at transonic speed, followed by a supersonic climbing acceleration. Essentially this path follows the sonic boom overpressure limit, as such it represents a typical acceleration profile to about Mach 2.0. The nominal V-h path is shown in Figure 3-2. The path following study divides this profile into 100 second intervals and attempts to steer to this succession of points. Guidance update occurs at about 5 second intervals. Control was executed with scalar pitch, bank angle and throttle. This study is intended to provide some basic insight into the operation of lambda guidance on atmospheric flight path guidance. The off-nominal conditions employed were a thrust error of -5% and a drag increase of 5% throughout the trajectory combined with an initial state error at t = 0 of -50 ft. in altitude and -50 ft/sec. in velocity. Since no inequality constraints were placed on throttle in this first study, guidance to the end points in fixed time is feasible. It can be seen from Figure 3-2 that the path followed by the lambda guidance simulator in the presence of this error is very close to the nominal path at all times. Control histories for the nominal and perturbed paths are shown in Figures 3-4 to 3-6. The control histories generally follow a saw-tooth pattern within each 100 second flight control segment. This is most noticeable in the throttle history of Figure 3-6. Throughout each 100 second segment the control history perturbations grow in magnitude, and the sawtooth shows a tendency to become more pronounced.

This behavior is attributable to the presence of vehicle characteristic errors. The control history at any update time is recomputed without knowledge of these errors. If errors of this type were not present, the trajectory would slowly approach the nominal as time passed and the perturbations apparently would exhibit a decaying character. The effect of the vehicle errors however steadily overpowers the effect of the corrective control actions. Nevertheless, it can be seen from Figure 3-2 that terminal control is maintained in a velocity-altitude-time sense. This is quite surprising in view of the violently changing control histories used to generate the nominal flight path. The pitch and bank-angle histories generally exhibit similar behavior to the throttle history.

The weighting matrix employed in these simulations varies linearly throughout each 100 second segment. Initial values were 1. for pitch and bank, and 0.01 for throttle inverse weighing matrix elements. At the termination of each segment all elements of this matrix were zero. This is equivalent to demanding that the control correction be completed by the end of the trajectory segment. This guidance to a sequence of points along the path effectively implements a path following mode with lambda guidance.

SHORT DURATION TRAJECTORY
PATH FOLLOWING

Velocity-Altitude Profile
Figure 3-2

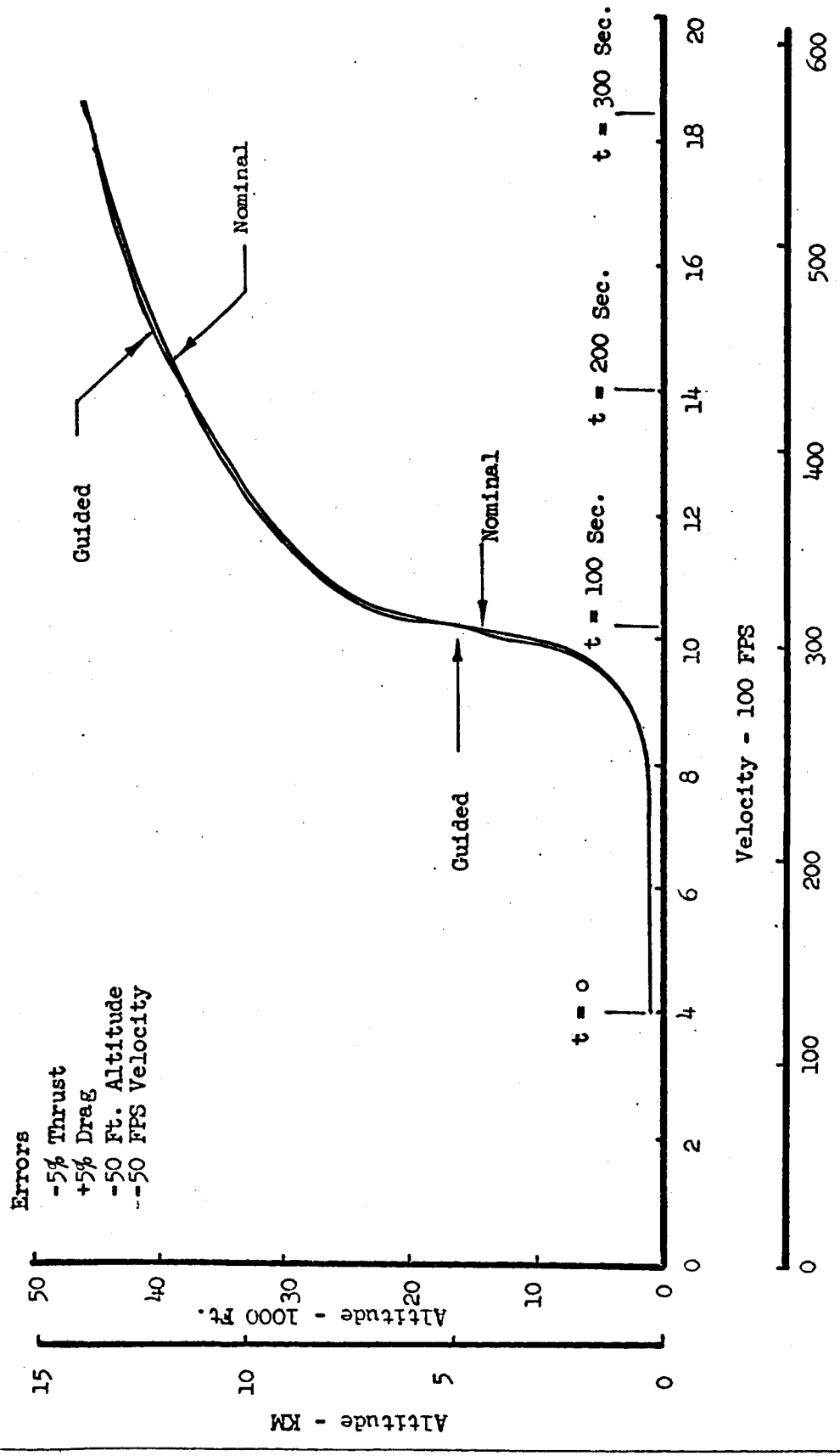

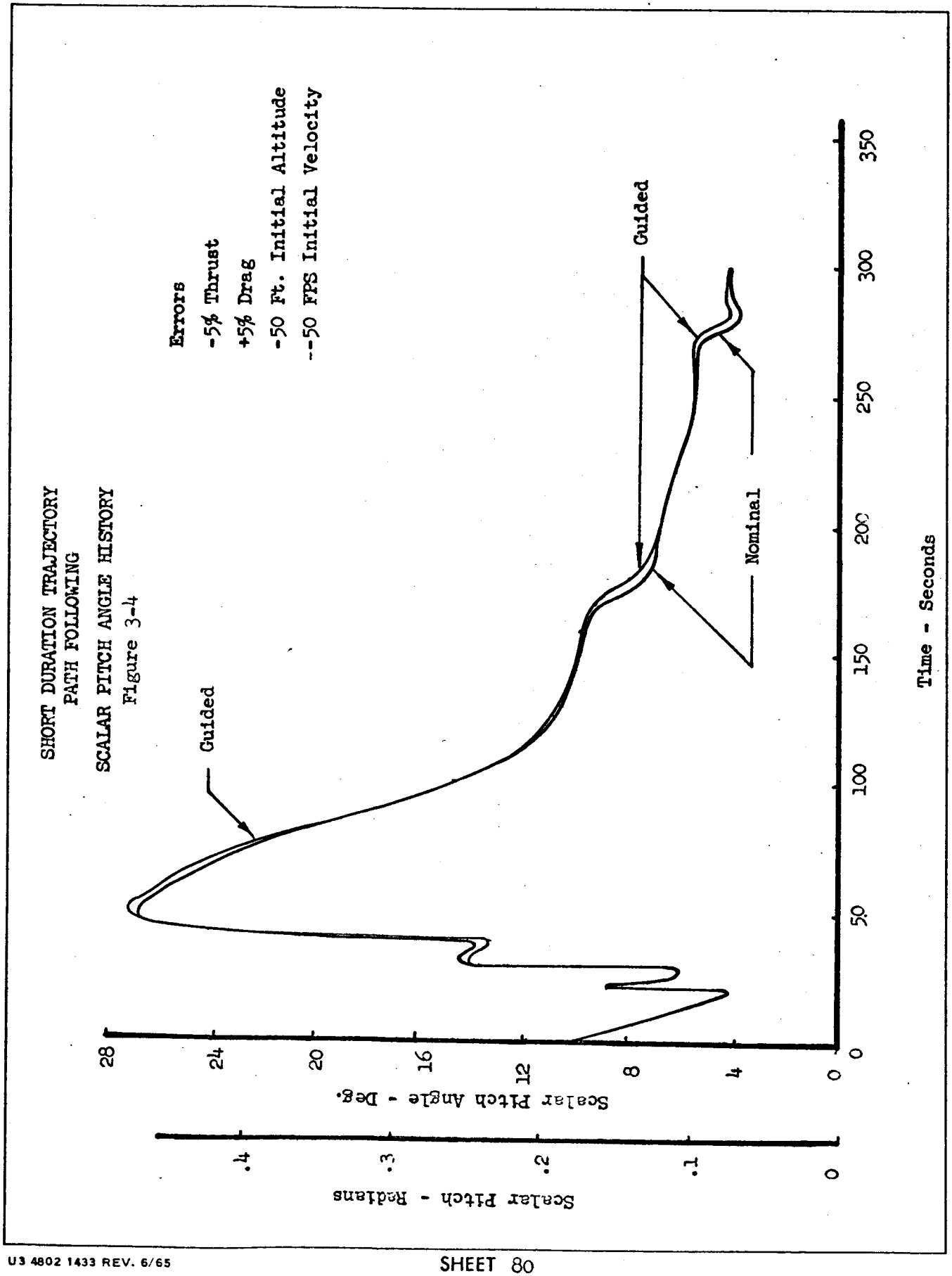

SHORT DURATION TRAJECTORY
PATH FOLLOWING
BANK ANGLE HISTORY

Figure 3-5

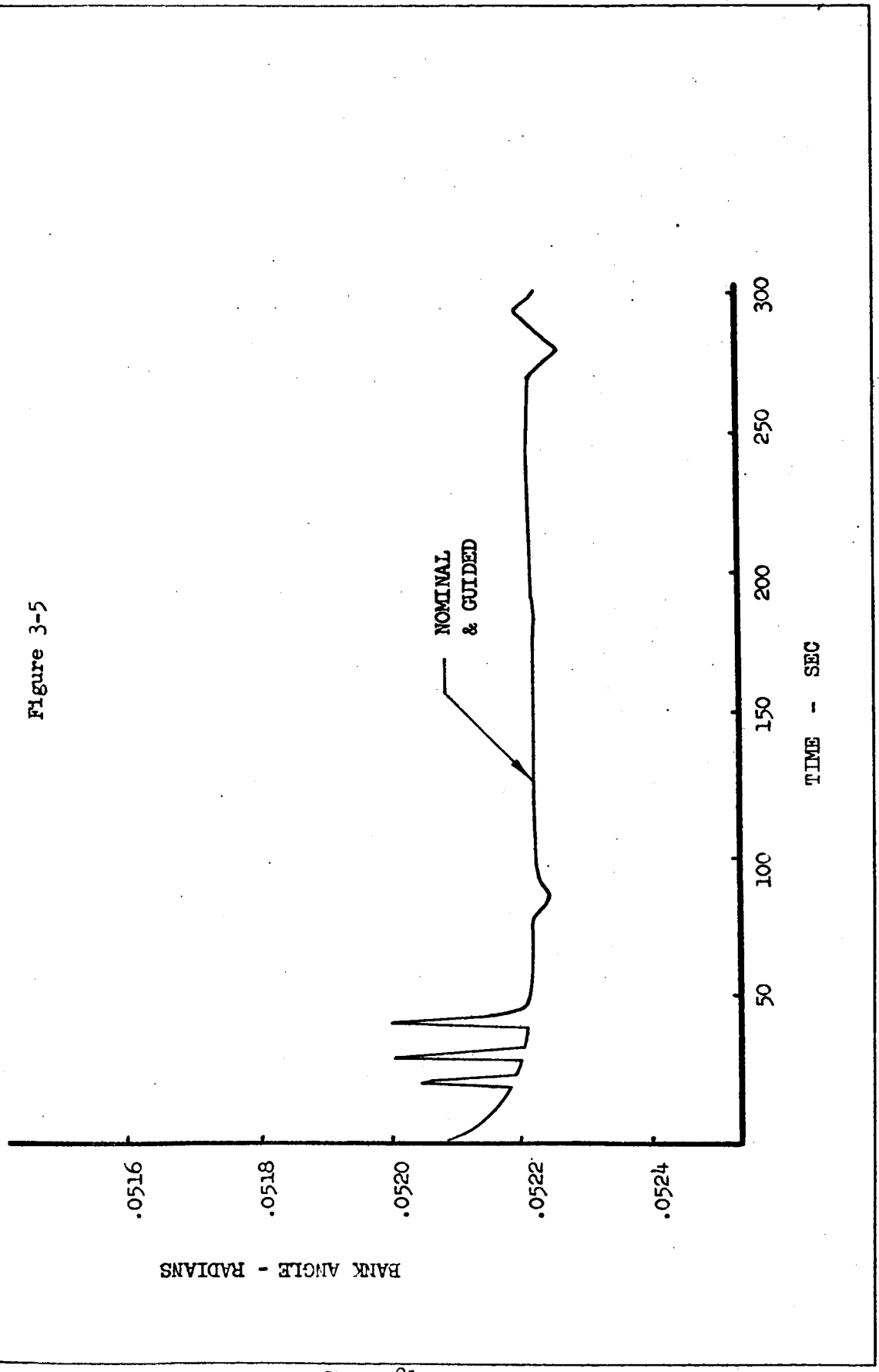

SHORT DURATION TRAJECTORY
PATH FOLLOWING
THROTTLE HISTORY
Figure 3-6

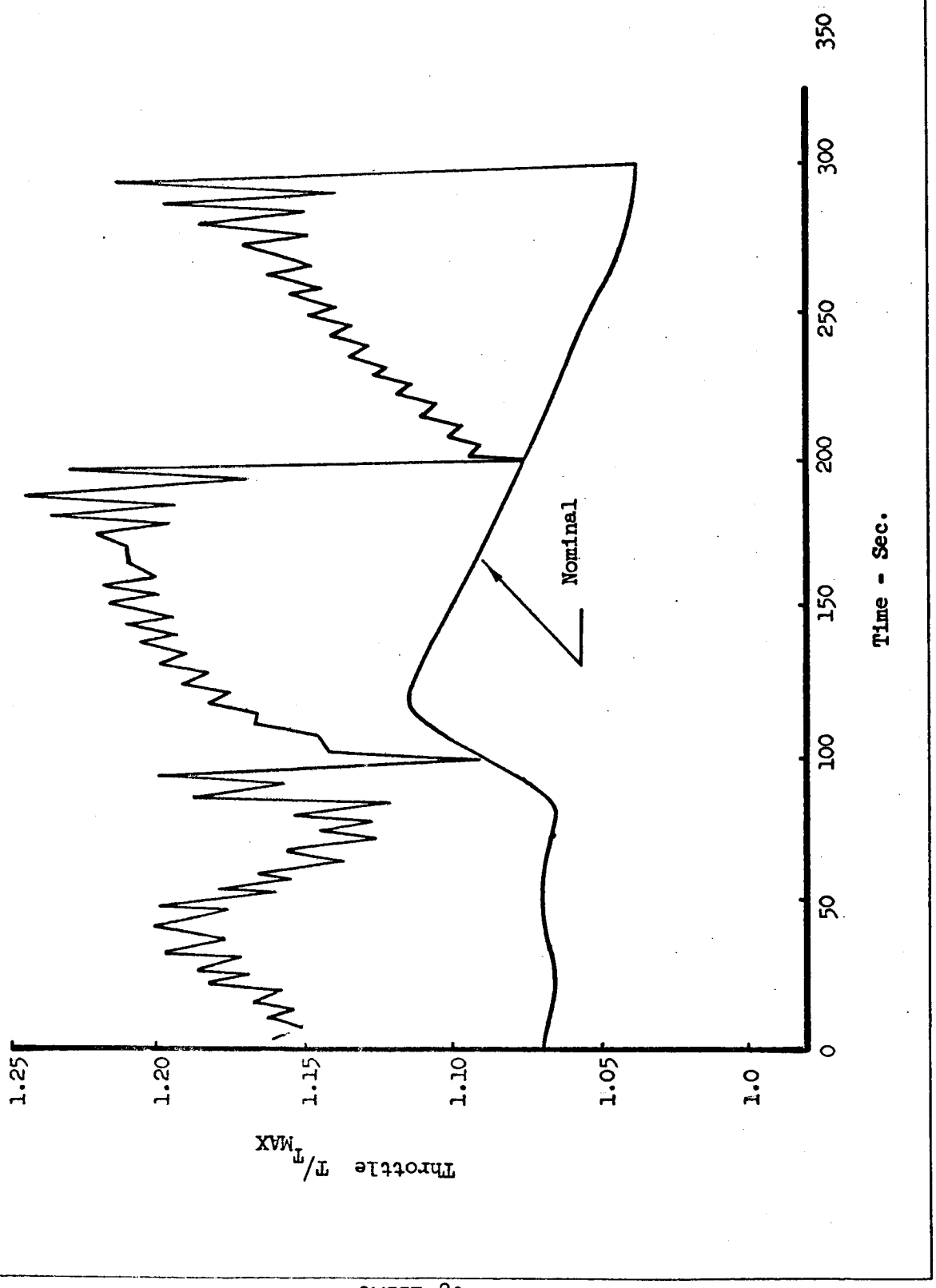

3.4.2 Short Duration Trajectory - Effect of Various Errors

It was concluded in the previous section that the saw-tooth nature of the control corrections was caused by the presence of vehicle characteristic errors. The effect of these error sources propagates without check between guidance update times as discussed in Section 3.4. A separate study of the effect of each error source was undertaken using the first 100 second segment of the preceding section. The results are presented in Figures 3-7 and 3-8. The velocity-altitude plot shows that all guidance trajectories remain in the neighborhood of the nominal path and terminal control is excellent in all cases, and better than the control in the presence of the combined disturbances. The throttle histories are presented in Figure 3-8. It can be seen that the control histories for errors in the state vector are smooth and tend to diminish in magnitude. The control histories for vehicle errors, however, retain the saw-tooth nature of the combined error study. Since the effects of vehicle errors tend to increase with the time in which they develop unchecked, there is a close relationship between the update frequency required and the spectrum of vehicle characteristic errors encountered.

3.4.3 Short Duration Trajectory - Weighting Matrix Variations

Since the weighting matrix used in the previous short duration studies was arbitrarily chosen, the effect of varying the elements is of interest. The dominant control corrections in the previous studies was clearly the throttle. Accordingly the throttle element in the inverse weighting matrix at t = 0.0 was parametrically varied while retaining the linear variation going to zero at the end of the particular 100 second segment. Further the terminal time constraint was abandoned, trajectory termination occurred in all cases on velocity, 568 m/sec. (V = 1863 ft/sec.).

Four guidance cases were simulated corresponding to W_N^{-1} = .1, .01, .001, .0001, where W_N^{-1} is the initial value of the throttle inverse weighting matrix element. The results arepresented in Figures 3-9 to 3-13. The resulting V-h paths are shown in Figures 3-9a to 3-9d. In all cases excellent terminal control results. Further, since the weighting matrix goes to zero after 100 seconds of flight, the control correction ceases at this point. A corollary to this is that the path should be regained after 100 seconds. This behavior can be seen in Figure 3-9.

The weighting matrix variation effect on pitch and bank is shown in Figure 3-10. The largest corrections to these variables occur for W_N^{-1} - .0001, and are shown in Figure 3-10. The correction for the other cases are almost identical to this plot. The throttle history on the other hand shows a marked variation with W_N^{-1} as shown in Figure 3-11. There is a pronounced difference between the corrections for the time free control case and the time fixed correction as shown in Figure 3-12. The terminal mass obtained in these simulations is plotted as a function of the inverse weighting element W_N^{-1} in Figure 3-13.

SHORT DURATION TRAJECTORY
SELECTED VEHICLE AND STATE ERRORS

VELOCITY ALTITUDE PROFILE

Figure 3-7

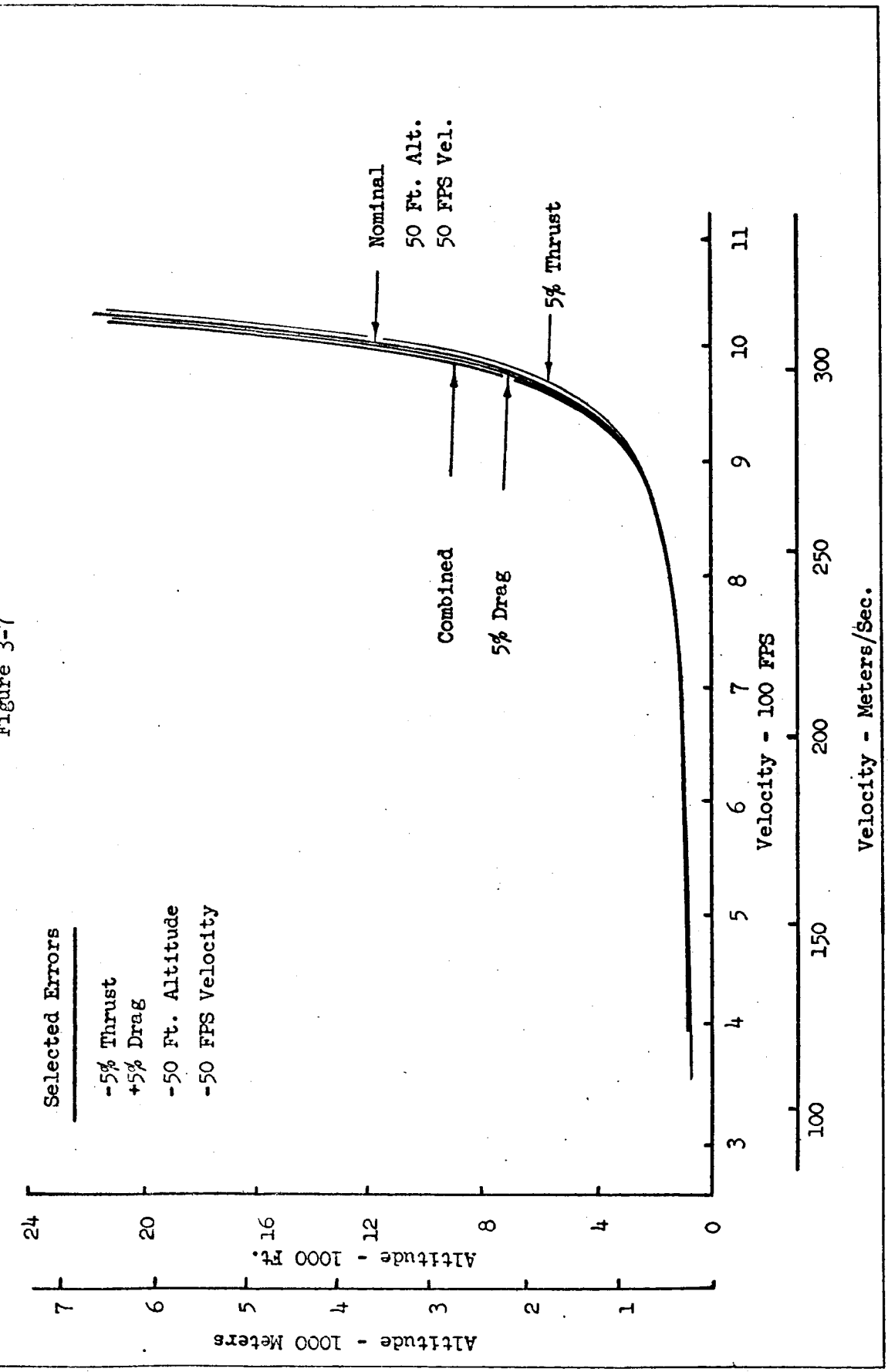

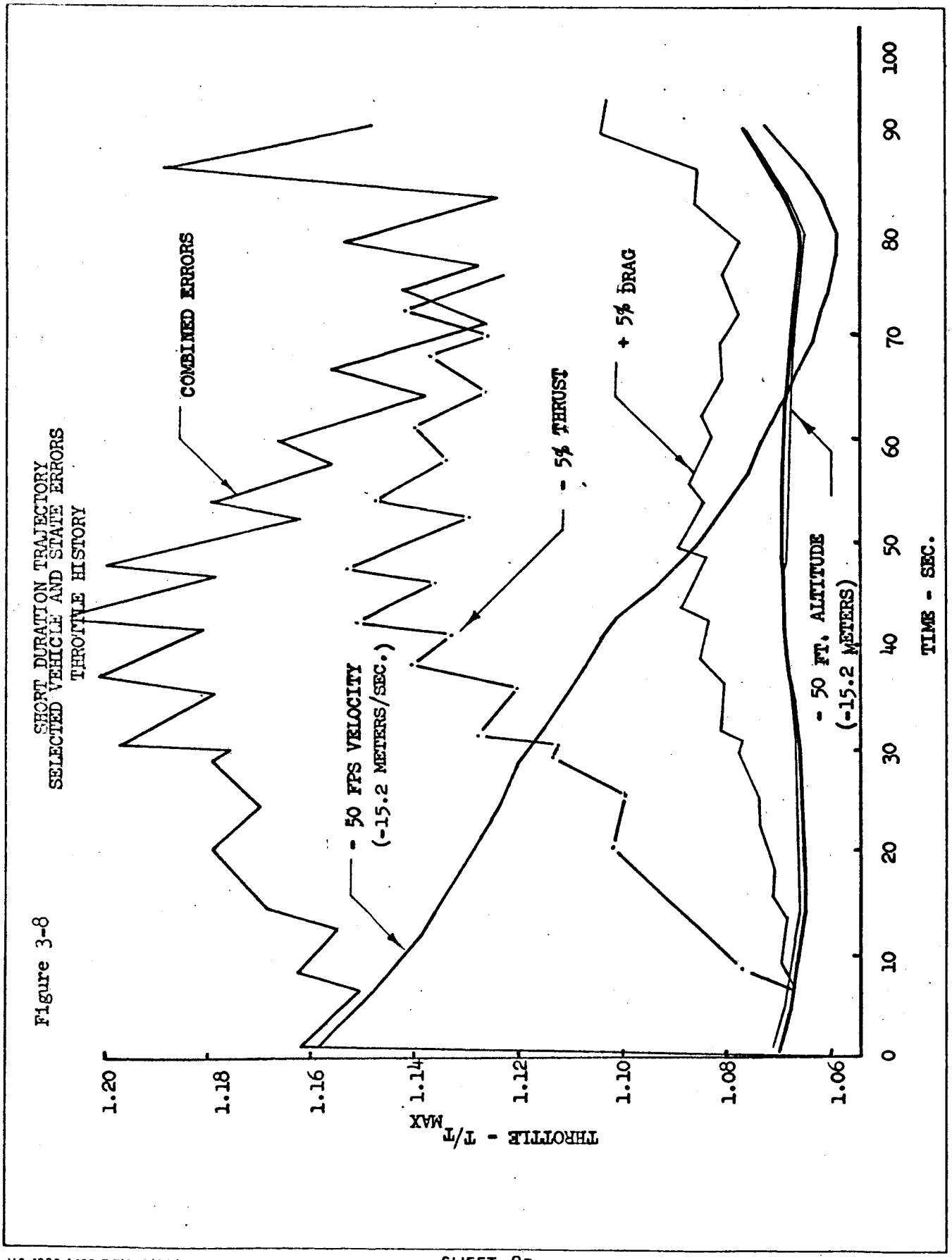

Figure 3-8

SHORT DURATION TRAJECTORY
WEIGHTING MATRIX VARIATION
VELOCITY ALTITUDE PROFILE

Figure 3-9

W_N^{-1} = Inital Value of Throttle Weighting Matrix Element

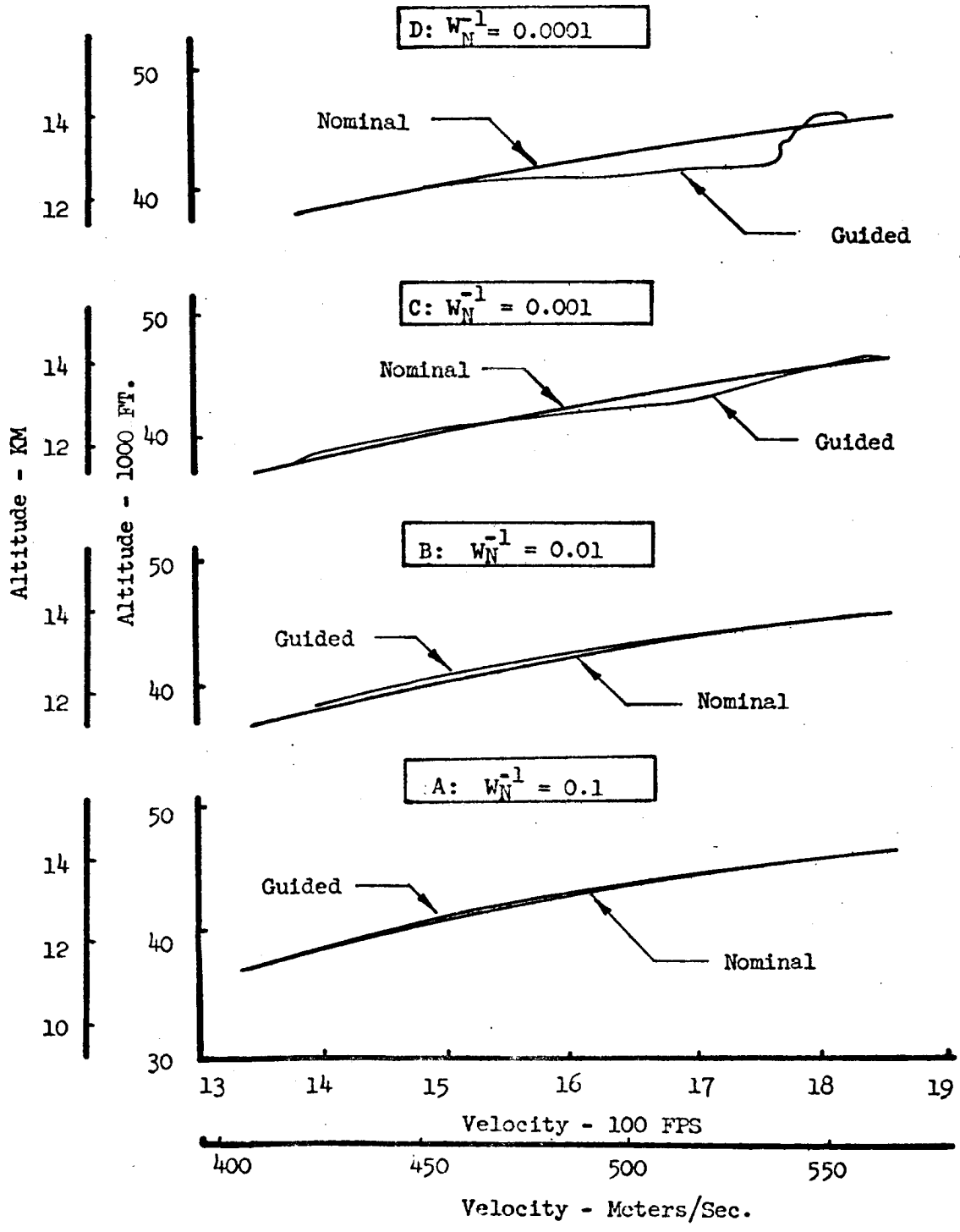

SHORT DURATION TRAJECTORY
WEIGHTING MATRIX VARIATION
SCALAR PITCH AND BANK ANGLE HISTORIES
Figure 3-10

Time Fixed

W_N^{-1} = Initial Value of Throttle Weighting Matrix Element

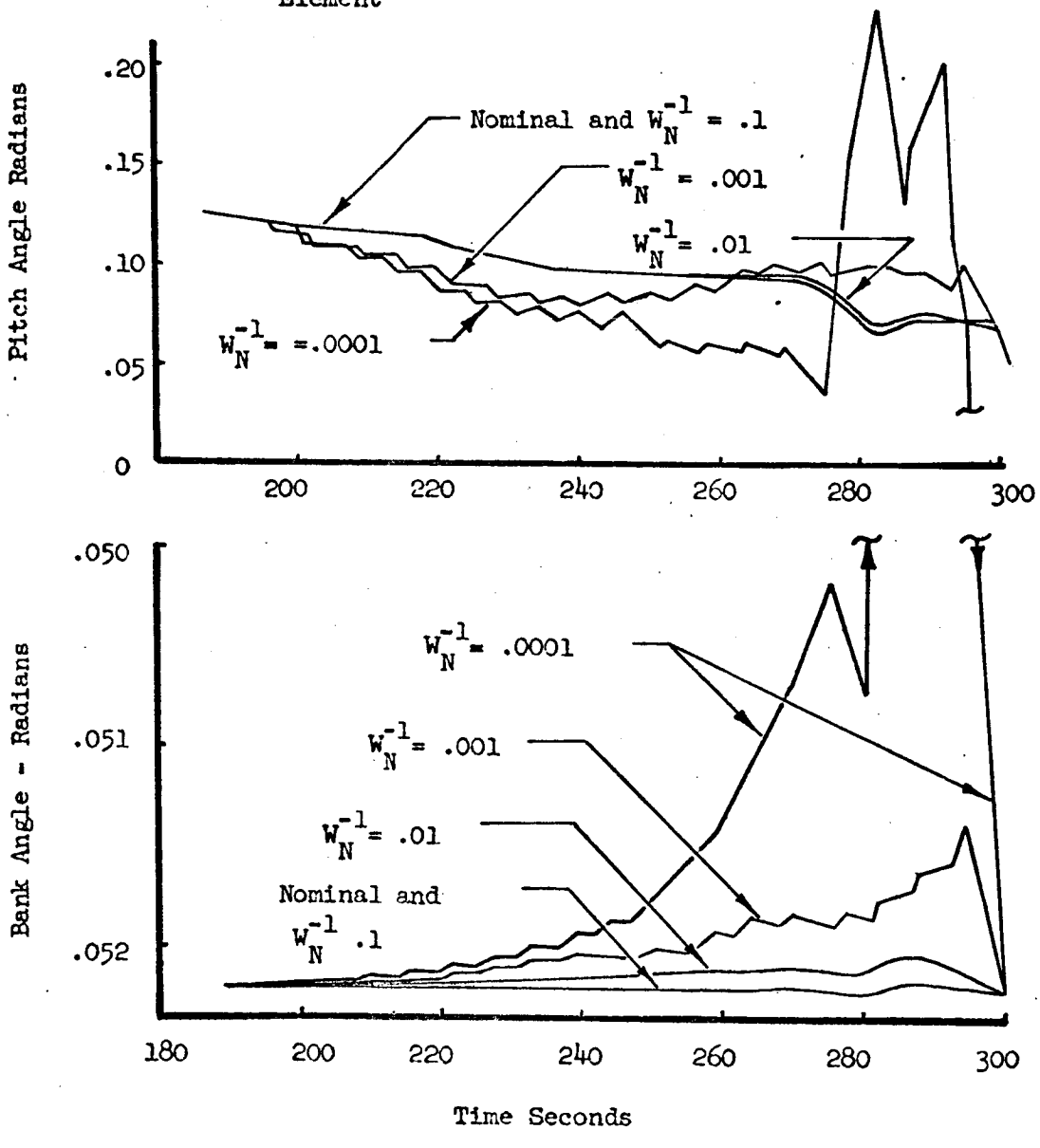

SHORT DURATION TRAJECTORY
WEIGHTING MATRIX VARIATIONS

THROTTLE HISTORY
Figure 3-11

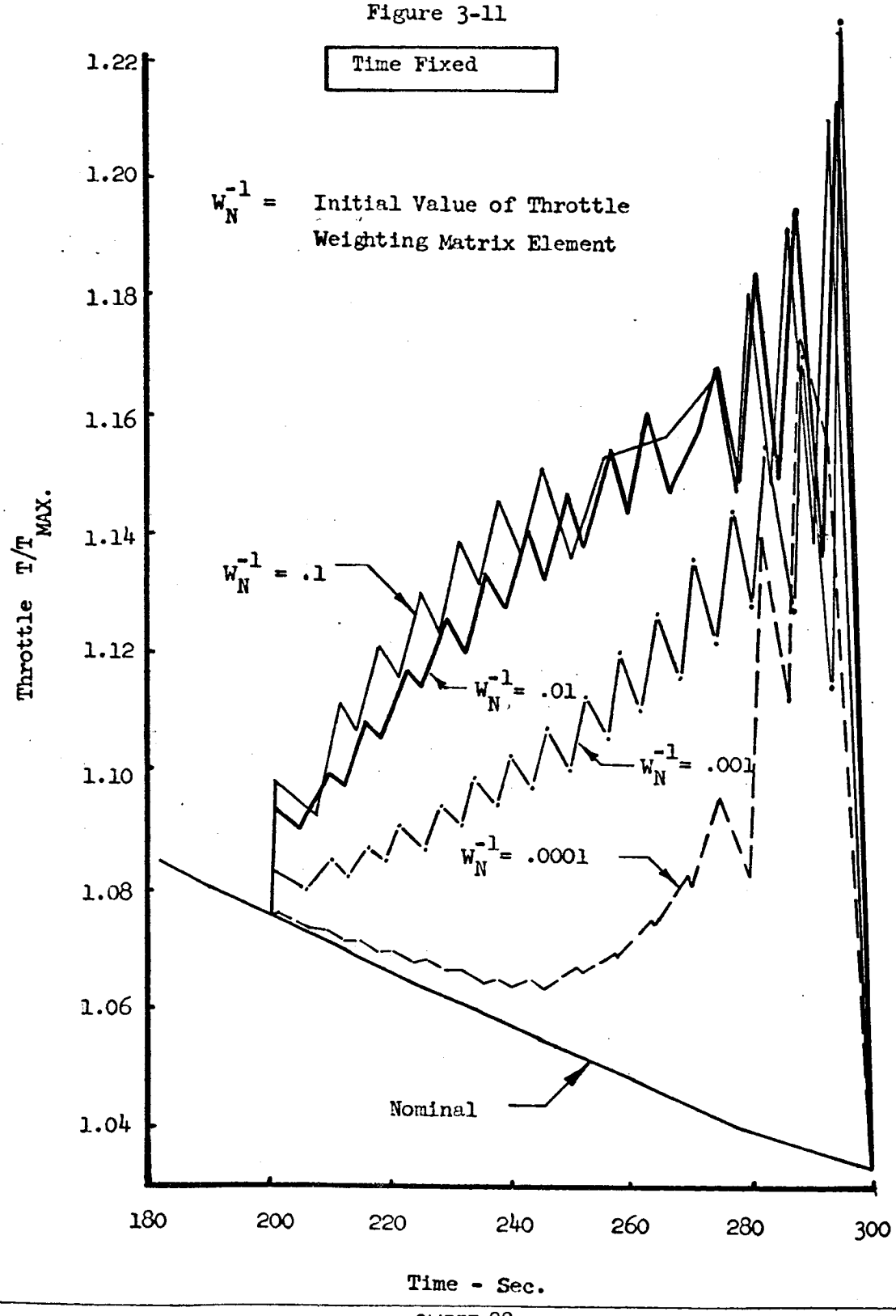

SHORT DURATION TRAJECTORY
TIME CONSTRAINT STUDY
THROTTLE HISTORY
Figure 3-12

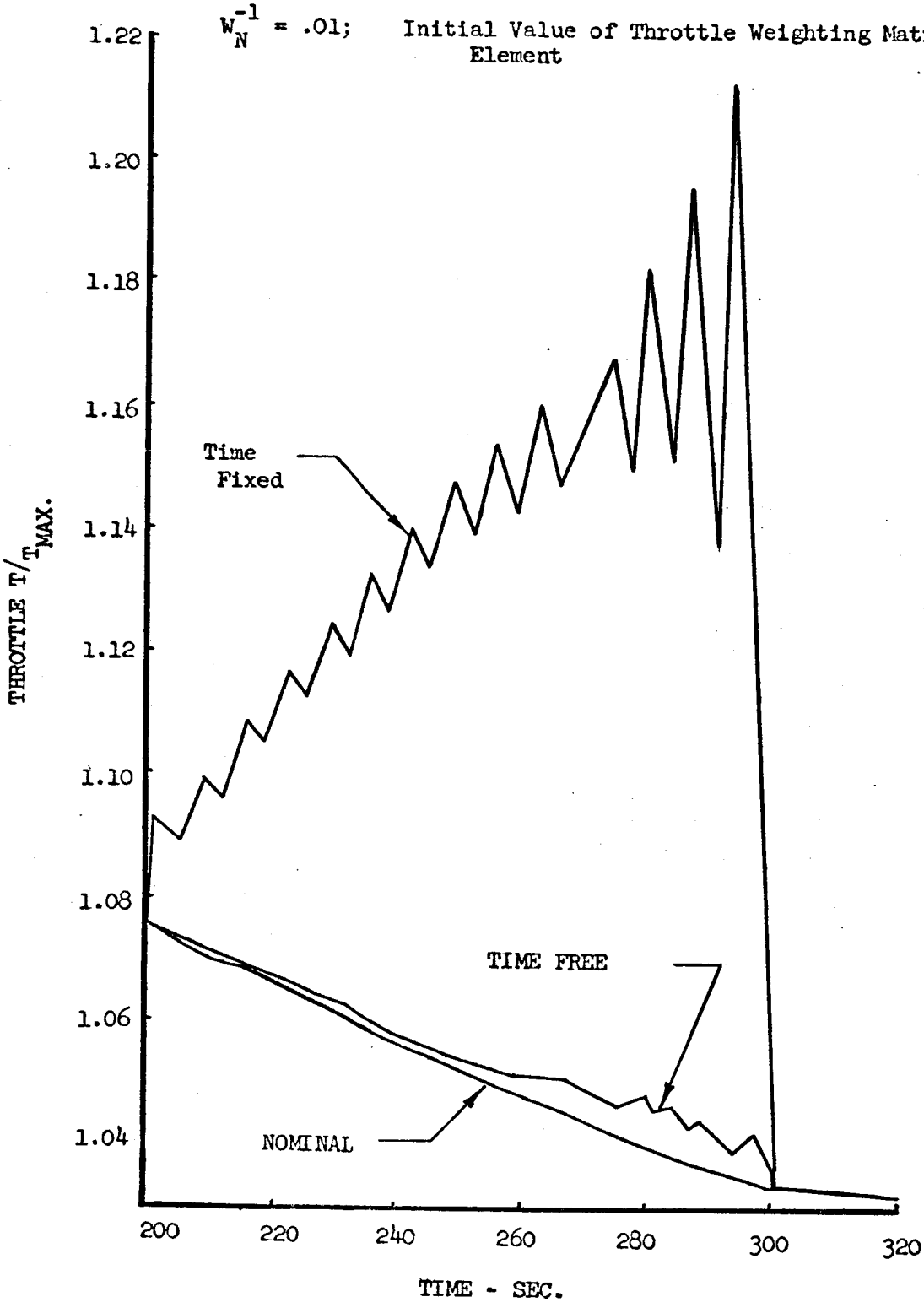

SHORT DURATION TRAJECTORY
EFFECT OF WEIGHTING MATRIX ELEMENT
ON GUIDANCE PENALTY

FIGURE 3-13

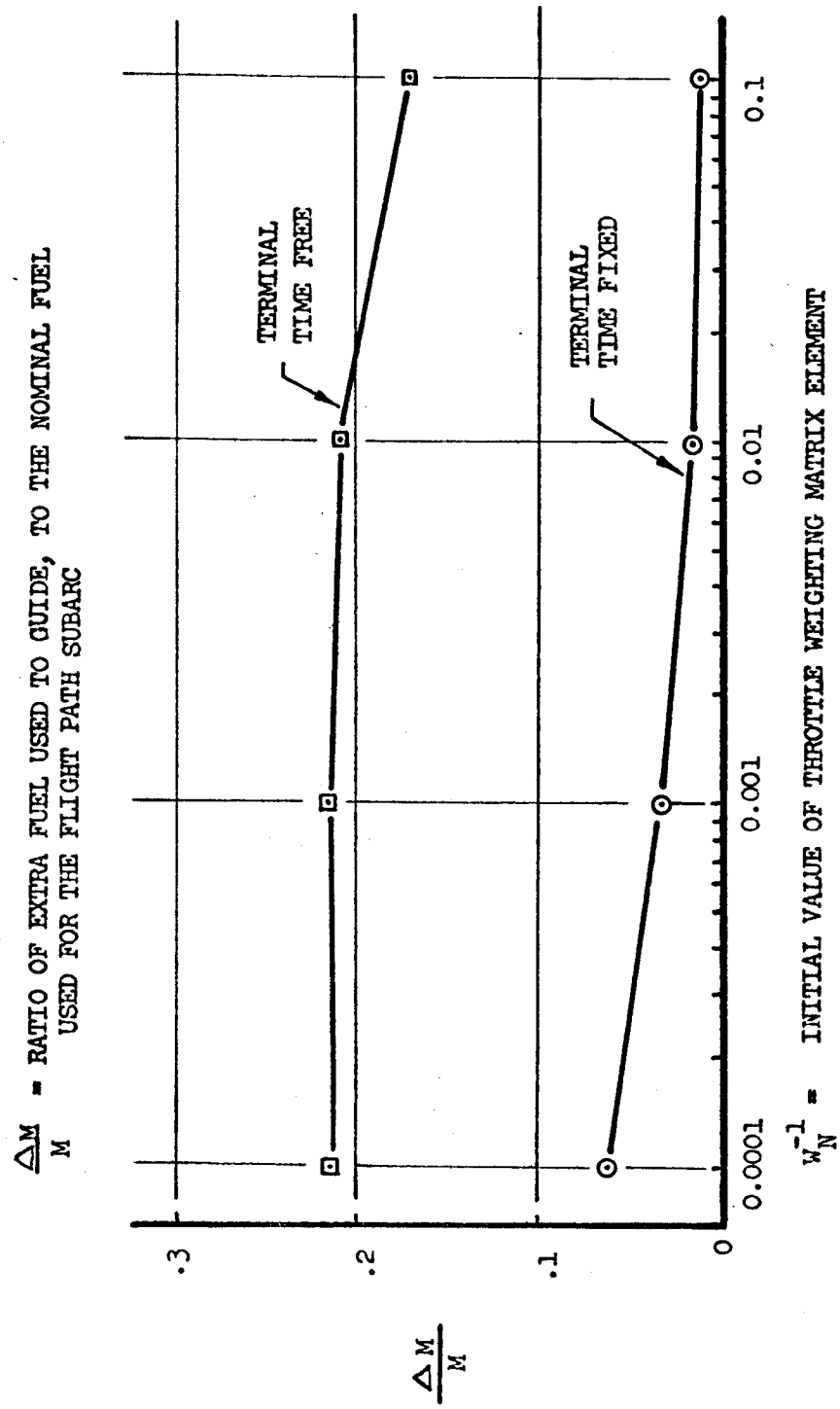

The experience gained by this study of weighting matrix selection on the short duration trajectory was used to guide the choice of the weighting matrix for the more complex problems discussed below.

3.4.4 Short Duration Trajectory - Update Period Study

The effect of update period has been studied on the final 100 second nominal segment with terminal time free and cutoff on velocity. Update periods of 10, 20, 40 and 80 seconds were employed. The resulting V-h profiles and throttle histories are shown in Figures 3-14a and 3-14b. All paths are practically coincident in the V-h plane. The throttle histories of Figure 3-14b show considerable variation with update period. Also shown is the comparable 5 second update from the weighting matrix study.

The maximum amplitude of control correction rises rapidly with increased time between updates. This is shown in Fig. 3-14c.

Later studies of lambda guidance of Stage 1 to the staging point and of Stage 1 from staging to the return base used an update period of 20 seconds. The Stage 1/Stage 2 guidance to the rendezvous point used an update period of 5 seconds.

3.5 The 3704 km (2000 N.M.) Offset Mission

The optimal 3704 km (2000 N.M.) mission flight path control histories from the optimal staging program were used to generate the nominal guidance flight paths of this section. The complete mission is treated in three ways during the following lambda guidance studies. These are

(1) Stage I - Outbound to Staging Point
(2) Stage I - Return
(3) Stage I/Stage II - Orbital Launch to Rendezvous

Since the nominal control histories were generated about an oblate earth whereas the lambda guidance simulator, Section 3.3, is limited to a spherical earth model, the nominal guidance trajectories do show some differences when compared to the final trajectories from the trajectory optimization work. Nevertheless the essential characteristics of the paths remain. It is therefore felt that the results obtained about the chosen nominal guidance paths present a realistic picture of the possibilities of lambda guidance for the vehicle mission under study. During this phase of the study, inequality constraints were not imposed and hence in some cases in-flight boundaries are exceeded. A method for incorporating inequality constraints was developed in the final phase of the study and is discussed in Section 3.6 below.

3.5.1 Stage I - Outbound Guidance to Staging Point

This mission covers the flight of the combined Stage I/Stage II module

SHORT DURATION TRAJECTORY
UPDATE FREQUENCY
FIGURE 3-14

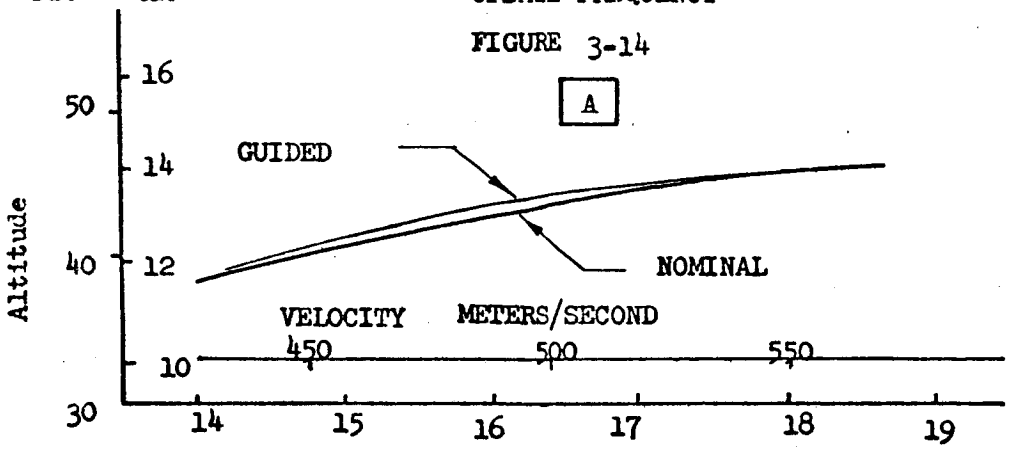

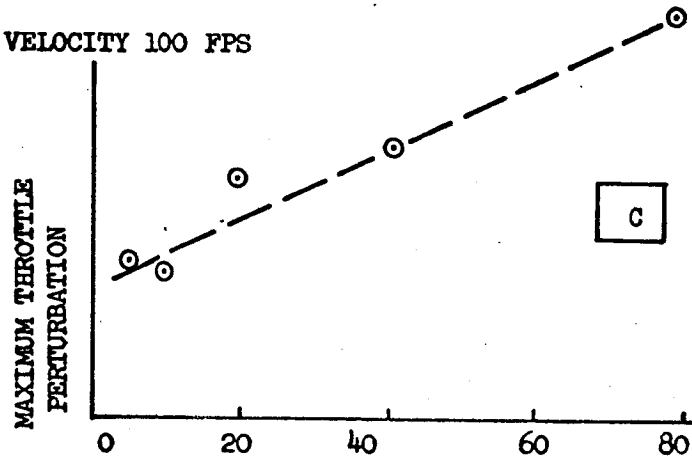

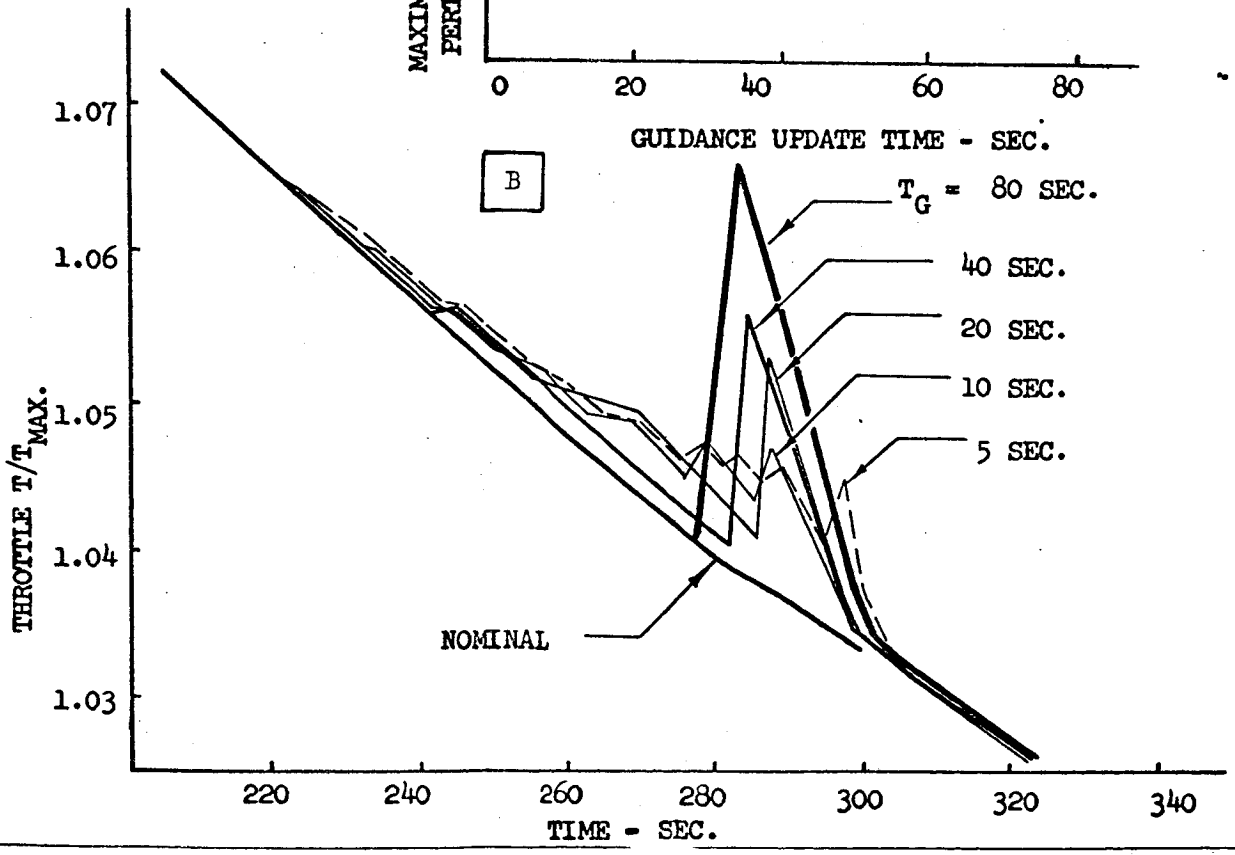

from a point immediately following take-off to the down range stage separation point. The ability of lambda guidance in the maintenance of terminal control at staging is studied when several types of error are encountered during the mission. Included in the error sources are:

(1) One minute timing errors
(2) Vehicle characteristic errors:
Thrust force, (-5%)
Fuel flow, (+5%)
Aerodynamic lift, (-5%)
Aerodynamic drag, (+5%)
(3) Initial state errors, +2,270 kg (+5000 lbs.)

The desired staging time is one of the terminal constraint equations and is used as the cutoff function for the guided case.

3.5.1.1 Timing Error Correction - Following Initial Acceleration and Climb

A timing error of one minute was introduced after 632 seconds of flight time. At this point on the nominal path, the vehicle is climbing through an altitude of 26.2 km (86,000 ft) at a Mach No. of 4.7 and a down range distance of about 417 km (225 N.M.) from the initial point. The timing error was created by the introduction of the state corresponding to t = 692 seconds. At this time the vehicle was passing through 26.8 km (88,000 ft) at M = 5.0, 500 km (270 N.M.) down range. The timing error study retains the nominal control history and control matrices as functions of time; the effect of introducing the state corresponding to t = 692 at the point t = 632 is to lengthen the effective flight time from M = 5.0 to the stage point by 60 seconds.

The nominal Stage I flight path in the altitude-mach plane is shown in Figure 3-15 together with the path generated by the lambda guidance simulator and the path flown if the control is uncorrected. The uncorrected path is the one obtained with the nominal control history in the presence of the timing error. In this plane the unguided path is almost identical to the nominal path whereas the guided path climbs immediately following the error while throttling back. The spatial paths flown are shown in Figs. 3-16 and 3-17 and the weight as a function of range in Fig. 3-18. The control behavior is shown in Figs. 3-19 to 3-21. It can be seen from Figures 3-16 to 3-18 that the lambda guidance simulator maintained good control.

In the Mach-altitude sense, Figure 3-15, an apparent anomaly arises in that the uncorrected control history maintains the end points somewhat better than the guided run did. This is largely fortuitions, being attributable to the nature of the nominal path. This is not surprising since the uncorrected path attains and maintains the cruise condition of about Mach 6.8, so that the terminal synergetic zoom is merely delayed in the order of 60 seconds. There is a small error during the zoom because the vehicle is a little lighter, of

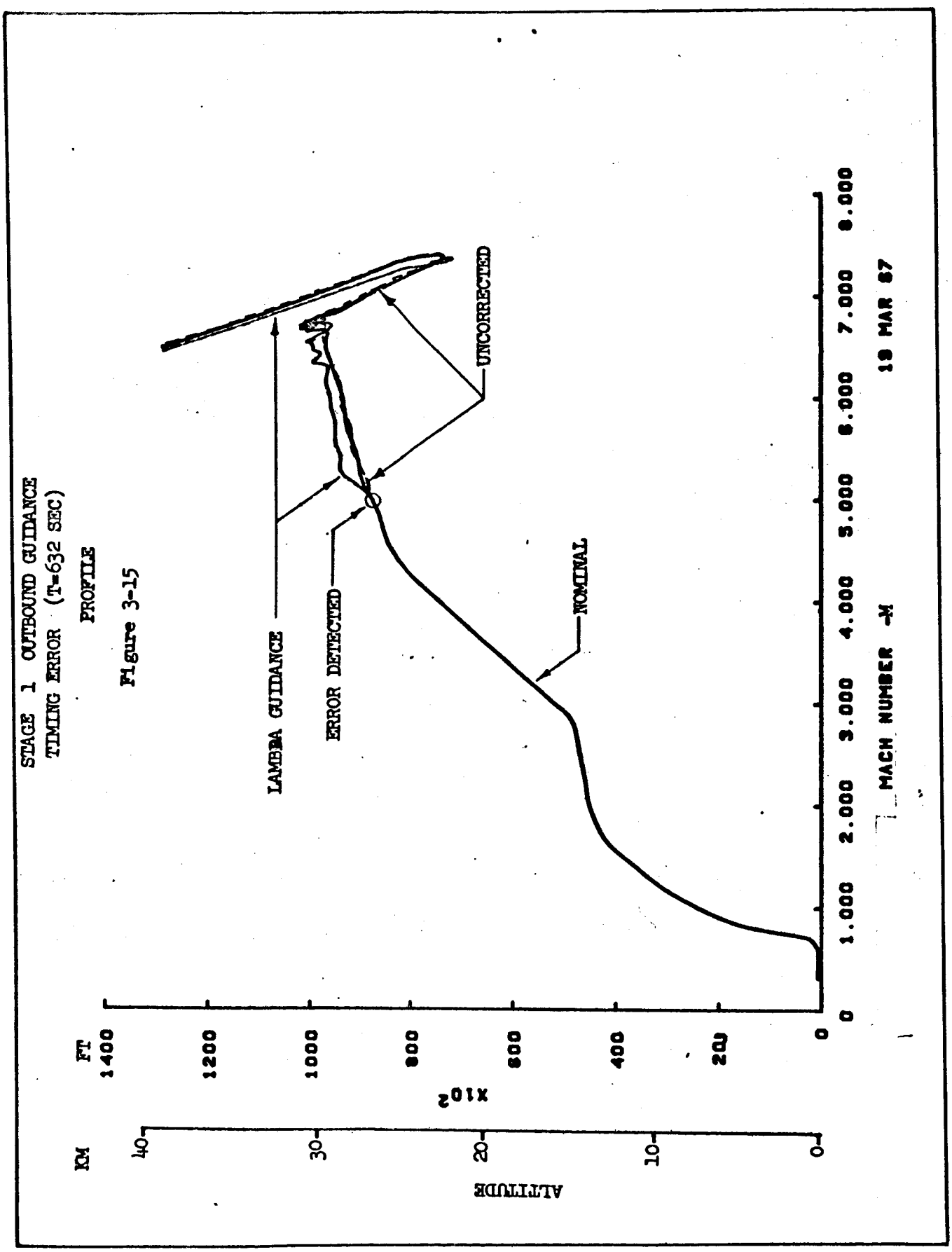

STAGE 1 OUTBOUND GUIDANCE
TIMING ERROR (T=632 SEC)
GROUND TRACK

Figure 3-16

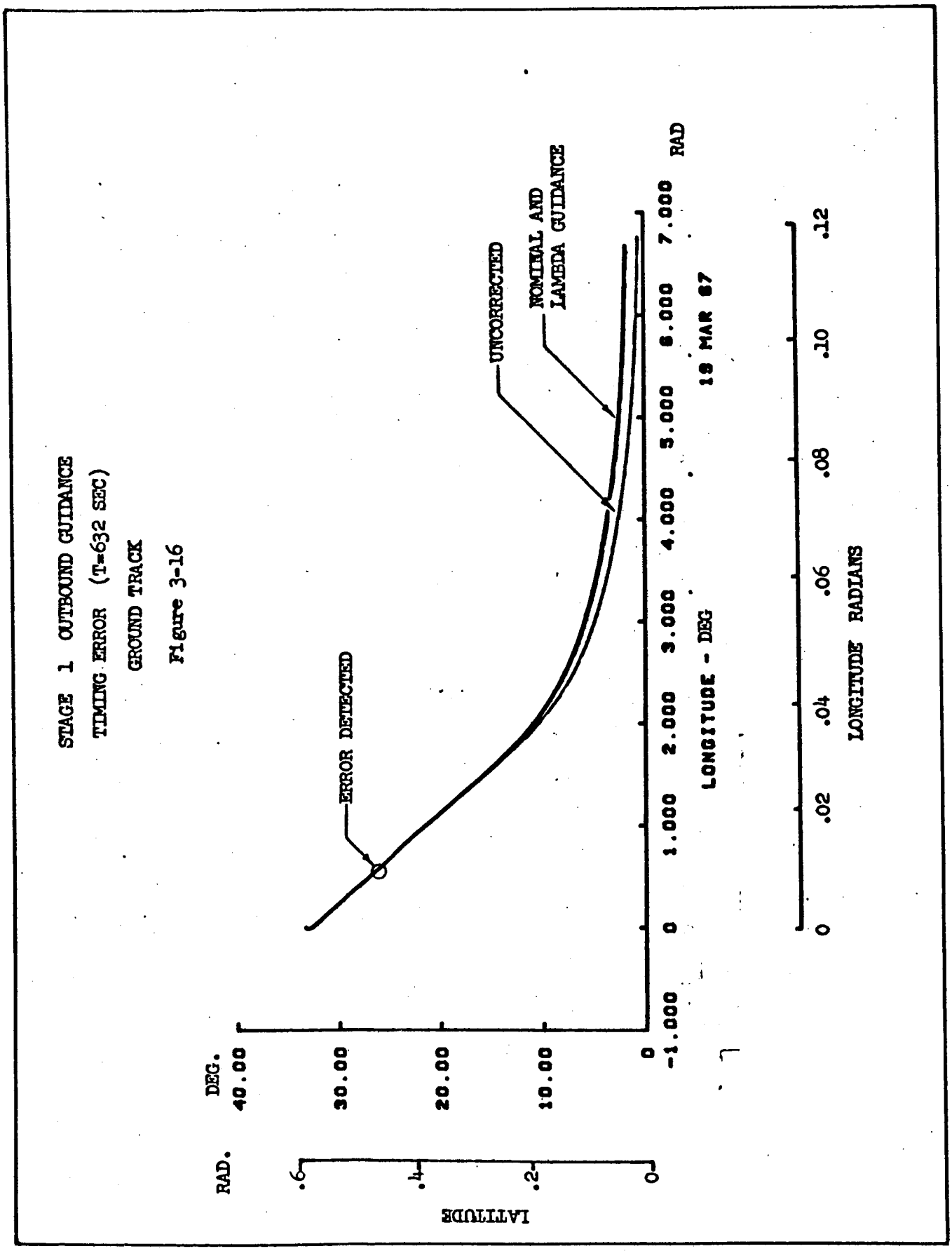

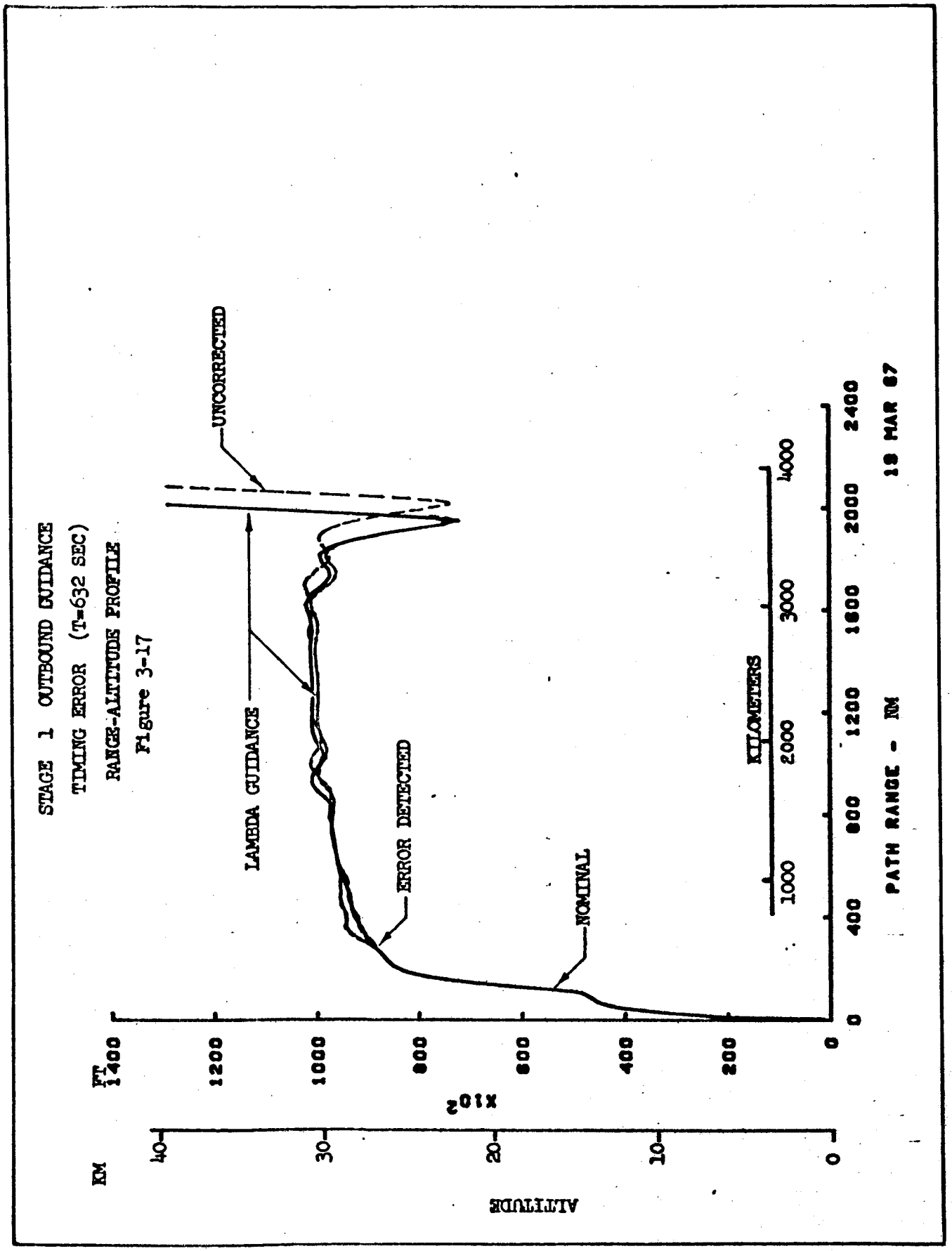

STAGE 1 OUTBOUND GUIDANCE
TIMING ERROR (T=632 SEC)
RANGE-MASS PROFILE

Figure 3-18

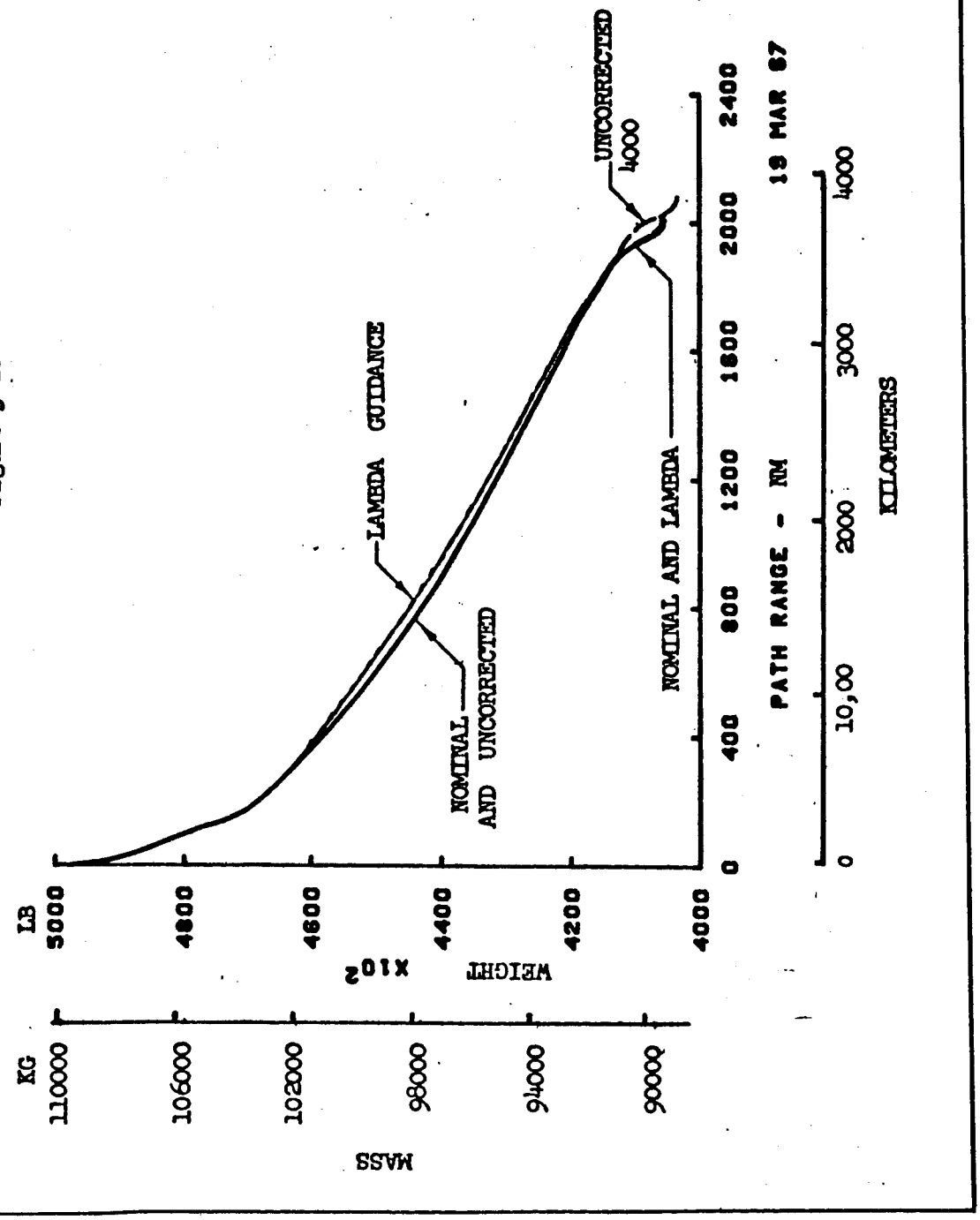

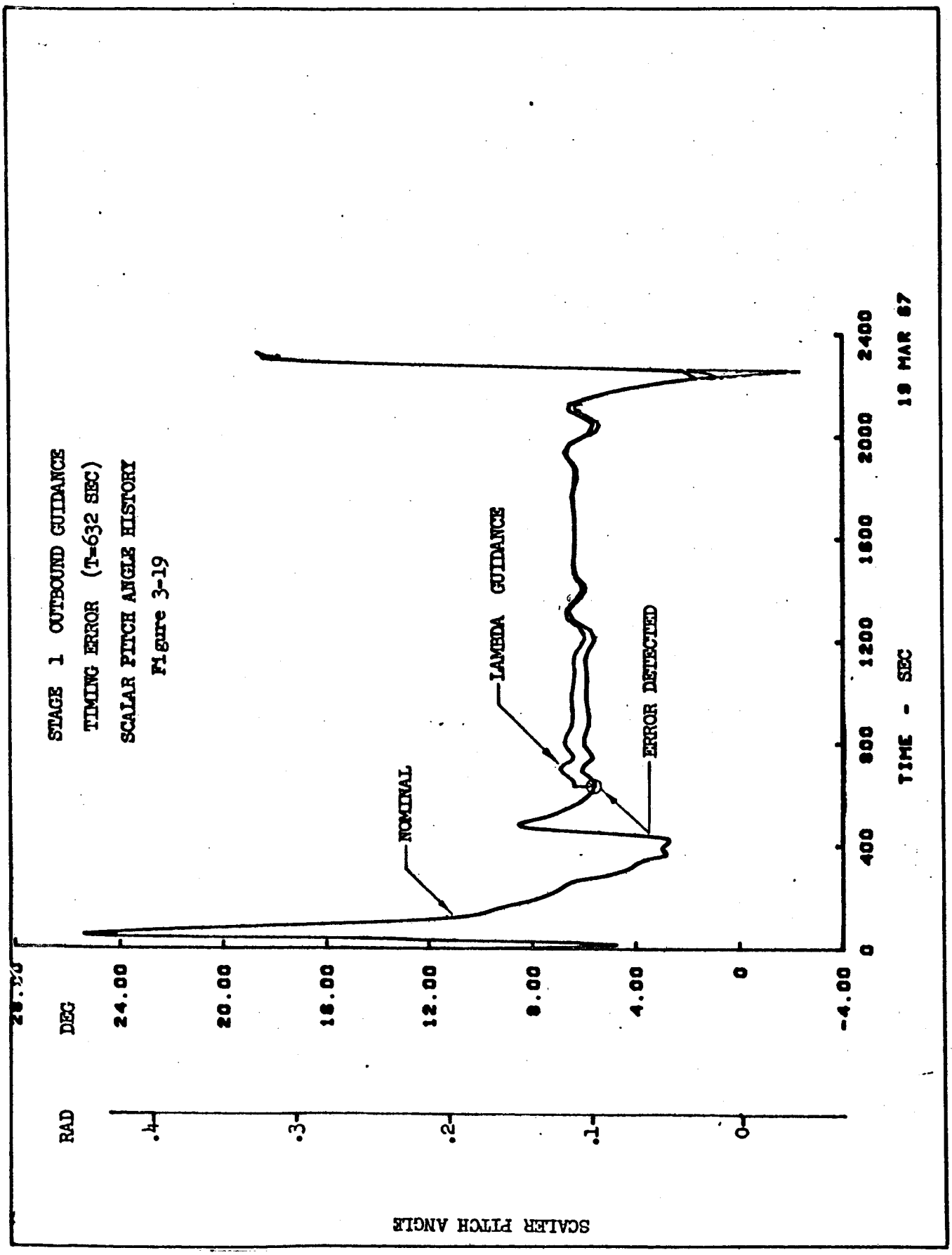

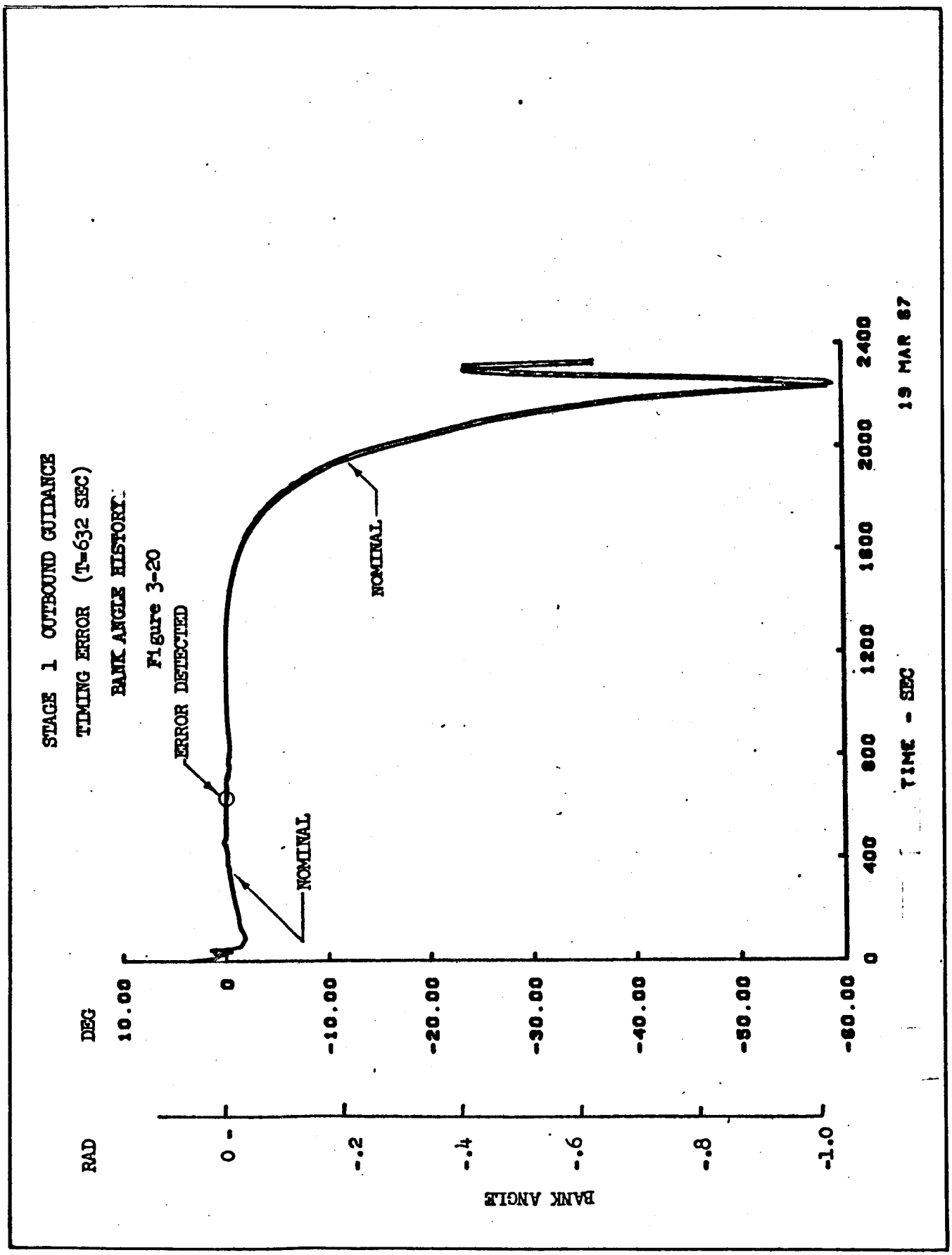

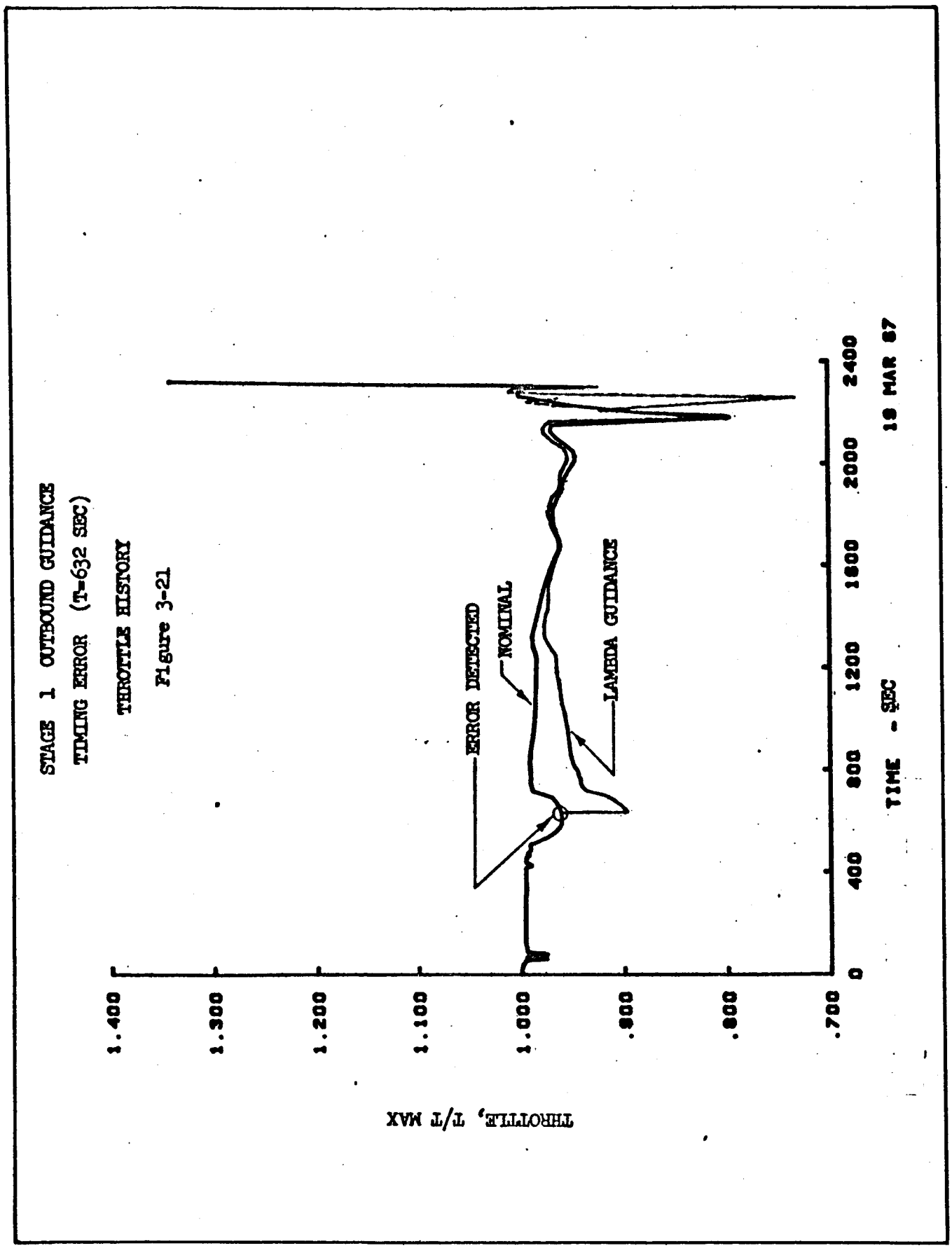

the order of $\frac{1}{2}\%$. This has little effect on the final maneuver and hence, in a V-h sense, the uncorrected path is in close agreement with the nominal. The actual terminal errors from this study for all state components were as follows:

State Component Error	Guided	Uncorrected
Weight, kg (lbs)	+ 225 (+496.1)	-805 (-1874.4)
Altitude, m (ft)	- 6.7 (-21.9)	+ 61.3 (+200.4)
Flight Path Angle, Deg.	+.075	-.004
Velocity, m/sec (FPS)	12.6 (-41.5)	+ 3.9 (+12.9)
Latitude, deg.	+ .004	- 1.2
Heading, deg.	- 0.83	- .15
Longitude, deg.	- .003	+ .082

The trajectory termination in this study occurred on time. This variable was constrained to the nominal trajectory value of 2322.6 seconds in all three flight paths discussed above, in view of the rendezvous condition imposed on the Stage II module.

3.5.1.2 Timing Error Correction - At Flight Commencement

A sixty second timing error was introduced at the initial condition, ($t = 0.0$), in the manner of the preceding section. The nominal and guidance V-h paths are shown in Figure 3-22 and the weight history as a function of path range in Figure 3-23. The ground track, as in the preceding section were practically identical and hence are not shown. The two significant control histories, pitch and throttle, are shown in Figures 3-24 and 3-25. The remaining control variable, bank angle, was not perturbed by a significant amount in this study. Terminal control was maintained to the following accuracy on the guidance trajectory,

State Component	Error
Weight	- 784 kg (-1729.2 lbs.)
Altitude	-37.1 m (-121.6 ft.)
Flight Path Angle	-.021°
Velocity	- 3.8 m/sec. (-12.4 ft/sec.)
Latitude	0.0 ($< .0005°$)
Heading	-.008°
Longitude	-.001°

Time is used as the cutoff condition at staging. The mass loss occurs largely in the initial climb and acceleration, Figure 3-23. It can be seen from the control history plots of Figures 3-24 and 3-25, that the major portion of the control correction occurs during the initial phase of the mission, for the weighting matrix chosen for the study. This result may be improved as further knowledge in the

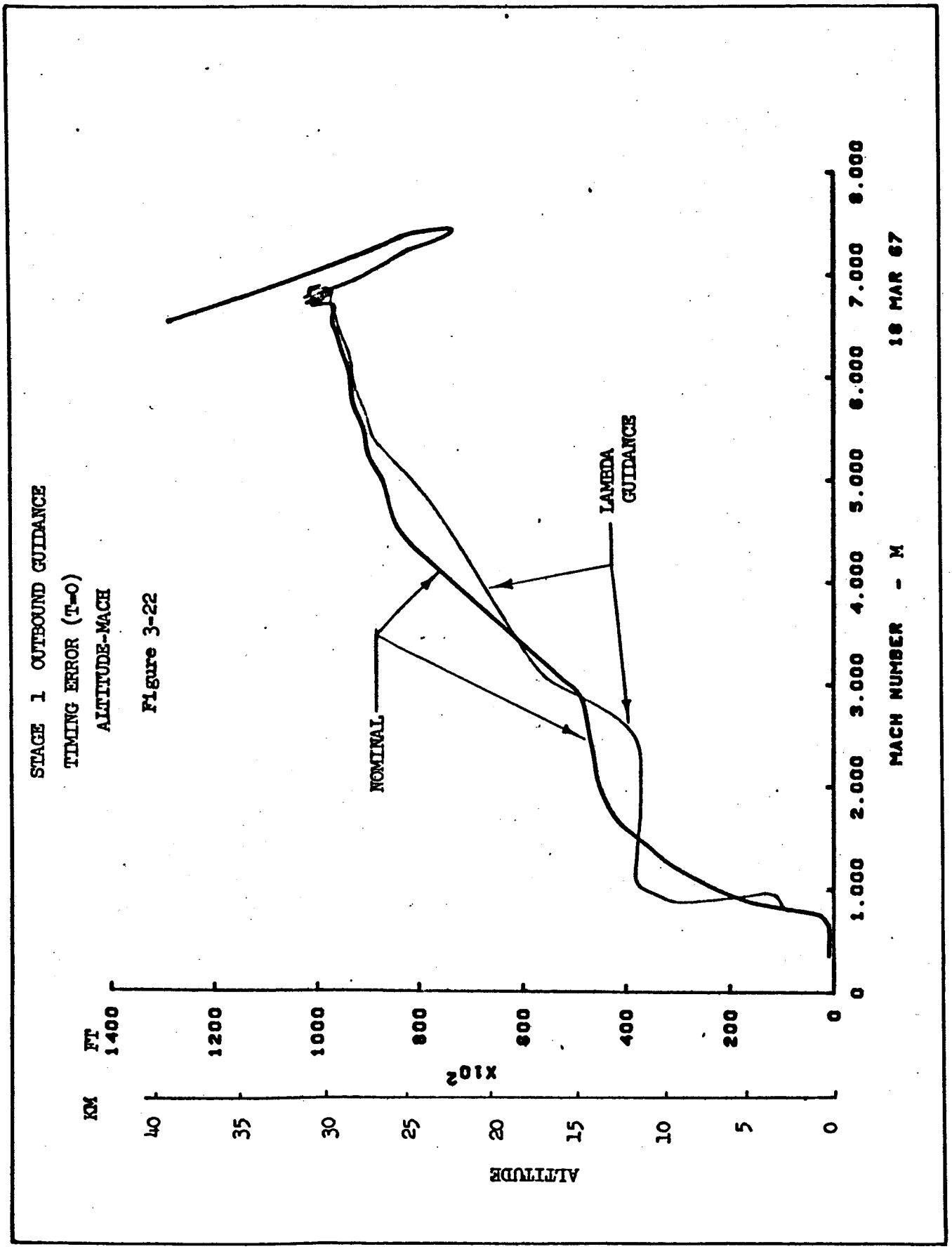

STAGE 1 OUTBOUND GUIDANCE
TIMING ERROR (T=0)
RANGE-ALTITUDE PROFILE

Figure 3-23

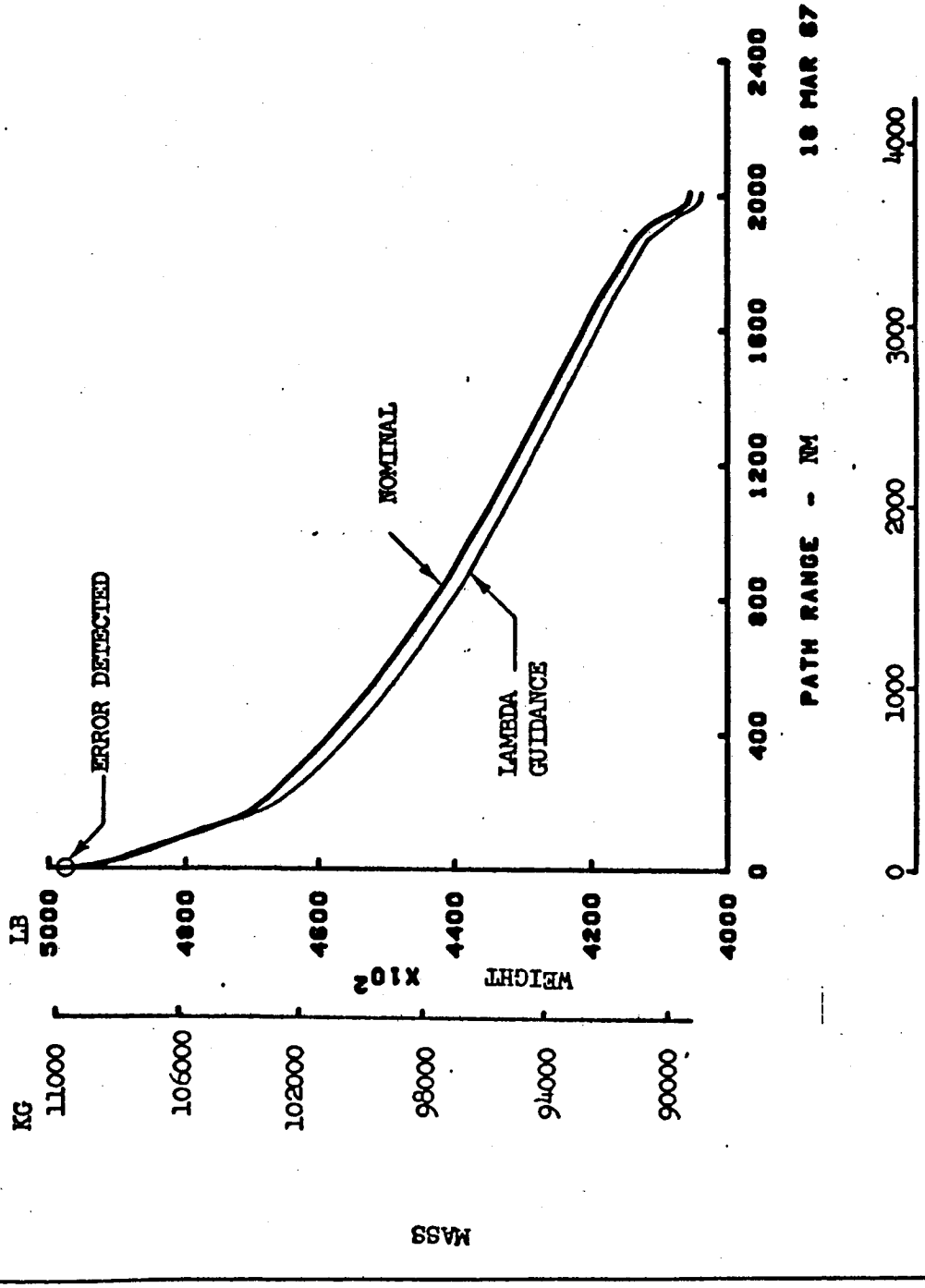

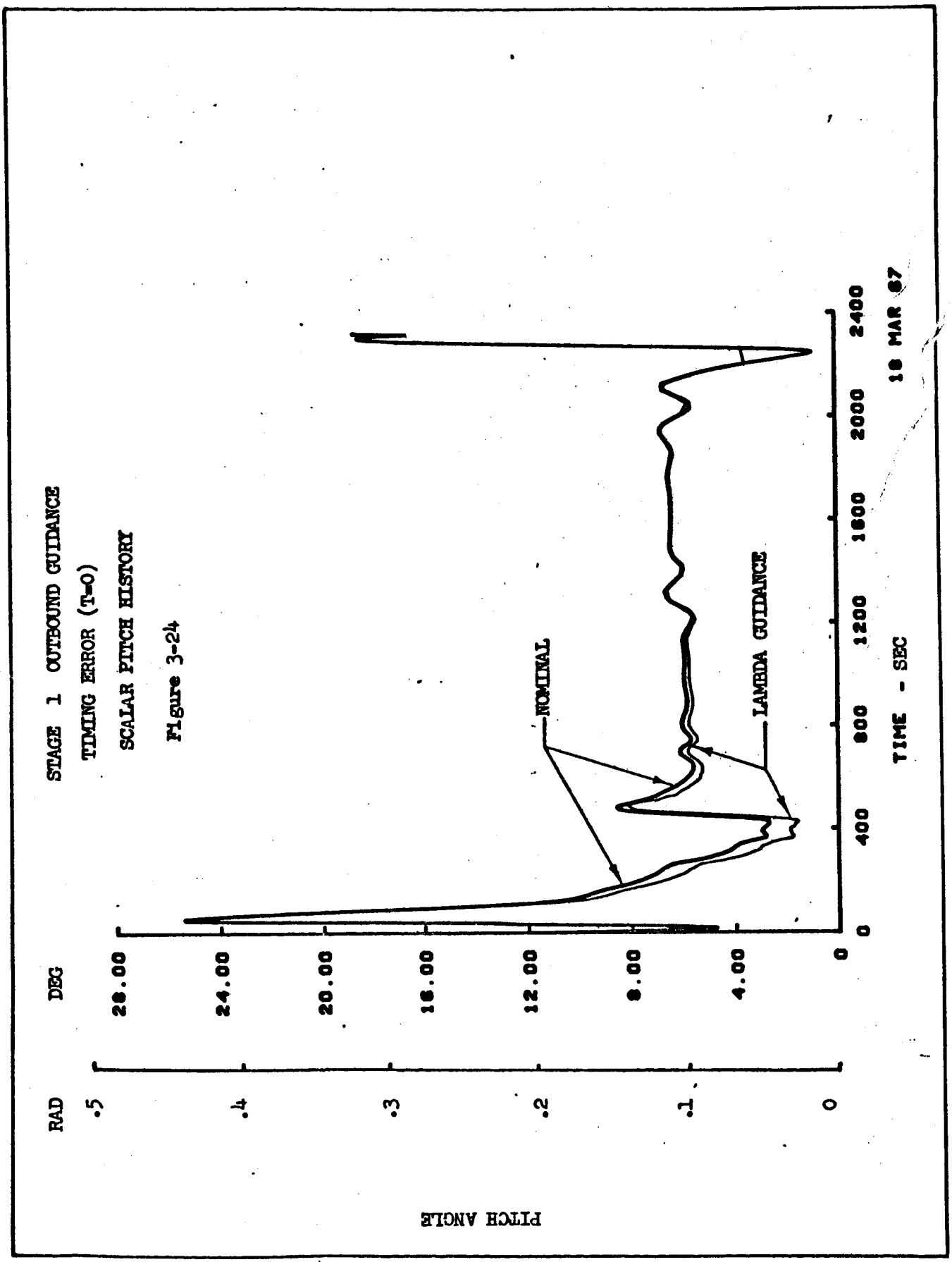

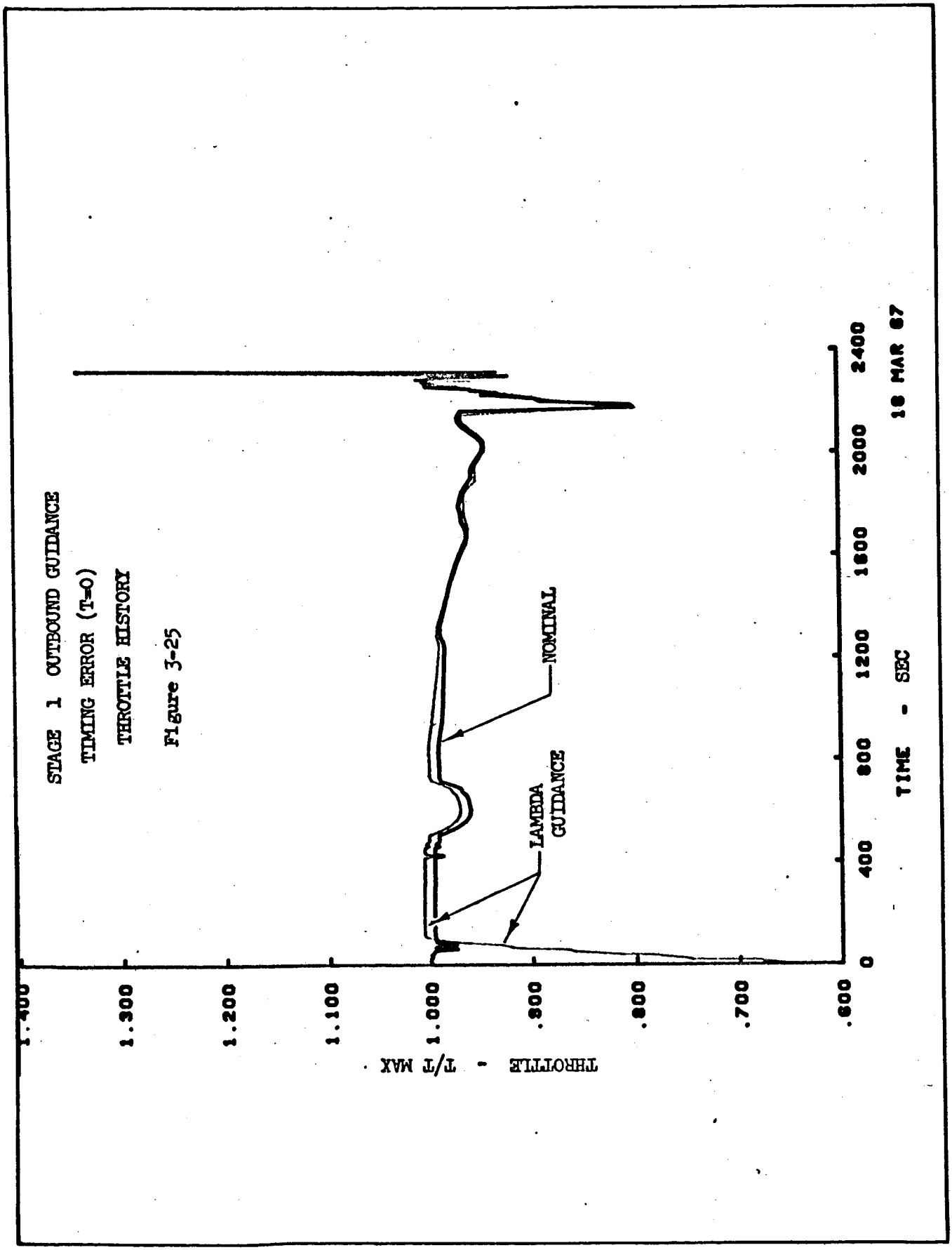

selection of these matrices is gained. The current method of correcting timing errors probably overestimates the control correction needed because the present lambda guidance simulator introduces timing errors in an indirect manner. The state corresponding to the time change, ΔT, is introduced at the error point; the nominal control history is then updated on the basis of corrections computed for the nominal time; hence an additional control error is present because of the time shift.

An alternate approach for correcting time errors would be to develop a lambda guidance implementation capable of controlling the time of staging. This would introduce timing changes during the cruise portion of the mission simultaneously with other corrective control perturbations. Significant performance improvements may also result if the cost criteria of Eqn. 3.26 were replaced by a minimum fuel cost index as discussed in Section 3.6.3.

3.5.1.3 Correction of Vehicle Characteristic Errors

Lambda guidance has been exercised on the complete Stage I outbound mission in the presence of the vehicle errors defined in Section 3.5.1. The results are shown in Figures 3-26 to 3-28. With the exception of the terminal zoom maneuver, the state errors caused by the vehicle off-nominal conditions are corrected with less deviation from the nominal profile, Figure 3-26, than required in correction of the timing errors of the preceding section. The ground track remains practically unaltered in these studies, as shown in Figure 3-27. The mass history of Figure 3-28 shows a similar variation for each vehicle error, the mass changes at any fixed range do show some variation however.

The terminal performance and constraint errors are presented in Figure 3-29.

The results of the Phase I open loop sensitivity study are included in this table. The Phase II results were obtained from a true closed loop guidance simulation. The Phase I results are merely sensitivities, obtained from a path-following climb-acceleration, followed by hand calculated constant W/δ (weight/pressure ratio) cruise.

Figures 3-30 to 3-33 show the result of flying the open loop control history in the presence of the vehicle characteristics errors. Altitude-range, altitude-Mach number, latitude-longitude, and weight-range plots are compared to the nominal path in these figures. These plots in a sense provide a measure of the size of error corrected by the lambda guidance simulation. It is apparent that the largest errors correspond to the thrust reduction and the drag increase.

3.5.1.4 Correction of Initial State Error

An error simulation was included in the Stage I - Outbound guidance

STAGE 1 OUTBOUND GUIDANCE
VEHICLE CHARACTERISTICS AND MASS ERRORS
GUIDED
ALTITUDE-MACH PROFILE

Figure 3-26

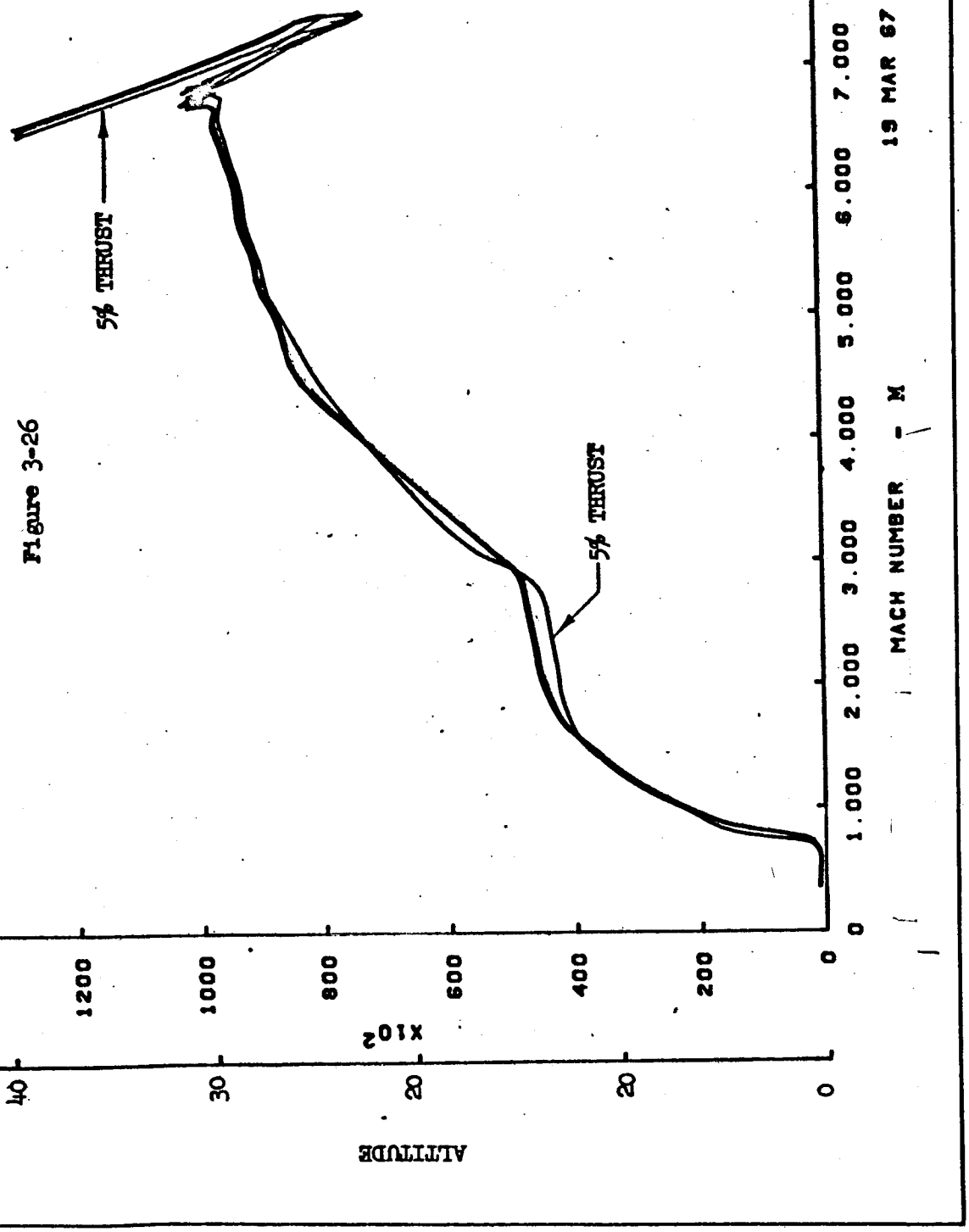

STAGE 1 OUTBOUND GUIDANCE
VEHICLE CHARACTERISTICS AND MASS ERRORS
LATITUDE-LONGITUDE PROFILE
GUIDED

Figure 3-27

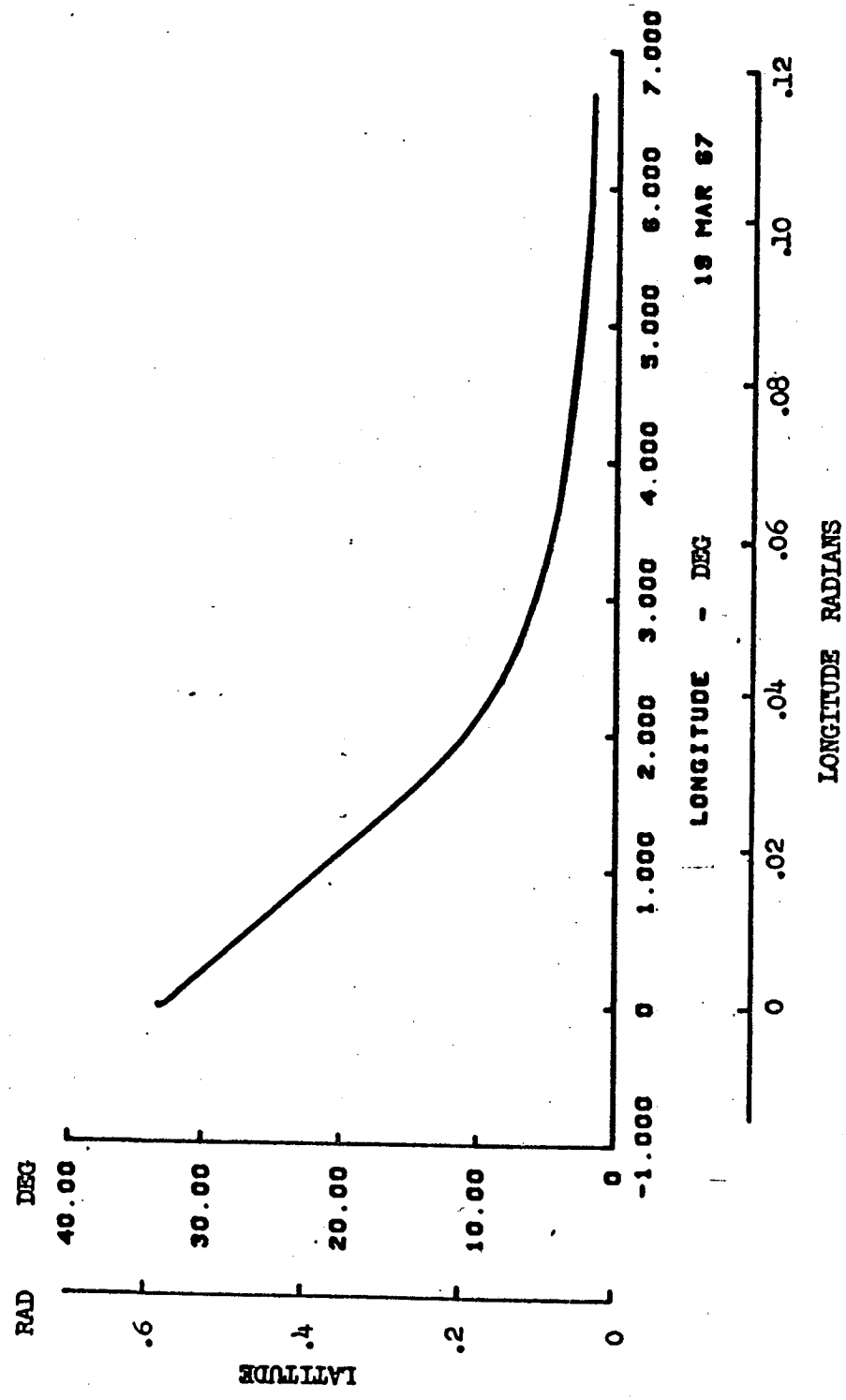

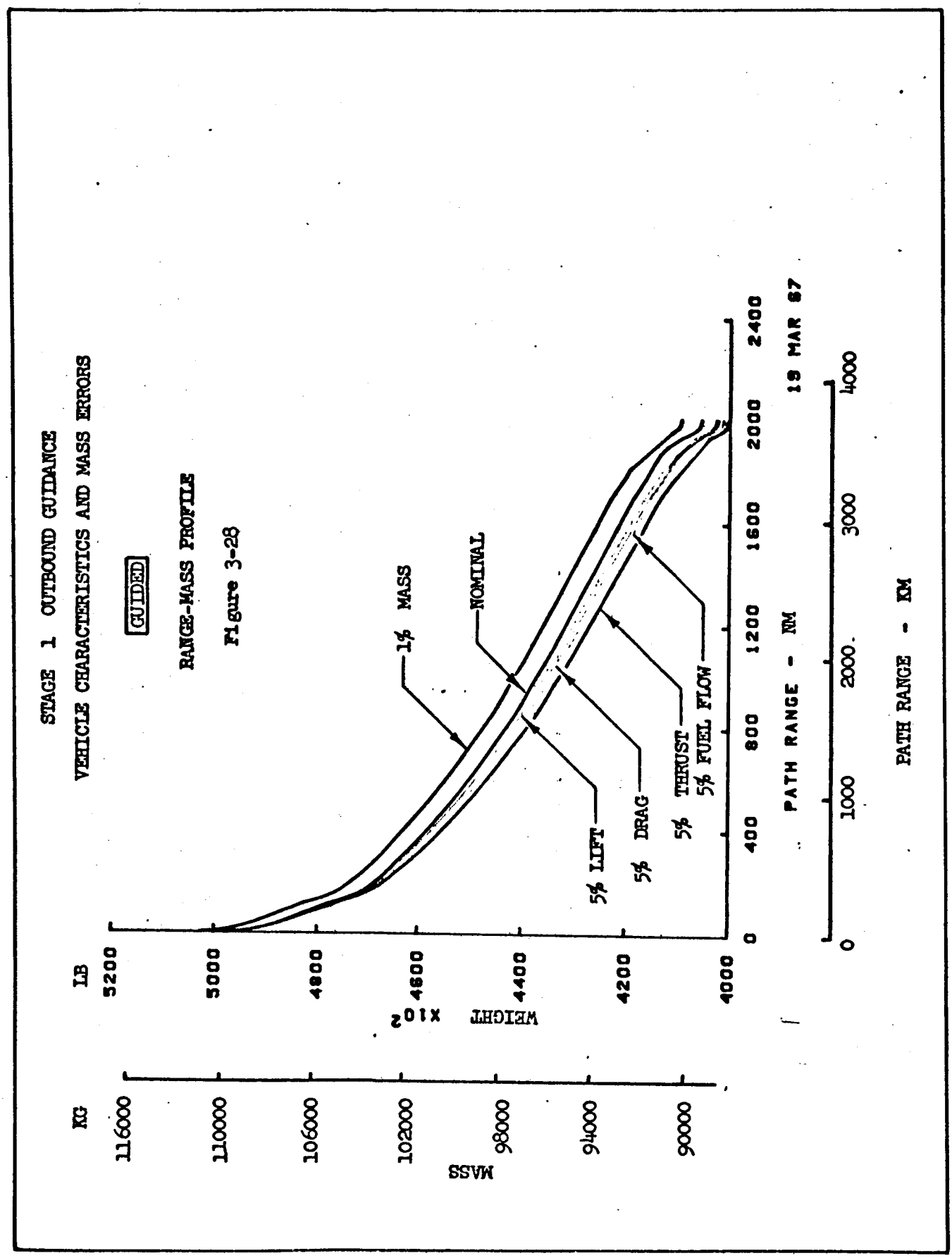

LAMBDA GUIDANCE PERFORMANCE
STAGE I OUTBOUND TO STAGING POINT

Figure 3-29

Error at Staging Due to Off-Nominal Conditions

Off-nominal effect / Constraints	Time + 1 min.	Thrust - 5%	Fuel Flow +5%	Lift -5%	Drag +5%	Initial Weight (+ 5,000 lbs.) + 2,270 kg
Altitude, m (ft.)	-6.7 (-22.)	-148 (-485)	+5.2 (+17)	-4.3 (-14)	-129 (-423)	+79 (+258)
Velocity, m/sec. (FPS)	-13 (-42.)	-21 (-70)	-0.02 (-0.07)	-7.3 (-24.)	-11 (-36.)	-2.4 (-8.0)
Flight Path Angle, deg.	+0.075	-0.02	+0.004	-0.22	-0.04	-0.05
Heading, Deg.	-0.083	+0.13	+0.002	-0.10	+0.041	+0.031
Latitude, Deg.	+0.004	+0.005	0.0	-0.001	+0.001	0.0
Longitude, Deg.	-0.003	-0.008	0.0	-0.002	-0.003	+0.001
Performance Terminal Mass Change kg (lbs.)	+225 (+496.)	-2,370 (-5,244)	-1,870 (-4,124)	-1,260 (-2,777)	-1,560 (-3,244)	-456 (-1,004)
Phase I Sensitivity, kg (lb)		-1450 (-3200)	-2400 (-5300)	-1350 (-2970)	-2220 (-4660)	-540 (-1190)

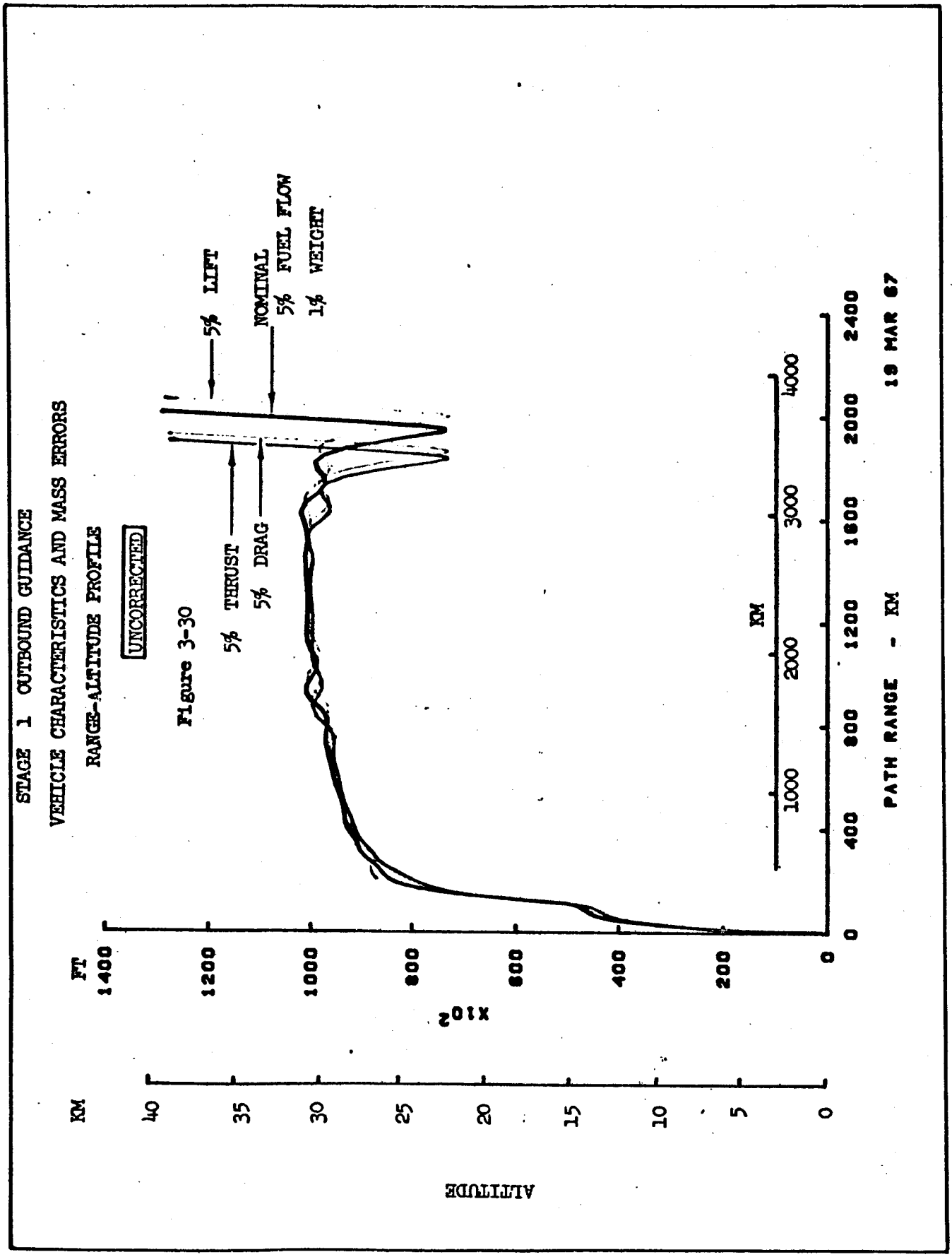

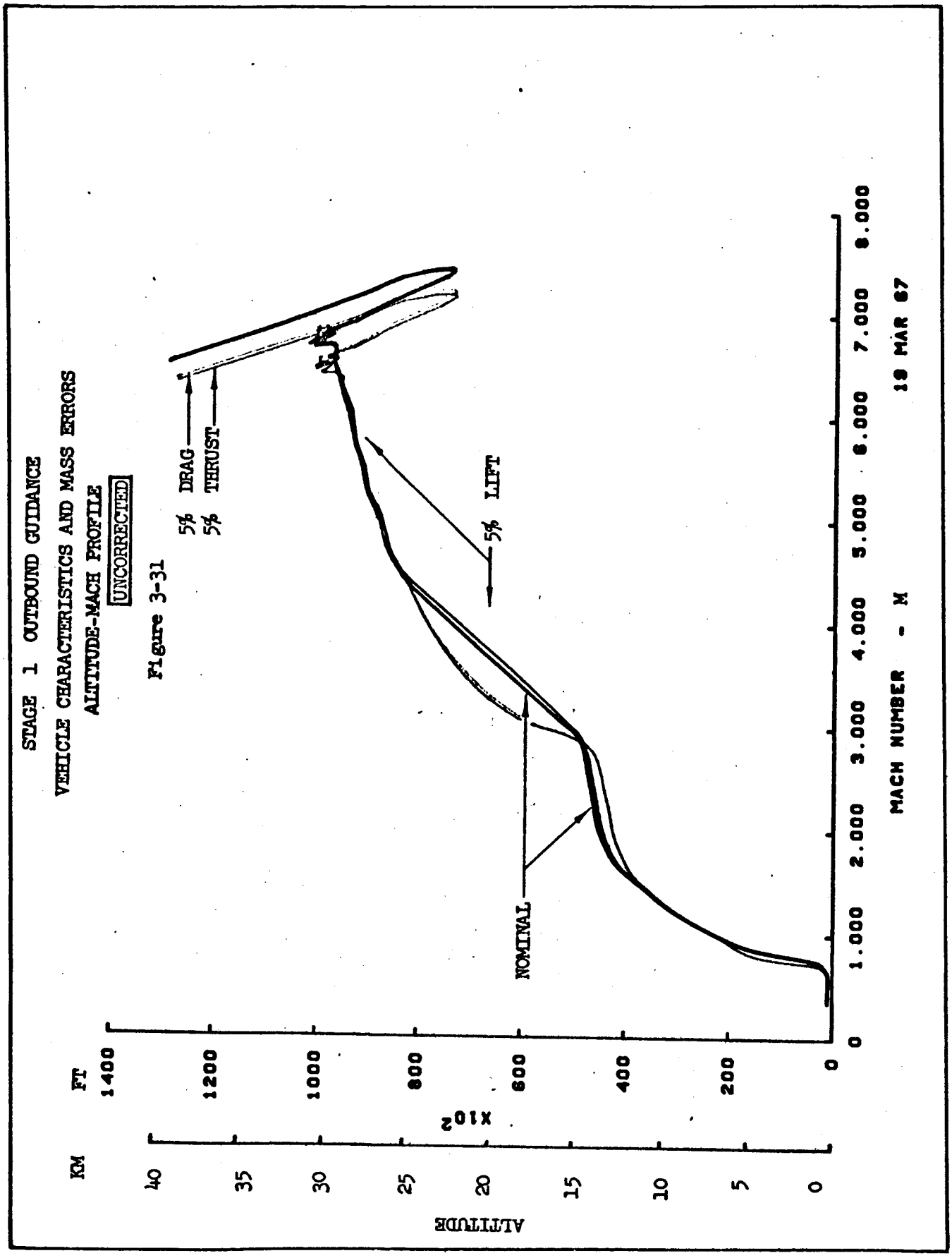

STAGE 1 OUTBOUND GUIDANCE
VEHICLE CHARACTERISTICS AND MASS ERRORS

FIGURE

UNCORRECTED

LATITUDE-LONGITUDE PROFILE

Figure 3-32

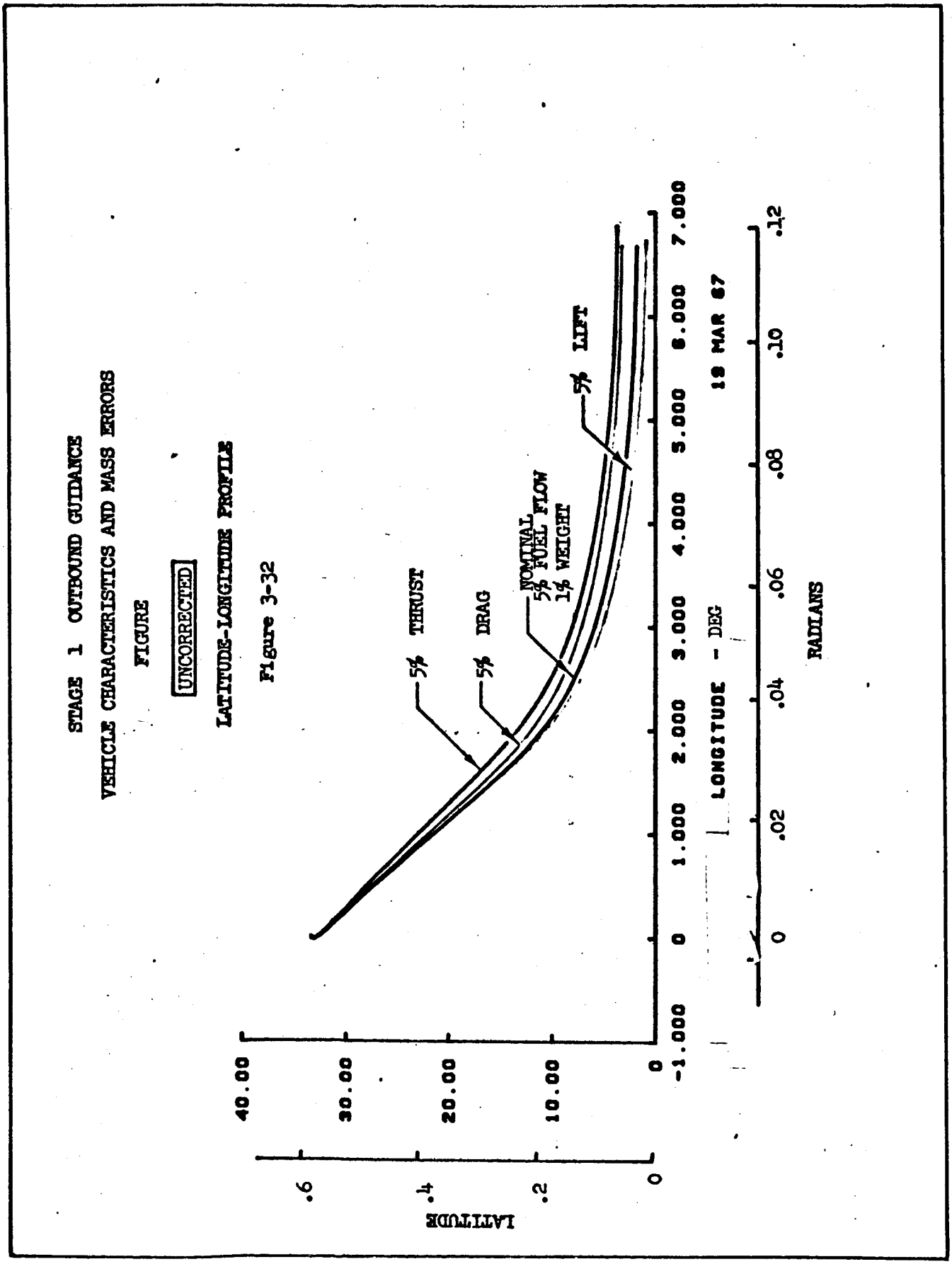

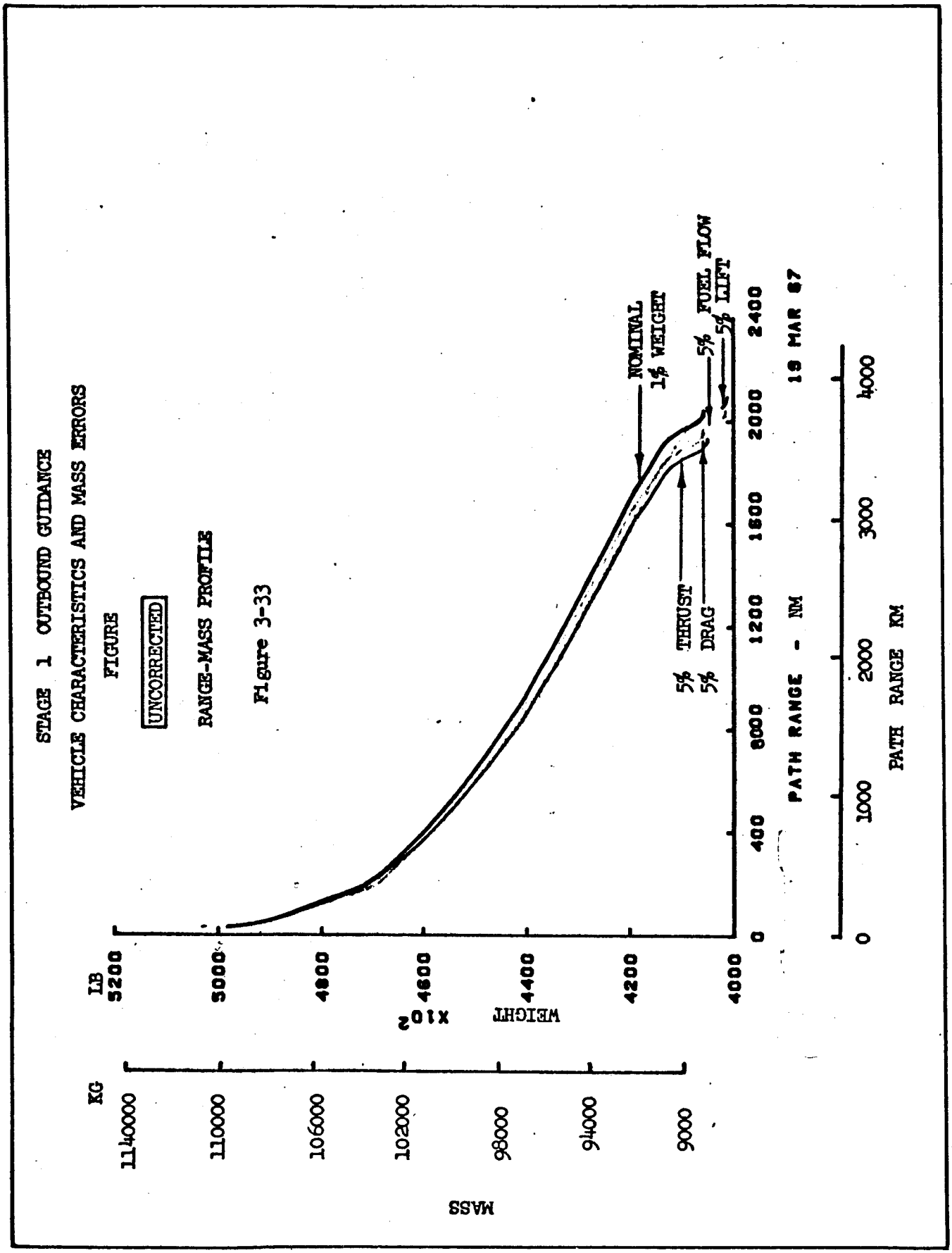

study for an initial mass error of +5% at t = 0.0. The results of this simulation have been included in Figures 3-26 to 3-33. The terminal mass error is the fuel difference between the nominal and the perturbed trajectories. The simulation resulted in a terminal mass which was 2,270 - 456 = 1,814 kg (5000 - 1004 = 3996 lbs), greater than that of the nominal path since the perturbed path commences with a vehicle mass increased by 2,270 kg (5000 lbs).

3.5.2 Stage I-Return Guidance to Base

This mission segment covers the flight of the Stage I module from the staging point in the vicinity of the equatorial plane to the base site at latitude 33.33°N, longitude 0°. The ability of lambda guidance to maintain terminal control at the base point was studied when the following errors were introduced:

(1) Vehicle characteristic errors

Thrust force, (-5%)
Fuel flow, (+5%)
Aerodynamic lift, (-5%)
Aerodynamic drag (+5%)

(2) Initial State Error

Weight, + 1,810 kg (+ 4000 lbs., 1.5%)

Guidance trajectories are terminated when at landing approach aids take over at a latitude of 3.825°N, an altitude of 86,459 ft., Mach number - 2.117, and longitude 2.017°E. The vehicle is therefore commencing the terminal descent and deceleration to subsonic speed.

3.5.2.1 Correction of Vehicle Characteristic Errors

The results of applying lambda guidance to the return mission segment are shown in Figures 3-34 to 3-39. In a Mach-altitude sense, Figure 3-34, the guidance trajectories all remain close to the nominal path, the greatest deviation being in the case of the aerodynamic lift force error. The ground track, Figure 3-35, in all cases is practically indistinguishable from that of the nominal. A measurable fuel penalty can be observed in Figure 3-36. Approximately the same amount of extra fuel is required in the maintenance of terminal control for all vehicle characteristic errors studied. It can be seen from the control histories of Figures 3-37 to 3-39 that the control corrections are essentially limited to throttle variations. This result is a direct function of the weighting matrices employed of course. The terminal errors in this study are presented in the following table.

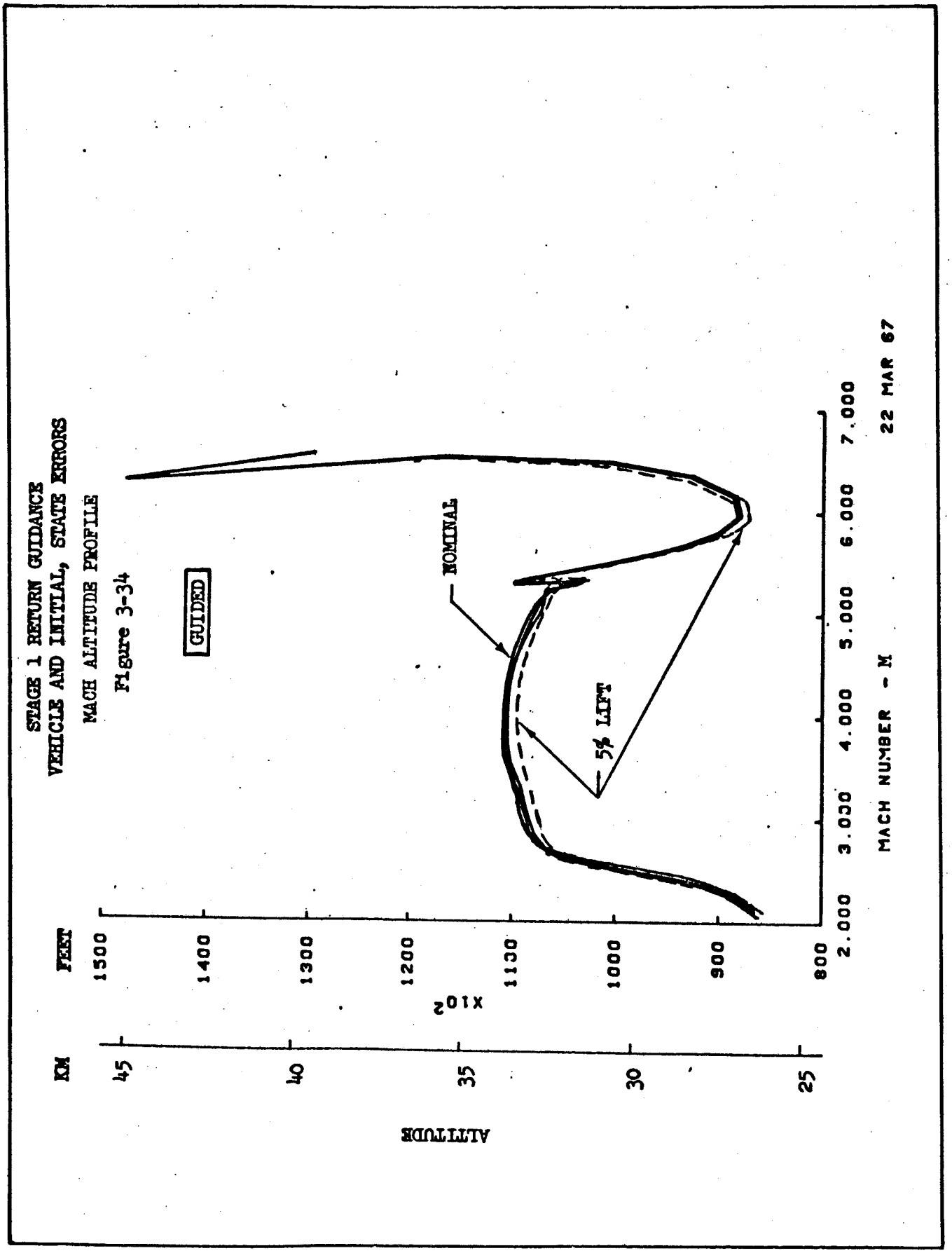

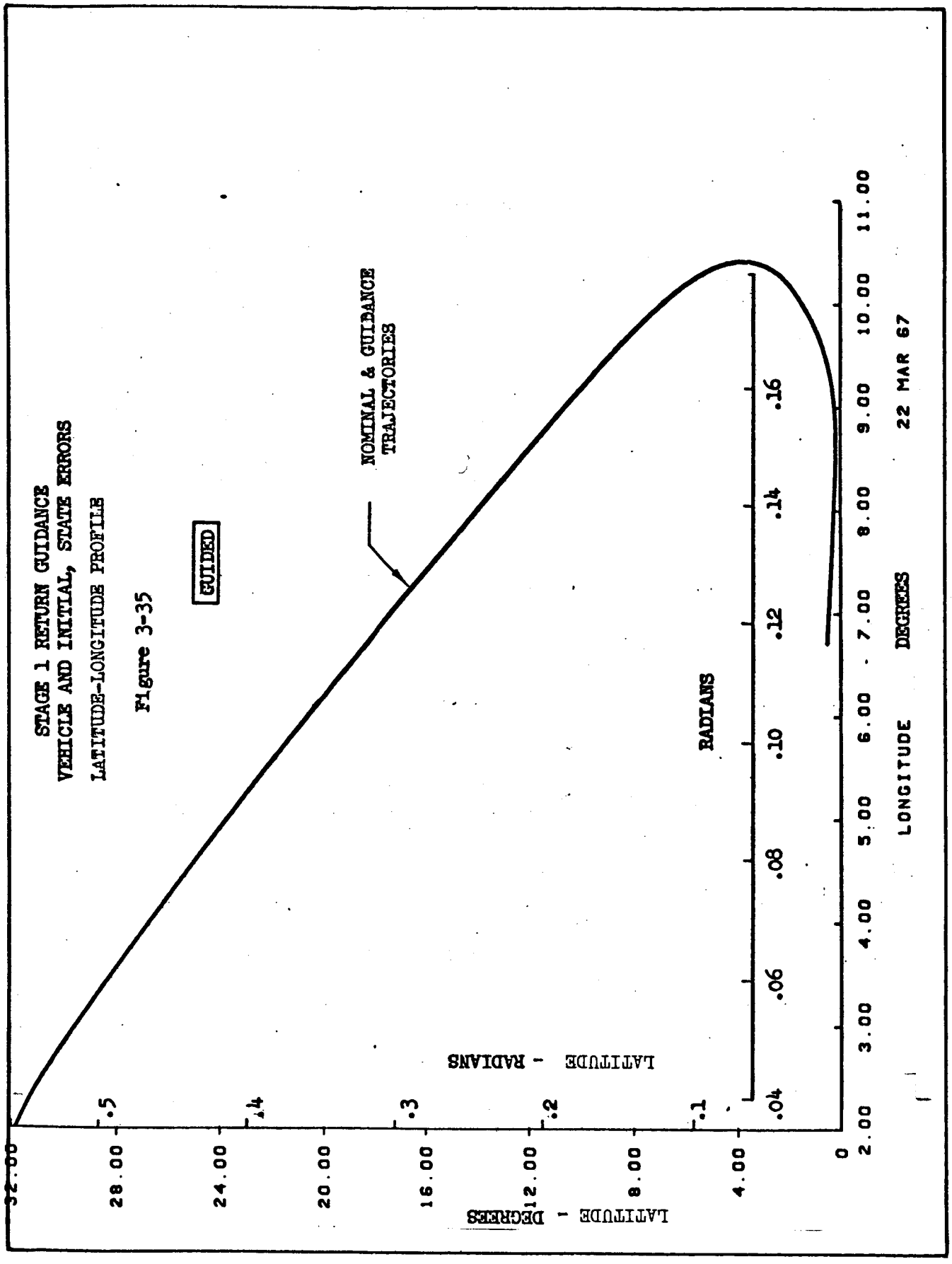

STAGE 1 RETURN GUIDANCE
VEHICLE AND INITIAL, STATE ERRORS

WEIGHT HISTORY

Figure 3-36

GUIDED

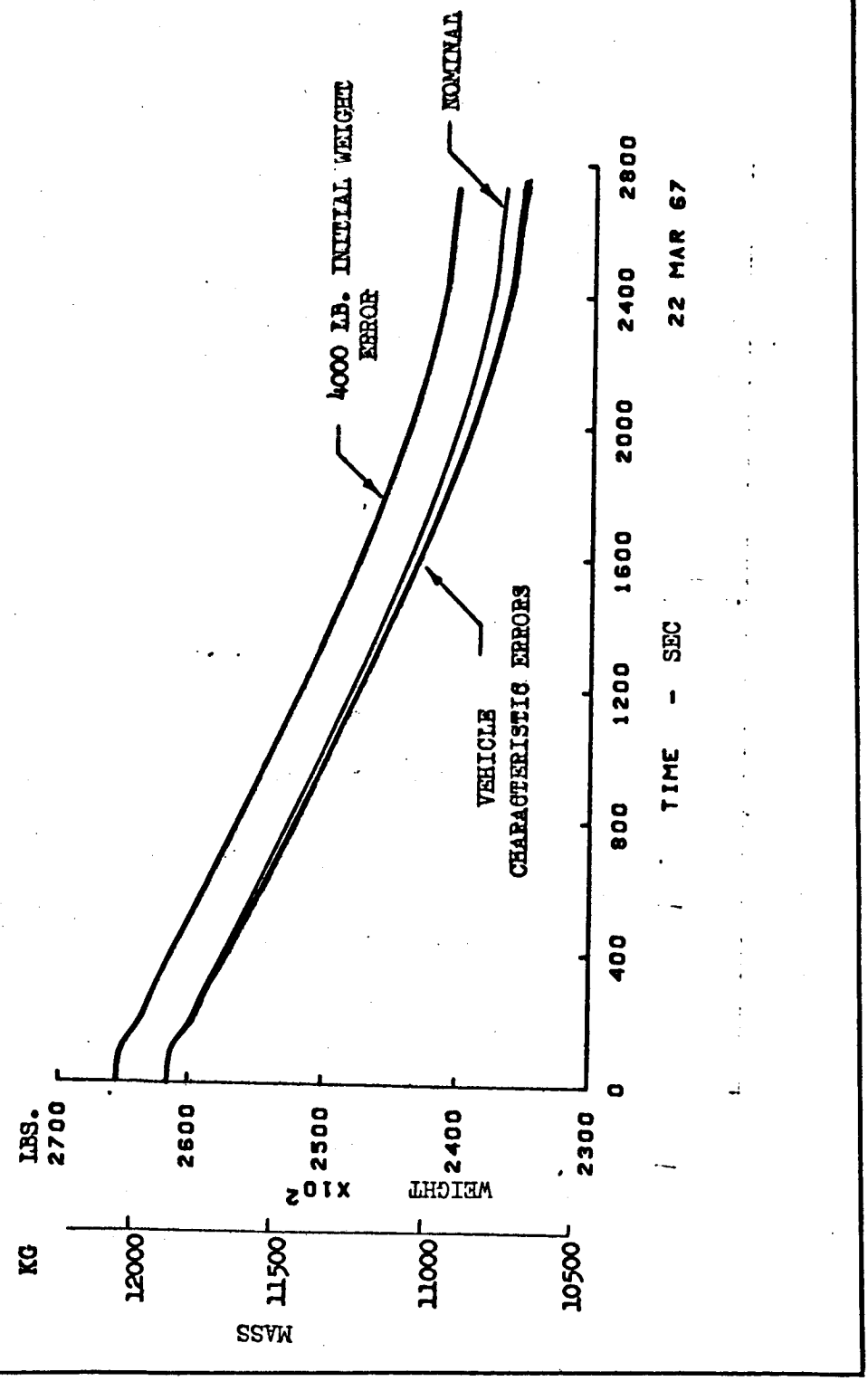

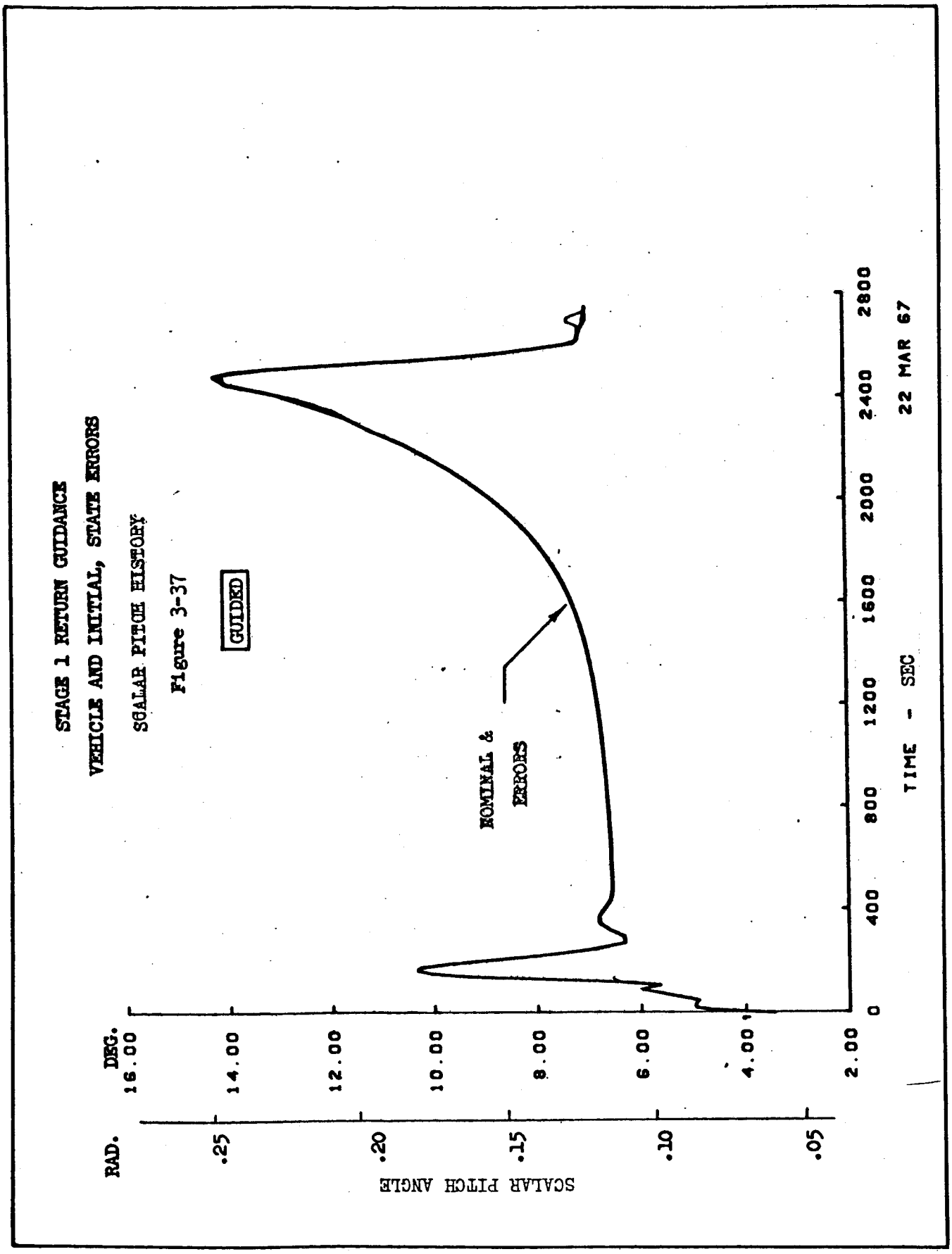

STAGE 1 RETURN GUIDANCE
VEHICLE AND INITIAL, STATE ERRORS
BANK ANGLE HISTORY

Figure 3-38

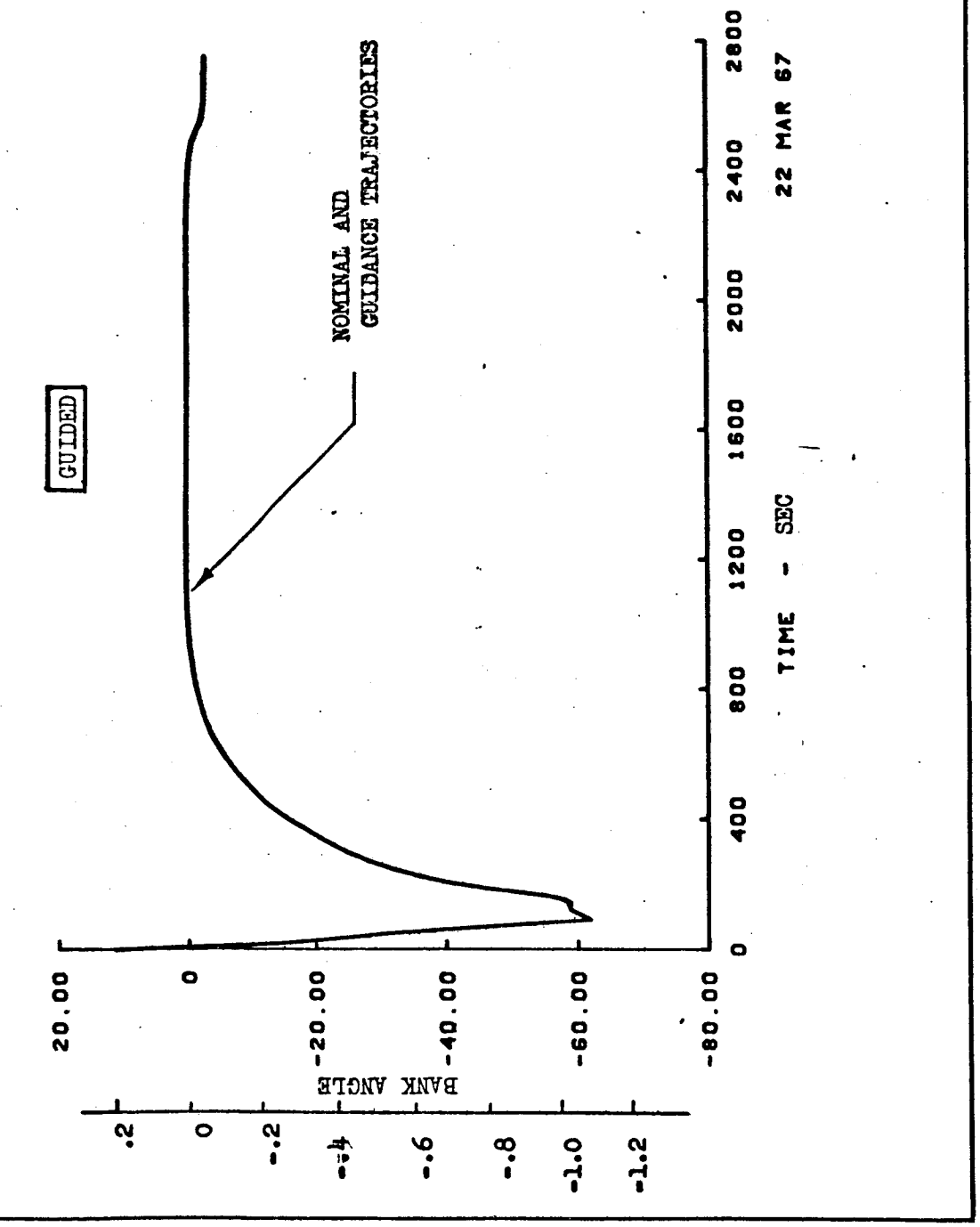

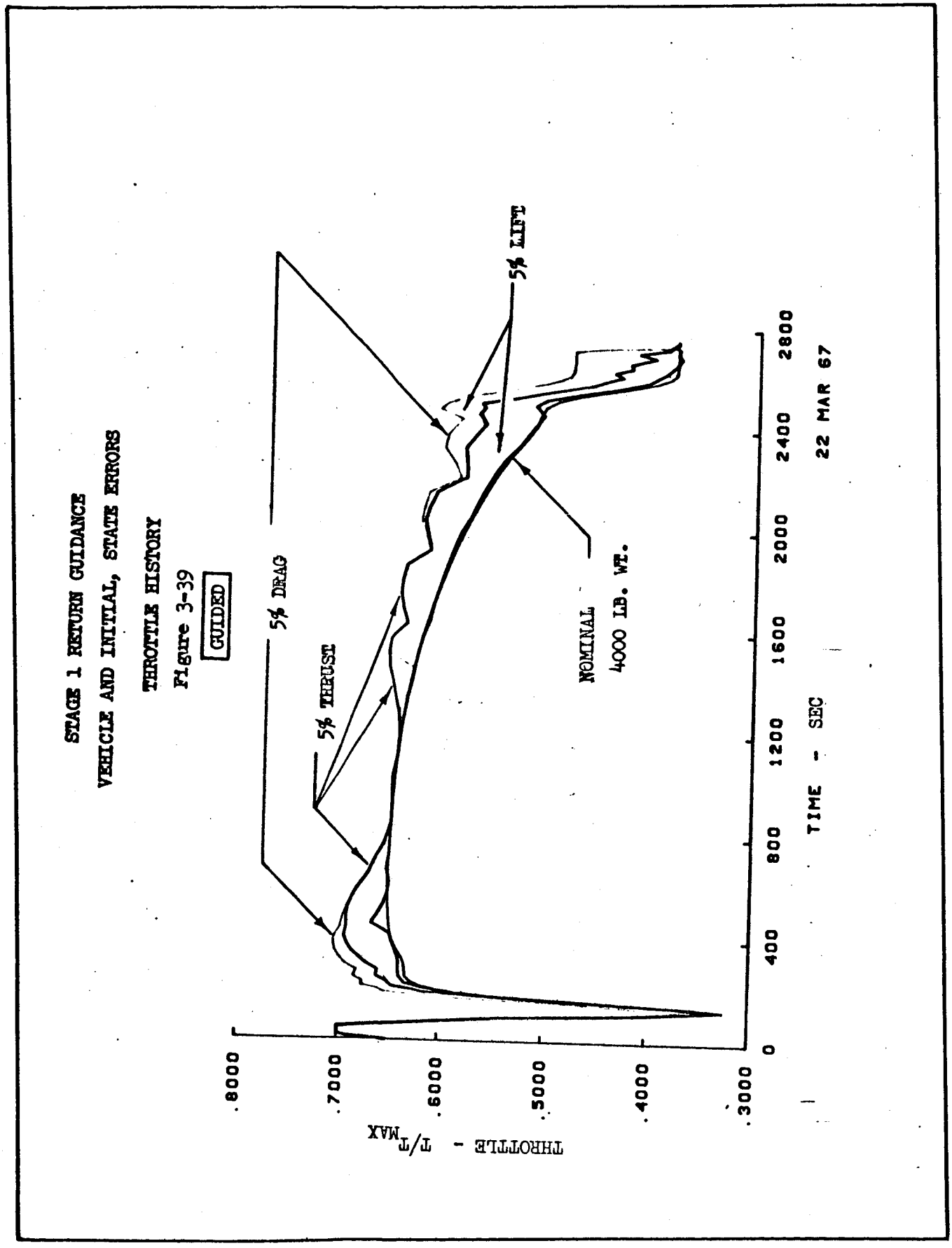

		ERROR SOURCE				
		Thrust -5%	Fuel Flow +5%	Lift -5%	Drag +5%	Initial Weight + 2,270 kg
Constraints	Altitude meters (feet)	33 (108.)	-0.07 (-.23)	-247 (-810.)	-125 (-409.)	-0.25 (-.83)
	Latitude degrees	0.001	0.	0.	0.001	0.
Performance	Phase II fuel, kg (lbs)	-635 (-1403.)	-530 (-1169.)	-822 (-1811.)	-771 (-1699.)	-197 (-434.)
	Phase I fuel, kg (lbs)	-616 (-1360)	-725 (-1600.)	-725 (-1600.)	-725 (-1600.)	-145 (-320.)

The Phase I results are open loop sensitivities and show reasonably good agreement with the Phase II closed loop results.

The results of flying the open loop nominal control histories in the presence of the above vehicle errors are presented in Figures 3-40 to 3-42.

Since the control perturbations depend strongly on the particular weighting matrix employed the above guidance study was repeated using a reduced inverse throttle weighting matrix element, $W_N^{-1}(t)$. The original calculation involved a weighting matrix whose inverse diagonal elements varied linearly between 1.0 at the trajectory commencement to zero at the trajectory termination. The second study retain these elements for the pitch and bank-angle controls; the throttle elements were everywhere reduced by a factor of 100.

Figures 3-43 to 3-46 show the resulting Mach-altitude paths and control histories. The terminal conditions attained are presented in the table below.

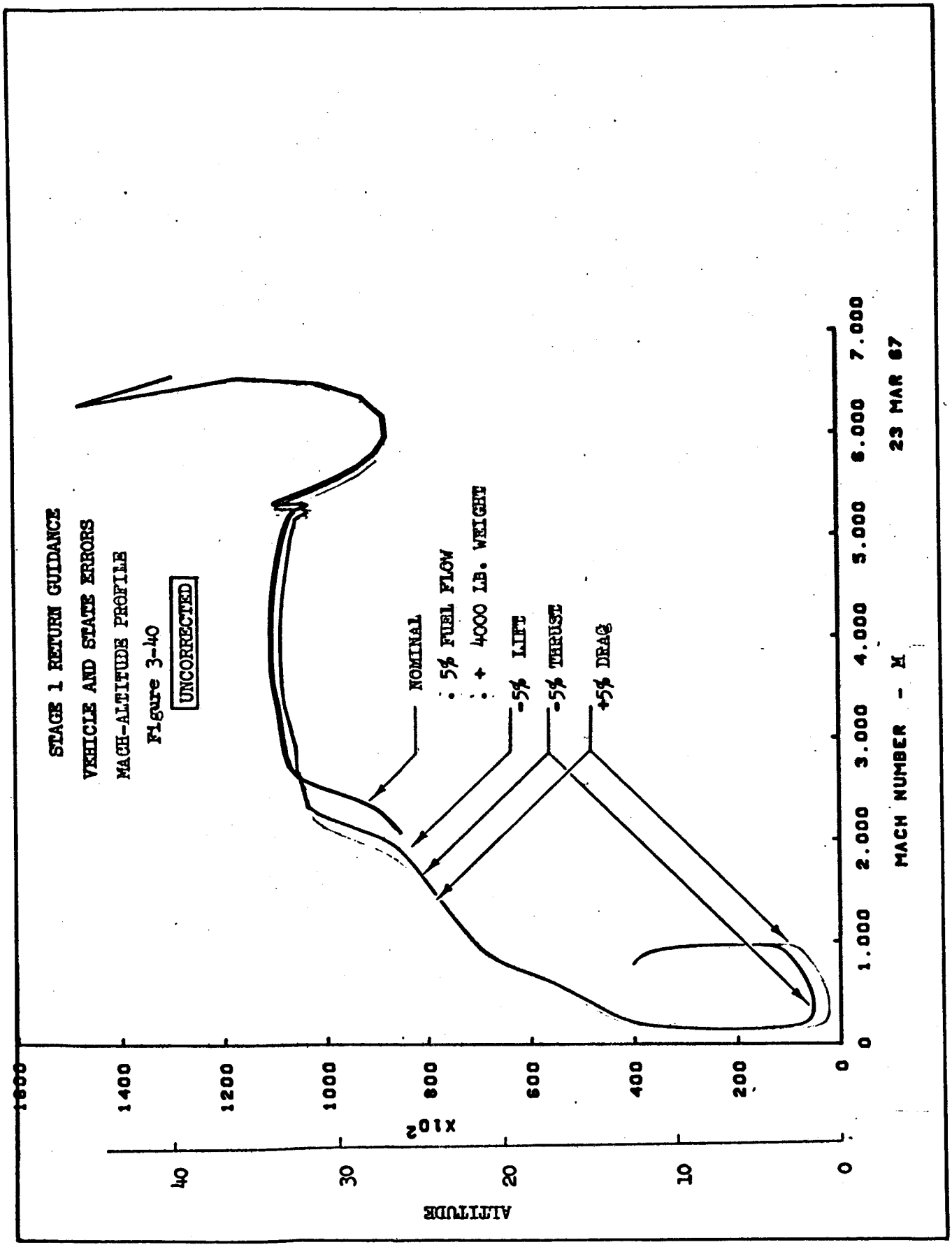

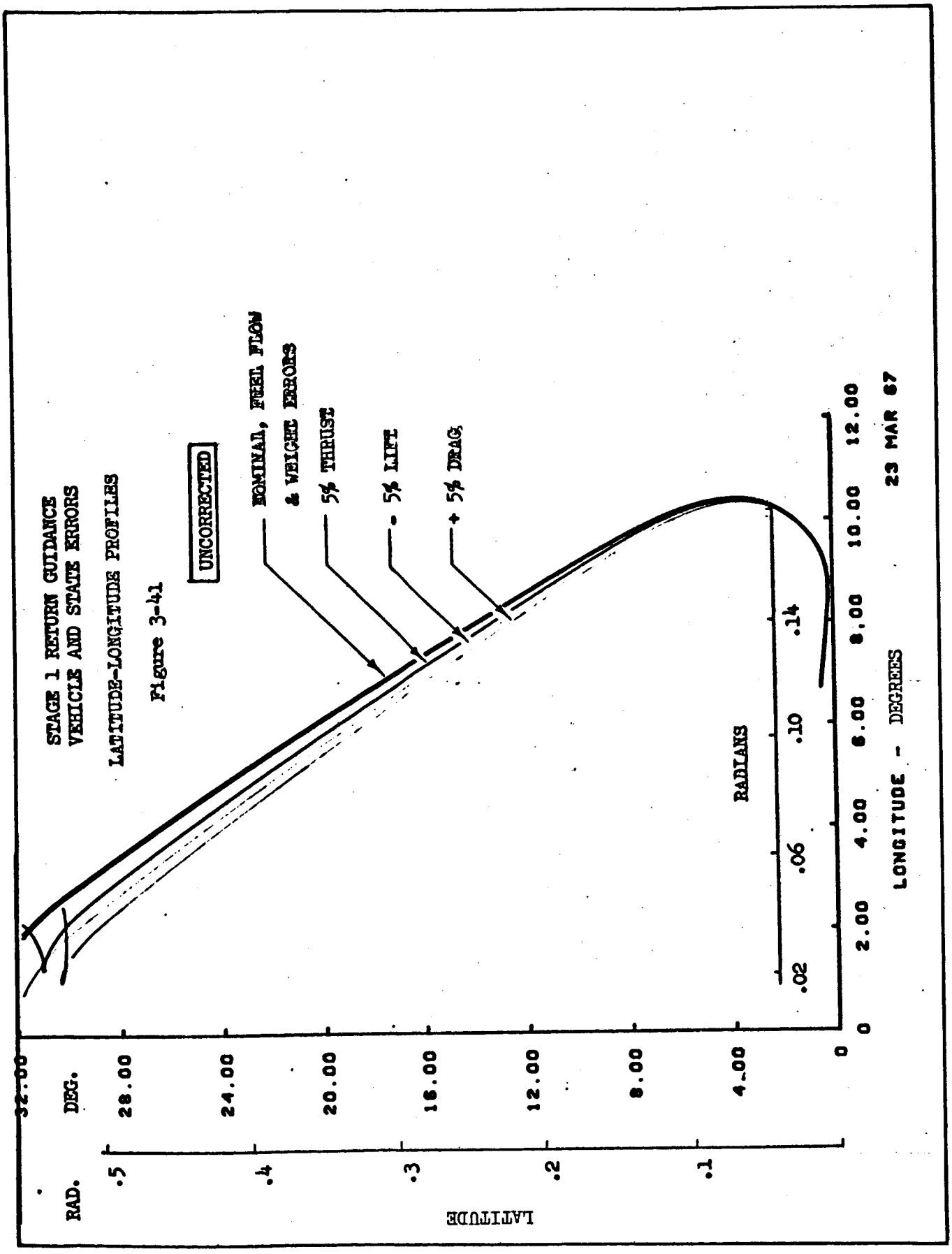

STAGE 1 RETURN GUIDANCE
VEHICLE AND STATE ERRORS

MASS HISTORY

Figure 3-42

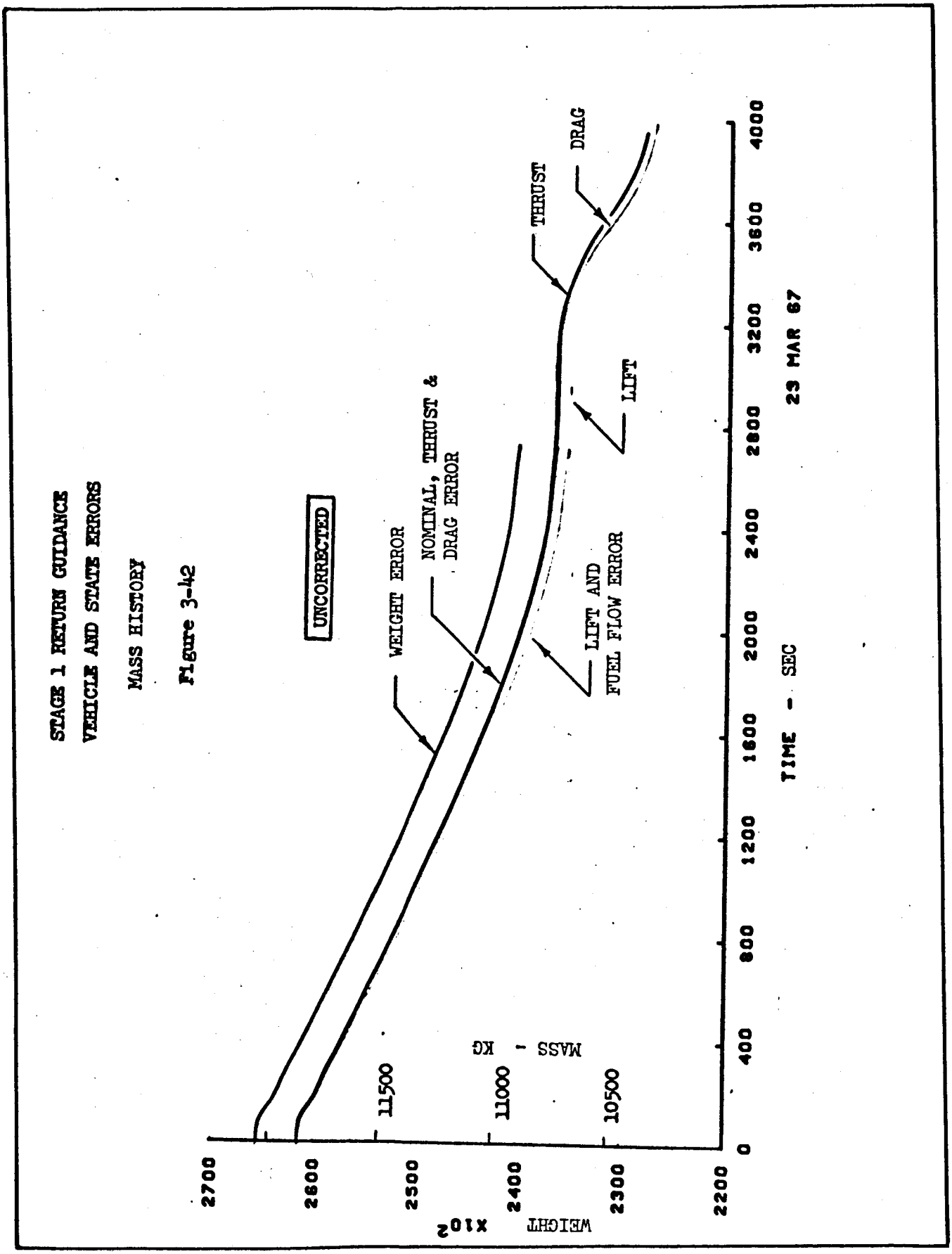

perturbations in the sensitive regions of large local response functions and large perturbations in the less sensitive regions of low local response functions. In such cases, weighting matrices based on the first derivative of the Hamiltonian, that is on the control impulse response functions as suggested in Reference 2, may be used to advantage.

At this time, therefore, it would appear that more work in the area of rational weighting matrix definition is required. In particular, for the class of trajectories studied in this report, further actual simulations involving realistic vehicle and environmental errors should be included in any such developmental effort. In the long term it seems that weighting matrices should be capable of automatic rational definition.

3.6.4 Vehicle Characteristic Errors

The corrective control perturbations in the presence of vehicle characteristics are quite different in nature to those employed for the correction of pure state errors. This point is discussed in some detail in Section 3.4.2. The differing nature of these two types of control corrections is attributed to the propagation of the vehicle characteristic errors which do not appear in the perturbation analyses of Sections 3 of Part II, Vol. 2.

It appears feasible to remove this discrepancy between the perturbed vehicle flight path and the above analysis by including selected vehicle characteristics in the state vector itself. For example, consider the thrust force, T_p. Since thrust appears in the state derivative equation 2.1.1, of Part II, Vol. 2, it follows that at the most we must have

$$T_p = T_p(x(t), \alpha(t), t) \qquad 3.37$$

Differentiating with respect to time

$$\dot{T}_p = \sum_{i=1}^{N} \frac{\partial T_p}{\partial x_i} \dot{x}_i + \sum_{j=1}^{M} \frac{\partial T_p}{\partial \alpha_j} \dot{\alpha}_j + \frac{\partial T_p}{\partial t} \qquad 3.38$$

Now suppose that the original control variables, $\bar{\alpha}$ are replaced by their derivatives, $\dot{\bar{\alpha}}$ as control variables. The original control variables now become part of the state, for let the new control variables be designated by $\bar{\beta}$ and the original control variables by $\bar{x}_\alpha$, then

$$\left\{\dot{x}_\alpha\right\} = \left\{f(x, \alpha, t)\right\} = \left\{\beta\right\} \qquad 3.39$$

which is of the form used in Equation 2.1.1, Part II, Vol. 2 follows from 3.30 that

$$\dot{T}_p = \sum_{i=1}^{N} \frac{\partial T_p}{\partial x_i} \dot{x}_i + \sum_{j=1}^{M} \frac{\partial T_p}{\partial x_{\alpha_j}} x_{\alpha_j} + \frac{\partial T_p}{\partial t} \qquad 3.40$$

which by Equations 3.39 and 3.40 is of the form

$$\dot{T}_p = f(x, x_\alpha, t) \qquad 3.41$$

STAGE 1 RETURN GUIDANCE

VEHICLE AND INITIAL STATE ERRORS

(REDUCED THROTTLE WEIGHTING MATRIX ELEMENT)

MACH-ALTITUDE PROFILE

GUIDED

Figure 3-43

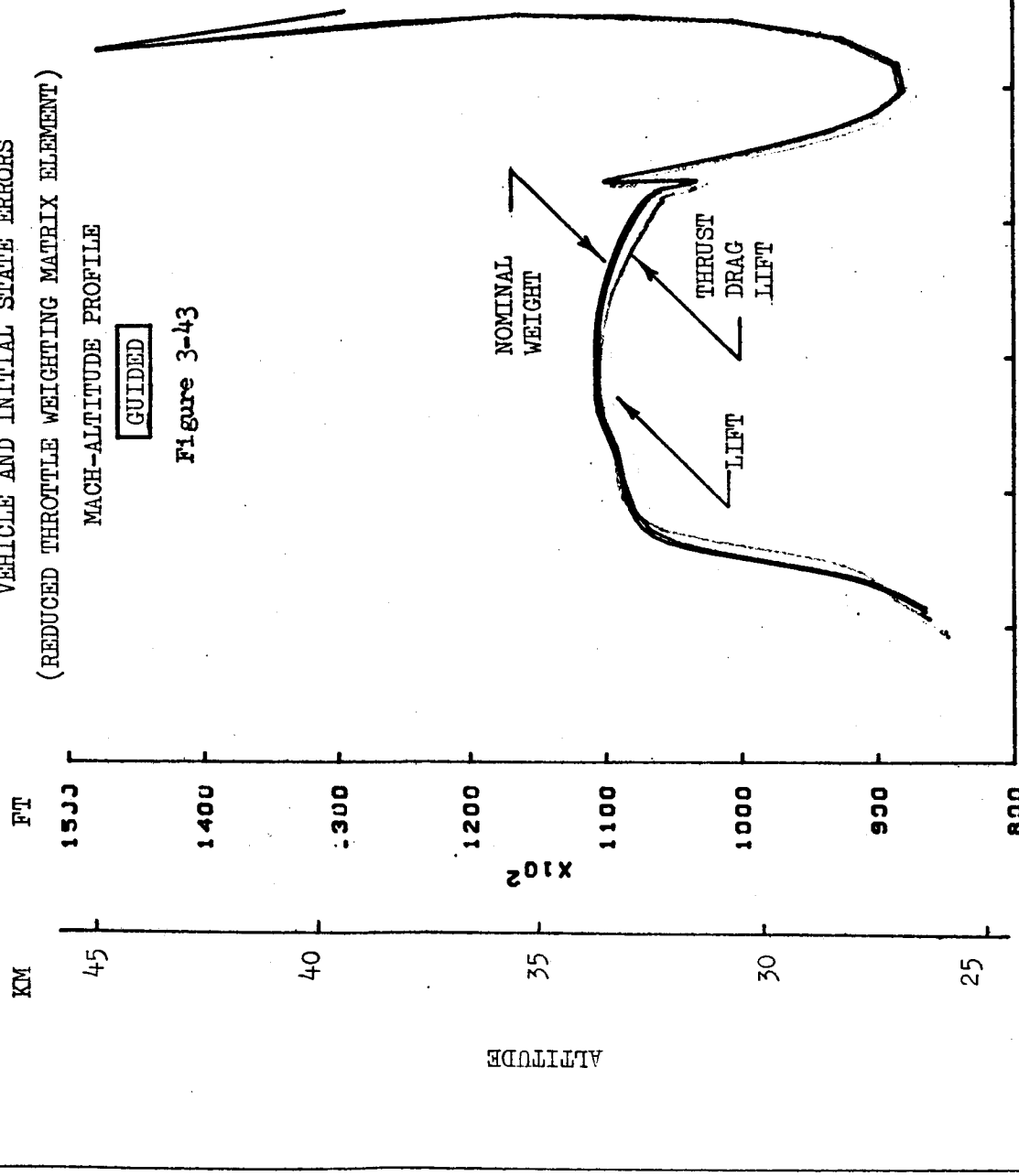

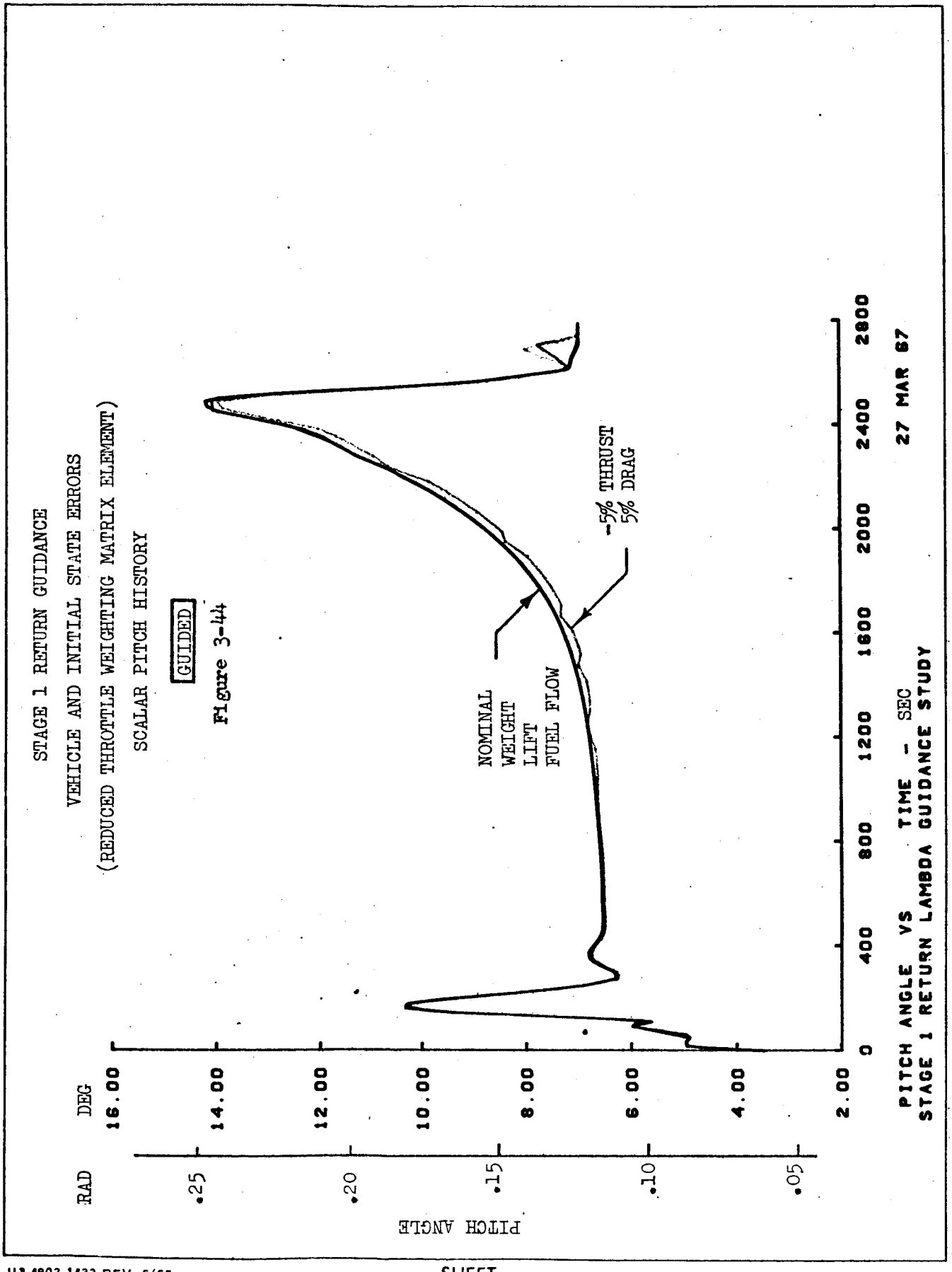

Figure 3-44

STAGE 1 RETURN GUIDANCE
VEHICLE AND INITIAL STATE ERRORS
(REDUCED THROTTLE WEIGHTING MATRIX ELEMENT)

GUIDED

Figure 3-45

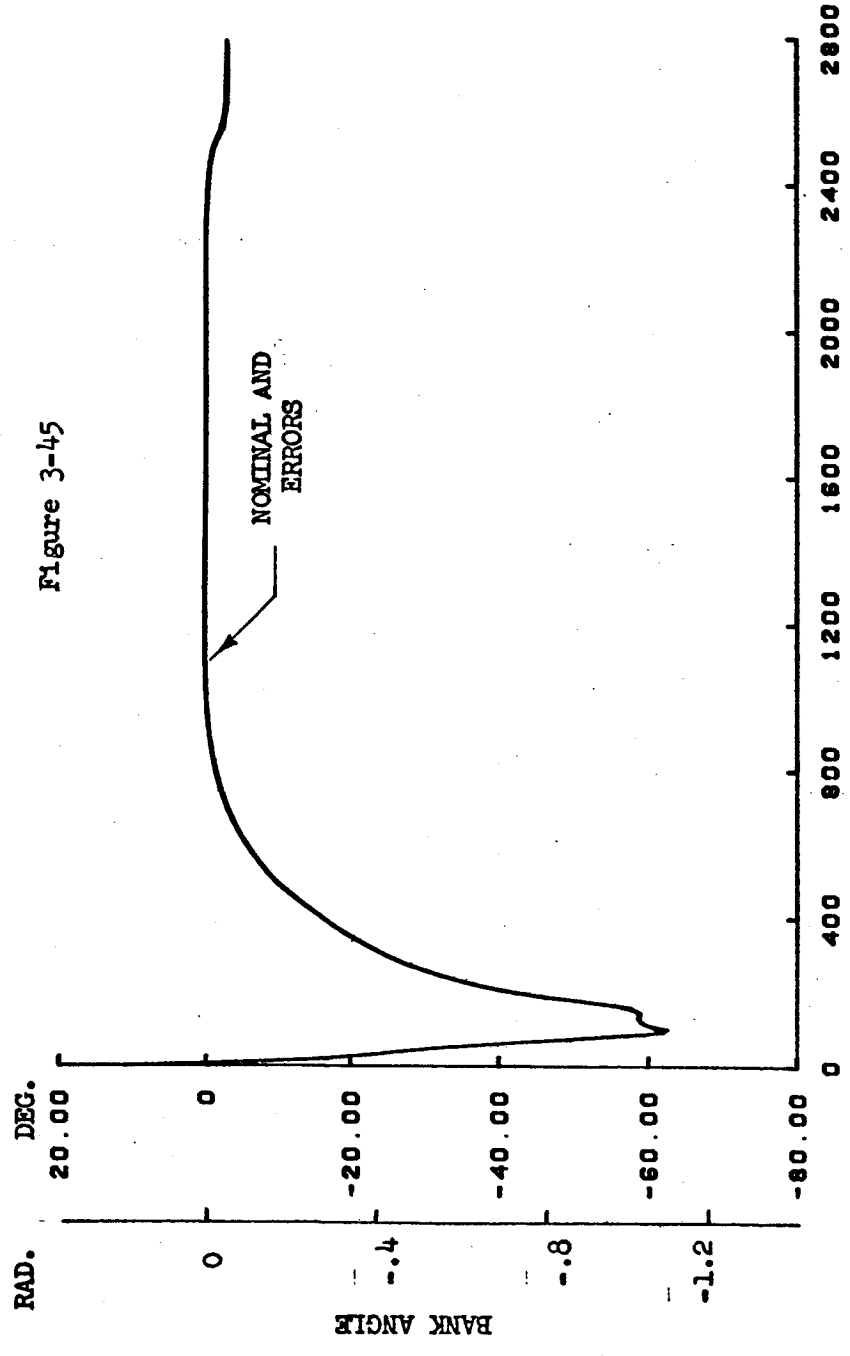

STAGE 1 RETURN GUIDANCE
VEHICLE AND INITIAL STATE ERRORS
(REDUCED THROTTLE WEIGHTING MATRIX ELEMENT)
THROTTLE HISTORY

Figure 3-46

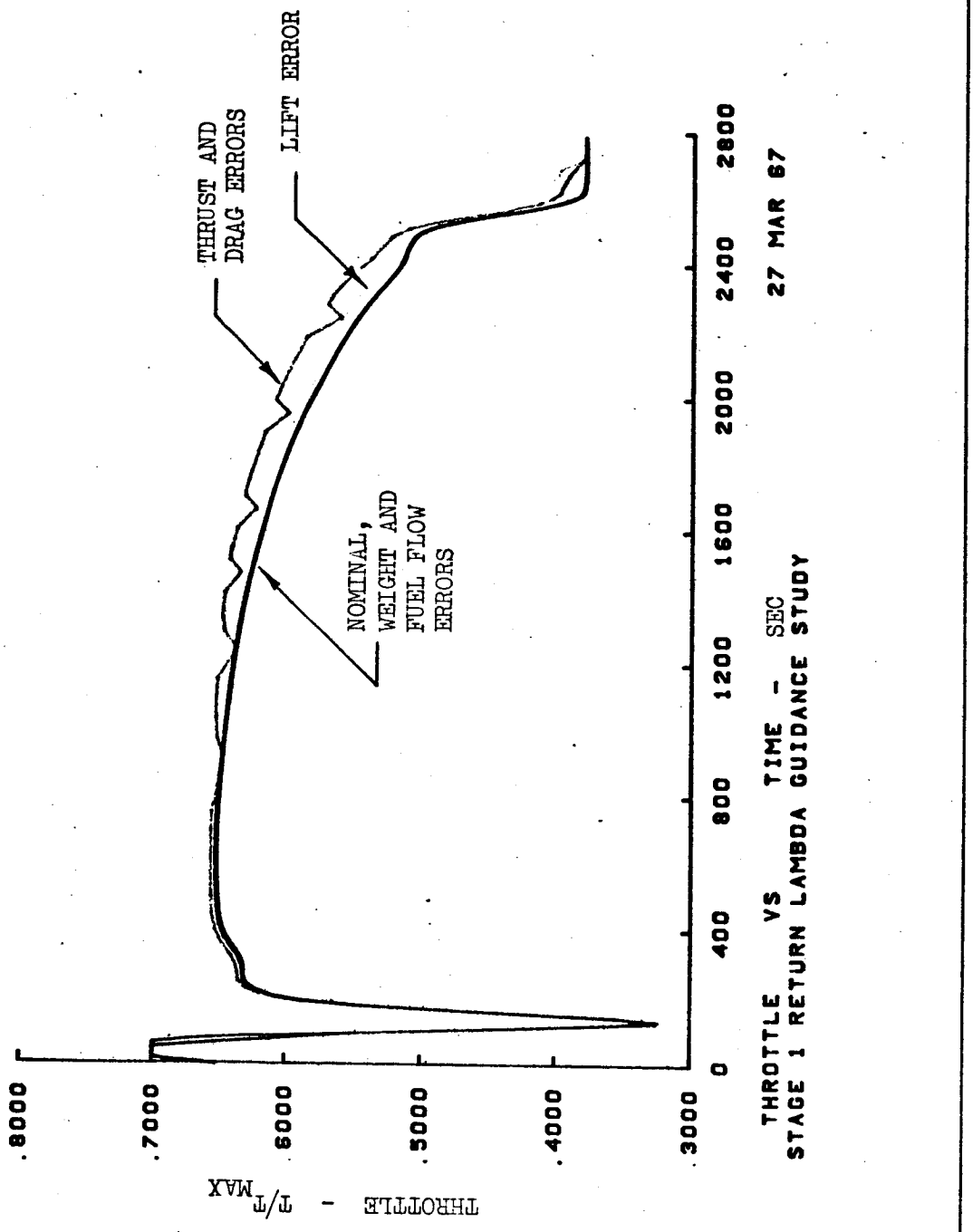

		ERROR SOURCES				
		Thrust -5%	Fuel Flow +5%	Lift -5%	Drag +5%	Initial Weight + 2,270 kg
Constraints	Altitude, Meters (feet)	-92 (-300)	+0.06 (+.19)	-481 (-1578.)	-511 (-1675)	-0.10 (-.34)
	Latitude, Degrees	0	0	0	0	0
Performance	Fuel kg(lbs)	-511 (-1128.)	-532 (-1173.)	-692 (-1526.)	-585 (-1290.)	-185 (-409.)

In all cases but one, the end points are reached with a smaller fuel penalty than that which occurs with the first choice of weighting matrix. In the fuel flow error case a negligible fuel difference resulted.

3.5.2.2 Correction of Initial State Error

An initial state error simulation was included in the Stage I return study, a 1,810 kg (4000 lb.) weight increase immediately following the stage point. The results of this simulation are included in Figures 3-34 to 3-46, and the tables of the preceding section. The terminal mass error quoted in these tables is the fuel difference between the nominal and perturbed trajectories so that most of the additional mass for the off-nominal case is retained in the terminal state.

3.5.3 Stage 1/Stage 2 Guidance to Rendezvous

The four month time scale of the lambda guidance study prohibited extensive investigation of the complete Stage I/Stage II mission. Some isolated results have been obtained and are discussed below.

The Stage I/Stage II nominal flight path is shown in Figure 3-47. This path was generated by flying the optimal control history of the Stage I/Stage II mission in an open loop fashion. It can be seen that the oblate earth control history from the optimization program of Section 5.2, Part II, Vol. 2, results in an altitude deficiency of about 45.8 km (150,000 ft.) when used in the spherical earth lambda guidance simulator of Section 3.3. The lambda guidance simulator was used

Bcc-466E

USE FOR DRAWING AND HANDPRINTING — NO TYPEWRITTEN MATERIAL

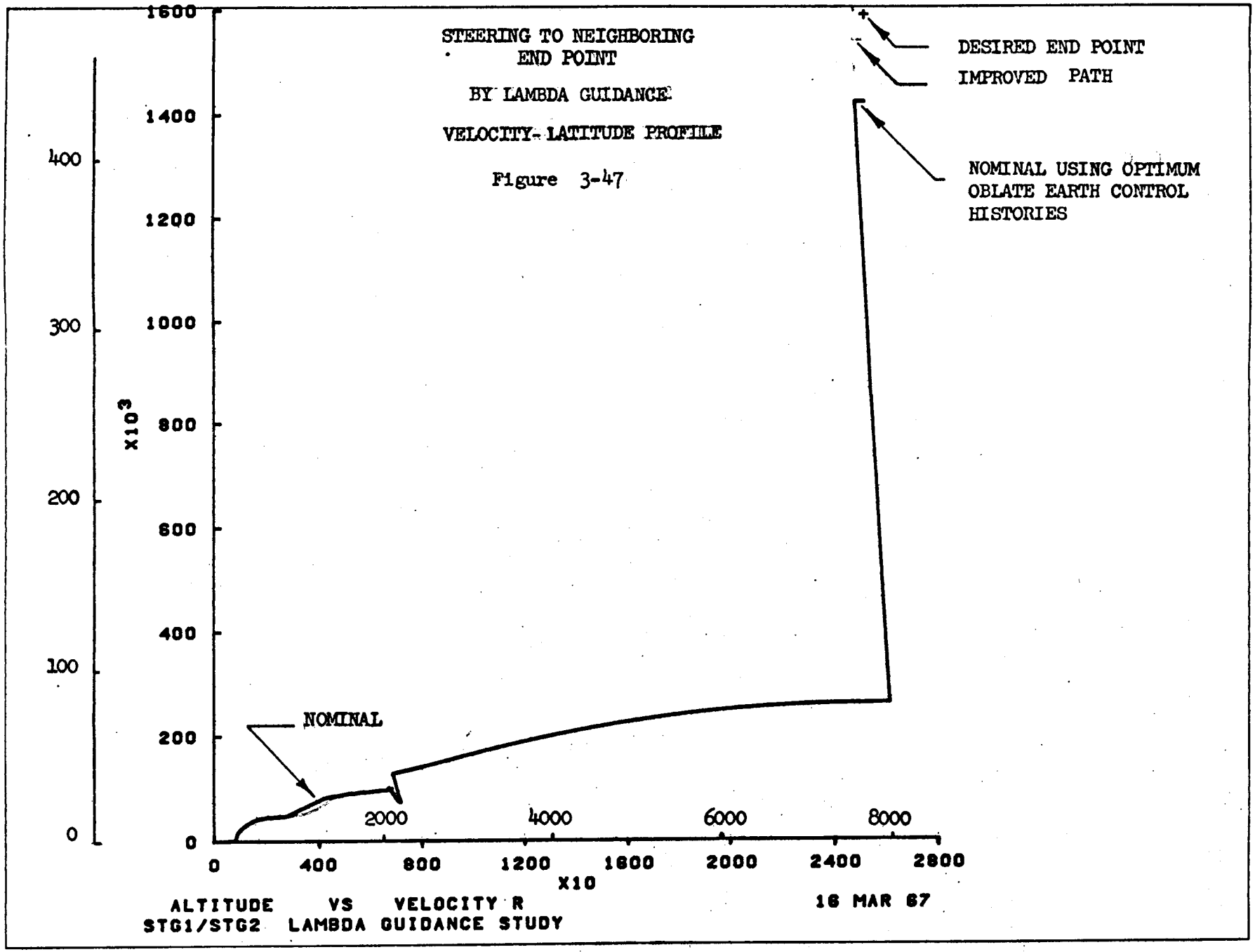

U3 4802 1433 REV. 6/65

SHEET 131

THE BOEING COMPANY

NUMBER D2-113016-7
REV LTR

in an attempt to eliminate this altitude discrepancy. To do this the simulator was modified to permit steering to a nearby point instead of to the nominal terminal conditions. It can be seen from Figure 3-47 that this attempt was partially successful in that the error discrepancy introduced by the change from oblate to spherical earth models, was reduced in magnitude by a factor of about two-thirds. To a degree this demonstrates the possibilities of lambda guidance throughout the complete Stage I/Stage II mission. It also demonstrates the ability of lambda guidance to steer to neighboring terminal points rather then to the nominal terminal point.

A second isolated example of Stage I/Stage II lambda guidance is presented in Figure 3-48. Here a 5% decrease in lift throughout Stage I generated an off nominal stage point. This vehicle error resulted in the following state errors at the stage point.

WEIGHT	-274 kg	(-609 lbs.)
ALTITUDE	-1810 m	(-5931 ft.)
FLIGHT PATH ANGLE		-0.23^{o}
VELOCITY	- 50m/sec.	(-164 ft/sec.)
LATITUDE		0.033^{o}
HEADING		-0.313^{o}
LONGITUDE		-0.179^{o}

The terminal Stage II errors resulting from this initial state error in Stage II were:

WEIGHT	-327 kg	(-723 lbs.)
ALTITUDE	+2.06 km	(+6750 ft.)
FLIGHT PATH ANGLE		-0.023^{o}
VELOCITY	-1.39 m/sec.	(-4.56 ft/sec.)
LATITUDE		0.005^{o}
HEADING		0.059^{o}
LONGITUDE		-0.070^{o}

Lambda guidance was employed throughout both stages in this example.

The above results should be treated with reservation since these two problems were the first multi-stage guidance problems studied with the aid of the lambda guidance simulator. Detailed inspection of these results revealed the presence of some numerical difficulties within the lambda guidance simulator when more than one stage is to be considered. These could not be eliminated within the time span of the present study. It is highly probable therefore, that further investigations would reveal substantially superior results to the two isolated examples quoted above.

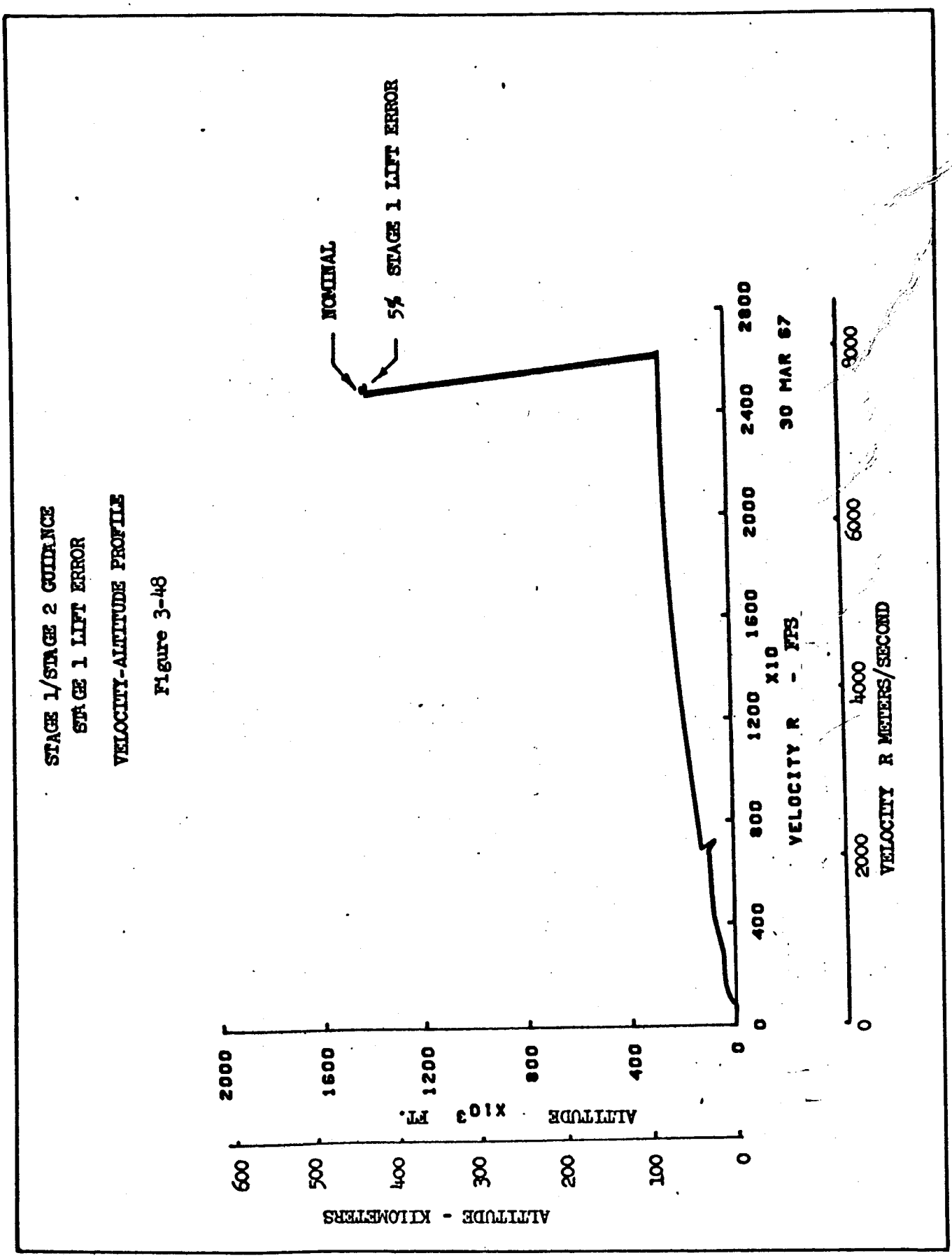

STAGE 1/STAGE 2 GUIDANCE
STAGE 1 LIFT ERROR
VELOCITY-ALTITUDE PROFILE

Figure 3-48

3.6 Lambda Guidance Developmental Studies

3.6.1 Inequality Constraints

The lambda guidance simulator of Section 3.3 does not include a direct method for the imposition of inequality constraints. Several straightforward devices can be used for indirect application of inequality constraints.

The simplest approach is to revert to path following in the neighborhood of the inequality boundary. Any conventional path following technique may be used for this purpose, or alternatively one might resort to short term lambda guidance in the manner of the demonstration problems of Section 3.4. For example, it can be seen from Figures 3-2 to 3-5 that this approach successfully negotiates the sonic boom over-pressure boundary of the Stage I outbound mission.

Since in-flight inequality constraints may be transformed to terminal equality constraints, Reference 2, it would appear that inequality constraints pose no additional problems. However it can be seen from Reference 2 that a trajectory satisfying the inequality constraints has zero partial derivatives, $\left\{\frac{\partial \gamma}{\partial \gamma} u\right\}$ and $\left\{\frac{\partial \gamma}{\partial \alpha} u\right\}$ throughout the flight path. Here x_u is the state variable that is introduced in the transformation of enroute inequality constraints to terminal equality constraints. In this case the analysis underlying the lambda guidance technique presented in Section 3.2 is unable to maintain terminal control. One might seek to replace the sharp edged inequality boundary by an approximate step function as in Reference 2, but this approach has proved tedious in the related problems of trajectory optimization and presumably would prove unwieldy here. An alternative is to create a false boundary D* such that

$$D^*(\gamma, \alpha, t) = \bar{D}(\gamma, \alpha, t) - D(\gamma, \alpha, t) \qquad 3.33$$

where the inflight inequality to be satisfied is

$$D(\gamma, \alpha, t) = \bar{D}(\gamma, \alpha, t) \qquad 3.34$$

This is illustrated in Figure 3-49.

A trajectory satisfying Eqn. 3.33 which violates the boundary, D = D*, throughout a total flight time of Tu*, will satisfy

$$x_u(t) \leq \Delta T_u^* \qquad 3.35$$

Constraining $x_u(t)$ to the nominal value will ensure that subsequent guidance trajectories remain in the neighborhood of the boundary in the above sense. Unfortunately this does not guarantee that the resulting guidance trajectories will be free of significant violations of the true in-flight inequality constraint, Eqn. 3.34. Steering to the nominal value of the false boundary constraint may result in paths which satisfy the true boundary as in Path 1 of Figure 3-50 or it

NOMINAL TRAJECTORY IN THE

PRESENCE OF FALSE BOUNDARY

Figure 3-49

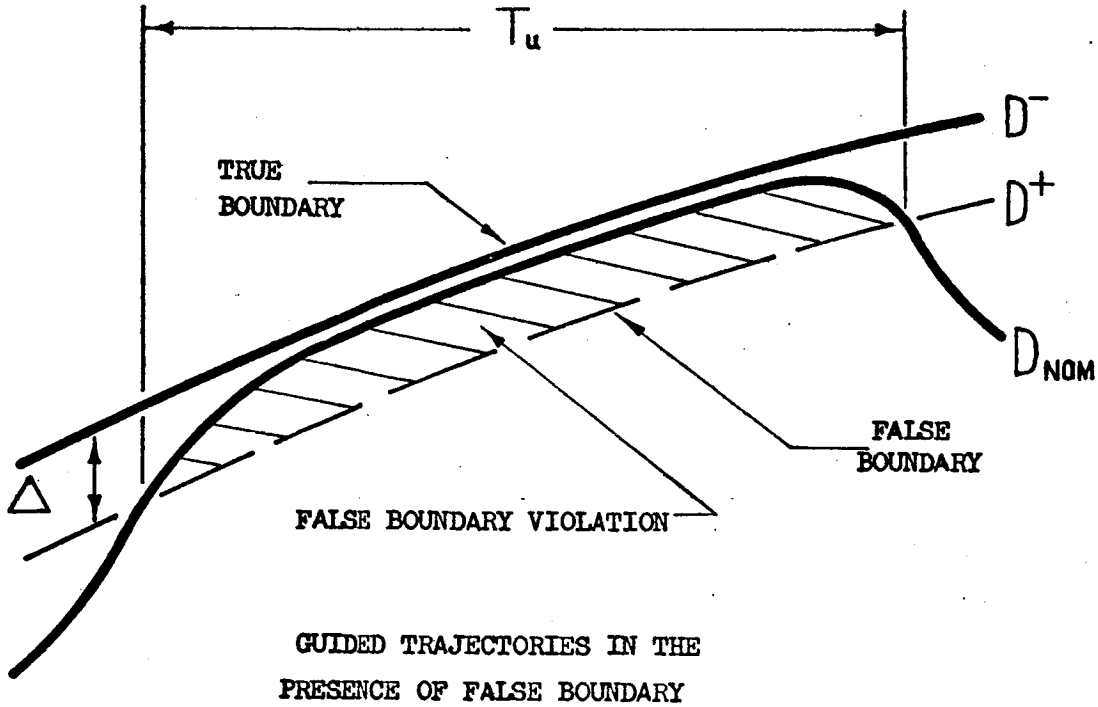

GUIDED TRAJECTORIES IN THE

PRESENCE OF FALSE BOUNDARY

Figure 3-50

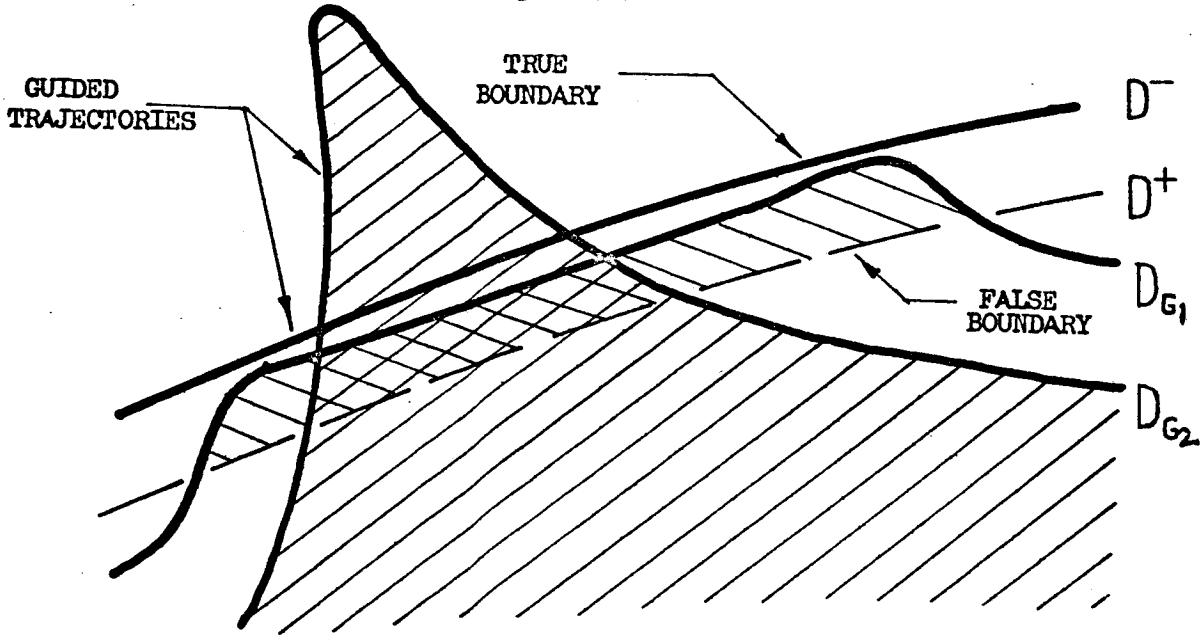

may involve significant violations of the true boundary as in Path 2 of Figure 3-50.

An example of this approach to the imposition of inequality constraints is shown in Figure 3-51 which shows the Mach-altitude profiles of the nominal, guided, and uncorrected paths in the presence of a +10% drag penalty. The path segment considered is the climb and acceleration along the sonic boom overpressure boundary. As noted in Section 6, Part II Volume 2, this involves some violation of the actual placard. Accordingly the false boundary, D*, was equated to the actual placard. The objective in this study is to maintain terminal control for the same integrated violation of D*. The guided path achieves this within 0.4%, the unguided path integrated violation was in error by 12.2%. It would appear that the false boundary method holds some promise as a device for maintaining in-flight inequality constraints. Further work in this area is needed however. This might include using higher order measures of the violation, i.e.,

$$x_u = (D-\bar{D})^{2N} \qquad 3.36$$

where N is a positive integer. This would tend to smooth out the resulting violation of the false boundary. Another possibility would be to steer to a zero violation of the false boundary rather than to the nominalviolation. Examples of steering to adjacent points are contained in Section 3.4.

A final possibility for the maintenance of in-flight inequality boundaries lies in the work of Bryson, Denham and Dreyfus, References 9 and 10. A generalized application of this work may well involve considerable effort for complex constraints, but if successful would provide explicit control for flight along the constraints.

3.6.3 Guidance Update Frequency

Section 3.4.3 illustrated the effect of update frequency on lambda guidance control. In the 100 second flight segment described there the terminal accuracy varied slowly with update frequency. The magnitude of the control perturbations required, however, rose rapidly with the time between successive updates.

A second update frequency study was undertaken in order to investigate the effect of this parameter for a more complex trajectory. Update times of 5, 10, 50, 100 seconds were employed. The results are shown in Figures 3-52 and 3-53. Also included is the trajectory resulting from the open loop control history. The error introduced in these calculations was a one minute early condition at the initial time.

Figure 3-52 shows the resulting Mach-altitude profiles, the terminal error increases quite rapidly with increasing time between update, the open loop control after staging results in rapid altitude loss followed by a decelerating descent. The vehicle energy for the 100 second update

REVISIONS			
LTR	DESCRIPTION	DATE	APPROVAL

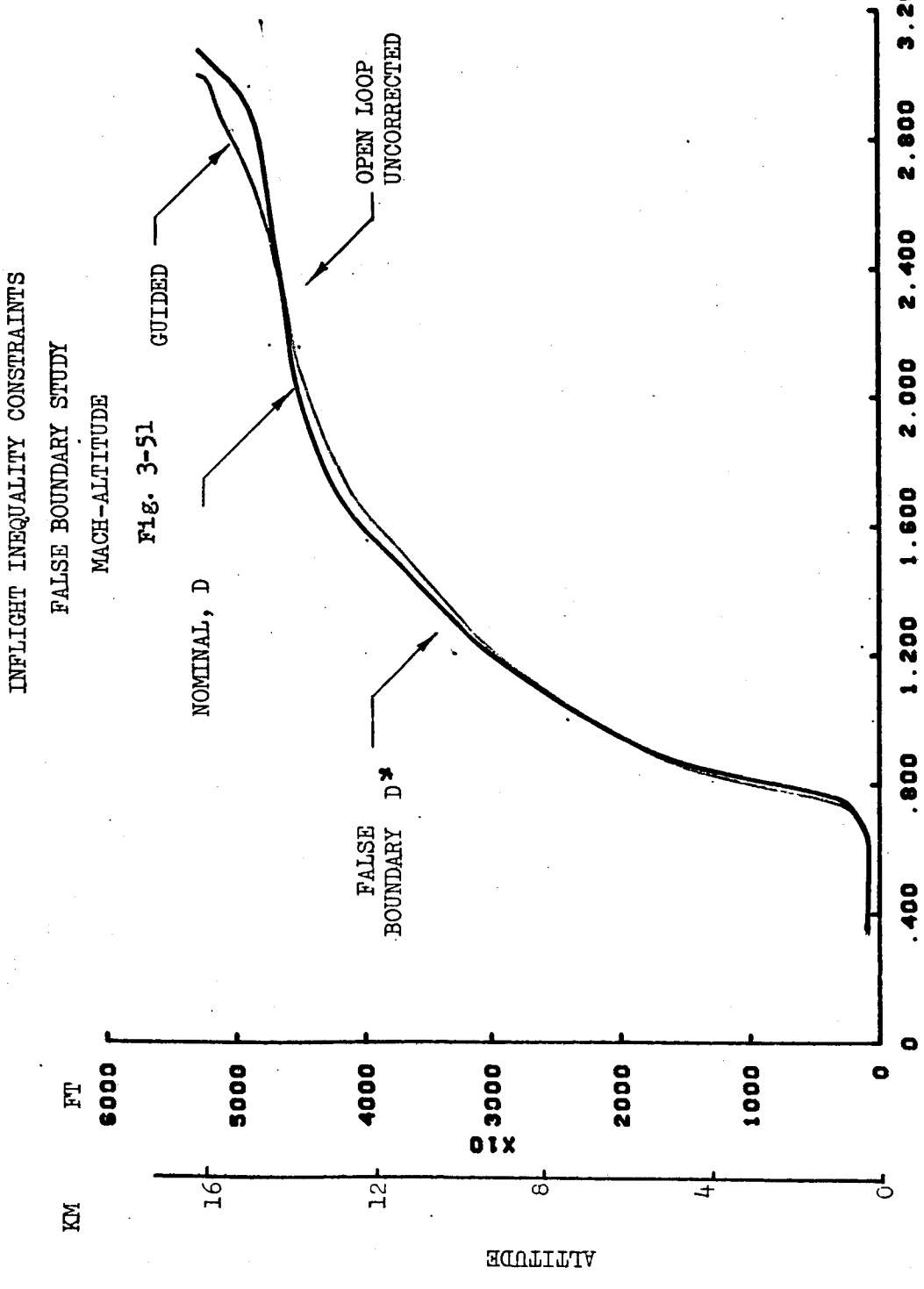

UPDATE FREQUENCY STUDY
STAGE 1/STAGE 2
VELOCITY-ALTITUDE PROFILE
Figure 3-52

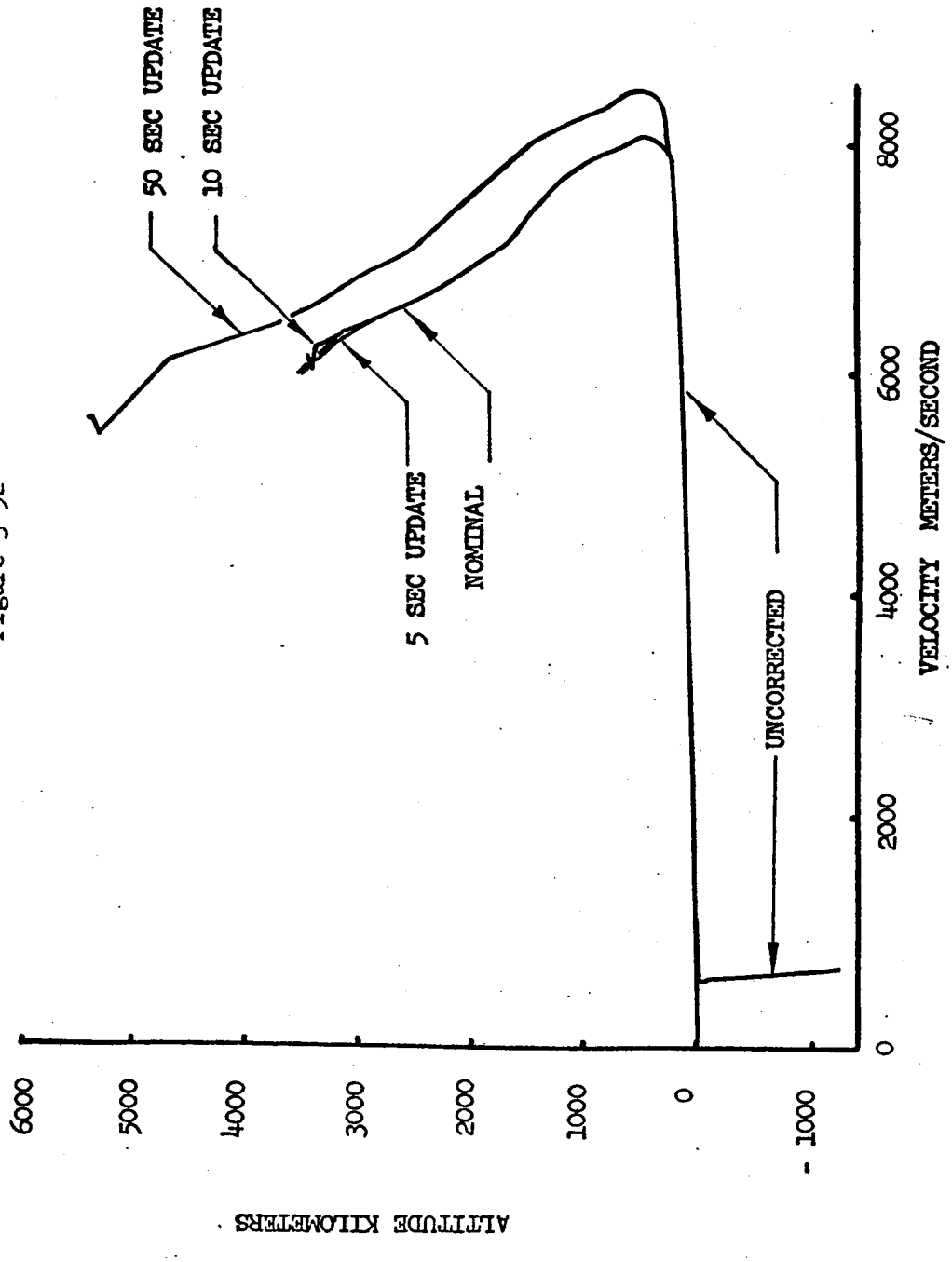

UPD TE FREQUENCY STUDY
STAGE 1/STAGE 2
GROUND TRACK

Fig. 3-53

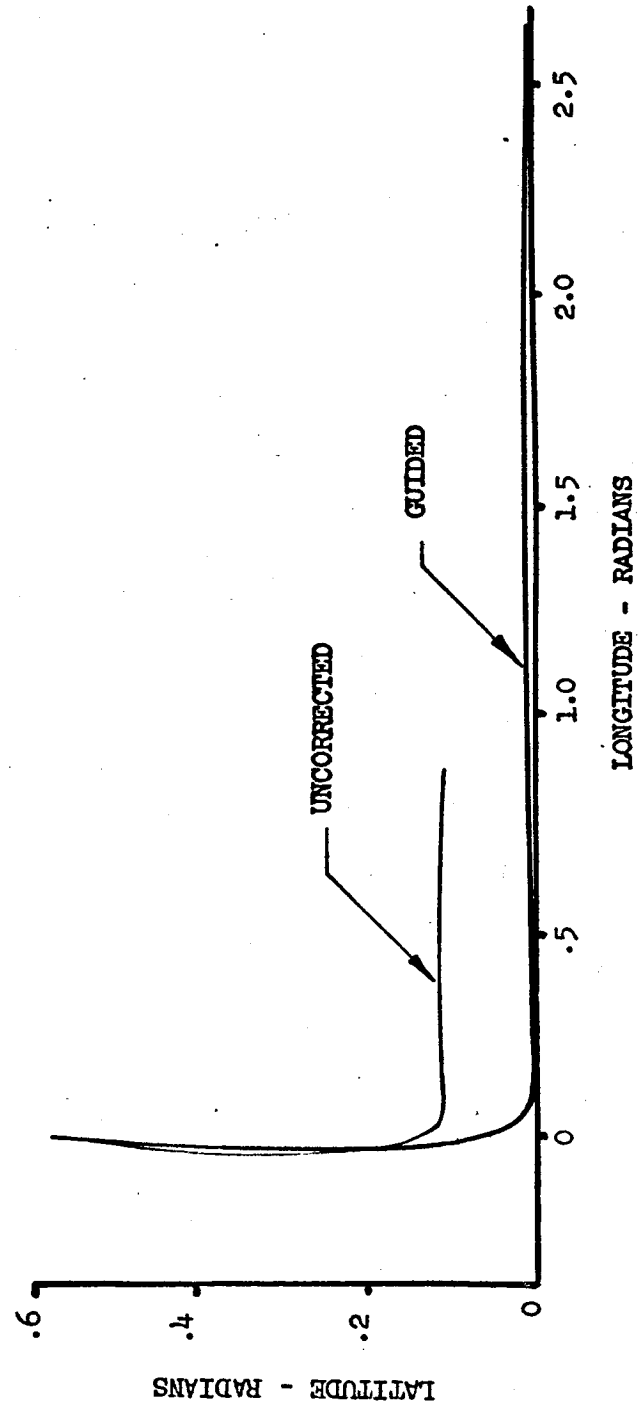

case exceeds the nominal coast energy so that the vehicle climbs to a much greater altitude in consequence. The remaining cases coast at about the expected energy level but show rapidly increasing terminal errors with increasing time between guidance updates. All the guided cases did achieve the desired orbital plane with reasonable accuracy, as can be seen from Figure 3-53.

Thus, the required update frequency in lambda guidance depends on the mission. On a short straightforward mission, update frequency would not appear to be a problem. On a long complex mission update frequency may drastically affect terminal accuracy. Presumably the required update frequency on such a mission will also depend strongly on the error source. No verification of this point by actual simulation has been made at this time.

3.6.3 Weighting Matrices

The control variable weighting matrix which defines a time varying metric tensor for the control space, plays a prominent role in lambda guidance application. By suitably manipulation of the weighting matrix the control perturbation can be made equal to any perturbation which satisfies the end points. In this sense the concept of a minimum control perturbation is almost meaningless in the absence of precise methods for determining the weighting matrix. A similar situation exists in the steepest-descent perturbation can be made equal to any performance improving perturbation that provides the specified end point changes. The repetitive application of the steepest-descent algorithm together with the weighting matrix concepts of Reference 2 largely overcome this difficulty in the trajectory optimization field, although even here further improvement could be sought.

In lambda guidance the problemis both more and less crucial. More crucial in that only one pass is made, less crucial in that the penalty involved is unlikely to be a strong function of the weighting matrix in the region of interest. The region of interest can usually be defined as that surrounding the minimum payoff cost perturbation. When guiding about an optimal path one solution to the weighting matrix problem is to base the weighting matrix on the second derivative of the Hamiltonian somewhat analogously to the approach suggested by Kelly in Reference 11 on the basis of second order reasoning.

In general this approach may not be satisfactory if the control has widely varying sensitivity along the flight path or if the nominal flight path is non-optimal, i.e., one determined by conventional performance analysis for example, or one in which the guidance and control payoff criteria differs from the basic flight path payoff criteria. This latter condition may be encountered frequently for it is in the nature of many flight mechanics problems that in those regions in which the governing response functions are greatest the terminal responses are most non-linear. Conversely, when the local response functions are small the terminal response is frequently quite linear. In situations of this type reliable guidance may well be associated with relatively small

that is, of the augmented state vector and time, hence T_p itself might be treated as a state variable and the state vector further augmented. Similar arguments hold for the aerodynamic forces and fuel flow, although in the trajectories of this study it is doubtful that is is worthwhile augmenting the state vector to account for fuel flow errors.

An approach of this nature would reduce vehicle characteristics errors to state errors and presumably eliminate the saw-tooth behavior observed in Section 3.4 , with consequent improved guidance.

To implement this approach would require estimation of the in-flight vehicle characteristic errors incorporated in the analysis. Obtaining this information from the available in-flight information might prove difficult, although optimal filtering theory presumably maybe of assistance here.

3.7 Summary

The lambda guidance simulations presented above demonstrate the feasibility of its use in Stage I guidance. There is little doubt that with some slight modification to the simulator, the complete Stage I/Stage II mission could also be controlled to similar accuracies. Further simulation appears necessary before a definitive judgement on the practicality of lambda guidance as a future method of control can be made.

This method has many attractive aspects. Computationally it is quite straightforward. It does provide optimal first order control once the time varying metric tensor of the control space is defined. It has considerable generality in that it provides a means for guiding to an arbitrary flight path whether optimal or not.

The problem of mechanization of the lambda guidance scheme has not received a detailed investigation. It does seem probable, in view of recent and anticipated increases in airborne computational capacity, that mechanization could be achieved within a reasonably short time, say before 1970. The mechanization may take several forms. If pre-flight computation of the control matrices were to be employed it is probable that present day airborne computer capacity would prove adequate. In the long term it seems / that on-board computation of these quantities is possible if conventional flight path determination techniques are employed. On-board computation of the control matrices for optimal paths would seem to require further advances in flight path optimization techniques, or at least significant improvement in the reliability of present methods before becoming feasible in the foreseeable future. Nevertheless in the long term this possibility should not be completely discounted.

It should also be noted that lambda guidance can have many variations. The present study is limited to fixed stage length problems and arbitrary weighting matrices. The state vector is limited to vehicle

mass and components of velocity and position. The indirect application of inequality constraints is required with the presently defined simulation. Each of these limitations could be removed with further effort. A final judgement on the power of lambda guidance awaits these developments. In the meantime the present results indicate it to be at least a promising future guidance technique.

SYMBOLS

(Reproduced from Reference 2)

A	Non-dimensional acceleration dose
$\bar{A}$	Non-dimensional acceleration dose with damping included
A_1, A_2, A_i	Integral measure of an inequality constraint violation
A_{ii}	Weighting matrix constant
A_m^s	Defined by Eqn. (7.2.4)
A_s^N	Defined by Eqn. (6.2.26)
$A(t)$	Control variable perturbation mode shape
$\mathring{A}(t)$	Desired control variable history for a vehicle flight path
$\dot{A}(t)$	Time derivative of non-dimensional acceleration dose
a, $a(t)$	Instantaneous acceleration
a_n	Acceleration in direction n
B_A	Bank angle
B_{ii}	Weighting matrix constant
B_m^s	Defined by Eqn. (7.2.5)
B_s^N	Defined as a column matrix by Eqn. (6.2.27), as a rectangular matrix in Eqn. (6.5.1)
C	The C^{th} iteration in a descent
$C_{D_\alpha}, C_{D_\alpha 2}, C_{D_\beta}, C_{D_\beta 2}, C_{D_{\alpha\beta}}$	Drag force slopes
C_{ii}	Weighting matrix constant
C_L, C_D, C_Y	Lift, drag and side force coefficients
$C_{L_o}, C_{D_o}, C_{Y_o}$	Lift, drag and side force coefficients when $\alpha = \beta = 0$
$C_{L_\alpha}, C_{L_\alpha 2}, C_{L_\beta}, C_{L_\beta 2}, C_{L_{\alpha\beta}}$	Lift force slopes
C_m^s	Defined by Eqn. (7.2.6)
C_N, C_A, C_Y	Force coefficients in body axis system
C_s^N	Defined by Eqn. (6.2.28)

C_{Y_α}, $C_{Y_{\alpha 2}}$, C_{Y_β}, $C_{Y_{\beta 2}}$, $C_{Y_{\alpha\beta}}$	Side force slopes
C_ψ	Non-dimensional amount of constraint error to be eliminated in a given cycle
c_q	Stagnation point heating coefficient
D	Any function to which an inequality constraint is to be added
D	Drag force
D	Summation defined by Eqn. (6.3.10)
DA^2	Algebraic control variable perturbation magnitude
D_{ii}	Weighting matrix constant
DP^2, DC^2	Control variable perturbation magnitudes
DP^2_{N-1}, DP^2_{N-2}	Value of DP^2 on final trajectory on last and last but one iterations
$DP_0{}^2$	Trial value of DP^2
$DP_1{}^2$	Minimum control variable perturbation magnitude which will eliminate a given constraint error
$DP_2{}^2$	Control variable perturbation magnitude when constraints are unaltered
DT^2	Stage point perturbation magnitude
$\bar{D}_U$, $\bar{D}_L$, $\bar{D}$	Upper and lower inequality constraints
D_1	Time history of D when inequality constraint is not satisfied
D_2	Time history of D when inequality constraint is satisfied
$df(\epsilon)$, df	Predicted change in a function for a very small perturbation
$d\beta$	Combined change in terminal constraints and initial state variable values
$d\beta^*$	Combination of $d\beta$ and cut-off function error
$d\phi$, $d\psi$, $d\Omega$	Change in payoff, constraint and cut-off functions

$d\phi_k$	Predicted change in ϕ for a step-size of magnitude k
$d\phi_o$, $d\psi_o$	Trial value of $d\phi$ or $d\psi$
E	Magnitude of maximum control variable error
E	A function to which a point constraint is to be applied
E	Distance between an interceptor and the first of two targets
$\bar{E}$, $\bar{E}(t)$	A point constraint
E_1	A function which fails to satisfy a point constraint
E_2	A function which satisfies a point constraint
F	Total vehicle force vector
F, F(t)	Matrix of partial derivatives $\frac{\partial f_i}{\partial x_j}$
F_n	Force in direction n
F_{x_e}, F_{y_e}, F_{z_e}	Components of force in X_e, Y_e, Z_e system
f, $f(x_n(t), \alpha_n(t), t)$	Function which gives the time derivative of a state variable
$\bar{f}$, $f(\bar{x}(t), \bar{\alpha}(t), t)$	Function which gives the time derivative of a state variable on the nominal trajectory
$f(X_i)$	Algebraic function of the variables X_i
f_1, f_2, f_v	Functions defining the state variables in the algebraic steepest descent analysis
G, G(t)	Matrix of partial derivatives, $\frac{\partial f_i}{\partial \alpha_j}$
grad ϕ	Gradient of ϕ when constraints are satisfied
g, g(x(T),T)	Any additional optimization function
g(x,y,z)	An algebraic constraint function

$H(D-\bar{D})$	Heaviside step function used to handle inequality constraints
h	Altitude
h_{min}	Minimum value of altitude permitted
h_s	Height of satellite's orbit
h_1, h_2	Height of target vehicles in interception problem
$I^{(-)}$, $I^{(+)}$	Number of regions in which $\lambda_{\phi\Omega}G$ is negative or positive
$I_{\phi\phi}$, $I_{\psi\phi}$, $I_{\psi\psi}$	Integrals of payoff and constraint sensitivities over whole trajectory
$I_{\phi\phi}(t')$, $I_{\psi\phi}(t')$, $I_{\psi\psi}(t')$	Integrals of payoff and constraint function sensitivities in the interval $t' \leq t \leq T$
i	Subscript indicating an element in the i^{th} row of a matrix
i,j,k	Unit vectors in direction of X_e, Y_e, Z_e
$J_{\phi\phi}$, $J_{\psi\phi}$, $J_{\psi\psi}$	Integrals defined by Eqns. (6.3.15) to (6.3.17)
J	Subscript indicating an element in the j^{th} column of a matrix
K_{N_ϕ}, K_{N_ψ}	Integrals defined by Eqns. (6.2.33) and (6.2.34)
K_s	Integrals defined by Eqn. (6.2.14)
$K_{\phi\phi}$, $K_{\psi\phi}$, $K_{\psi\psi}$	Functions defined by Eqns. (6.4.25) to (6.4.27)
k	Magnitude of control variable perturbation
k	Step-size parameter
$k(a,t-t')$	Acceleration dose damping function
k_{high}, k_{low}	Working limits on step-size parameter k
$k_{\phi TVL}$, $k_{\psi TVL}$	Value of step-size parameter based on dimensional change of payoff or constraint functions
L	Lift force
$L(t)$, $\dot{L}(t)$	Solution to the adjoint equations which at some time $t = T$, becomes the unit matrix
$L(t')$, $L(\bar{t})$	Particular values of L(t) at $t = t'$ or $\bar{t}$
$L_{\phi\phi}$, $L_{\psi\phi}$, $L_{\psi\psi}$	Integrals defined by Eqns. (6.3.7) to (6.3.9)

M	The number of control variables
M_N	Mach number
M_μ, M_ω	Constants used to improve convergence in numerical solution of variational equations
$M_{\phi\phi}$, $M_{\psi\phi}$	Functions defined by Eqns. (7.4.7) and (7.4.9)
m	Subscript or superscript indicating a typical control variable
m	Vehicle mass
m	Exponent of density in stagnation point heating
$\dot{m}$	Time derivative of vehicle mass
N	Exponent in approximate step function
N	The number of state variables
N	The number of completed iterations
N	Throttle setting
n	A direction
n	Exponent on velocity in stagnation point heating
n	Subscript or superscript indicating a typical state variable
$n_{x,a,y}$	Body axis forces
$O(P)$, $O(Q)$	Orders of magnitude
P	Argument of an order of magnitude
P	The number of constraints
P_1, P_2, etc.	Trajectories followed if the errors at the first, second, etc., predetermined sampling points are uncorrected.
p	Suffix indicating a typical constraint
P_s	Matrix which transforms state variable perturbations to the left of the s^{th} stage point into those on the right

$\dot{Q}$	Rate at which heat is created at the stagnation point
Q_s	Product of P_s and $\bar{\lambda}_{x\Omega s}$'
Q_1, Q_2, etc.	Expected trajectory after errors at first, second, etc., predetermined sampling points are corrected for
q	Dynamic pressure
R	Radius vector from center of the earth to vehicle
R	Range inhibiting force
R_e	Planet equatorial radius
R_p	Planet polar radius
r,s	Suffix indicating r^{th} and s^{th} control variables
S	A switching function
S	Vehicle reference area
S', $\bar{S}$	Number of stages being specified directly and optimized, respectively.
S^{ϕ}	A typical control variable sensitivity
S_r, S_s, S_t	Typical control variable sensitivities of order R,S,T, respectively
S^{ϕ}_{α}	Integrated payoff function sensitivities
$S^{\phi}_{\alpha\psi}$	Integrated mixed payoff function sensitivities
s', $\bar{s}$	Suffix indicating typical stage points being specified directly and optimized, respectively.
s^{ϕ}_{α}	Instantaneous payoff function sensitivities
$s^{\phi}_{\alpha\psi}$	Mixed control variable sensitivities
T	Trajectory termination time
$T_i(-)$, $T_i(0)$, $T_i(+)$	Upper time boundary on the i^{th} region in which $\lambda_{\phi\Omega}{}^0$ is negative, zero, or positive, respectively
T_s	Cut-off point for s^{th} stage in stage time
T_1, T_2	Actual conditions at predetermined sampling points along a trajectory
T_1', T_2', etc.	Anticipated conditions at predetermined sampling points along a trajectory
t	The independent variable, in this report time
t	A time point between the time an error is noted, t', and the trajectory termination

t'	Time at which an acceleration dose is received
t'	Time at which an error in a desired flight path is detected
t'	Time at which a function which fails to satisfy a point constraint is nearest to doing so
t'	A point in time separating regions of differing control variable power
t'	Time at which a stage point occurs
t'	A point at which it is desired to impose boundary conditions on the adjoint equation solution
$t_i(-)$, $t_i(0)$, $t_i(+)$	Lower time boundary on the i^{th} region in which $\lambda_\phi \Omega^G$ is negative, zero, or positive, respectively
t'_s	Time at which the s^{th} stage point occurs
t_{max}	Maximum value of time permitted.
t_o	Trajectory commencement time
U	Weighting function used in penalty function technique, Eqn. (6.4.42)
U, $\bar{U}$	Augmented payoff function
u,v,w	Velocity components of body axis system
u_e, v_e, w_e	State variables of velocity in X_e, Y_e, Z_e system
V, V_e	Vehicle velocity vector
V_{c_s}	Satellite velocity
V_I	Inertial velocity
$V_{\bar{s}}$	Stage point weighting functions
V_1, V_2	Velocity of targets in interception problem
W, $W(t)$	Control variable weighting function
W_α	Algebraic control variable weighting function
X_e, Y_e, Z_e	Rotating rectangular coordinate system at center of the earth
$\dot{X}_e$, $\dot{Y}_e$, $\dot{Z}_e$	Velocity components in X_e, Y_e, Z_e system
$\ddot{X}_e$, $\ddot{Y}_e$, $\ddot{Z}_e$	Acceleration components in X_e, Y_e, Z_e system
$\dot{X}_g$, $\dot{Y}_g$, $\dot{Z}_g$	Velocity components in local geocentric coordinates
X_i	Algebraic variables
$X(t)$	Desired flight path of a vehicle

$x_e(t)$, $\dot{x}_e$	A state variable and its derivative used in point constraint analysis
$x_n(t)$	The n^{th} state variable history
$\dot{x}_n(t)$	The nth state variable time derivative
x_o, x_{1_o}, x_{2_o}	Position of interceptor, and two target vehicles at $t = t_o$
$\dot{x}_s(T_s)$, $\dot{\bar{x}}_s$	Value of state variable derivative at $\tau = T_s$
$x(t)$	A state variable history
$\bar{x}(t)$	A nominal state variable history
$x(t_o)$, x_o	Initial state variable value
$x(T_s)$	Values of state variables at $\tau = T_s$
x_u, $x_u(t)$, x_L, $x_L(t)$	State variables which measure the integrated violation of an inequality constraint
$\dot{x}_u$, $\dot{x}_L$	Time derivatives of x_u, x_L
x,y,z	Body axis coordinates
x_1, x_2, x_v	State variables in algebraic steepest descent analysis
x , $\dot{x}$ (t)	A state variable and its derivative, used in the penalty function analysis
Y	Side force
z(x,y)	An algebraic function which is to be maximized
α , $\alpha(t)$	Control variable, control variable history
α	Angle of attack
$\alpha_m(t)$	The m^{th} control variable history
$\bar{\alpha}_m(t)$, $\bar{\alpha}(t)$	Nominal control variable history
α_1, α_2	A powerful and a weak control variable
α_1, α_2	Control variables in algebraic steepest descent solution

β	Sideslip angle
γ_I	Inertial flight path climb angle
ΔC_ψ	Attempted incremental change in C_ψ on each cycle
$\overline{\Delta P_i}^*$, $\overline{\Delta P_s}^*$, $\overline{\Delta P_r}^*$	Integral measure of total change in the i^{th}, s^{th} or r^{th} control variable between nominal and optimal trajectories
$\overline{\Delta P_i}(C)$, $\overline{\Delta P_s}(C)$, $\overline{\Delta P_r}(C)$	Integral measure of change in the i^{th}, s^{th} or r^{th} control variable, between the nominal and C^{th} iteration
$\overline{\Delta P_s}(\infty)$, $\overline{P_r}(\infty)$	Integral measure of change in the s^{th} or r^{th} control variable history as the number of ierations increases without limit
ΔP^2	Magnitude of control variable correction
ΔT	Change in cut-off time
ΔT_s	Stage time perturbation at the termination of the s^{th} stage
$\Delta T_s'$	Directly specified stage point perturbations
ΔT_s^*	Optimal stage point perturbations
ΔU	Change in augmented function produced by control variable perturbation
$\Delta f(\epsilon)$, Δf	Actual change in a function during a very small perturbation
$\Delta\alpha_i$	Difference between nominal and optimal values of i^{th} control variable at any point
$\overline{\Delta\alpha_s}$	Mean control variable change as the number of interations increases without limit
$\overline{\Delta\alpha^*_s}$	Mean control variable change between nominal and optimal trajectories
$\Delta\alpha(t)$	A control variable history correction or error
$\Delta\alpha(t')$	Size of a pulse correction to the control variable history at $t = t'$
$\Delta\beta$	Defined by Eqn. (III.23)
$\Delta\phi$, $\Delta\psi$	Terminal errors introduced by uncorrected state variable error at $t = t'$
$\Delta\phi(k)$, $\Delta\psi(k)$	Actual change in payoff or constraint functions for a perturbation step-size of magnitude k
$\Delta\Omega$	Cut-off function error introduced by terminating trajectory at the predicted time at which $\Omega = 0$
$\Delta\Omega_s$	Perturbation in the s^{th} stage point cut-off function
$\Delta\psi(-)$, $\Delta\psi(+)$	Upper and lower bounds on constraint function changes caused trajectory errors
Δx_s, Δx_s^P	Additional state variable perturbations specified directly by at the commencement of the s^{th} stage

$\Delta x(t')$	Error in desired flight path at $t = t'$
$\Delta\varphi(-)$, $\Delta\varphi(+)$	Upper and lower bounds on constraint function changes caused by trajectory errors
Δx_1^{ϕ}, Δx_1^{θ}	Perturbations in latitude and longitude at commencement of first stage
δU, $\delta\bar{U}$	Change in augmented payoff function
$\delta(d\phi)$	Change in ϕ caused by a pulse in the control variables at $t = t'$
δk	Change in control variable perturbation magnitude
$\delta(t-t')$	Dirac Delta Function applied at $t = t'$
$\delta x(t)$	State variable perturbation
$\delta x(\bar{t})$	State variable error induced at $t = \bar{t}$ by uncorrected error at $t = t'$
$\delta x_s(T_s + \Delta T_s)$	State variable perturbations at the termination of the s^{th} stage
$\delta x_s(0)$, δx_s	State variable perturbations at the commencement of the s^{th} stage
$\delta x_{s+1}(-)$, $\delta x_{s+1}(+)$	State variable perturbations induced by perturbations in preceding portion of the trajectory to the left and right of the s^{th} stage point
$\delta\alpha(t)$, $\delta\alpha$	Control variable variation (perturbation)
$\delta^2\alpha$, $\delta(\delta\alpha)$	Control variable second variation
$\delta\alpha_{ij}$, $\delta\alpha_{sj}$, $\delta\alpha_{rj}$	Change in the i^{th}, s^{th} or r^{th} control variable on the j^{th} descent
$\delta\alpha_o$	Trial value of $\delta\alpha$
$\delta\alpha_k$	Values of $\delta\alpha$ corresponding to a value k of the step-size parameter
$\delta\alpha(t)_{min}$, $\delta\alpha(t)_{max}$	The maximum and minimum control variable perturbation magnitudes at any point along the trajectory
$\delta\alpha_1$	Control variable perturbation corresponding to DP_1^2
$\delta\alpha_2$	Control variable perturbation which leaves the constraints unaltered
$\delta l'$	Defined by Eqn. (6.2.50)
$\delta\bar{\Gamma}$	Defined by Eqn. (7.4.1)

$\delta\Psi(T_s)$	Change in Ψ_s at $\tau_s = T_s$
$\delta\phi, \delta\psi, \delta\Omega$	Change in payoff, constraint and cut-off functions
θ_I	Inertial longitude
θ_L	Longitude
Λ	Sum of a set of vector solutions, or multiple of a solution, to the adjoint equations
$\Lambda_{\phi\Omega}, \Lambda_{\psi\Omega}$	Adjoint variables defined by Eqns. (6.2.35) and (6.2.36)
$\lambda, \lambda(t)$	The adjoint variables
$\dot{\lambda}, \dot{\lambda}(t)$	The adjoint variable derivatives
λ_T	Thrust angle rotation
$\lambda_e, \dot{\lambda}_e$	Adjoint variable corresponding to a point constraint state variable
$\lambda_i, \dot{\lambda}_i$	Adjoint variables which do not correspond to a point constraint state variable
$\lambda_j, \dot{\lambda}_j$	Vector solution to the adjoint equation and its time derivative
$\lambda_s^{(-)}, \lambda_s^{(+)}$	Values of the adjoint variables to the left and right of a stage point
$\lambda_{x_s}, \lambda_{x\Omega_s}$	Adjoint variables corresponding to the choice $\Psi = x$
$\bar{\lambda}_{x\Omega_s}, \lambda_{x\Omega_s}(0)$	Value of $\lambda_{x\Omega_s}$ at $\tau_s = 0$
$\lambda_\phi, \lambda_\phi(t)$	Payoff function adjoint variable, measures sensitivity of ϕ at unperturbed cut-off time to state variable changes at t
$\lambda_\psi, \lambda_\psi(t)$	Constraint function adjoint variable, measures sensitivity of constraint at unperturbed cut-off time to state variable changes at t
$\lambda_\Omega, \lambda_\Omega(t)$	Cut-off function adjoint variable, measures sensitivity of Ω at unperturbed cut-off time to state variable changes at t
$\lambda_{\Psi_s}, \lambda_{\Omega_s}, \lambda_{\psi\Omega_s}$	Adjoint variables defined in the s^{th} stage
$\lambda_{\phi\Omega}, \lambda_{\phi\Omega}(t)$	Payoff function sensitivity to state variable changes at t
$\lambda_{\psi\Omega}, \lambda_{\psi\Omega}(t)$	Constraint function changes to state variable changes at t

$\Psi, \Psi(x)$	Algebraic constraint function
$\Psi_s, \Psi_s(T_s + \Delta T_s)$	The value of any function of the state variables and stage time at the s^{th} stage termination
$\dot{\Psi}_s, \dot{\Psi}_s(T_s + \Delta T_s)$	Time derivative of Ψ_s
Ψ_1, Ψ_2	Constraints in algebraic steepest descent analysis
$\psi, \psi(x_n(T),T)$	A constraint function
$\dot{\psi}, \dot{\psi}(T)$	Constraint function time derivative at trajectory
ψ_{ERR}	Control system constants, Section I.4.5
ψ_{FWD}, ψ_{BWD}	Permissable favorable or unfavorable non-dimensional change in constraints
ψ_{NL}	Non-linearity of constraints
ψ_{NL_o}	Desired non-linearity of constraints
ψ_{TOL}	Desired accuracy of constraints
$\psi_\alpha(t')$	Constraint function sensitivity to control variable pulse at $t = t'$, in optimal staging problem
$\psi_{\Delta x_s}$	Constraint function sensitivity to perturbations in the state variable which are directly specified at the commencement of the s^{th} stage
$\psi_{\Delta T_s}$	Constraint function sensitivity to stage point perturbations
$\Omega, \Omega(x_n(T),T)$	The trajectory final cut-off function
$\dot{\Omega}, \dot{\Omega}(T)$	Cut-off function time derivative at trajectory termination
$\Omega_s, \Omega_s(x(T_s), T_s)$	Cut-off function for s^{th} stage
$\dot{\Omega}_s(T_s)$	Time derivative of s^{th} stage cut-off function at T_s
Ω	Longitude of ascending node
ω	Lagrangean multiplier on stage point perturbations
ω_p	Magnitude of earth's angular velocity
ω_p	Earth's angular velocity vector
ω_s	Angular velocity of satellite

ω_0, ω_1	Particular values of ω used in numerical solution of variational equations
$\phi, \phi(x)$	Algebraic payoff function
$\phi, \phi(x_n(T),T)$	The payoff function
$\dot{\phi}, \dot{\phi}(T)$	Payoff function time derivative at trajectory termination
ϕ_{ADV}	Maximum permissable adverse change in payoff function
ϕ_{max}	The greatest absolute value of the payoff function over the preceding iterations
ϕ_{NL}^{L}	Latitude Payoff function non-linearity
ϕ_{NL_o}	Desired payoff function non-linearity
ϕ_T	Thrust cone angle
$\phi_\alpha(t)$	Payoff function sensitivity to control variable pulses at $t = t'$, in optimal staging problem
$\phi_{\Delta T_s}$	Payoff function sensitivity to stage point perturbations
$\phi_{\Delta x_s}$	Payoff function sensitivity to state variable perturbations which are directly specified at the commencement of the s^{th} stage
φ	Central angle measured from ascending node
φ_s	Satellite central angle
$\mu\varphi s_o$	Initial satellite central angle
	Lagrangean Multiplier for control variable magnitude constraint
μ_g	Gravitational constant
μ_0, μ_1	Particular values of μ used in numerical solution of variational equations
ν	Lagrangean Multiplier for terminal constraints
ϑ	Lagrangean Multiplier used in optimal staging analysis
ϑ_0, ϑ_1	Particular values of used in numerical solution of variational equations
σ_I	Inertial heading angle

τ	Stage time
$\tau(a)$	The length of time that a vehicle or crew can withstand an acceleration a
τ_s	Stage time in the s^{th} stage
ψ	Longitude difference between vehicle and ascending node

Matrix Notation

$[\ ]$	Rectangular matrix
$\{\ \}$	Column matrix
$[\ ]$	Row matrix
$[\ ]$	Diagonal matrix
^{t}	Transposed matrix
$[\ ]^{-1}$	Inverse matrix

REFERENCES

1. A. E. Bryson and W. F. Denham, A Steepest-Ascent Method for Solving Optimum Programming Problems, Raytheon Report B31303.

2. D. S. Hague, Three-Degree-of-Freedom Problem Optimization Formulation, Volume 3 Analytical Development, FDL-TDR-64-1, Part I, Volume 3, AF Flight Dynamics Laboratory, Air Force Systems Command, Wright-Patterson AFB, October 1964.

3. A. A. Morgan and G. W. Brandaway, An Explicit Multi-Stage Boost Guidance for Minimum Fuel Consumption, Boeing Document D2-90200, November 1962.

4. D. S. Hague, "The Optimization of Multiple-Arc Trajectories by the Steepest-Descent Method", pp 489-517; Recent Advances in Optimization Techniques, edited by Lavi and Vogl, John Wiley, 1966.

5. FDL-TDR-64-1, Part II, Volume 3, Users Manual for Part I, Volume 3 (reference 2 above)

6. Part I of D2-113016-5.

7. L. H. Stein, M. L. Matthews, and J. W. Frenk, "STOP-A Computer Program for Supersonic Transport Trajectory Optimization", Contract NAS 1-5293, Final Report, January 1967.

8. D. W. Hahn and B. F. Itzen, "The Space Trajectory Optimization/Steepest Ascent Digital Computer Program (AS 2080)", Boeing Document D2-23374, June 1964.

9. W. F. Denham and A. E. Bryson, Jr., "Optimal Programming Problems With Inequality Constraints II: Solution by Steepest-Ascent", AIAA Journal, January 1964, pp. 25-34.

10. A. E. Bryson, Jr., W. F. Denham, S. E. Dreyfus, "Optimal Programming Problems With Inequality Constraints I: Necessary Conditions for Extremal Solutions", AIAA Journal, November 1963, pp. 2544-2550.

11. Optimization Techniques with Applications to Aerospace Systems, edited by George Leitmann, Academic Press, 1962.

4.0 Navigation-Guidance Mechanization and Related Studies

4.1 Stage 1 Navigation Equipment and Mechanization

A block diagram of the Stage 1 G & N system is shown in Figure 4-1. Table 4-1 shows the weight, volume, and power of the navigation and communication equipment for the Stage 1 vehicle. The communication equipment is included as part of the avionics system. For the most part, two units are provided for each function, following more-or-less standard airplane practice of providing separate equipment for each control position. Equipment for the current technology concept is shown in Table 4-1. The advanced technology concept differs from the current technology concept in the inclusion of a navigation satellite receiver and the use of a strapdown inertial system in place of the gimbaled system.

4.1.1 Inertial Navigation System

The inertial navigation system is required for two functions, navigation and the attitude reference for the vehicle. The pilot-aircraft control interface is an area for research to assure flight safety. Techniques need to be developed to minimize the effects of attitude reference failures. Manual control by the pilot to follow navigation-guidance commands will require simulation test for malfunction situations. To provide maximum safety, three inertial systems with majority logic error detection are recommended. The first failure will fail operational, and the second failure can be detected by auxiliary failure detection logic and crew decision. Choice of three inertial systems also improves navigation accuracy. If all three systems are 1.8 km/hour (1 N.M./hour) systems, total inertial navigation accuracy after filtering is 1.05 km/hour (0.58 N.M./hour). A third advantage in the choice of three systems is that dispatch reliability is improved. Failure of one system during preflight does not necessarily scrub the flight as it can continue with two systems operating with a small penalty in safety.

Results of the Phase 1 study indicated that 1.85 km/hour inertial navigation accuracy is near optimum in terms of cost and performance. This is the accuracy currently being specified for many military aircraft, advanced subsonic commercial aircraft, and supersonic commercial aircraft. Following is a list of companies currently producing systems in the 3.7 km/hour (2 N.M./hour) or better accuracy range:

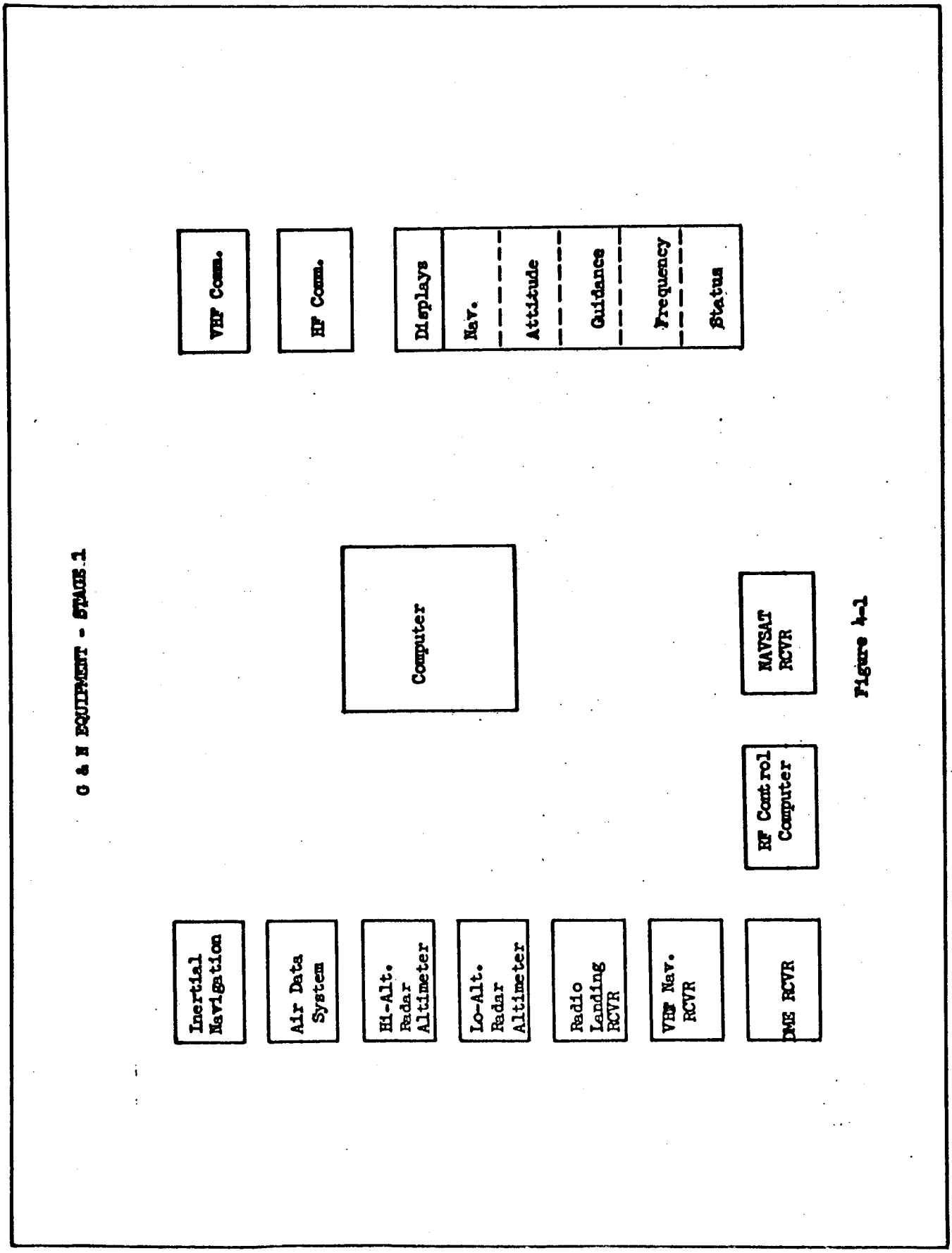

Figure 4-1

Table 4-1

STAGE 1 NAVIGATION EQUIPMENT - CURRENT TECHNOLOGY CONCEPT

Unit/Subsystem	Number of Units	Weight/Unit KG(lb)	Volume/Unit M^3 (ft^3)	Power Unit-W	Total Weight KG(lb)	Total Volume M^3 (ft^3)	Total Power-W
Inertial Navigation-Gimbaled System	3	27 (60)	.043 (1.5)	300	81 (180)	.129 (4.5)	600
Air Data	2	2.7 (6)	.0043 (.15)	15	5.4 (12)	.0086 (.3)	30
Hi-Alt Radar Altimeter	1	11.3 (25)	.017 (.6)	75	11.3 (25)	.017 (.6)	75
Low-Alt Radar Altimeter	2	4.5 (10)	.0028 (.1)	75	9 (20)	.0056 (.2)	150
Radio Landing Receiver	2	4.5 (10)	.014 (.5)	50	9 (20)	.028 (1)	100
VHF Nav Receiver	2	9 (20)	.008 (.3)	56	18 (40)	.016 (.6)	112
DME Receiver	2	17 (37)	.014 (.5)	200	34 (74)	.028 (1)	400
Radar ATC Transponder	2	5.5 (12)	.008 (.3)	75	11 (24)	.016 (.6)	150
Navigation Displays	2	9 (20)	.014 (.5)	50	18 (40)	.028 (1)	100
Central Nav. Computer	2	23 (50)	.057 (2)	100	46 (100)	.114 (4)	200
VHF Communications	2	7.7 (17)	.008 (.3)	33(193)*	15.4 (34)	.016 (.6)	66
HF Communications	2	25 (55)	.025 (.9)	20(1600)*	50 (110)	.05 (1.8)	40
RF Control Unit	2	2.25 (5)	.0028 (.1)	20	4.5 (10)	.0056 (.2)	40
RF Device Control Computer	2	11.3 (25)	.014 (.5)	40	22.6 (50)	.029 (1)	80
RF System Displays	2	3.6 (8)	.008 (.3)	65	7.2 (16)	.016 (.6)	130
TOTAL		163 (360)	.24 (8.5)	1174	342 (755)	.5 (18)	2273

*Power when transmitting

Company	System
AC Electronics	Carousel
Autonetics	N-16
Bell Aerosystems	Hipernas
General Precision	ASN-58
Honeywell	H-386
Litton	LN-15
Nortronics	NIS-105
Sperry	SGN-10

A typical set of parameters for a representative system would be as follows:

Performance	1.85 km/hour (1 N.M./hour)
Weight	27 kg/systems (60 lb/system)
Power	300 W
Volume	.0425 M^3 (1.5 cubic feet)
Computer	GP parallel
Storage	16,000 words, 24 bits/word
Speed	12 μ SEC add time
Reliability	1000 hour MTBF/system

4.1.2 Radio Navigation Aids

VOR/DME

The standard radio navigation aid for aircraft is the VHF Omni Range (VOR) system. Air navigation overland relies almost entirely on this system. The VOR measurement provides the magnetic bearing of the VOR station with respect to the aircraft. Crossing of two bearing lines, together with knowledge of altitude fixes the aircraft position. In recent years, the addition of radio distance measuring equipment (DME) has been implemented at many VOR stations. Using bearing and range, a fix can be obtained from one station. The accuracy of VOR bearing information is on the order of 2.5 degrees (2σ). At a 365 km (200 Mile) range, this results in a line at position uncertainty of 14.5 km (eight miles). The distance measurement is much more accurate, being about 0.27 km (0.15 miles) 2σ. Fixes obtained from DME measurements from two stations would be within 0.55 KM (0.3 miles) for a reasonable fix geometry. The usable range of DME fixes is from 185 to 550 km (100 to 300 miles), depending to a large extent on aircraft altitude.

VOR/DME position fixes will be used to update the Stage 1 inertial system when it is flying overland and when it enters the terminal area on the return mission phase.

OMEGA

The OMEGA system, when completed, will provide near world-wide navigation coverage. Expected accuracy is on the order of 4 km (2.2 N.M.) 2σ. Since this accuracy is not competitive with inertial system accuracy, the OMEGA system would not be used for a prime navigation aid. It could possibly have some use as a backup system, but its value would be questionable in view of the fact that three inertial navigators are recommended.

Loran C

The Loran C radio navigation system, while not offering world-wide coverage, does provide fairly high accuracy 0.36 km (0.2 mile) fixes over many parts of the Earth. If a large percentage of flights are expected to traverse areas covered by Loran C, installation of a Loran C receiver in the Stage 1 vehicle may be seriously considered as a means to increase navigation accuracy and reliability.

Automatic Landing System

An instrument landing system is desirable for this mission to provide all-weather capability. There is a general dissatisfaction in some circles on the adequacy of the current standard instrument landing system (ILS). Some specific complaints include the following:

- o ILS ground system calibration is not stable. Factors affecting beam accuracy include: nearby structures, nearby aircraft, ground conductivity, water table level and tide level.
- o Accuracy is not adequate, especially near the runway.
- o The system costs too much to install at some of the smaller airports, especially those in more primitive countries.

Pilots complain of numerous "disengages" (automatic decoupling of ILS from autopilot upon signal loss) during approaches. In one instance, it was found that disengages occurred at the same point in the approach path whenever a particular hangar door was closed. Anyone who has watched TV when an airplane was flying overhead can appreciate this phenomenon. The problem of providing an automatic all-weather landing system even for subsonic airplanes is acute. It is expected to be even more acute for supersonic airplanes which will have larger attitude response times. For a hypersonic aircraft, landing approach speeds may be above 365 km/hour (200 knots), control response will be slow, and pilot visibility in approach and touchdown attitude will be limited. In addition, the fuel required for a go-around after a missed landing may be excessive. It is doubtful that the current ILS system will provide accurate enough guidance for such an aircraft. It is probable that an ILS system that will meet the requirements will be available contemporary with the hypersonic launch vehicle.

A number of studies have been done on developing an improved landing guidance system. One system which has reached the testing state is the STATE system. This system is essentially an improvement on the current ILS technique, with the major difference being the use of high frequency (C band) to permit formation of a narrow beam, thereby avoiding reflection from nearby objects, and the addition or range information. Other systems under study utilize an onboard radar which interrogates radar beacons on the runway. A system like the STATE system may be applicable, since it is designed for portable operation, ground equipment is relatively inexpensive, and the beam elevation angle can be tailored to fit the desired glide slope.

Radar Altimeters

Two radar altimeters are shown in the first stage G & N equipment list. One is a high altitude radar altimeter for use during the high altitude cruise portion of the mission. The output of the high altitude radar altimeter will be used to correct the output of the altitude computed by the inertial navigation system, as the error in altitude computed by the inertial system grows with time. The Saturn V radar altimeter is used as an example of the high altitude radar altimeter.

The low altitude radar altimeter has an altitude range of 0-1500 Meters (0-5000 ft) and is used for the automatic landing function. This altimeter is used for altitude control during final descent through the point of the flare maneuver. The AN/APN 167 radar altimeter is a typical example.

4.1.3 Air Data Sensors

It is expected that some development will be required for an air data system for the cruise vehicle. Accurate measurement of static pressure becomes difficult because of the low pressure at cruise altitude. The atmospheric pressure at 30 km (100,000 feet) is about 8 mm (0.32 inches) of mercury. Pressure sensing accuracies of 0.08 mm (±0.003) inches of mercury can be attained. A 0.08 mm of mercury error in static pressure sensing at Mach 7 results in an error in computed Mach No. of 0.08.

At Mach 7, the air stagnation temperature is about 2155 degrees C (3900 degrees F). Platinum wire resistance elements are usually used for measuring stagnation temperatures at lower Mach numbers. Platinum melts at 1760 degrees C (3200 degrees F). Tungsten may possibly be used as the sensing element.

Because of the high temperature environment, cooling of the pressure sensors may be necessary.

4.1.4 Navigation and Guidance Displays

The G & N displays can be grouped into four general categories. These are (1) displays of vehicle state, (2) displays of vehicle attitude, (3) displays of predicted vehicle state, and (4)displays of G & N subsystem status. Primary displays in each of these categories are identified below.

(1) Position Displays

- o Inertial navigator position
- o Radio update position
- o Position deviation
- o Mach/airspeed
- o Inertial navigator ground speed
- o Heading
- o Heading deviation
- o Acceleration
- o Radar altitude
- o Pressure altitude
- o Altitude rate

The radio update position is the position obtained from the last update and carried forward in time using inertial navigation. The pilot can, at his discretion, update the inertial navigator depending on his judgement of the quality of the radio update.

(2) Attitude Displays

- o Vehicle pitch and roll
- o Pitch and roll deviation
- o Pitch and roll rate

(3) Predicted Position Display

- o Time to destination
- o Time deviation
- o Distance to destination

(4) Subsystem Status Displays

- o Subsystem malfunction indication
- o Nav receiver signal to noise ratio
- o Inertial navigator mode, alignment state
- o Receiver, transmitter frequency settings

During all airborne phases of the cruise vehicle mission, the vehicle will be under control of a precomputed flight plan stored in the control computing system. The crew will monitor the displays and provide human decision and backup capability for situations which are difficult to control using the computer.

Conventional flight instruments, geared to manual operation of subsonic aircraft may not be adequate for hypersonic flight. However, the use of a central computing system allows a great deal of flexibility in display management in that display modes and sequences can be programmed on the computer. Both special and general displays should be used. An example of a general display is a cathode ray tube display on which messages of interest are written upon manual command or computer command. Special displays are used for parameters which must be monitored continuously, such as position, velocity, and attitude. A common concept for a position display is a film map display which uses a computer driven "bug" to denote the vehicle position. The map display is often integrated with the CRT display using a single display tube which combines the film projection and electron beam writing.

One of the considerations in the design of the display and control system for navigation and guidance is integration with a central electronic management system. Modern high performance airplanes are reaching a level of complexity that greatly increases pilot workloads and electronic system requirements.

Besides controlling the vehicle, a central electronic management system would also perform other flight functions which in subsonic airplanes traditionally have been done manually. These include:

- o Communication frequency switching
- o Automatic navigation updates
- o Automatic position reporting
- o Central data recording
- o Malfunction detection
- o Display management
- o Provide control response to certain malfunctions such as engine out.

4.1.5 Communications

Communications is basically a separate function that is included in the navigation equipment because of the requirement for enroute target orbit parameter updating. Standard communications equipment is VHF and HF transmitters, receivers, displays and controls. A radio frequency device control computer is included for automatic tuning to reduce crew work load requirements.

4.1.6 Packaging

Packaging of the first stage guidance and navigation equipment will for the most part follow standard airplane rack units. Figure 4-2 shows a typical layout for the navigation and communications equipment. Some of the units require forced air cooling. This is usually done with a fan mounted on the rear of the package. Ambient temperature around the equipment rack should be below 43°C (110°F) for adequate cooling. A typical packaging arrangement for the inertial navigation unit is shown in Figure 4-3.

4.1.7 Advanced Technology Concept - Stage 1

The advanced concept Stage 1 navigation system differs from the current technology concept in that a world-wide navigational satellite system is assumed to exist. Moreover, the satellite system is assumed to provide a high enough fix frequency to be useful to the hypersonic cruise vehicle application. This would require an update about every five minutes. Most satellite navigation systems currently under study provide continuous coverage. Navigation accuracy is $\pm$1.85 km ($\pm$ 1 N.M.) or better. The use of a high accuracy, high frequency navigation satellite system allows the use of a less accurate inertial navigation system. A strapdown inertial navigation system is proposed for the advanced technology configuration on the Stage 1 vehicle. Such a system would have a navigation accuracy of 3.7 km/hour (2 N.M./hour) CEP, a weight of 18 kg (40 pounds), a volume of .028 M^3 (one cubic foot), a power of 150 watts, and a 2000 hour MTBF. The weight, volume, and power of the navigation satellite receiver is 9 kg, .014 M^3, and 20 watts. Table 4-2 shows the Advanced Technology Stage 1 equipment.

The use of a high accuracy world-wide navigational satellite system allows the deletion of short range radio navigation aids (VOR and DME) for terminal area navigation. In the advanced technology concept, two navigation satellite receivers will be provided. Table 4-2 shows the advanced technology Stage 1 navigation equipment. The possibility also exists that (a) depending upon the Navsat type there may not be a need for the high altitude altimeter, and (b) voice and other communications could also be handled by Nav Sat.

The degradation of strapdown inertial systems because of environmental efforts is only approximately known. A flight test program is recommended to evaluate strapdown technology.

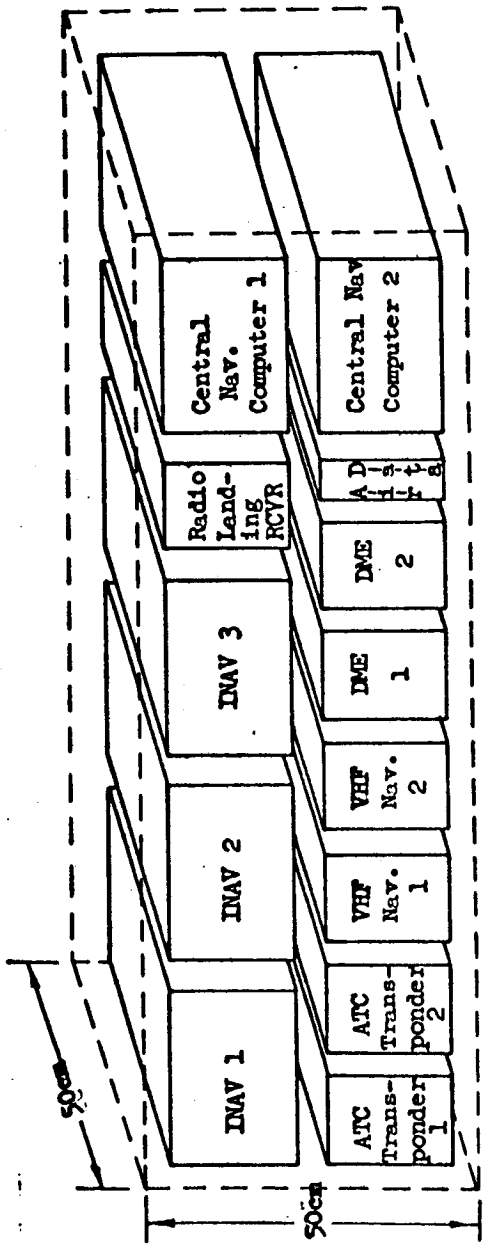

Guidance and Navigation Equipment

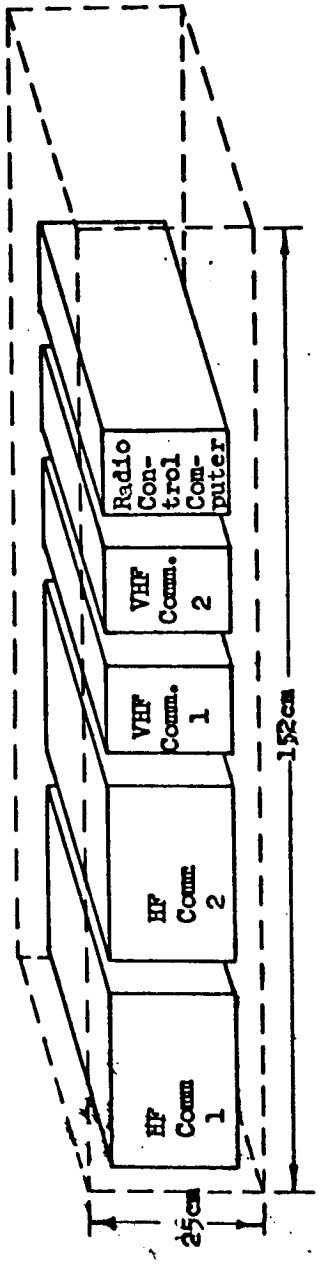

Communications Equipment

Figure 4-2

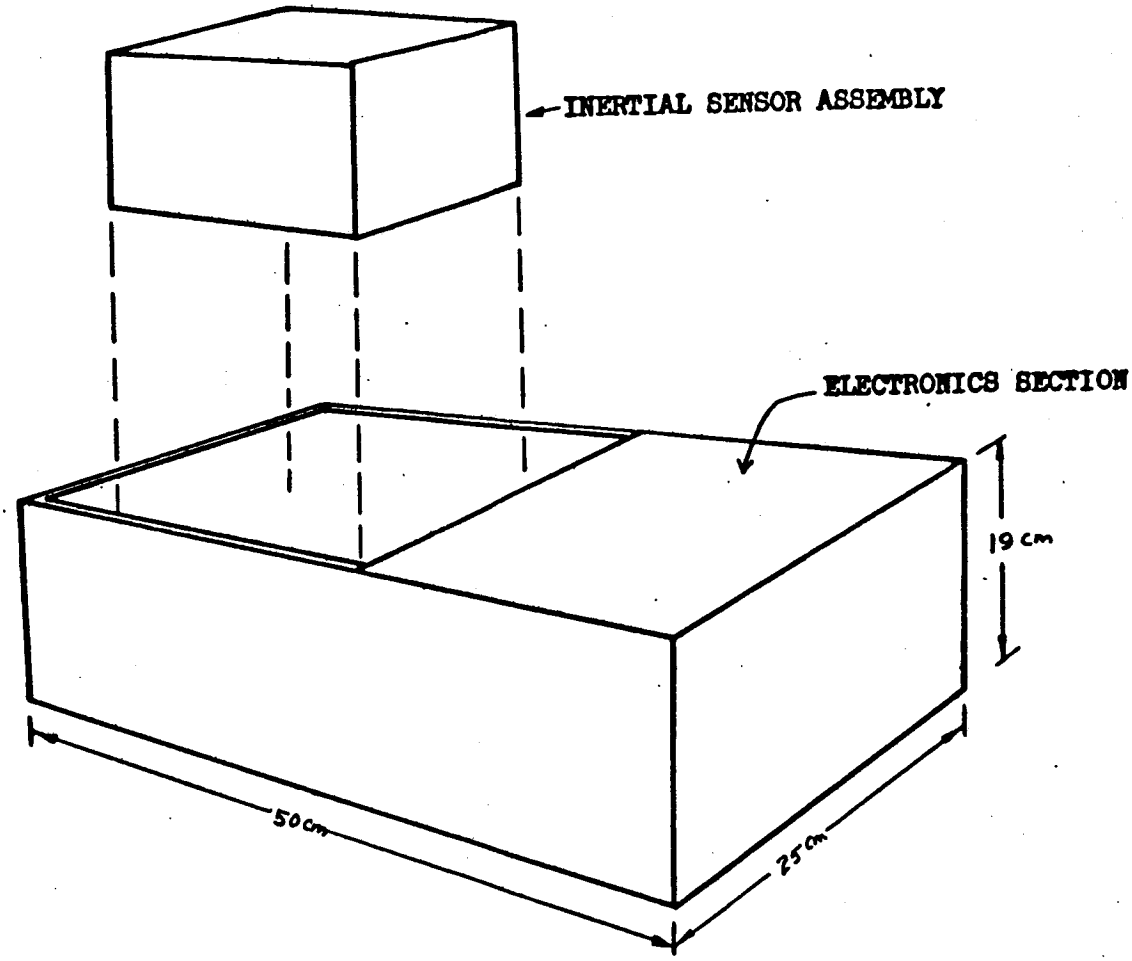

TYPICAL INERTIAL NAVIGATION UNIT PACKAGING

Figure 4-3

Table 4-22

Stage 1 Navigation Equipment - Advanced Technology Concept

Unit/Subsystem	Number of Units	Weight/Unit KG (lb)	Volume/Unit M^3 (ft^3)	Power Unit-W	Total Weight KG (lb)	Total Volume M^3 (ft^3)	Total Power-W
Inertial Navigation - Strapdown System	3	18 (40)	.028 (1)	150	54 (120)	.084 (3)	450
Air Data	2	2.7 (6)	.0043 (.15)	15	5.4 (12)	.0086 (.3)	30
Hi-Alt Radar Altimeter	1	11.3 (25)	.017 (.6)	75	11.3 (25)	.017 (.6)	75
Lo-Alt Radar Altimeter	2	4.5 (10)	.0028 (.1)	75	9 (20)	.0056 (.2)	150
Radio Landing Receiver	2	4.5 (10)	.014 (.5)	50	9 (20)	.028 (1)	100
Radar ATC Transponder	2	5.5 (12)	.008 (.3)	75	11 (24)	.016 (.6)	150
Navigation Displays	2	9 (20)	.014 (.5)	50	18 (40)	.028 (1)	100
Navsat Receiver	2	9 (20)	.014 (.5)	20	18 (40)	.028 (1)	40
Central Nav. Computer	2	23 (50)	.057 (2)	100	46 (100)	.114 (4)	200
VHF Communications	2	7.7 (17)	.008 (.3)	33	15.4 (34)	.016 (.6)	66
HF Communications	2	25 (55)	.025 (.9)	20	50 (110)	.05 (1.8)	40
RF Controls/Displays	2	15 (33)	.022 (.8)	80	30 (66)	.044 (1.6)	160
TOTALS		135 (298)	.214 (7.65)	743	277 (611)	.424 15.7	1561

4.2 Stage 2 Guidance-Navigation Equipment and Mechanization

4.2.1 Current Technology Concept

The Gemini guidance and navigation system is chosen as an example of current technology equipment which can meet the accuracy and reliability requirements of the Stage 2 mission. Major elements of the Gemini guidance system include a gimbaled inertial measurement unit, a general purpose digital computer, a rendezvous radar, and a horizon scanner. Although current Gemini equipment is described for the current technology concept, it is expected that advances in the state of the art will be taken advantage of in implementing a Gemini-type guidance system for the cruise-launch application. Primary advance is expected in increased reliability and lower weight. A block diagram of the Stage 2 G & N system is shown in Figure 4-4, and a summary table of the Stage 2 G & N equipment is given in Table 4-3.

Inertial Measurement Unit

The inertial measurement unit chosen for the current technology Stage 2 system is the Gemini system. This is an all attitude platform using three gyros and three accelerometers. The IMU weighs approximately 13.6 kg (30 pounds), has a volume of 0.025 M^3 (0.76 cubic feet) and has a power consumption of 100 watts. An installation drawing of the Gemini IMU is shown in Figure 4-5.

Computer

A computer meeting requirements is a general purpose serial computer having a memory capacity of 8,000 twenty-four bit words. The weight of the computer is 27 kg (60 pounds), it has a volume of 0.0425 M^3 (1.5 cubic feet) and a power consumption of 85 watts.

Rendezvous Radar

The rendezvous radar is a L Band radar which measures the range, range-rate, angle, and angular rate to a transponder in the target vehicle. The acquisition range is 460 km (250 N.M.). The antenna is composed of four archimedes spiral antennas. Measurement of the angle of the incident wave from the transponder is achieved by rotating the spiral antenna to form an interferometer phase measuring system. The angle of rotation is proportional to the angle of the received signal from the reference axis. The weight, size and power of the Gemini rendezvous radar is 31 kg (68 pounds), 0.05 M^3 (1.75 cubic feet), and 78 watts. An advanced version has been proposed having a weight of 13.5 kg (30 pounds), a volume of .035 M^3 (1.25 cubic feet), and a power of 23 watts. Figures 4-6 and 4-7 show the Gemini rendezvous radar installation.

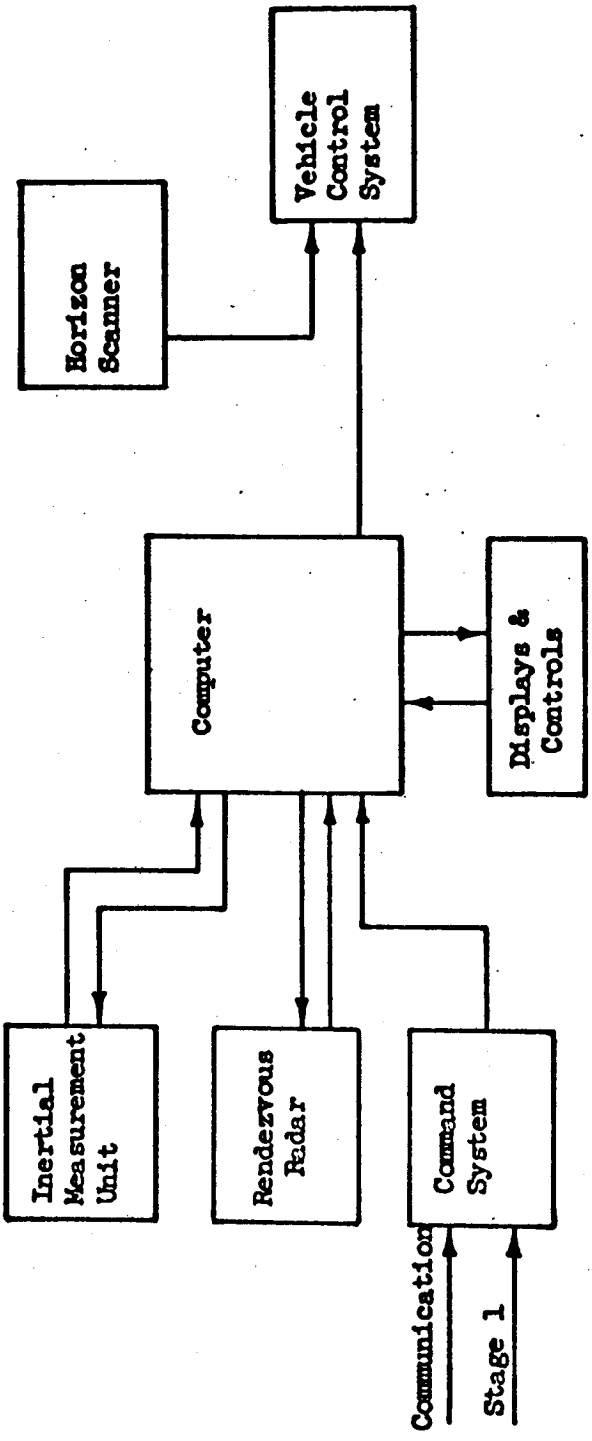

Stage 2 G & N SYSTEM

Figure 4-4

STAGE 2 G&N EQUIPMENT - CURRENT TECHNOLOGY CONCEPT

Unit	Number of Units	Weight KG (lb.)	Volume M^3 ($ft.^3$)	Power W
IMU	1	13.6 (30)	.025 (.76)	100
IMU Electronics	1	9 (20)	.0056 (.2)	30
Computer	1	27 (60)	.043 (1.5)	90
Rendezvous Radar	1	31 (68)	.05 (1.75)	78
Horizon Scanner	1	8.2 (18)	.009 (.3)	20
Displays/Controls*	1	6.8 (15)	.0057 (.2)	30
Command System	1	9 (20)	.007 (.25)	20
	System Totals	105 (231)	.145 (4.96)	368

*Manned Only

Table 4-3

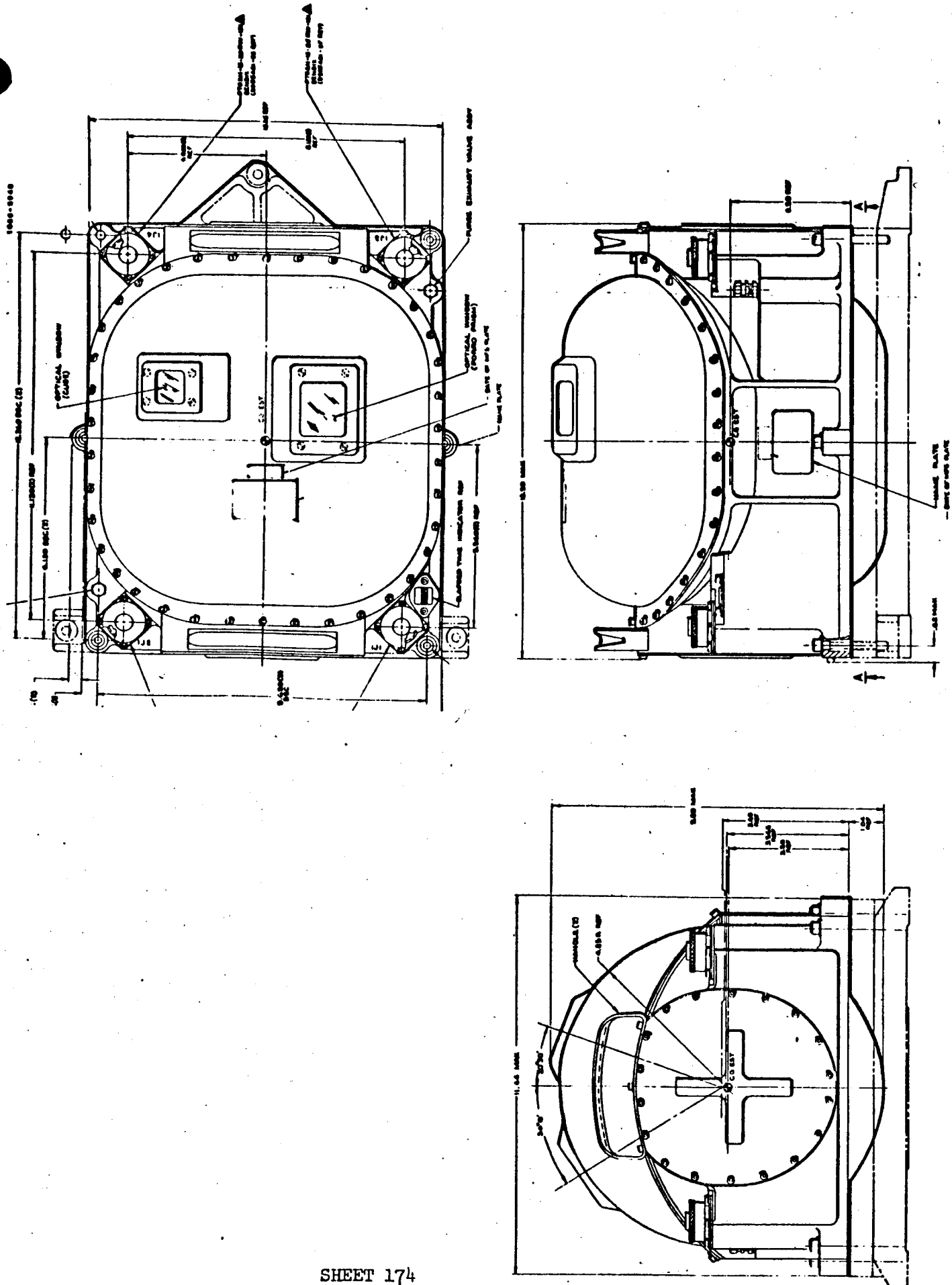

Figure 4-5

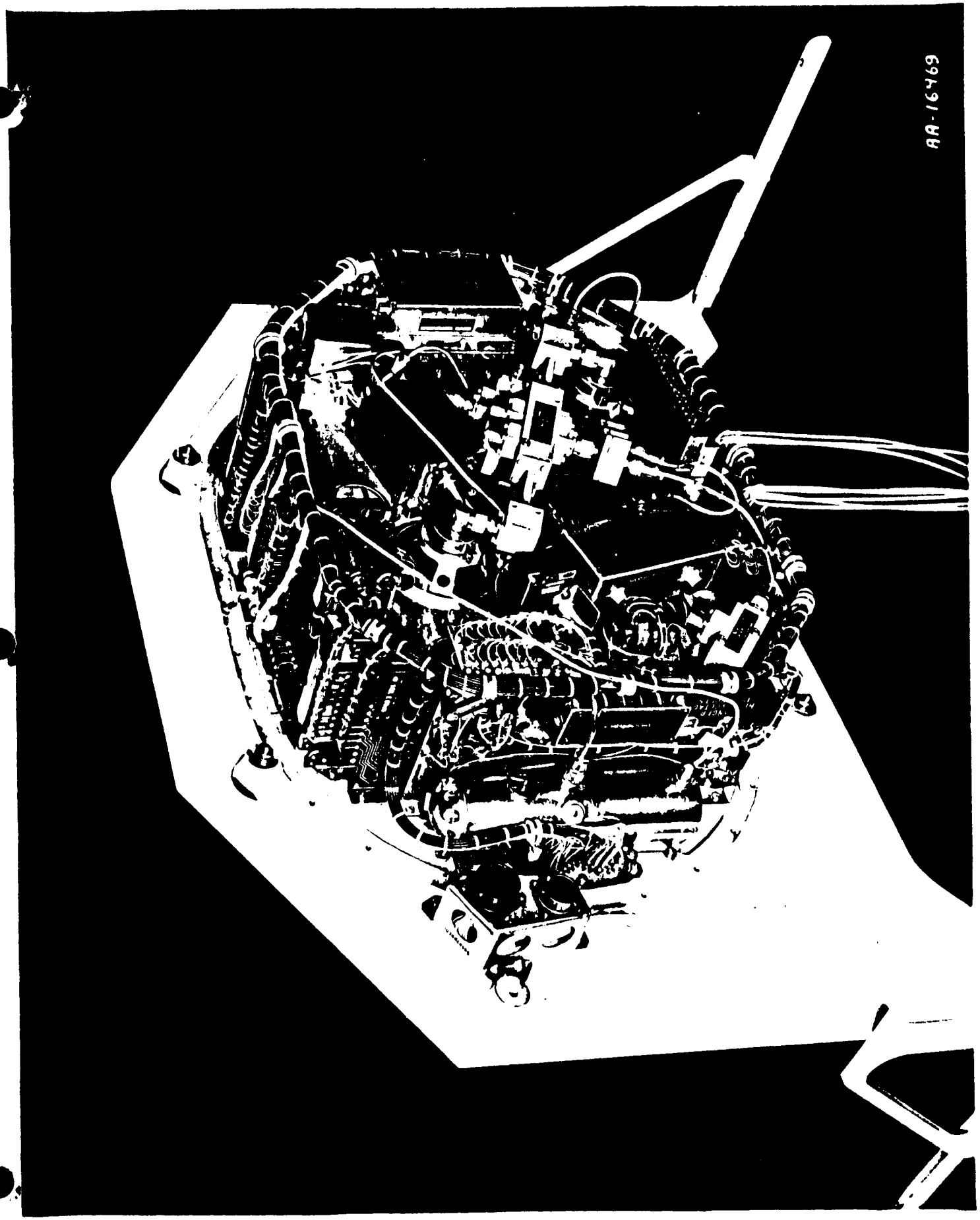

Figure 4-6

Gemini Radar - Rear View

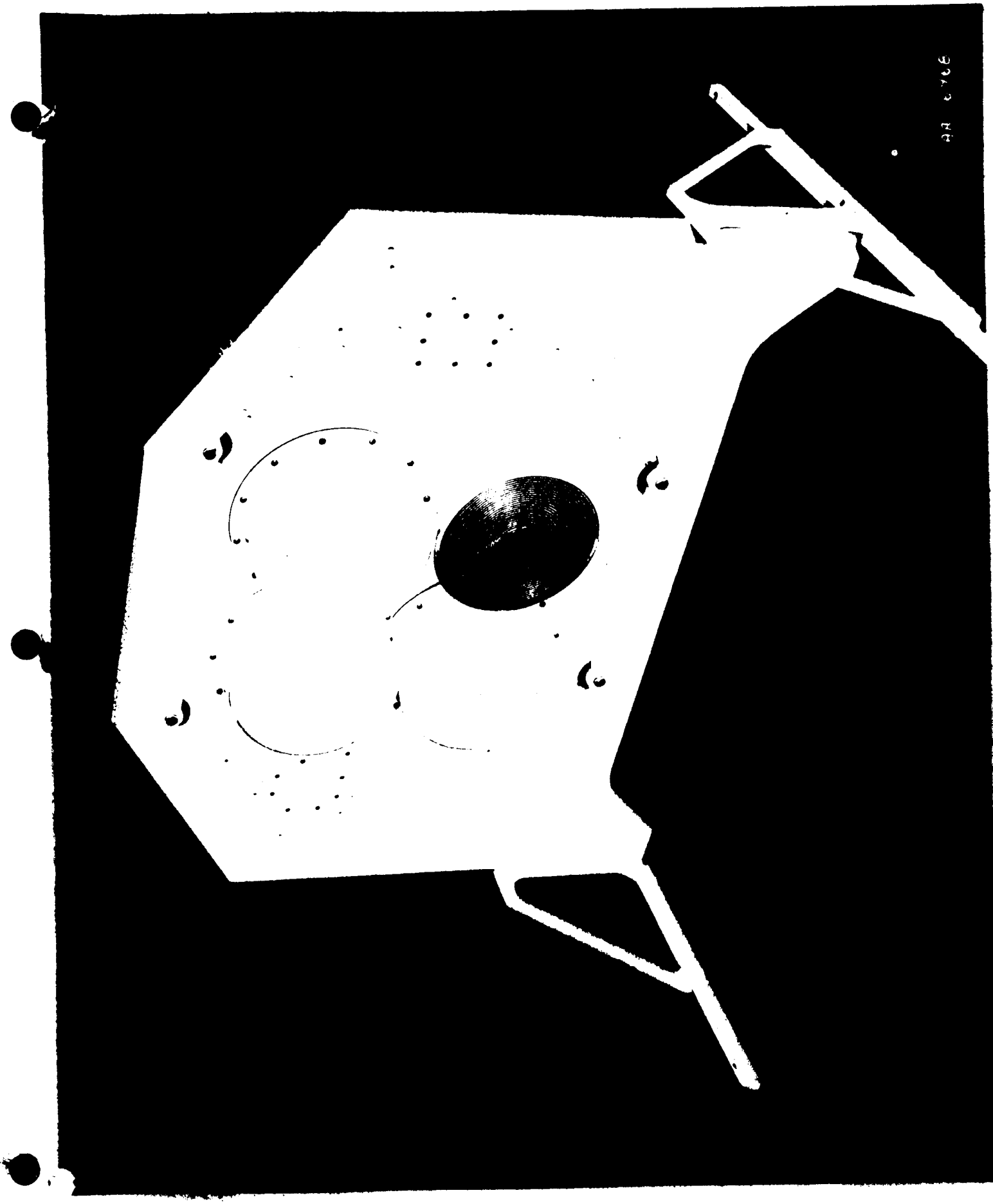

Figure 4-7

Gemini Radar - Front View

Displays

Gemini displays are considered representative of current technology Stage 2 G & N displays. These displays consist of the following:

- o Rendezvous radar range and range rate indicator
- o Computer manual data display unit
- o Incremental velocity indicator
- o Attitude display

Command System

The command system is used to accept commands from the ground control system. These commands are either stored for execution at a later time (stored program command) or are routed for immediate execution (real time command).

Horizon Scanner

The horizon scanner is used for in-orbit attitude reference and as a means of aligning the inertial guidance system. Aligning the inertial reference is accomplished by slaving the pitch and roll gyros to the horizon scanner local vertical reference and rotating the vehicle yaw axis until the sensed roll rate is zero. The error in horizon scanner sensed local vertical at a 460 km (250 N.M.) altitude is expected to be less than 0.15 degrees. An advanced version of the Gemini horizon sensor, similar to that used in OGO can be used. The weight of the system is 4.5 kg (10 pounds) and the power of 6W. Figure 4-8 shows a picture of the horizon sensor. Two tracking heads are used, providing four tracking fields of view. One electronics assembly supports both tracking heads. Figure 4-9 shows a schematic of the tracker head.

4.2.2 Advanced Technology Concept - Stage 2

The advanced technology concept for the Stage 2 navigation-guidance system is not too dissimilar from the current technology concept. The major differences are:

1. Use of a strapdown guidance system in place of the gimbaled IMU.
2. Use of an advanced version of the Gemini rendezvous radar.

For the second stage vehicle in particular, a strapdown inertial system appears attractive. Because of the short thrusting time, gyro drift errors do not produce substantially large navigation errors. A gyro drift error of one degree/hour for example, will cause a maximum position error at apogee of 5.2 km (2.8 N.M.). A

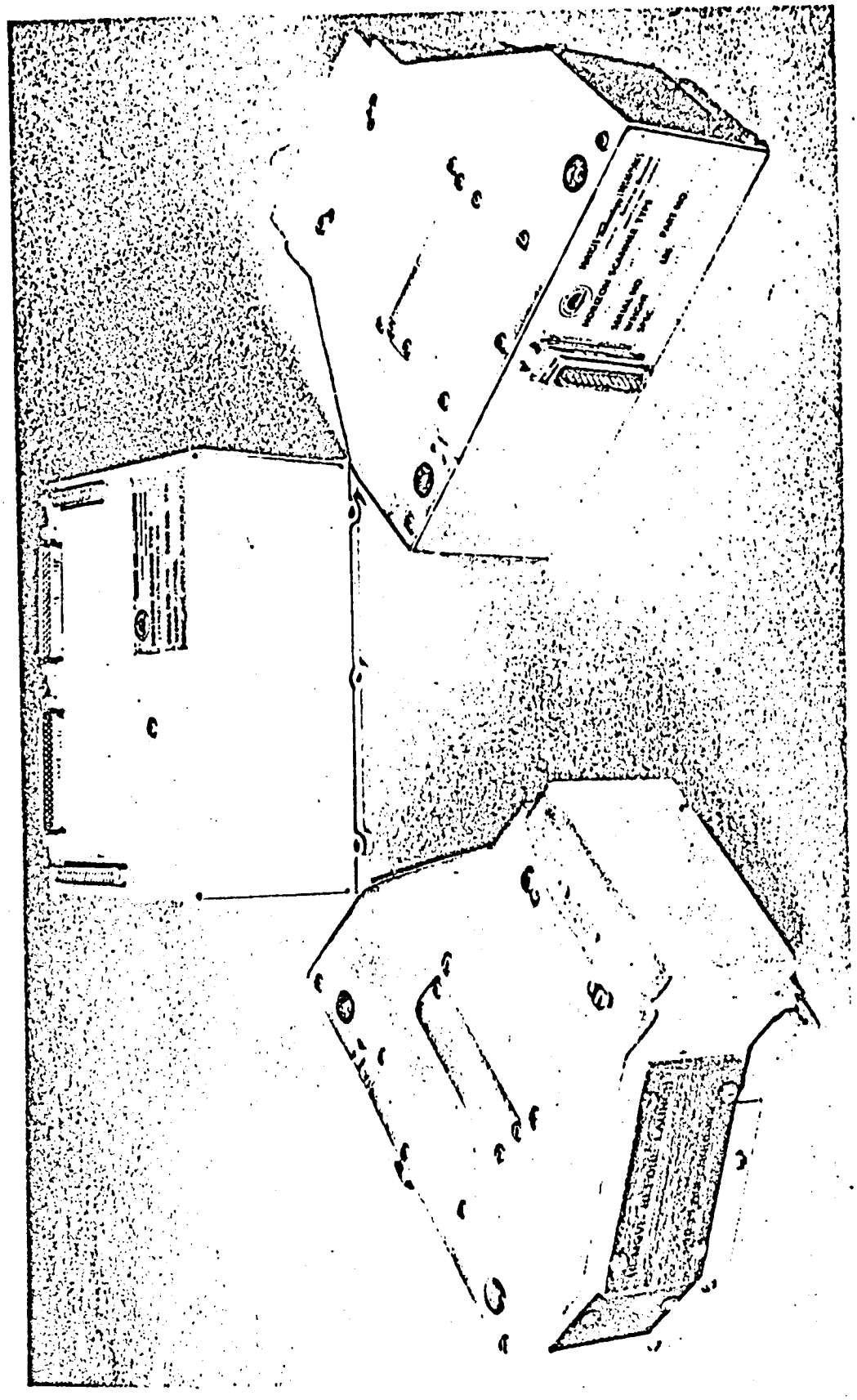

Fig. 4-8 OGO horizon sensor.

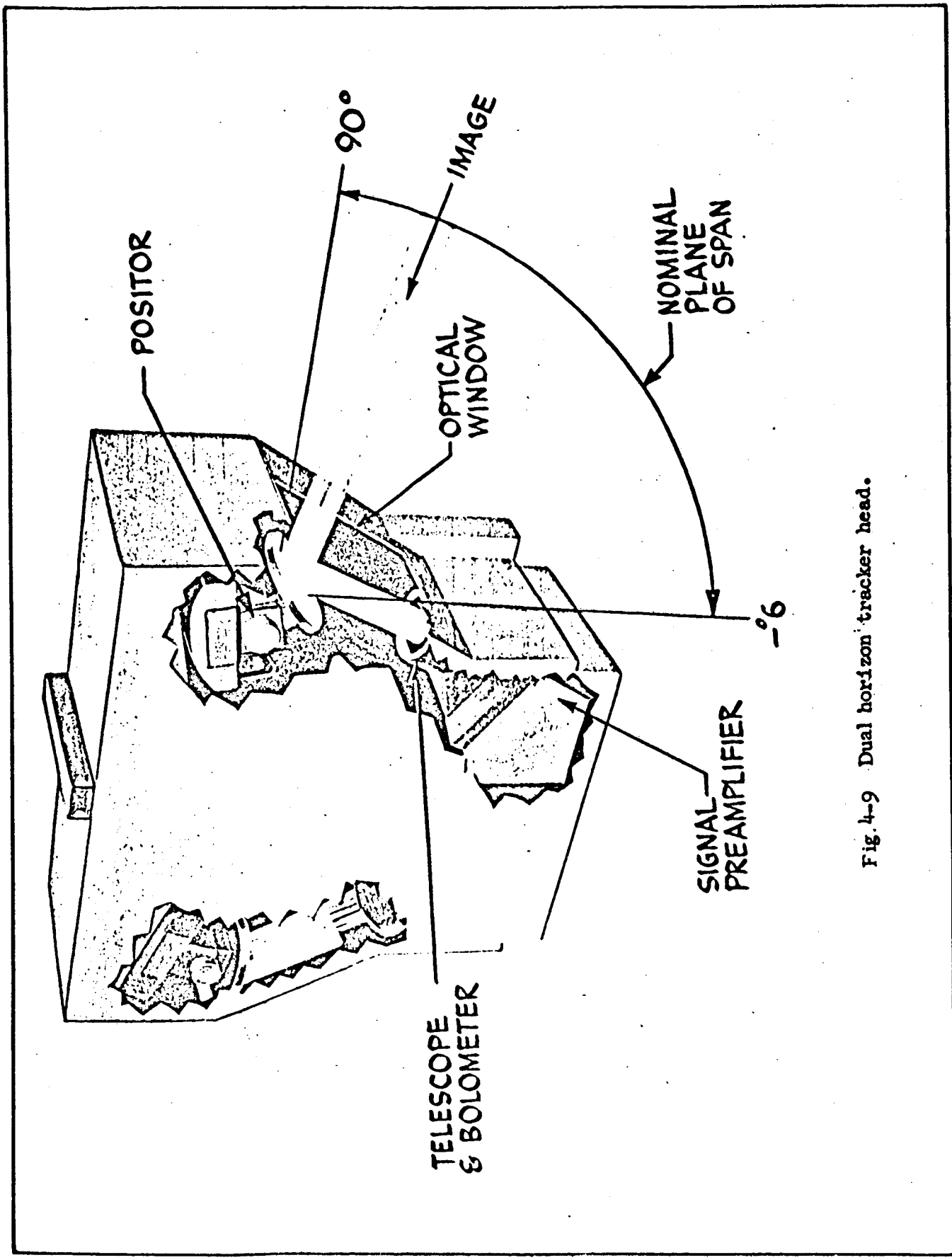

Fig. 4-9 Dual horizon tracker head.

reasonable value of drift for a strapdown system would be 0.2 degree/hour using medium quality gyros. A summary table of the advanced technology Stage 2 G & N system is given in Table 4-4.

Strapdown Inertial Guidance System

Figure 4-10 shows a block diagram of a typical strapdown guidance system mechanization. In this particular example, a digital differential analyzer (DDA) type computer is used for the direction cosine computation and velocity resolution computation. A general purpose computer section is used for the guidance law computations. Using a DDA for the invariant part of the equation mechanization results in a minimum of hardware complexity. The estimated weight, volume and power for a complete strapdown guidance system is estimated at 15 kg (33 pounds), 0.01 M^3 (658 cubic inches) and 124 watts. This system would have an accuracy commensurate with Stage 2 requirements, with an expected gyro drift rate of 0.2 degrees/hour and an accelerometer bias of 5×10^{-5}g.

STAGE 2 G&N EQUIPMENT - ADVANCED TECHNOLOGY CONCEPT

Unit	Number of Units	Weight KG (lb.)	Volume M^3 ($ft.^3$)	Power W
Strapdown Inertial Guidance System	1	15 (33)	.011 (.38)	125
Rendezvous Radar	1	13.6 (30)	.035 (1.25)	23
Horizon Scanner	2	8.2 (18)	.0085 (.3)	20
Displays & Controls*	1	9 (20)	.0056 (.2)	30
Command System	1	9 (20)	.007 (.25)	20
	System Totals	54.8 (121*)	.067 (2.38*)	218*
		46 (101)	.062 (2.18)	188

*Manned Vehicle Only

Table 4-4

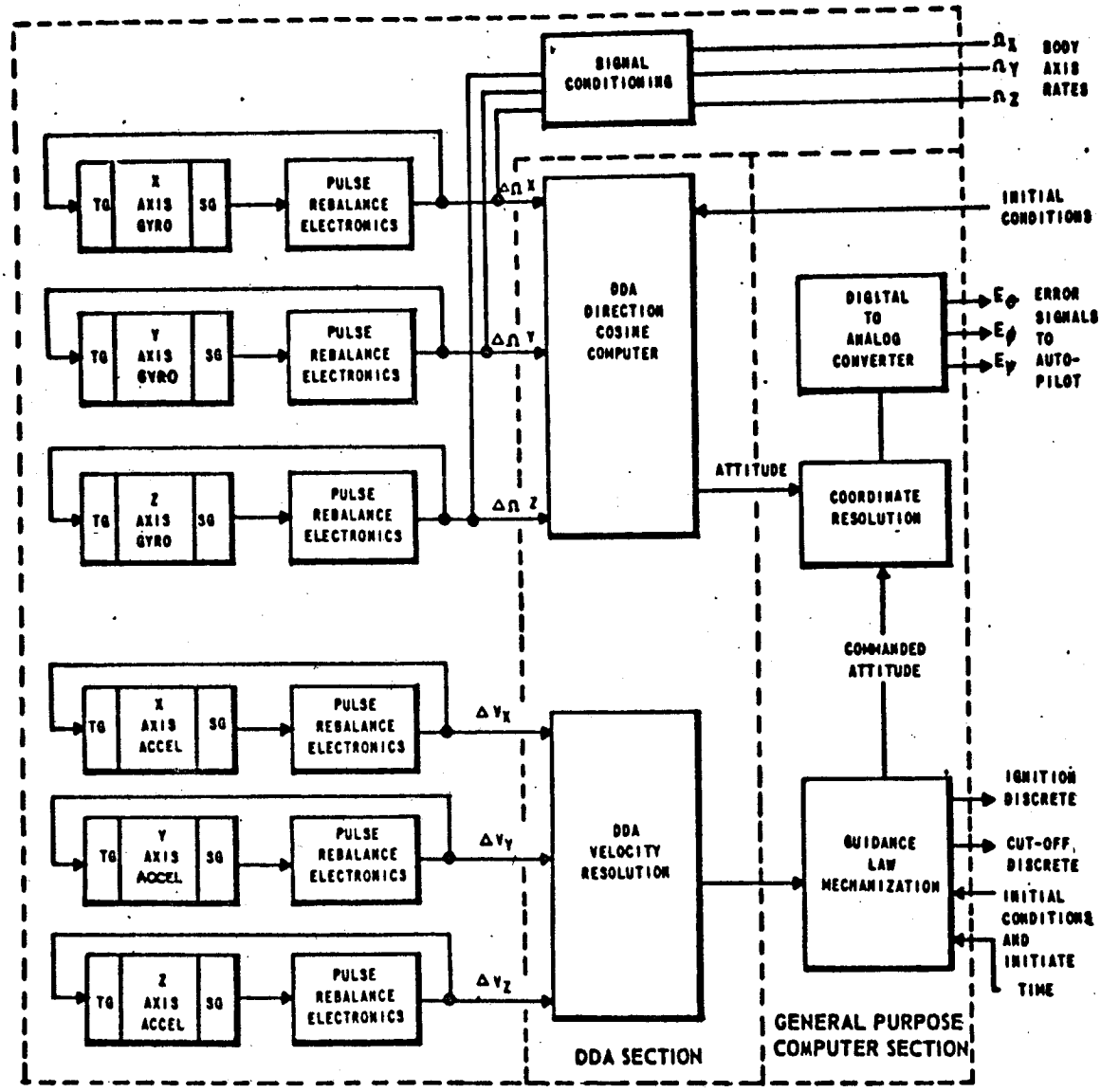

FIGURE 4-10 STRAPDOWN GUIDANCE SYSTEM BLOCK DIAGRAM

4.3. Operational Studies

4.3.1 Crew Functions

The role of the pilot and crew of the first stage vehicle will not be solely one of system monitors in that capability for manual control will always be provided. Manual operation of the first stage may be difficult during the hypersonic portion of the mission because of the precision required. An important area of research is the investigation of the optimum pilot, display, and airplane control relationships for best performance when consideration is given to both normal and emergency modes of operation. The capability of the crew to control the aircraft with adequate precision under the guidance of suitable displays must be established through simulations, both ground based and inflight. These simulations would be used to establish crew size and interactions.

One of the more important crew functions is the control of the vehicle for approach and landing. Normal landings are expected to be manually controlled. In bad weather situations the vehicle would be flown under air traffic control direction to the point of acquisition of the glide slope beam. Subsequent descent and landing would utilize the instrument landing system.

Besides actual flying of the stage one vehicle, the crew must provide the following function:

- o Communication with Mission Control
- o Communications with ATC
- o Communications with Stage 2
- o Insertion of mission data into the computer
- o Monitoring G & N displays, selection of backup modes
- o Monitoring Stage 2 systems
- o Providing mission abort decision

Operation of the Navigation and Guidance System for the Stage 1 vehicle will normally be almost entirely automatic, with the central computer providing functions which have more often been done manually. Examples of such functions are frequency switching, position plotting, and navigation fixes. Crew duties will consist primarily of malfunction monitoring and to select backup modes for failures which are not readily sensed by automatic means.

4.3.2 Preflight Checkout

To minimize ground support equipment, most of the preflight checkout should be performed aboard the first stage. The first stage checkout system would provide for checkout of both first and second stage vehicles. Preflight function sequencing and system checkout will be done using a central computer system. To as large an extent as possible, the preflight sequencing and checkout will be entirely automatic. The role of the crew will be to insert mission data, monitor the computer displays, investigate indicated malfunctions (possibly

by calling up subsystem checkout subroutines from the computer) and control the checkout sequence. Critical parameters must be continuously displayed at appropriate crew stations.

Checkout and countdown of the second stage will continue from preflight until the point of second stage release.

4.3.3 Preflight Alignment

First Stage Alignment

Because of the relatively short mission time, the error due to gyro drift, which is usually the predominant error in cruise inertial navigation systems, is on the same order as the accelerometer errors and alignment erors. The azimuth alignment error is the worst offender. Azimuth alignment of airplane inertial navigation is usually done by gyrocompassing-sensing the horizontal component of Earth rotation with a level gyro to determine the platform orientation about the vertical axis. This method suffers from errors caused by gyro bias, gyro noise, and noise due to vehicle movements, from wind buffets, for example. A gyro bias error of 0.01°/hr causes a 0.06° error in azimuth alignment with a 10°/hr (45° latitude). Instrument noise and vehicle noise degrades the accuracy further. If sufficient time for filtering is available, the noise affects can be reduced. Performing 180° platform azimuth rotations permits a determination of the level gyro bias.

The practical limit on the accuracy of gyrocompass azimuth alignment is about 0.05 to 0.1 degree. To obtain higher accuracy, an external reference must be used, using optical sightings on a reference mirror or reference mark aligned with respect to North. An opening port or window must be provided for optical access to a reference prism on the stable element of the inertial measurement unit.

Strapdown First Stage Alignment

The alignment of a strapdown first stage inertial navigation system is more difficult than that of a gimbaled system because the gyros are not isolated from the angular motion of the vehicle. Because of motion due to wind gusts, crew motion, fuel loading, etc., it is doubtful that accurate self-contained alignment can be accomplished in a reasonable time. Alternatives are possible, however. One method is to measure the strapdown reference unit orientation with respect to a fixed reference using optical reference surfaces on the package. Providing the optical path into the aircraft can be a very difficult problem. A second method is to physically align the reference unit to accurately machined surfaces mounted near the aircraft which are aligned to true North and level. This requires removing the package from the aircraft, using either a battery supply or an extension cable. Careful handling of the package is necessary to avoid subjecting it to high rates.

Despite these disadvantages, the latter method appears to offer the most convenient solution.

Second Stage Alignment

In-flight leveling of a Stage 2 inertial platform can be accomplished by using a Stage 1 master platform as a reference. The difference in velocity between the masterplatform and secondary platform is used as an input to the torquers of the secondary platform gyros. The secondary platform is torqued until the two platforms have the same velocity output when averaged over the time constant of the leveling loop. In a third order mechanization gyro drift error effects are eliminated and the accuracy of level is determined by the secondary platform accelerometer bias. A 10^{-4}g bias gives a 20 second of arc leveling error. Structural oscillations between the two platforms and master platform noise errors may double the error. Thus, a level accuracy of 40 seconds of arc can be expected at separation of stage 2 with an inexpensive stage 2 platform.

Azimuth Alignment or Transfer

The technical critical problem with a master platform - secondary platform configuration is azimuth alignment of the secondary platform. A number of alternate transfer methods and alignment methods can be considered.

(1) Ground-based alignment

Pre-takeoff leveling and azimuth alignment of the stage 2 inertial platform requires a low drift rate azimuth gyro. Level of the stage 2 can be held relative to a stage 1 master platform by the leveling mode. After a 40 minute flight to the staging point the azimuth accuracy for various gyro drift rates is, assuming perfect preflight alignment:

Effective Gyro Drift Rate (Degrees/hour)	Azimuth Error Degrees
1.	0.7
0.1	0.07
0.01	0.007
0.001	0.0007

(2) Gyro-compassing

In-flight gyrocompassing with an accurate azimuth gyro on a stage 2 platform is limited by the accuracy of vehicle velocity. Better performance is obtained with preflight alignement with the accurate azimuth gyro required for gyrocompassing and the relatively short flight time of the basic mission. Gyrocompassing is one of the

potential modes of preflight azimuth alignment.

(3) Velocity change matching

Azimuth transfer can be accomplished by comparing the velocity change measured by the master platform with the velocity change measured by the secondary platform and attributing differences to azimuth errors. A velocity change or vehicle turn is required for the comparison. Three error sources determine the resulting azimuth accuracy: (a) the master platform azimuth error, (b) vehicle azimuth oscillations (say 3M/sec (10 fps)) divided by the input velocity change (say 1000 M/sec (3000 fps)) gives an azimuth error in radius (3×10^{-3} radians = 0.2° in the example), (c) the ability of the secondary platform to hold the alignment after the maneuver.

(4) Position data use for azimuth alignment

Position data obtained from the master platform is compared with the position data output of a stage 2 inertial navigator using a weighted least squares filter (or Kalman filter). The filtering process gives estimates of stage 2 navigator errors including azimuth alignment errors. Gyro bias drift errors can also be estimated. For a single turning maneuver comparison the position data method reduces to the velocity change matching result. However, the position data filter method has several advantages. Data over a longer time interval is used so that smaller maneuvers are required for a given azimuth error; this may provide a significant operational advantage for some launch vehicle missions. Also, the effect of vehicle azimuth oscillations can be estimated using multiple position data comparisons over several oscillations. This potentially could improve the azimuth accuracy compared to velocity match methods. Further detailed study is required to establish the magnitude of the accuracy advantage.

Alignment Study Conclusion

For a gimbaled second stage inertial measurement unit, the preferred alignment method is to independently align the platform with respect to local level and true North during preflight and to subsequently update the alignment during flight using an optimum filtering technique with the Stage 1 inertial navigation system as a master. For a strapdown stage 2 system, the unit will be aligned with respect to the airplane body axes at prelaunch and fine aligned in flight using the stage 1 inertial navigation system as a master.

4.4 Accuracy Analysis

To obtain a comparison of the performance to be expected with the cruise-launch vehicle G & N concepts considered, a simplified error analysis was done. Only major error sources were considered. Errors accrued during the first stage cruise and the second stage boost are propagated to the apogee point using the following relation:

$$\begin{bmatrix} \delta h \\ r\delta\theta \\ r\delta\dot{\theta} \\ \delta\dot{h} \\ \delta z \\ \delta\dot{z} \end{bmatrix} = \begin{bmatrix} 2-\cos\theta & 0 & 2\frac{r}{V}(1-\cos\theta) & \frac{r}{V}\sin\theta & 0 & 0 \\ 2-\sin\theta-3\theta & 1 & \frac{r}{V}(4\sin\theta-3\theta) & \frac{2r}{V}(\cos\theta-1) & 0 & 0 \\ \frac{V}{r}(\cos\theta-1) & 0 & 2\cos\theta-1 & -\sin\theta & 0 & 0 \\ \frac{V}{r}\sin\theta & 0 & 2\sin\theta & \cos\theta & 0 & 0 \\ 0 & 0 & 0 & 0 & \cos\theta & \frac{r}{V}\sin\theta \\ 0 & 0 & 0 & 0 & -\frac{V}{r}\sin\theta & \cos\theta \end{bmatrix} \begin{bmatrix} \delta h_o \\ r\delta\theta_o \\ r\delta\dot{\theta}_o \\ \delta\dot{h}_o \\ \delta z_o \\ \delta\dot{z}_o \end{bmatrix}$$

where

θ = orbital angle
V = velocity
r = radius from Earth center
δh = altitude error
$r\delta\theta$ = down range error
$r\delta\dot{\theta}$ = horizontal velocity error
$\delta\dot{h}$ = altitude rate error
δz = cross plane error
$\delta\dot{z}$ = cross plane velocity error

For a Hohmann transfer, $\theta = 180°$, and r and V are approximately 6500 km (3550 nautical miles) and 7300 M/sec (24,000 ft/sec). The matrix then reduces to:

$$\begin{bmatrix} \delta h \\ r\delta\theta \\ r\delta\dot{\theta} \\ \delta\dot{h} \\ \delta z \\ \delta\dot{z} \end{bmatrix} = \begin{bmatrix} 1 & 0 & 3.56 & 0 & 0 & 0 \\ -8.5 & 1 & -8.4 & -3.56 & 0 & 0 \\ -1.78 & 0 & -3 & 0 & 0 & 0 \\ 0 & 0 & 0 & -1 & 0 & 0 \\ 0 & 0 & 0 & 0 & -1 & 0 \\ 0 & 0 & 0 & 0 & 0 & -1 \end{bmatrix} \begin{bmatrix} \delta h_o \\ r\delta\theta_o \\ r\delta\dot{\theta}_o \\ \delta\dot{h}_o \\ \delta z_o \\ \delta\dot{z}_o \end{bmatrix}$$

With velocity in M/sec and position in km.

First Stage Error

The errors assumed for the first stage navigation system are considered representative of a 1.8 to 3.6 km/hour (1 to 2 N.M./hour) gimbaled system: Table 4-5 shows the error at staging. A major portion of the error is due to heading alignment. A high accuracy alignment technique using optical alignment would reduce the cross track position error from 3.48 km to 1.7 km.

The accuracy of a strapdown first stage system with navigation satellite updates is assumed to be on the same order as the gimbaled inertial system.

Second Stage Error

The errors after the end of second stage thrust are due to (1) the first stage position and velocity errors, (2) second stage alignment error due to first stage error and transfer error, and (3) error in measuring the second stage velocity. Tables 4-6 and 4-7 show the error after second stage thrust for a gimbaled second stage system and a strapdown second stage system.

The errors at apogee due to the accumulated errors after second stage thrust are found by applying the error transformation matrix.

Comparison of the apogee errors for the assumed errors of the two second stage guidance systems show the errors of the gimbaled system are about half that of the strapdown system. The weight of the fuel required to correct the velocity errors are approximately 18 kg (40 pounds) and 8 kg (18 pounds) for the strapdown and gimbaled concepts respectively, assuming a 4500 kg (10,000 pounds) vehicle.

TABLE 4-5

FIRST STAGE NAVIGATION ERROR

	Cross Track	Along Track
Position Error - KM (N.M.)		
Gyro Drift - .01°/hour	1.4 (.76)	1.4 (.76)
Heading Alignment - .05°	3.05 (1.67)	0
Accelerometer Bias 5 x 10^{-5}g	.314(.172)	.314(.172)
Accelerometer Scale Factor - .05%	.88 (.481)	.88 (.481)
RSS	3.48 (1.9)	1.67 (.915)
Velocity Error - M/Sec. (ft/sec)		
Gyro Drift	.305(1)	.305(1)
Heading Alignment	1.83 (6)	0
Accelerometer Bias	.4 (1.3)	.4 (1.3)
Accelerometer Scale Factor	0	0
RSS	1.9 (6.2)	.49 (1.6)

TABLE 4-6

SECOND STAGE NAVIGATION ERROR - GIMBALED SYSTEM

	Error After Transfer ΔV					
	KM (N.M.)			M/Sec (ft/sec)		
	Altitude δh	Along Track $r\delta\theta$	Cross Track δz	Velocity $r\delta\dot{\theta}$	Vertical Velocity $\delta\dot{h}$	Cross Velocity $\delta\dot{z}$
Initial Condition Error	.018(.01)	1.67(.915)	3.98(1.9)	.49(1.6)	0	1.9(6.2)
Alignment Error = .05° Az.						4.6(15)
Level Error = .01°					.9(3)	
Accelerometer Scale Factor = $.5(10^{-4})$ g/g				.27(.9)		
Accelerometer Bias = $.5(10)^{-4}$g				.15(.5)	.15(.5)	.15(.5)
TOTAL RSS	.018(.01)	1.67(.915)	3.48(1.9)	.58(2.07)	.91(3.03)	5(16.2)

Error after 180° Hohmann transfer

δh = 2.06 KM (1.13 N.M.)

$r\delta\theta$ = 6.1 KM (3.3 N.M.)

δz = 3.48 KM (1.9 N.M.)

$r\delta\dot{\theta}$ = .91 M/Sec (3 ft/sec)

$\delta\dot{h}$ = 1.74 M/Sec (5.7 ft/sec)

$\delta\dot{z}$ = 5 M/Sec (16.4 ft/sec)

Total Position Error = 7.32 KM (4 N.M.)

Total Velocity Error = 5.37 M/Sec (17.6 ft/sec)

TABLE 4-7

SECOND STAGE NAVIGATION ERRORS - STRAPDOWN SYSTEM

Error After Transfer ΔV

	KM (N.M.)			M/sec (ft/sec.)		
	Altitude δh	Along Track $r\delta\theta$	Cross Track δz	Velocity $r\delta\dot{\theta}$	Vertical Velocity $\delta\dot{h}$	Cross Velocity $\delta\dot{z}$
Initial Condition Error	.018(.01)	1.8(1)	3.6(2)	.49(1.6)	0	1.9(6.2)
Alignment Error = .1° Az.						(30)
Alignment Error = .05° level					4.5(15)	
Accelerometer Scale Factor = .7 x 10^{-4} g/g				.425(1.4)		
Accelerometer Bias = 10^{-4} g				.305(1)		
TOTAL	.018(.01)	1.8(1)	3.6(2)	.715(2.35)	4.6(15)	11(36.2)

Error after 180° Hohmann Transfer

δh = 2.5 KM (1.32 N.M.)

$r\delta\theta$ = 17.7 KM (9.7 N.M.)

δz = 3.6 KM (2.7 N.M.)

$r\delta\dot{\theta}$ = 2.15 M/Sec (7.05 ft/sec)

$\delta\dot{h}$ = 4.6 M/Sec (15 ft/sec)

$\delta\dot{z}$ = 11 M/Sec (36.2 ft/sec)

Total position error = 18 KM (9.8 N.M.)

Total Velocity error = 12 M/Sec (40 ft/sec)

4.5 Reliability Analysis

The data obtained in the reliability analysis is based on the following assumptions:

- o First stage mission time of two hours with a reliability degradation factor of 5 used for the airplane environment. This results in an equivalent operating time of 10 hours.

- o Second stage mission time of 1.5 hours, with reliability degradation factors of 5 for the outbound cruise, 125 for the 4.4 minute thrusting period, and 1 for the coast period. This results in an equivalent operating time of 13 hours.

Tables 4-8 and 4-9 show the reliability estimates for the Stage 1 and Stage 2 vehicles. For the Stage 1 vehicle, the reliability ranges from .943 to .948 for a single thread system, and from .9968 to .9973 for a system where every unit is redundant. The reliability of the second stage system ranges from .985 for the current technology concept to .989 for the advanced technology concept. Total mission reliability then ranges from .934 for the minimum reliability combination to .986 for the maximum reliability combination.

These reliability estimates consider basic equipment reliability only, assuming that it must all function to complete the mission. This is quite conservative since the crew will detect malfunctions and select alternate modes, and many of the equipments considered are auxiliary aids that are not absolutely essential for normal missions. Even in the basic equipment, such as the inertial platform or computer, many malfunctions will degrade performance but will not affect the ability to complete the mission. Finally, the estimates given represent the current state-of-the-art; significant reliability improvements with time are expected.

Table 4-8 /

Reliability Estimates - Stage 1 Equipment

	MTBF-Hrs.	Reliability - Two Hour Mission, K-factor = 5
Inertial Navigation System		
a. Gimbaled	1000	.99
b. Strapdown	2000	.995
Air Data	6000	.9983
High ALT Radar Altimeter	1000	.99
Lo ALT Radar Altimeter	2000	.995
Radio Landing RCVR	7500	.9987
VHF Nav. RCVR	1000	.99
DME RCVR	1000	.99
Radar ATC Transponder	3300	.997
Nav. Displays	4000	.9975
Navsat RCVR	10,000	.999
Central Nav Computer	5000	.998

Probability of no function failing: Gimbaled - .943 single thread, .9968 redundant

Strapdown - .948 single thread, .9973 redundant

Table 4-9

Reliability Estimates - Stage 2 Equipment

	MTBF - Hrs.	Reliability - Equiv. 13 Hr. Mission
Inertial Measurement Unit		
a. Gimbaled	5000	.9974
b. Strapdown	7000	.9981
Computer	4000	.9968
Rendezvous Radar		
Current	3000	.9957
Advanced	10,000	.9987
Displays & Controls	5000	.9974
Horizon Scanner	15,000	.9991
Command System	10,000	.9987

Probability of no system failing: Current Technology - .985

Advanced Technology - .989

5.0 Alternate Missions

5.1 Cruise Mission Capability

The cruise mission performance has been estimated from the results of the outbound climb/acceleration and cruise segments combined with the inbound descent/deceleration segments by using the data of Figure 6-3 of D2-113016-5 (Volume 2). Figure 5.1 shows an approximate weight schedule generated by this method. These data indicate the payload for the 9260 km (5000 N.M.). cruise mission of approximately 29,478 kg (65,000 lb) can be expected by using the optimization techniques of this report. The complement of guidance and navigation equipment chosen for the stage one vehicle of the cruise-launch mission allows operation as a pure cruise vehicle with essentially no change except guidance computer reprogramming and removing second stage functions. The navigation systems chosen are essentially the same as those used on current aircraft and advanced transport aircraft such as the supersonic transport. Because of the very high speed of the hypersonic cruise vehicle, air traffic control clearances must be obtained before takeoff to allow an unimpeded flight. Since the flight path is highly predictable, no problem would be anticipated in obtaining priority clearances.

For the cruise mission, the required inertial navigation accuracy is not as high as that for the launch mission. A 3.7 km/hr (2 N.M./hr) system (CEP) will result in navigation error well within existing and predicted future Air Traffic Control (ATC) separation requirements. Radio navigation updates (VOR, DME, and ATC radar) are used in operation near terminal areas and during overland flights. The total time when the aircraft is out of range of radio fixes would be less than 20 minutes for most flights.

If a navigation satellite system is used, the period between updates would be on the order of five minutes.to limit error buildup.

5.2 Refueling Rendezvous Mission

For those missions which require a maximum payload injected at a 3650 km (2000 nautical miles) offset, an inflight refuleing must be accomplished for the Stage 1 return. Rendezvous guidance with the tanker vehicle will rely to a great extent on the use of a refueling rendezvous radar system. This consists of a radar transmitter on the tanker vehicle with a beacon transponder on the Stage 1 vehicle. Replies from the transponder are coded to contain the Stage 1 vehicles' speed, heading, and altitude. The tanker vehicle would perform the active part in rendezvous. An example if a rendezvous beacon is an advanced AN/APN-135 beacon. This beacon operates on K_u band and has a weight of 9 kg (20 pounds), a volume of $0.01M^3$ (0.35 cubic feet), and a power consumption of 100 watts.

FIGURE 5-1

MASS SCHEDULE-CRUISE MISSION

NOTE: DATA TAKEN FROM 3704 KM OFFSET LAUNCH MISSION, OUTBOUND AND INBOUND LEGS

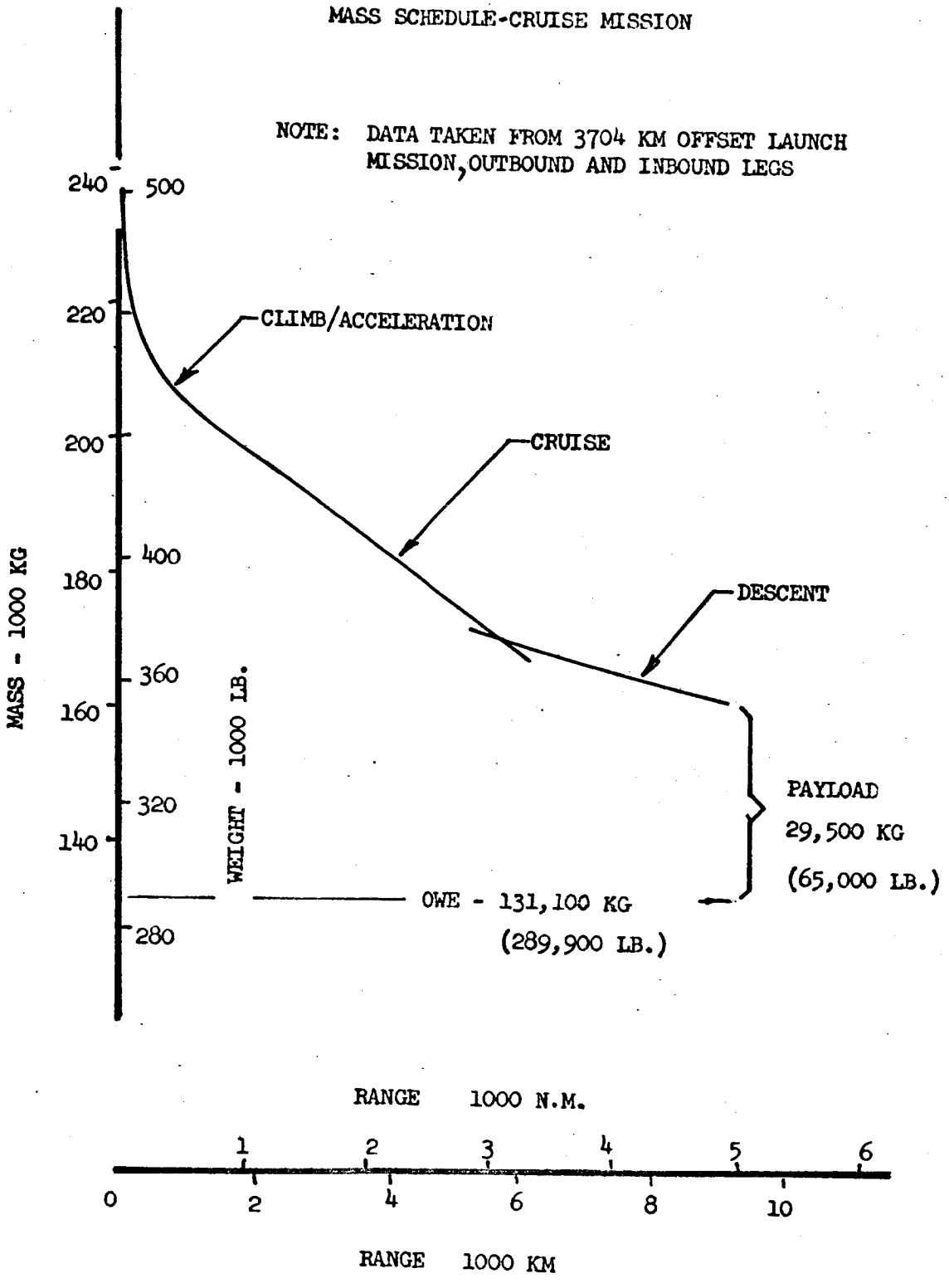

6.0 GUIDANCE AND NAVIGATION COSTING SECTION

6.1 ESTIMATING TECHNIQUES

The Guidance and Navigation costing performed during the Phase II portion of this study reflects values derived from both standard estimating practices and specialized parametric estimating techniques. The standard practices encompass suppliers catalogs, documents, data banks, historical statistics and other sources of data relating to specific cost areas of this estimate. Parametric estimating techniques were relied upon to develop costs when design definition and other pertinent information was limited to basic criteria lacking cost visibility.

The Guidance and Navigation cost estimates which follow were generated entirely within these guidelines. These estimates must, therefore, be construed as budgetary or planning tools until such time as more definitive criteria becomes available.

An evaluation was made to assure that all estimated costs are realistic by comparing the major components with comparable commercial quality avionic equipment being used or anticipated during the 1965 through 1975 time period.

6.2 GENERAL APPROACH

The Guidance and Navigation Equipment identified by block diagrams (Figure 4-1 and 4-4) were used as baseline for costing all purchased equipment.

Unit average recurring costs were assigned to each item after consultation with avionic buyers, reviewing current and historical accounting ledgers or by arriving at some costs parametrically. After the average recurring unit cost was established for each item, it was computed back to a theoretical number one unit in order to equate all G&N equipment on an equal basis. From this point, estimating relationships from aircraft/space programs were used to develop ratios and factors to extrapolate from the known unit cost to development costs.

Deviations from standard estimating techniques were made on a few items after Finance/Engineering judgment indicated equipment peculiarities caused higher than usual costs, i.e., Inertial Navigation System and computers; these costs were adequately adjusted.

In the case of the Inertial Navigation System (INS), an assumption was made in the advanced technology estimate, that the state-of-the-art for hypersonic aircraft electronics

GENERAL APPROACH (Continued)

would be at about the same relative point in time as the supersonic transport is today. Developmental costs in the advanced INS should, therefore, be indicated by today's cost, assuming, of course, that a normal evolution of G&N technology continues throughout the next decade. Costs have not been included for technology growth (development).

Nonrecurring costs are displayed as a range of costs, low and high, and indicates those costs which would be experienced in further developing Guidance and Navigation components to meet the specific technical requirements for the proposed missions. The cost ranges are realistic, based on historical data for similar hardware usage, reliability, and maintainability.

Since the engineering studies of each equipment type for the hypersonic vehicle application have been on a conceptual design level of detail, there is some risk that significant development problems have been overlooked or discounted. An offsetting factor is that the results of the SST avionics development should, for the most part, be directly applicable to the hypersonic vehicle.

Another consideration is that conservative weight and electrical power estimates have been used. It is potentially possible that significant reductions can be made for the advanced time period. However, this would imply complete redesign of each equipment component and would considerably increase development costs.

6.3 GROUND RULES

In addition to the basic ground rules expressed under the heading, General Approach, the following assumptions were used as guidelines in the development of the following costs:

- Nonrecurring costs are the direct labor, indirect costs, and material costs for the effort to develop a G&N component and to provide production capabilities for that component. Typical nonrecurring costs are:

  a. Preliminary design and analysis
  b. Design engineering (hardware drawings)
  c. Design, development, and qualification tests, test spares, mock-ups, and models
  d. Costs of all tooling, manufacturing and procurement effort specifically incurred in performing development or design development and qualification test.

GROUND RULES (Continued)

- Recurring costs are the direct labor, indirect costs, and material costs for the production effort. Except for item specifically defined above as nonrecurring, recurring costs include the costs of the following:

  a. Engineering re-design and associated evaluation and liaison (sustaining effort)
  b. Direct labor, material and associated indirect costs
  c. Production testing including systems testing and integration.

- Not included in these costs are:

  - the integration and interfacing of the G&N system with other subsystems within the cruise vehicle or second stage vehicles
  - allowance for spares
  - allowance for technical services or crew training
  - Prime Contractor's fee or profit

- Production costs for the cruise vehicle G&N do not reflect a learning process due to the limited number of units to be built. Cruise vehicles are assumed to remain in a prototype category; it is assumed that three to five vehicles are to be built. Therefore, the number one unit production cost will be used.

- A 91% learning curve for the second stage G&N estimate was used. This is in keeping with cost trades performed earlier in the study and given in cost tables in Volume I of the final report. Production quantities of 20 units are reflected in the recurring costs for the second stages.

KEY WORDS

Cruise Vehicle -	A hypersonic aircraft, which for the purpose of this study, assumes the role of a first stage boost vehicle capable of launching a space vehicle into an Earth orbit. G&N technology for this vehicle is based on current and proposed SST, 747, 727, and 707 equipment requirements.
Unmanned Second Stage -	A theoretical space vehicle of the Gemini/Apollo generation to be used for Earth orbital missions. G&N design criteria is basically that which was proposed for Gemini/Apollo with allowances and deletions made for an unmanned mode of operation as a prime requirement.

KEY WORDS (Continued)

Manned Second Stage - Basically the same description as the above, however, emphasis is placed on the man-rated requirements for the Gemini/Apollo missions. Displays and controls were added to accomplish this function.

Purchased Equipment (P.E.) - All avionic/space oriented "black boxes" required to perform mission guidance and navigation functions within the technology of this study are assumed to be Purchased Equipment. The point is conceded that portions of this equipment would be subcontracted; this fact is irrelevant to the purpose or mechanics of these estimated costs, and was, therefore removed from the rationale.

GUIDANCE AND NAVIGATION COSTING SUMMARY

(All dollars are in thousands)

	Current Technology		Advanced Technology	
	Low	High	Low	High
CRUISE VEHICLE				
Nonrecurring Costs	$14,030	$19,950	$13,820	$19,620
Recurring Costs (5 units)	10,905	10,905	10,270	10,270
Total	$24,935	$30,855	$24,090	$29,890
UNMANNED SECOND STAGE				
Nonrecurring Costs	$ 9,400	$18,800	$ 7,400	$14,800
Recurring Costs (20 units)	11,080	11,080	8,700	8,700
Total	$20,480	$29,880	$16,100	$23,500
MANNED SECOND STAGE				
Nonrecurring Costs	$19,950	$28,500	$16,400	$23,500
Recurring Costs (20 units)	13,440	13,440	11,060	11,060
Total	$33,390	$41,940	$27,460	$34,560

Costs exclude: Spares, Technical Services, Interfacing and Fee.

Revised April 12, 1967

CURRENT TECHNOLOGY COST ESTIMATE

(All dollars are in thousands)

	Nonrecurring Costs (RDT&E) Low	Nonrecurring Costs (RDT&E) High	P.E. Quantity Per Ship Set	Total Recurring Unit Costs
CRUISE VEHICLE (1st Stage)				
Inertial Navigation	$ 5,250	$ 6,500	3	$ 557
Air Data System	1,370	2,110	2	301
High Alt. Radar Altimeter	90	130	1	10
Low Alt. Radar Altimeter	90	130	2	19
Radio Landing Receiver	110	160	2	23
VHF Navigation Receiber	110	160	2	23
DME Receiver	210	330	2	47
RF Control Computer	150	230	2	33
Computer	3,250	5,000	2	716
VHF Communications	190	290	2	41
HF Communications	320	490	2	70
Displays	2,760	4,220	Misc.	302
RF Unit	40	70	2	10
Radar ATC Transponder	90	130	2	29
Total Costs	$14,030	$19,950		$2,181
UNMANNED Second Stage				
IMU	$ 4,000	$ 8,000	1	$ 237
Computer	1,600	3,200	1	94
Rendezvous Radar	3,000	6,000	1	177
Horizon Scanner	400	800	1	23
Command System	400	800	1	23
Total Costs	$ 9,400	$18,800		$ 554
MANNED Second Stage				
IMU	$ 7,000	$10,000	1	$ 237
Computer	2,800	4,000	1	94
Rendezvous Radar	5,250	7,500	1	177
Displays and Controls	3,500	5,000	1	118
Horizon Scanner	700	1,000	1	23
Command System	700	1,000	1	23
Total Costs	$19,950	$28,500		$ 672

Revised: April 12, 1967

ADVANCED TECHNOLOGY COST ESTIMATE

(All dollars are in thousands)

Components	Nonrecurring Costs (RDT&E) Low	Nonrecurring Costs (RDT&E) High	P.E. Quantity Per Ship Set	Total Recurring Unit Costs
CRUISE VEHICLE (1st Stage)				
Inertial Navigation	$ 5,250	$ 6,500	3	$ 489
Air Data System	1,370	2,110	2	301
High Alt. Radar Altimeter	90	130	1	10
Low Alt. Radar Altimeter	90	130	2	19
Radio Landing Receiver	110	160	2	23
RF Control Computer	150	230	2	33
Nav. Satellite Receiver	110	160	1	11
Computer	3,250	5,000	2	716
VHF Communication	190	290	2	41
HF Communication	320	490	2	70
Displays	2,760	4,220	Misc.	302
RF Unit	40	70	2	10
Radar ATC Transponder	90	130	2	29
Total Costs	$13,820	$19,620		$2,054
UNMANNED Second Stage				
IMU	$ 2,000	$ 4,000	1	$ 118
Computer	1,600	3,200	1	94
Rendezvous Radar	3,000	6,000	1	177
Horizon Scanner	400	800	1	23
Command System	400	800	1	23
Total Costs	$ 7,400	$14,800		$ 435
MANNED Second Stage				
IMU	$ 3,500	$ 5,000	1	$ 118
Computer	2,800	4,000	1	94
Rendezvous Radar	5,200	7,500	1	177
Displays and Controls	3,500	5,000	1	118
Horizon Scanner	700	1,000	1	23
Command System	700	1,000	1	23
Total Costs	$16,400	$23,500		$ 553

Revised: April 12, 1967